NORTH ATLANTIC TREATY ORGANIZATION

ADVISORY GROUP FOR AEROSPACE RESEARCH AND DEVELOPMENT

(ORGANISATION DU TRAITE DE L'ATLANTIQUE NORD)

AGARD Advisory Report No.182

PROPULSION AND ENERGETICS PANEL

WORKING GROUP 14

on

SUITABLE AVERAGING TECHNIQUES IN NON-UNIFORM INTERNAL FLOWS

Edited by

M.Pianko
Office National d'Etudes et de
Recherche Aérospatiales
29 Avenue de la Division Leclerc
92320 Châtillon sous Bagneux
France

and

F.Wazelt
Lehrstuhl für Flugantriebe
Technische Hochschule Darmstadt
Petersenstrasse 30
6100 Darmstadt
Germany

This Advisory Report was prepared at the request of the Propulsion and Energetics Panel of AGARD.

THE MISSION OF AGARD

The mission of AGARD is to bring together the leading personalities of the NATO nations in the fields of science and technology relating to aerospace for the following purposes:

- Exchanging of scientific and technical information;
- Continuously stimulating advances in the aerospace sciences relevant to strengthening the common defence posture;
- Improving the co-operation among member nations in aerospace research and development;
- Providing scientific and technical advice and assistance to the North Atlantic Military Committee in the field of aerospace research and development;
- Rendering scientific and technical assistance, as requested, to other NATO bodies and to member nations in connection with research and development problems in the aerospace field;
- Providing assistance to member nations for the purpose of increasing their scientific and technical potential;
- Recommending effective ways for the member nations to use their research and development capabilities for the common benefit of the NATO community.

The highest authority within AGARD is the National Delegates Board consisting of officially appointed senior representatives from each member nation. The mission of AGARD is carried out through the Panels which are composed of experts appointed by the National Delegates, the Consultant and Exchange Programme and the Aerospace Applications Studies Programme. The results of AGARD work are reported to the member nations and the NATO Authorities through the AGARD series of publications of which this is one.

Participation in AGARD activities is by invitation only and is normally limited to citizens of the NATO nations.

Published June 1983

ISBN 92-835-1452-1

Set and Printed by Specialised Printing Services Limited
40 Chigwell Lane, Loughton, Essex IG10 3TZ

AGARD Advisory Report No.182 (Eng.)
Advisory Group for Aerospace Research and Development, NATO
PROPULSION AND ENERGETICS PANEL WORKING GROUP 14 on SUITABLE AVERAGING TECHNIQUES IN NON-UNIFORM INTERNAL FLOWS
Edited by M.Pianko and F.Wazelt
Published June 1983
172 pages

In 1979 the Propulsion and Energetics Panel of AGARD established a Working Group named WG14 whose terms of reference were to study the averaging techniques used for non-uniform internal flows. This problem is relevant to gas turbine systems, in which the actual flows are usually heterogeneous and three-dimensional. Nevertheless, the test analysis and performance prediction methods are presently based upon simple one-dimensional models. Members of WG14 first reviewed

P.T.O.

AGARD-AR-182 (Eng.)

Internal flow
Averaging techniques
Equivalent flow
One dimensional flow
Heterogeneous
Mean value
Turbine engine component

AGARD Advisory Report No.182 (Eng.)
Advisory Group for Aerospace Research and Development, NATO
PROPULSION AND ENERGETICS PANEL WORKING GROUP 14 on SUITABLE AVERAGING TECHNIQUES IN NON-UNIFORM INTERNAL FLOWS
Edited by M.Pianko and F.Wazelt
Published June 1983
172 pages

In 1979 the Propulsion and Energetics Panel of AGARD established a Working Group named WG14 whose terms of reference were to study the averaging techniques used for non-uniform internal flows. This problem is relevant to gas turbine systems, in which the actual flows are usually heterogeneous and three-dimensional. Nevertheless, the test analysis and performance prediction methods are presently based upon simple one-dimensional models. Members of WG14 first reviewed

P.T.O.

AGARD-AR-182 (Eng.)

Internal flow
Averaging techniques
Equivalent flow
One dimensional flow
Heterogeneous
Mean value
Turbine engine component

AGARD Advisory Report No.182 (Eng.)
Advisory Group for Aerospace Research and Development, NATO
PROPULSION AND ENERGETICS PANEL WORKING GROUP 14 on SUITABLE AVERAGING TECHNIQUES IN NON-UNIFORM INTERNAL FLOWS
Edited by M.Pianko and F.Wazelt
Published June 1983
172 pages

In 1979 the Propulsion and Energetics Panel of AGARD established a Working Group named WG14 whose terms of reference were to study the averaging techniques used for non-uniform internal flows. This problem is relevant to gas turbine systems, in which the actual flows are usually heterogeneous and three-dimensional. Nevertheless, the test analysis and performance prediction methods are presently based upon simple one-dimensional models. Members of WG14 first reviewed

P.T.O.

AGARD-AR-182 (Eng.)

Internal flow
Averaging techniques
Equivalent flow
One dimensional flow
Mean value
Turbine engine component

AGARD Advisory Report No.182 (Eng.)
Advisory Group for Aerospace Research and Development, NATO
PROPULSION AND ENERGETICS PANEL WORKING GROUP 14 on SUITABLE AVERAGING TECHNIQUES IN NON-UNIFORM INTERNAL FLOWS
Edited by M.Pianko and F.Wazelt
Published June 1983
172 pages

In 1979 the Propulsion and Energetics Panel of AGARD established a Working Group named WG14 whose terms of reference were to study the averaging techniques used for non-uniform internal flows. This problem is relevant to gas turbine systems, in which the actual flows are usually heterogeneous and three-dimensional. Nevertheless, the test analysis and performance prediction methods are presently based upon simple one-dimensional models. Members of WG14 first reviewed

P.T.O.

AGARD-AR-182 (Eng.)

Internal flow
Averaging techniques
Equivalent flow
One dimensional flow
Mean value
Turbine engine component

current practices as employed by research and development teams in various research establishments and industry. The Group also undertook a theoretical analysis of the relations which may be correctly applied to steady flows. Consequently it was possible to discuss and classify known averaging methods. The theoretical study concludes by proposing refinements to known methods and a new approach to averaging for use with engine components and propulsion system analysis.

A large variety of possible averaging techniques were identified. Some were based on theoretical considerations, others were without justification except in their simplicity or common usage. All the averaging procedures were tested and compared by preparing a number of sample calculations in ducted flows, turbojet components and a complete propulsion system.

The Group arrived at several conclusions concerning the merits and the limitations of the methods studied. One method is recommended for stagnation temperature averaging. No single method is recommended for stagnation pressure averaging; the choice must depend on the particular circumstances.

This Advisory Report was prepared at the request of the Propulsion and Energetics Panel of AGARD.

ISBN 92-835-1452-1

current practices as employed by research and development teams in various research establishments and industry. The Group also undertook a theoretical analysis of the relations which may be correctly applied to steady flows. Consequently it was possible to discuss and classify known averaging methods. The theoretical study concludes by proposing refinements to known methods and a new approach to averaging for use with engine components and propulsion system analysis.

A large variety of possible averaging techniques were identified. Some were based on theoretical considerations, others were without justification except in their simplicity or common usage. All the averaging procedures were tested and compared by preparing a number of sample calculations in ducted flows, turbojet components and a complete propulsion system.

The Group arrived at several conclusions concerning the merits and the limitations of the methods studied. One method is recommended for stagnation temperature averaging. No single method is recommended for stagnation pressure averaging; the choice must depend on the particular circumstances.

This Advisory Report was prepared at the request of the Propulsion and Energetics Panel of AGARD.

ISBN 92-835-1452-1

current practices as employed by research and development teams in various research establishments and industry. The Group also undertook a theoretical analysis of the relations which may be correctly applied to steady flows. Consequently it was possible to discuss and classify known averaging methods. The theoretical study concludes by proposing refinements to known methods and a new approach to averaging for use with engine components and propulsion system analysis.

A large variety of possible averaging techniques were identified. Some were based on theoretical considerations, others were without justification except in their simplicity or common usage. All the averaging procedures were tested and compared by preparing a number of sample calculations in ducted flows, turbojet components and a complete propulsion system.

The Group arrived at several conclusions concerning the merits and the limitations of the methods studied. One method is recommended for stagnation temperature averaging. No single method is recommended for stagnation pressure averaging; the choice must depend on the particular circumstances.

This Advisory Report was prepared at the request of the Propulsion and Energetics Panel of AGARD.

ISBN 92-835-1452-1

current practices as employed by research and development teams in various research establishments and industry. The Group also undertook a theoretical analysis of the relations which may be correctly applied to steady flows. Consequently it was possible to discuss and classify known averaging methods. The theoretical study concludes by proposing refinements to known methods and a new approach to averaging for use with engine components and propulsion system analysis.

A large variety of possible averaging techniques were identified. Some were based on theoretical considerations, others were without justification except in their simplicity or common usage. All the averaging procedures were tested and compared by preparing a number of sample calculations in ducted flows, turbojet components and a complete propulsion system.

The Group arrived at several conclusions concerning the merits and the limitations of the methods studied. One method is recommended for stagnation temperature averaging. No single method is recommended for stagnation pressure averaging; the choice must depend on the particular circumstances.

This Advisory Report was prepared at the request of the Propulsion and Energetics Panel of AGARD.

ISBN 92-835-1452-1

AGARD
NATO OTAN
7 RUE ANCELLE · 92200 NEUILLY-SUR-SEINE
FRANCE
Telephone 745.08.10 · Telex 610176

DISTRIBUTION OF UNCLASSIFIED AGARD PUBLICATIONS

AGARD does NOT hold stocks of AGARD publications at the above address for general distribution. Initial distribution of AGARD publications is made to AGARD Member Nations through the following National Distribution Centres. Further copies are sometimes available from these Centres, but if not may be purchased in Microfiche or Photocopy form from the Purchase Agencies listed below.

NATIONAL DISTRIBUTION CENTRES

BELGIUM
Coordonnateur AGARD -- VSL
Etat-Major de la Force Aérienne
Quartier Reine Elisabeth
Rue d'Evere, 1140 Bruxelles

CANADA
Defence Science Information Services
Department of National Defence
Ottawa, Ontario K1A OK2

DENMARK
Danish Defence Research Board
Østerbrogades Kaserne
Copenhagen Ø

FRANCE
O.N.E.R.A. (Direction)
29 Avenue de la Division Leclerc
92320 Châtillon sous Bagneux

GERMANY
Fachinformationszentrum Energie,
Physik, Mathematik GmbH
Kernforschungszentrum
D-7514 Eggenstein-Leopoldshafen 2

GREECE
Hellenic Air Force General Staff
Research and Development Directorate
Holargos, Athens

ICELAND
Director of Aviation
c/o Flugrad
Reykjavik

ITALY
Aeronautica Militare
Ufficio del Delegato Nazionale all'AGARD
3, Piazzale Adenauer
Roma/EUR

LUXEMBOURG
See Belgium

NETHERLANDS
Netherlands Delegation to AGARD
National Aerospace Laboratory, NLR
P.O. Box 126
2600 A.C. Delft

NORWAY
Norwegian Defence Research Establishment
Main Library
P.O. Box 25
N-2007 Kjeller

PORTUGAL
Direcção do Serviço de Material
da Forca Aerea
Rua da Escola Politécnica 42
Lisboa
Attn: AGARD National Delegate

TURKEY
Department of Research and Development (ARGE)
Ministry of National Defence, Ankara

UNITED KINGDOM
Defence Research Information Centre
Station Square House
St. Mary Cray
Orpington, Kent BR5 3RE

UNITED STATES
National Aeronautics and Space Administration (NASA)
Langley Field, Virginia 23365
Attn: Report Distribution and Storage Unit

THE UNITED STATES NATIONAL DISTRIBUTION CENTRE (NASA) DOES NOT HOLD STOCKS OF AGARD PUBLICATIONS, AND APPLICATIONS FOR COPIES SHOULD BE MADE DIRECT TO THE NATIONAL TECHNICAL INFORMATION SERVICE (NTIS) AT THE ADDRESS BELOW.

PURCHASE AGENCIES

Microfiche or Photocopy
National Technical
Information Service (NTIS)
5285 Port Royal Road
Springfield
Virginia 22161, USA

Microfiche
Space Documentation Service
European Space Agency
10, rue Mario Nikis
75015 Paris, France

Microfiche or Photocopy
British Library Lending
Division
Boston Spa, Wetherby
West Yorkshire LS23 7BQ
England

Requests for microfiche or photocopies of AGARD documents should include the AGARD serial number, title, author or editor, and publication date. Requests to NTIS should include the NASA accession report number. Full bibliographical references and abstracts of AGARD publications are given in the following journals:

Scientific and Technical Aerospace Reports (STAR)
published by NASA Scientific and Technical
Information Facility
Post Office Box 8757
Baltimore/Washington International Airport
Maryland 21240, USA

Government Reports Announcements (GRA)
published by the National Technical
Information Services, Springfield
Virginia 22161, USA

Printed by Specialised Printing Services Limited
40 Chigwell Lane, Loughton, Essex IG10 3TZ

ISBN 92-835-1452-1

REPORT DOCUMENTATION PAGE

1. Recipient's Reference	2. Originator's Reference	3. Further Reference	4. Security Classification of Document
	AGARD-AR-182 (Eng.)	ISBN 92-835-1452-1	UNCLASSIFIED

5. Originator Advisory Group for Aerospace Research and Development
North Atlantic Treaty Organization
7 rue Ancelle, 92200 Neuilly sur Seine, France

6. Title PROPULSION AND ENERGETICS PANEL WORKING GROUP 14 on SUITABLE AVERAGING TECHNIQUES IN NON-UNIFORM INTERNAL FLOWS

7. Presented at

8. Author(s)/Editor(s)	9. Date
Edited by M.Pianko and F.Wazelt	June 1983
10. Author's/Editor's Address	**11. Pages**
See flyleaf	172

12. Distribution Statement This document is distributed in accordance with AGARD policies and regulations, which are outlined on the Outside Back Covers of all AGARD publications.

13. Keywords/Descriptors

Internal flow
Averaging techniques
Equivalent flow
One dimensional flow
Heterogeneous flow
Mean value
Turbine engine component

14. Abstract

In 1979 the Propulsion and Energetics Panel of AGARD established a Working Group named WG 14 whose terms of reference were to study the averaging techniques used for non-uniform internal flows. This problem is relevant to gas turbine systems, in which the actual flows are usually heterogeneous and three-dimensional. Nevertheless, the test analysis and performance prediction methods are presently based upon simple one-dimensional models. Members of WG 14 first reviewed current practices as employed by research and development teams in various research establishments and industry. The Group also undertook a theoretical analysis of the relations which may be correctly applied to steady flows. Consequently it was possible to discuss and classify known averaging methods. The theoretical study concludes by proposing refinements to known methods and a new approach to averaging for use with engine components and propulsion system analysis.

A large variety of possible averaging techniques were identified. Some were based on theoretical considerations, others were without justification except in their simplicity or common usage. All the averaging procedures were tested and compared by preparing a number of sample calculations in ducted flows, turbojet components and a complete propulsion system.

The Group arrived at several conclusions concerning the merits and the limitations of the methods studied. One method is recommended for stagnation temperature averaging. No single method is recommended for stagnation pressure averaging; the choice must depend on the particular circumstances.

This Advisory Report was prepared at the request of the Propulsion and Energetics Panel of AGARD.

PREFACE

Working Group 14 was established as a consequence of two primary issues in the field of gas turbine engine technology. The first is the trend toward lower aspect ratio, more heavily loaded blading. The second is the increasing need to understand the effects of flow non-uniformities on engine performance and on its stability. The latter statement reflects the growing awareness that non-uniformities tend to reduce the stall margin on high performance engines. This is particularly true for engine-airplane combinations that expect to face wide operating ranges in speed, altitude and attitudes. The objectives and scope of work for Working Group 14 is given below.

Approval Date: March 1978

Starting Date: January 1979

Finishing Date: Spring 1982

Objectives: Numerous investigations have been made into how to average properties across a non-uniform or unsteady flow so as to characterize it for the purpose of one-dimensional performance analysis of gas turbine powerplant.

The Working Group will make firm recommendations where possible as to the best techniques to adopt, and will identify areas in which more research is needed before firm recommendations can be made.

In particular, the Working Group will:

- collect and review existing practice or proposals for averaging non-uniform and/or unsteady flows,
- identify averaging techniques which are in principle correct when seeking to calculate heat, power, thrust and efficiency,
- quantify where applicable the uncertainty levels of different averaging methods,
- recommend methods for adoption (these methods may of course be already standard practice),
- recommend further research activities needed to resolve uncertainties where a significant effect on performance analysis is involved.

Scope of Work: It is planned to limit participation in this Working Group to about 10 members only. This Working Group will need about six meetings. Findings and recommendations will be published preferably as an Advisory Report.

The Working Group was made up of the following people:

Panel Members		*Non-Panel Members*	
E.E.Covert	US	P.Carrière	Fr
D.Dini	It	G.Meauze	Fr
J.Dunham	UK	H-W.Happel	Ge
J.Fabri	Fr	H.Kruse	Ge
Ch.Hirsch	Be	J.L.Livesey	UK
M.Pianko	Fr	S.Wehofer	US
F.Wazelt	Ge		

The following organizations provided the working Group with information relating to their procedures:

Arnold Engineering Development Center, USAF
CEPr – Centre d'Essais des Propulseurs
DFVLR – Deutsche Forschungs-und Versuchsanstalt für Luft-und Raunfahrt
Detroit-Diesel Allison Division, General Motors
General Electric Company, Aircraft Gas Turbine Division
MTU – Motoren-und Turbinen-Union
NASA Lewis Research Center
ONERA – Office National d'Etudes et de Recherches Aérospatiales
Pratt and Whitney Government Products Division
Rocketdyne Division of Rockwell International, Inc.
Teledyne CAE, Inc.
UK National Gas Turbine Establishment

The Advisory Report is the product of these studies, and the contributors are indicated below:

E.E.Covert	Chapter 2
H-W.Happel	Section 3.1
H.Kruse	Section 4.3
J.Livesey	Section 4.1
M.Pianko	Sections 3.2 and 4.4
F.Wazelt	Chapter 1
S.Wehofer	Chapter 2 and Section 4.2

The final editing was accomplished by Professor Wazelt and Mr Pianko, who assumed much of the responsibility during Professor Wazelt's illness.

Every attempt was made by each of us to be as accurate as possible in interpreting the work of others so generously provided for us. Further, we tried to ensure proper literature and report citations. It is likely in fact that we have not caught all the errors of omission or commission. Please, accept our apologies in advance if you were misquoted or not cited. Comments would be welcome. Please send them to:

Panel Executive
Propulsion and Energetics Panel
AGARD
7 rue Ancelle
92200 Neuilly sur Seine
France

Eugene E. Covert, Chairman
Propulsion and Energetics Panel

ACKNOWLEDGEMENTS

1. Dr J. Dunham (UK National Gas Turbine Establishment) has contributed to Sections 4.1, 4.2 and 4.3.

2. Dr H.Kruse (DFVLR, Germany) has contributed to Section 4.2.

3. Acknowledgement for assistance with Section 4.1 to Dr E.M. Laws and Dr D.V.Roscoe (University of Salford, UK).

AR-182 (ENG)

CONTENTS

GENERAL NOMENCLATURE

A	Area
C_d	Nozzle discharge or flow coefficient
C_g	Nozzle thrust coefficient
C_p	Specific heat at constant pressure
C_v	Nozzle velocity coefficient
E_c	Kinetic energy
FAR	Fuel Air Ratio
F_G	Gross thrust
FHV	Fuel Heating Value (or calorific value)
h_s	Static specific enthalpy
h_t	Total specific enthalpy
H_s	Static enthalpy
H_t	Total enthalpy
I	Impulse
$\dot{m}$	Mass flow rate
$\dot{m}_A$	Air mass flow rate
$\dot{m}_F$	Fuel mass flow rate
M	Mach number
P_s	Static pressure
P_t	Total pressure
r	Radius
R	Gas constant
s	Specific entropy
S	Entropy
T_s	Static temperature
T_t	Total temperature
V	Absolute velocity
W	Relative velocity
α	Flow angle of absolute velocity with tangential direction
β	Flow angle of relative velocity with tangential direction
γ	Ratio of specific heats
δ	Boundary layer thickness
Δ	Difference
ϵ	Slope angle
η	Efficiency
θ	Circumferential angle
ρ	Density
ω	Angular velocity

Subscripts

AV	Average
AX	Axial
CAL	Calculated
e	Exit

i	Inlet
LOC	Local
m	In direction of meridian
n	Number of measurements
REF	Reference
s	Static
t	Total
u	Tangential
θ	In circumferential direction
o	Free stream ambient conditions

Superscripts

–	Average or mean values for either radial or circumferential variations
=	Average or mean values for combined radial and circumferential variations
*	Sonic conditions

ENGINE STATION IDENTIFICATION

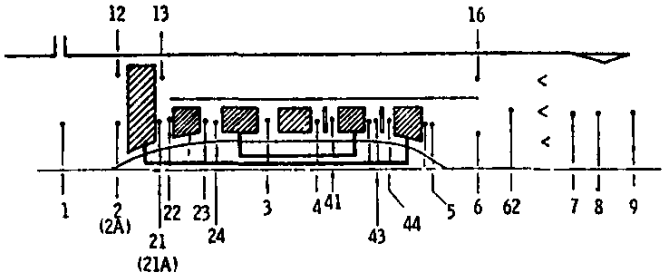

Station Number	*Station Identification*
1	Inlet/engine interface
12	Fan inlet (tip section)
2	Fan inlet (hub section)
2A	Fan inlet (average)
13	Fan discharge (tip section)
21	Fan discharge (hub section)
21A	Fan discharge (average)
22	Intermediate compressor inlet
23	Intermediate compressor discharge
24	High-pressure compressor inlet
3	High-pressure compressor discharge
4	Burner discharge
41	High-pressure turbine nozzle discharge
43	High-pressure turbine discharge
44	Low-pressure turbine nozzle discharge
5	Low-pressure turbine discharge
16	Bypass duct mixer inlet
6	Core engine mixer inlet
62	Augmenter inlet
7	Engine/exhaust nozzle interface
8	Exhaust nozzle throat
9	Exhaust nozzle discharge

Chapter 1

INTRODUCTION

1.1 BACKGROUND

In flight propulsion systems both propulsive power and thrust is generated by adding energy to, and exerting forces and moments on a working fluid which passes through the system. The working fluid may vary in composition as it passes through the system. It is generally a gas composed of atmospheric air and gaseous combustion products. This gas is compressible and its thermodynamic characteristics can be approximated by the thermally ideal state equation.

The complete propulsion system is composed of different components, which are arranged in series and/or in parallel. Each of these components exerts specific actions on the gas as it passes through the components which changes the gas flow and state quantities. The individual component types are selected and arranged in such a way that the flow and state changes at the interface between successive components which together complete an open thermodynamic cycle for the power plant system, thereby assuring continuous system operation.

1.2 PERFORMANCE ANALYSIS

For system and component performance analysis, the specific actions exerted by individual components on the gas flow must be known. These specific component effects are distributed internally within the component flow (e.g. viscous stresses, heat conduction, chemical reactions) and over the component internal surfaces (normal and tangential stresses). The distributed local action can be summarized as the sum of the individual component (component performance) in terms of forces, moments, work, heat and losses due to dissipation. In most applications these quantities cannot be derived from direct measurements. They can, however, be determined indirectly from flow and state changes, which the working gas experiences when it passes through the component. Therefore, the basic information required for experimental determination of component and system performance analysis is the three-dimensional distribution of measured velocity components and state quantities at the component interfaces of the system.

The quantitative relationships between the velocity and state changes from component inlet to outlet face and the sum of component actions (forces, moments, energy changes and dissipation) are derived from the conservation laws of fluid dynamics using a stationary control volume which bounds the component inlet and outlet areas and the component interior solid surfaces. The thermodynamic state changes of the working gas flow, which also enter into these integral relations, are governed by the laws of thermodynamics.

It must be realized that such integral relationships relate the total action within the component to the resultant integrated changes in velocity and state quantities and do not offer detailed information about local effects. Even if complete and precise information about the three-dimensional distribution of all velocity and state quantities is available for both the component inlet and outlet faces, the description of overall component forces, which act on the flow as it passes from inlet to outlet, cannot be separated into the individual contribution by different physical phenomena. Only the combined effect of all forces occurring within the control volume can be determined in this way. Therefore, employing relations derived from control volume averaging always results in loss of detailed information.

1.3 SIMPLIFICATION BY AVERAGING

An averaging technique may be used with design data or with measured data. Design data, obtained by computation, are always consistent. But the experimental determination of the distributed flow and state quantities, which enter into these integral relationships, requires the application of extensive traversing instrumentation at all component interfaces. In propulsion systems, such extensive instrumentation cannot be provided safely and economically. Experimental efforts of this magnitude are usually limited in application to special component test rigs during the research and development phase.

To simplify steady state component and system analysis and to verify the results experimentally, employing only limited fixed instrumentation at the component interfaces, the real, non-uniform, three-dimensional flows with time periodic velocities and state quantities (rotating wakes and turbulence), it would be desirable to represent or approximate the real flow by uniform steady flow models, which transport the same amount of mass, momentum, moment of momentum and energy through the interfaces as the real, non-uniform flow. The velocity and state quantities of the

uniform flow models can be determined by applying suitable time- and position-averaging procedures to the distributed velocity and state quantities of the real flow.

Introduction of representative average velocities, momentum flows and state quantities, allow one to evaluate component and system performance simply. The quantitative results obtained from such simplified performance analysis methods can describe the steady state performance parameters with adequate accuracy. In addition, suitable averaging techniques define locations within the flow field where local velocity and state quantities coincide with the averaged velocity and state properties. Fixed instrumentation therefore should be positioned at these locations in order to obtain truly representative experimental performance data.

Many different averaging procedures of non-uniform internal flows are currently in use. Therefore the question arises, if performance parameters derived by using different averaging methods remain comparable with each other. Simple calculations are used to illustrate this comparison.

1.4 OBJECTIVE AND SCOPE

The objective for the work reported here is to review known averaging methods and to present their differences, to quantify inaccuracies or uncertainties inherently associated with different averaging procedures and to arrive at recommendations for practical applications. In view of the increased capabilities of modern instrumentation and computation equipment, more sophisticated averaging techniques may become practicable and therefore are considered in the present work.

For the present study the scope of work was restricted to consider only the following propulsion systems: Turbojet (with and without reheat); Turboshaft-Engines (without heat exchange or propellers) and Turbofan-Engines (with and without mixing or reheat). Furthermore, the averaging methods considered here are applicable only to steady-state component and system performance analysis.

Certain aspects of the work presented in this report are closely related to instrumentation, its capabilities, accuracies and limitations. Since new capabilities and improvement in the field of instrumentation are occurring at a rapid rate, the present capabilities of data gathering and acquisition systems were not considered to be limiting. Effects of instrumentation aspects are included when one deals with the time-averaging of time periodic data.

1.5 APPROACH

Initially, existing models of component and system performance analysis were reviewed. The information presented in this part of the report was collected through direct contact with the specialists in the respective organizations, and provide perspective as to procedures presently in use.

Next, a theoretical analysis of component and system performance based upon integral relations for stationary finite control volumes with fixed boundaries. The general compressible fluid relations are then specialized for steady (time-averaged) flows. Their representation as uniformly distributed averaged quantities then are derived. In this context, consideration is given to the inherent limitations of performance analysis results derivable from averaged quantities and to those statements, which are in principle correct. On the basis of this work, known averaging methods are discussed, classified and their limitations are defined. This theoretical presentation is concluded by proposing new refinements to known methods and a novel approach to simplified component and system analysis.

The averaging procedures are subsequently tested by completing a selected group of typical sample calculations. Quantitative comparisons of the results are presented and their uncertainty levels are specified.

The work concludes with a summation and critique of the results obtained. Recommendations for acceptable averaging procedures are offered. Finally, those problem areas are identified, where additional efforts are needed to achieve further progress.

Chapter 2

CURRENT FLOWPATH-AVERAGING PRACTICES

SUMMARY

This chapter discusses the flowpath-averaging practices and philosophies used by companies and governmental agencies currently engaged in aircraft turbine engine component and system development. Flowpath-averaging practices vary depending on the engine component, the User's design philosophies, the User's test facilities and equipment, accuracy requirements, and available resources. In general, most of the current turbine engine flow-averaging practices involve some form of area or mass flow weighting. In engine systems where there are severe internal space limitations and instrument installation restrictions, energy and work balances based on measured airflow, thrust/torque, and fuel flow are used to define single values of component interface flow properties. An area of flowpath averaging which is receiving increased attention is the error evaluation process. An error evaluation is required of the measurement systems and flow averaging procedures to insure that test results are meeting engine component and system performance specification requirements.

DEFINITION OF FLOWPATH-AVERAGING METHODS

Area Average

Parameter integral with respect to flow area divided by total flow area.

Area-weighted average pressure:

$$\bar{P}_t = \frac{\int P_t dA}{A} .$$

Area-weighted average temperature:

$$\bar{T}_t = \frac{\int T_t dA}{A} .$$

Mass Average

Parameter integral with respect to mass flow divided by total mass flow rate.

Mass flow-weighted average pressure:

$$\bar{P}_t = \frac{\int P_t \rho V_{AX} dA}{\dot{m}} .$$

Mass flow-weighted average enthalpy:

$$h_t = \frac{\int h_t \rho V_{AX} dA}{\dot{m}} .$$

Mass flow-weighted average entropy:

$$\bar{s} = \frac{\int s \rho V_{AX} dA}{\dot{m}} .$$

With the definition of any two of the mass flow-weighted parameters listed above, the third parameter can be obtained from a Mollier diagram.

Mass flow-weighted average velocity:

$$\bar{V} = \frac{\int V \rho V_{AX}\, dA}{\dot{m}} .$$

Two-Dimensional Mass Average

Parameter circumferential and radial integral with respect to mass flow divided by total mass flow rate.

Two-dimensional mass flow-weighted average pressure:

$$\bar{\bar{P}}_t = \frac{\iint P_t (\rho V_{AX}) r\, d\theta\, dr}{\iint (\rho V_{AX}) r\, d\theta\, dr} .$$

Two-dimensional mass flow-weighted average isentropic enthalpy equivalent of a total pressure change:

$$\bar{\bar{P}}_{t_e} = \bar{P}_{t_i} \left[\frac{\int [(\bar{P}_t / \bar{P}_{t_i})^{\gamma - 1/\gamma} - 1] \bar{\rho}\, \bar{V}_{AX}\, r dr}{\int \bar{\rho} V_{AX}\, r dr} + 1 \right]^{\gamma/\gamma - 1}$$

where the single bar parameters are circumferential mass averaged values.

Two-dimensional mass flow-weighted average temperature is:

$$\bar{\bar{T}}_t = \frac{\iint T_t (\rho V_{AX}) r\, d\theta\, dr}{\iint (\rho V_{AX}) r\, d\theta\, dr} .$$

Numeric Average

Parameter arithmetic sum divided by the number of measurements:

Numeric averaged pressure:

$$\bar{P}_t = \frac{\Sigma P_t + \cdots P_{t_\eta}}{\eta} .$$

Numeric averaged temperature:

$$\bar{T}_t = \frac{\Sigma T_t + \cdots T_{t_\eta}}{\eta} .$$

DZUNG Average

The mean or average values are consistent with the following equations, which represent the conservation laws with a rotating frame (ω = constant):

Continuity:

$$\bar{\rho} \bar{W}_m = \frac{\int \rho W_m\, dA}{A} .$$

Momentum (in direction of meridian):

$$\bar{\rho} \bar{W}_m^2 + \bar{P}_s = \frac{\int (\rho W_m^2 + P_s)\, dA}{A} .$$

Moment of Momentum:

$$r(\omega \bar{r} + \bar{W}_\theta) \bar{\rho} \bar{\bar{W}}_m = \frac{\int r(\omega r + W_\theta) \rho W_m\, dA}{A} ,$$

Energy:

$$\left(\bar{h}_s + \frac{\bar{W}^2}{2} - \frac{(\omega \bar{r})^2}{2} \right) \bar{\rho} \bar{W}_m = \frac{\int \left(h_s + \frac{W^2}{2} - \frac{(\omega r)^2}{2} \right) \rho W_m\, dA}{A} .$$

Equation of State:

$$\bar{h}_s = (\gamma/\gamma - 1)(\bar{P}_s/\bar{\rho})$$

and $\bar{r}$ is given by

$$\bar{r}^2 \equiv \frac{\int r^2 \rho W_m \, dA}{\int \rho W_m \, dA} .$$

Hence, there are six equations with six unknown variables: P_s, $\bar{p}$, h_s, W_m, W_θ, and $\bar{r}$. For the case of an absolute frame ($\omega = 0$), the relative velocity, W, is replaced by absolute velocity, V.

2.1 INTRODUCTION

The aerospace turbine engine community presently has no recognized standards or guidelines concerning averaging of flowpath gas properties with the exception of engine face distortion indices. The problem is that each engine manufacturer has different restrictions and requirements for selecting an averaging method. Restrictions are generally imposed by available resources and test facilities. Requirements are dictated by the program goals and the type engine component being evaluated. Factors usually considered when selecting a method of flowpath averaging are:

Compatibility with the design analyses.

Fundamental consistency with the particular component performance parameter being evaluated such as thrust, torque or efficiency.

Required instrument measurement systems including consideration of instrument type, measurement range, quantity, and required accuracies.

Conformity with existing informational data banks.

Available resources and test facilities.

The purpose of this chapter is to discuss the flowpath-averaging practices and philosophies used by the companies and governmental agencies engaged in aircraft turbine engine development. Since instrumentation plays an important role in the averaging selection process and the component performance evaluation process, developmental engine component and system flowpath measurement practices are also discussed. The material is presented in four parts: flowpath measurement and averaging practices for (1) turbomachinery, (2) combustors, and (3) turbine engine systems, as well as (4) a discussion of flowpath-averaging error evaluation practices. The flowpath-averaging practices used at the major government turbine engine component and system test centers are presented in tabular form. The practices presented in this chapter apply to steady-state flows and not necessarily to dynamic, or time-variant, flows. Fan and compressor inlet flow-averaging practices are discussed, but turbine engine inlet flow distortion methodology is not discussed, as it is already being addressed by other committees (e.g., Ref.2.1).

The test centers which contributed to this effort are as follows:

Arnold Engineering Development Center (AEDC)
Centre d'Essais des Propulseurs (CEPr)
Deutche Forschungs-und Versuchsanstalt fur Luft-und Raumfahrt (DFVLR)
National Aeronautics and Space Administration – Lewis Research Center (NASA-Lewis)
National Gas Turbine Establishment (NGTE)

The manufacturers which contributed to this effort are as follows:

Detroit Diesel Allison
General Electric Aircraft Engine Group
Motoren-und Turbinen-Union
Pratt and Whitney Aircraft
Rocketdyne
Teledyne CAE

2.2 TURBOMACHINERY (COMPRESSORS/TURBINES)

Design Practices

The type of flowpath-averaging used for the design phase is dictated by the type of analyses used for the design phase. For turbomachinery, the design effort includes evaluation of the radial flow distributions within the proposed blade passages, evaluation of the component thermodynamic cycle efficiencies, and evaluation of meanline component design and aerodynamic losses. The analysis procedures used in turbomachinery design vary from the solution of simple radial equilibrium equations to determine flow distributions within blade passages, to complex three-dimensional flow equations using the complete radial equilibrium momentum equation, energy equation, and continuity conditions (Refs 2.2 2.4). The basic analytical tools for most turbomachinery designs are streamline curvature methods and matrix inversion schemes that account for both streamline curvature and radial gradients in entropy and enthalpy. Torque, power, and the work per unit mass of fluid (total head) are determined using Euler's rotating machinery power relations

(Ref.2.5). For streamline curvature methods and matrix inversion schemes, component inlet and exit flow properties are generally specified at equal radial increments or at stations that correspond to the entrance and exit of each airfoil row for the stator vanes and rotor blades. The equations define flow properties along streamlines or stream tubes (i.e., lines or surfaces of constant mass flow) so that flowpath averaging of the analytical results is equivalent to one- and two-dimensional mass averaging procedures. The numerical mass-averaged properties from the streamline analyses are also used to evaluate the component power relations. In general, flowpath parameters in the design phase tend to be a form of mass averaging including one- and two-dimensional mass averaging of pressures and temperatures, with radial and circumferential mass averaging of momentum, and energy terms.

Test Practices

The objective of the component test phase is to fix the basic hardware configuration and establish actual performance and reliability. Component performance is generally evaluated by substituting the test data into the design model. Flowpath areas and losses in the design model are adjusted so that the numerical results correspond to the measured data. By using the airfoil geometry along with the measured overall interstage temperature and pressure profiles and by assuming casing blockage distribution and stator loss correlations, one can formulate a computational model of the turbomachinery from which the blade element performance can be obtained. Generally, computational models require the addition of flow correlation coefficients or other such terms to the equation which are in some ways related to flowpath averaging. Presently, there is no general consensus as to what specific form of flowpath averaging is to be used for correlation of test data. The selection of a flowpath property-averaging method for the component test phase should be consistent with requirements of the general design model (i.e., some form of mass averaging) and both consistent and representative of the component fundamental performance parameters such as torque and efficiency. Current flowpath-averaging methods, however, are not always this sound, principally because of experimental considerations. In practice, the selection of an experimental flowpath-averaging method is highly dependent on the available measurement systems. The limiting factors include measurement capability, probe flow-field interference, instrument accessibility, required measurement accuracies, and resource requirements. To clarify these limits, a discussion of current experimental flowpath-averaging practices must be prefaced with some discussion of turbomachinery measurement practices.

Test Rig Measurements -- For performance testing of isolated turbomachinery components, mass flow, torque, and component inlet/exit flow properties, are measured. Flow rates are measured with calibrated bellmouths, or, if sufficient pressure is available, with critical flow venturis (Ref.2.6) or calibrated orifices (Ref.2.7). All airflow rates are corrected to dry air rates. Uncalibrated orifices are used for secondary flows such as compressor interstage bleeds and turbine secondary cooling flows. Flowpath-averaging methods are not used for primary measuring systems; instead, flow conditioning equipment is used to achieve one-dimensional bulk flow. Flow coefficients are used to account for boundary-layer and flow curvature effects. For inlet flow distortion testing, a numerical summation of flows per unit area is made (Ref.2.8). The analyses described in References 2.9 and 2.10 are used at AEDC to evaluate flow rates when symmetrical or planar flow distortions are present.

Turbomachinery component inlet stagnation pressures and temperatures are generally measured with fixed rakes spaced in circumferential quadrants. The number of measurements made at the inlet station is configuration dependent and can vary from 20 to 100 combined pressure and temperature measurements. As an example to illustrate the number and location of probes at the engine inlet face the Society of Automotive Engineers (US) suggests in its Aerospace Recommended Practice (ARP 1420 of March 1978) eight equiangual space rakes with five probes per rake location at the centers of the equal areas. An exception to this practice is turbine testing behind a combustor. For this case, turbine inlet temperature spatial variations and levels usually make the use of probes impractical so that average inlet flow values are determined from a turbine work balance. Wall static pressure taps are generally located in the inlet circumferential plane at increments from 15 to 90 degrees. Flow-field static pressures are not measured in most circumstances.

For each stage, instrumentation for interstage performance may consist of two to four temperature and pressure rakes with each rake having anywhere from three to six probes. If possible, static pressure taps are located on the case and inner wall between the airfoil rows.

Component exit stagnation pressures and temperatures are normally measured with a circumferential traversing rake system so that a detailed survey, which generally includes 200 to 500 individual measurements of the exit flow stagnation conditions, is possible. Wall static pressure taps are located in a manner similar to the component inlet plane. For turbine component testing, flow angle probes are generally incorporated into the pressure- and temperature-traversing rake system.

Flowpath Averaging – On the basis that the test data be consistent with the design analyses, the flowpath averaging for the component test data would basically incorporate mass-averaging procedures; however, the component test data are not readily amenable to mass averaging procedures. For instance, direct mass flow averaging requires rake probes to be located at centroids of equal mass flow, momentum, or energy. However, since the required probe positions are not known prior to the evaluation of the test results, the general practice is to locate probes on centroids of equal cross-sectional area. Using this criterion, the probes can be accurately positioned prior to the test. The equal area position is independent of test settings, and for low flow distortion levels, equal area positions are more closely aligned to streamlines than other positioning criteria such as equal radial increments. To mass average test data, a local static flow

property (usually static pressure) is required. For low subsonic Mach numbers, the general practice is to assume that the radial static pressure is constant and equal to the circumferential numeric average of the wall static pressure measurements; alternately, a static pressure profile based on experimental or analytical results may be assumed. The mass-averaging procedure increases the measurement uncertainty level of the averaged flow properties compared to using simple area-averaged flow properties. The task is to determine whether the less accurate mass flow-averaged properties are preferable to area-averaged values. It is not uncommon to find combinations of both area- and mass-averaging-type procedures being used to reduce component test data. For instance, some of the practices used for flowpath-averaging turbomachinery inlet and exit temperature and pressure measurements are:

Area or mass average the measured values.

Area average the circumferential values and mass average the resultant radial profile.

Two-dimensional mass average the measured values.

Use the measured mass flow, the circumferential numeric average of the wall static pressure, an effective flow area, and area-averaged temperature to calculate stagnation pressure.

Effective exit flow swirl angles are defined using either area- or mass-averaging practices (Ref.2.11). Another common practice for compressor testing is to mass average the isentropic enthalpy equivalent of the total pressure change (see definitions) across the compressor to arrive at an average exit total pressure. For turbine testing behind a combustor, turbine work is generally determined from a measurement of shaft work as opposed to measurement of flow-stream enthalpy drop, and turbine inlet gas temperature is determined from a measurement of turbine torque.

Some of the general flowpath-averaging practices used at the various governmental test centers for compressor and turbine testing are presented in Tables 2.I and 2.II, respectively. References 2.12 - 2.28 provide a more detailed description of some of the experimental facilities and practices used for turbomachinery component testing.

2.3 COMBUSTOR

Design Practices

A mathematical model of a combustor requires formulation of equations which describe the complex aerothermodynamic and chemical interactive processes that occur in the combustor. A number of combustor analytical models have been and are presently being developed (Refs 2.29 and 2.30) and are providing some perceptive insight into combustor designing. The models vary from simple analyses which treat the combustor as a perfectly stirred reactor to complex three-dimensional analyses that include finite-rate chemistry. The existing analytical models, however, do not account for all the interactive phenomena; they implicitly assume steady-flow and in this way are at variance with actual combustors. Therefore, the basic design tools for combustor development are still based on empirical-type models. Combustor empirical models are usually formulations of influence coefficients for the interrelationships of the various combustor variables. The empirical correlations normally assume single value initial conditions for approach temperature and pressure, and then calculate values for overall performance parameters (i.e., parameters such as combustor efficiency and burner pressure loss). As a result, flowpath averaging is not a major consideration for most combustor prehardware analytical design practices.

Test Practices

Results of combustor development tests are used to evaluate performance factors such as temperature profile patterns, combustion efficiency, and burner pressure loss that require spatial averaging of measured flow properties. Just as for turbomachinery components, the selection of an experimental flowpath-averaging method is dependent on the available measurement systems. For combustors, the measurement problem is particularly difficult because of the chemical reactions and the hostile temperature environment.

Test Rig Measurements The various parts of the combustor are identified in Figure 2.1. The basic combustor test measurements are mass flow, pressure, temperature, and gas composition. The airflow measurement systems are the same as used for turbomachinery component testing. For combustor testing behind a compressor, the airflow rates are determined from compressor airflow minus leakage and turbine cooling flow. Fuel flows are measured with calibrated turbine-type flowmeters.

At the combustor diffuser inlet, the measured quantities are total pressure, total temperature, and wall static pressure. Combustor inlet pressure and temperatures are measured with fixed rakes spaced on equal circumferential increments with the probes located on equal increments of the inlet cross-sectional flow area. Wall static pressure taps are installed on the outer and inner diameters of the diffuser case and generally located in the plane simulating the trailing edge of the compressor exit guide vanes. The number of measurements is dependent on the combustor size and design and can vary from 10 to 60 individual temperature and pressure measurements each and from 4 to 20 wall statics. For combustor testing behind a turbine engine compressor, combustor inlet flow conditions are inferred from the compressor exit measurements.

Wall static pressure taps are located at various axial locations in the diffuser and combustor shrouds and are used to evaluate burner pressure losses. Generally from 1 to 4 static pressure taps are placed at each axial location. Total pressure rakes placed in the combustor shroud are used to evaluate flow splits and liner Mach numbers.

At the combustor exit, total temperature and pressure are measured with either a circumferential traversing or a fixed-rake system. The pressure rake probe heads are water cooled. The sampling and temperature probes are made of platinum to withstand the combustor exhaust temperatures. Aspirated temperature probes are generally used, and in most cases also serve as gas-sampling probes. Individual rake probes are radially spaced so that each probe samples an equal increment of cross-sectional flow area. Typically, for fixed rakes, a total of 20 to 40 stagnation pressures and 40 to 80 stagnation temperatures are measured. For traversing rake systems, as many as 300 to 600 individual measurements can be recorded. Static pressure at the combustor exit is measured with wall static pressure taps located on both the outer and inner annulus wall, and a total of anywhere from 4 to 20 taps used.

Flowpath Averaging – Combustor flowpath-averaging practices vary for different design concepts and among the various developers and test centers. The current practices, however, for the most part, consist of either area-weighting or mass flow-weighting procedures. As discussed in the turbomachinery component subsection, area weighting is straightforward since it generally requires only numeric averaging of the probe data, whereas mass averaging requires assessment of the local flow Mach numbers. Combustor flowpath-averaging procedures for the evaluation of combustor efficiency, burner pressure loss, temperature pattern factors, and flow Mach numbers are discussed below.

Combustor efficiency is determined by dividing the measured enthalpy rise across the combustor by the theoretical enthalpy rise. In practice, the average combustor inlet temperature may be determined using either mass flow-weighted or area-weighted flowpath-averaging procedures. The average exit temperature is generally determined using mass flow-weighted procedures, or if numerous measurements are made, the numeric average of the exit temperatures is used. An average exhaust gas temperature can also be determined from an evaluation of the gaseous emission products by using combustor theoretical frozen and equilibrium chemical analyses (Ref.2.31). A widely accepted technique for computing combustor efficiency directly is to determine the amount of unrecovered heat of combustion related to the measured unburned hydrocarbons (HC) and carbon monoxide (CO). If this technique is used, aspirated temperature probes are commonly used to channel the gas samples into a manifold that provides an average reading for CO and HC. This technique is usually used for combustor systems where the quantity of equilibrium CO is small.

Combustor or burner pressure loss is defined as the loss in average total pressure between the diffuser inlet and combustor exit expressed as a percentage of the diffuser inlet average total pressure. The diffuser inlet and combustor exit total pressures are determined using either area- or mass flow-weighting procedures. On occasion, the combustor total pressure is evaluated using the numeric average of the combustion chamber wall static pressure measurements and an estimate of the chamber Mach number. The diffuser inlet Mach number used to correlate the burner pressure loss is determined from the numeric average of the inlet wall static pressure measurement, measured airflow, and either a mass flow-weighted or area-weighted inlet total temperature.

To describe the quality of the combustor outlet temperature profile, the stator, rotor, and pattern temperature distribution factors are evaluated. The stator factor is the largest temperature difference between the highest local radial temperature and either the design or the average radial temperature normalized by the average temperature rise across the combustor. The rotor factor is the same ratio but is for the largest temperature difference in the circumferential direction. The pattern factor is the difference between the highest local combustor exit temperature and the average combustor exit temperature divided by the combustor temperature rise. Nonweighted temperatures are used for the evaluation of the temperature distribution parameters, and the average temperature required for these evaluations is the simple numeric average of the measurements. However, since the temperature probes are placed on increments of equal area, the numeric averaged temperature corresponds to an area-weighted value.

These verbal descriptions may be written algebraically as

Stator Factor

Maximum of

$$\frac{T_t(r)_{MAX} - T_{t\,DESIGN}}{\overline{\Delta T}_{t\,COMBUSTOR}} \quad \text{or} \quad \frac{T_t(r)_{MAX} - \overline{T}_t(r)}{\overline{\Delta T}_{t\,COMBUSTOR}}$$

Rotor Factor

Maximum of

$$\frac{T_t(\theta)_{MAX} - T_{t\,DESIGN}}{\overline{\Delta T}_{COMBUSTOR}} \quad \text{or} \quad \frac{T_t(\theta)_{MAX} - \overline{T}_t(r)}{\Delta T_{COMBUSTOR}}$$

Combustor Pattern Factor

$$\frac{[T_t(r,\theta) - \bar{T}_t(r,\theta)]_{\text{COMBUSTOR EXIT}}}{\bar{\Delta T}_{t\,\text{COMBUSTOR}}} .$$

The general combustor flowpath-averaging practices used at the various governmental test centers are presented in Table 2.III. References 2.31 -2.36 give a more detailed description of some of the experimental facilities and practices used for combustor component testing.

2.4 TURBINE ENGINE SYSTEMS

Design Practices

The design and development of a turbine engine system requires the use of analyses which can relate changes in component configuration to changes in both steady-state and transient operating conditions. In actual practice, data generated from component analyses and previous engine experimental results are stored in high-speed computers in the form of tables and coefficients and are used to predict engine performance. The type of information stored is aerothermodynamic properties of air and products of combustion, aerothermodynamic performance of the various engine components as a function of the controlling independent variables including the effects of Reynolds number and flow distortion, power losses by auxiliary units and bleed flows, and data that relate geometric changes to engine performance. The data used to generate the performance program tables and coefficients are flow averaged in accordance with the users' particular component flow-averaging test practices.

Test Practices

Methods of acquiring and averaging flow data in engine system tests are considerably different from those used for cascade and component rig testing. Space limitations and installation problems frequently prevent the use of extensive instrumentation; therefore, many of the measurements made for component testing such as combustor gas composition, flow angularity surveys, and torque are not practical for most engine system tests. As a result, energy and work balances are used extensively to define component interface average flow properties. Another practice is to use component test rig data and scale model data to enhance limited engine system component flowpath data. The advantage, however, of engine system testing is duplication of the component actual operating environment, and this is difficult to simulate in component and scale model tests. There have been several studies on the importance of simulating the correct flow distortion patterns for component performance evaluation. For example, Reference 2.36 discusses the effect of inlet distortion patterns on axial compressors, and Reference 2.37 points out some of the adjustments required to use scale model uniform, cold-flow nozzle data to evaluate full-scale nonuniform, hot-flow nozzle performance. Isolated component and scale model test factors applied to engine system data must be carefully analyzed and evaluated.

Test Cell Measurements – Engine system performance tests require the measurement of engine airflow, fuel flow, and thrust. Engine airflow rates are measured using the standard or calibrated airflow metering devices described in the turbomachinery test section. Metering systems, flow distortion, and averaging requirements for engine transient airflow measurement are discussed in Reference 2.38. For turbofan engines, high-pressure compressor mass flow rates are calculated using: (1) core engine averaged inlet flow properties and a calibration flow coefficient, or (2) a high-pressure compressor and turbine work balance, or (3) a known value of high-pressure turbine inlet mass flow function. Interstage mass flows are determined using flow coefficients or bleed pipe flow-metering orifices. Engine fuel flows are calculated using calibrated turbine flowmeter data, and thrust is calculated using calibrated load cell data and redundant analytical force balance procedures. Analytical force balance procedures which take into consideration flow nonuniformities are described in References 2.39 and 2.40.

Typical engine test instrumentation for a low bypass mixed flow and a high bypass dual stream turbofan are shown in Figures 2.2 and 2.3, respectively. Temperature and pressure rakes are generally included in developmental engine tests at the stations indicated. The general practice is to locate instrument probes on centers of equal stream areas. There are exceptions to this placement, such as using centers of "estimated equal mass flow", but this arrangment is individually justified and does not often occur in practice. On occasion, instrument measuring systems such as flow angle measuring devices, interstage instruments, and optical measuring devices are used for development engine testing; however, these systems are considered nonstandard or special requirements. For a typical transient test, 20 to 40 percent of the engine pressure instrumentation consists of close-coupled systems with a frequency response of 1 to 100 Hz. For dynamic testing such as engine stall margin evaluations, 50 to 80 percent of the pressure instrumentation are high-frequency response systems with a frequency response of 100 to 1,000 Hz.

Flowpath Averaging – Pressures and temperatures used to compute engine gas generator performance parameters are usually area averaged, although, mass flow-averaged schemes are sometimes used. In all instances, individual measurements are corrected for effects such as recovery factors, flow misalignment, and stem and radiation corrections prior to averaging or use in computation. Calculation of engine performance parameters requires in addition to averaged pressures and temperatures, flow thermodynamic properties (e.g., Ref.2.41) and calibration factors such as flow coefficients, burner efficiency, and turbine mass flow function. The fluid average enthalpy and entropy are determined as functions of the

fluid average pressure, temperature, and fuel/air ratio. The specific practices used for each engine component are described in the following paragraphs.

Fan flow is reduced to a dry air state, and inlet total pressures and temperatures are area averaged. Fan inlet Mach number is calculated using an area-averaged total pressure and temperature and the numeric average of the wall static pressures. The fan discharge pressure and temperature is completely area averaged or combined with mass averaging. For instance, fan tip and hub exit bulk properties are determined using area-averaging procedures. However, fan exit bulk pressure is determined by mass flow-averaging the tip and hub area-averaged measurements, and fan exit bulk temperature is determined by an energy balance of the tip and hub area-averaged measurements. Fan efficiencies are evaluated using enthalpies derived using an area-averaged total pressure and temperature and calculated gas properties.

Compressor average inlet total pressure and temperature are inferred from the fan exit, or, if inlet rakes are present, area averaged. Compressor inlet mass flow, as previously discussed, is calculated in one of the three ways; usually, however, the mass flow is determined from a known value for the high-pressure turbine inlet mass flow function. Compressor exit total pressures are area averaged and the exit total temperature is either area or numerically averaged. Inlet and exit Mach numbers and efficiencies are calculated in the same manner as the corresponding fan terms.

The combustor (burner) inlet measurements are generally obtained from the compressor exit measurements. Combustor discharge total pressure is the numeric average of the burner wall static pressure measurements while burner discharge temperature is calculated by one of two methods. The first temperature method uses an assumed value for the burner efficiency and an energy balance across the combustor. The second method uses measured high-pressure turbine discharge conditions and a high-pressure compressor and turbine work balance. The latter includes an assessment of the average rate of energy input by the compressor into the airstream, the available and unavailable turbine cooling flow energy, high-pressure turbine combustor power extraction, and the high-pressure spool power loss from inefficiencies such as friction.

Turbine inlet conditions are obtained either from measured turbine discharge conditions and a compressor-turbine work balance, or from burner discharge conditions with the subsequent addition of the effect of turbine cooling flow available for turbine work. The turbine exit total pressures are area averaged and the exit total temperatures either area or numerically averaged. On occasion, probe measurements at the exit are numerically averaged on circumferential rings and the ring averages area weighted. This procedure is used when radial flow variations are considered to be much more severe than the circumferential variations. Turbine Mach numbers are calculated in the same manner as those of the fan and compressor. Turbine efficiency is calculated using area-averaged pressure and temperature, and calculated gas properties.

For the case of an augmented, twin-spool turbofan engine having a single exhaust nozzle, the bypass mass flow and the core engine mass flow are combined prior to afterburning. This region of the engine is referred to as the afterburner inlet diffuser. In the diffuser, the bypass and core flow bulk properties are determined using area-averaging procedures. The diffuser exit bulk pressure is determined by mass flow averaging the bypass and core area-averaged measurements, and the exit bulk temperature is determined by an energy balance of the bypass and core area-averaged measurements.

The afterburner inlet flow properties are determined from either the turbine exit properties, afterburner inlet diffuser properties, or, if measured, using area-averaging methods. The exit pressure, if measured, is area averaged. For the case with afterburning, the average exit pressure is estimated using the pressure drop characteristics of the afterburner or from the exit wall static pressures and a mass flow calibration. The average afterburner exhaust total temperature is calculated from an assumed burner efficiency or from measured exhaust nozzle thrust, nozzle thrust coefficient, and mass flow. The exhaust nozzle inlet flow properties are determined from the afterburner exit flow property evaluation. The nozzle exit pressure corresponds to the measured ambient pressure.

General engine flowpath-averaging practices used at the various governmental test centers are presented in Table 2.IV. References 2.42 -2.46 give a more detailed description of some of the experimental facilities and practices used for turbine engine testing.

2.5 ERROR EVALUATION

The error evaluation process for flowpath averaging consists of assessing both the flowpath measurement and averaging error and propagation of this error into an engine component or system performance error. Such estimates are necessary to verify that the experimental results will be meaningful to the overall program performance requirements. In practice, two types of errors are generally considered -- measurement uncertainty and sampling error. Measurement uncertainty is defined (Ref.2.47) as the maximum error which might reasonably be expected and is a measure of the closeness of the measurement to the true value. Uncertainty assessment consists of an audit of the random (precision) and fixed (bias) errors from the measurement, calibration, data acquisition, and data reduction processes and probe/tap fixed errors from aerodynamic and thermal effects that contribute to the final uncertainty of the measured value. The assessed measurement errors are quantified as a difference between the measured value and a true value defined by a standard; therefore, all measurement apparatus and measurement practices must be traceable to a recognized standard.

Sampling error is defined as that error in an averaged property which is the result of limited spatial measurements in a distorted flow field. There are both steady-state and time-variant sampling errors.

Comparative accuracies of different flow-averaging methods are not reported in the literature, possibly because either such specialized studies have not been documented, or the results are too user-dependent meaning that the accuracies are only applicable to the user's equipment, test practices, and installation. General measurement accuracies and practices used to evaluate and propagate flow-averaging measurement and sampling errors, however, are available and are presented in the remaining portion of this chapter.

Measurement Uncertainty

Methodology (Ref.2.47) - Measurement uncertainty evaluation is a complex process which requires a knowledge of both measurement engineering and statistics. Several treatises on measurement error are contained in the literature (Refs 2.48 -2.60). In the United States, the Abernethy-Thompson uncertainty evaluation method (NBS) is rapidly becoming an accepted standard evaluation practice for US Turbine Engine Industry and Test Centers. The method is relatively simple, yet perceptive. The methodology is described in the following documents:

JANNAF "ICRPG Handbook for Estimating the Uncertainty in Measurements Made with Liquid Propellant Rocket Engine Systems". CPIA Publication 180, AD 851127, and

USAF AEDC-TR-73-5, "Handbook Uncertainty in Gas Turbine Measurements". AD 755356 (Ref.2.47).

The Abernethy-Thompson method defines the maximum error (U) that can reasonably be expected for a single measurement as follows:

$$\pm U = \pm(B + t_{95} S)$$

where B is the upper limit of the bias error from the true value, S is the precision index, which is an estimate of the true standard deviation of repeated values of the measurement, and t_{95} is the Student-t statistical parameter at the 95-percent confidence level. The t_{95} value is a function of the number of degrees of freedom used in calculating the precision index. (The degrees of freedom are calculated using the Welch-Satterthwaite formula, Reference 2.47.) It is a function of the degrees of freedom and magnitude of each elemental precision index. Flowpath-averaged parameters, however, are not single measurements but are determined as a function of several individual measurements. To assess the measurement uncertainty of flowpath parameters, it is necessary to propagate individual measurement uncertainties through a function that relates the flowpath parameter and the individual measurements. Abernethy and Thompson (Ref.2.47) approximate the error propagation with a first-order Taylor's series method. For a three-variable function

$$Z = f(X, Y, W)$$

and expanding the right-hand side with a first-order series expansion for ΔZ gives

$$\frac{\Delta Z}{Z} = f\left(\frac{X}{Z}\frac{\partial Z}{\partial X}\frac{\Delta X}{X} + \frac{Y}{Z}\frac{\partial Z}{\partial Y}\frac{\Delta Y}{Y} + \frac{W}{Z}\frac{\partial Z}{\partial W}\frac{\Delta W}{W}\right) .$$

The term $\Delta Z/Z$ expresses the error propagation to Z from errors represented by $\Delta X/X$, $\Delta Y/Y$, and $\Delta W/W$. The terms $X\partial Z/Z\partial X$, $Y\partial Z/Z\partial Y$, and $W\partial Z/Z\partial W$ are defined as the influence coefficients (I_X, etc.) of x, y, w on z. The final measurement uncertainty for the function z is then:

$$\pm U_Z = \pm(B_Z + t_{95} S_Z)$$

where

$$B_Z = [I_X^2 B_X^2 + I_Y^2 B_Y^2 + I_W^2 B_W^2]^{1/2}$$

(B_Z, B_X, B_Y, and B_W are the bias errors for the Z, X, Y, and W component terms, respectively) and where

$$S_Z = [I_X^2 S_X^2 + I_Y^2 S_Y^2 + I_W^2 S_W^2]^{1/2}$$

(S_Z, S_X, S_Y, and S_W are the precision errors for the Z, X, Y, and W component terms, respectively).

Application – The expression for flowpath area-averaged pressure is used as a simple example for the application of the measurement uncertainty methodology to flowpath-averaged parameters. For multiple measurements of the *same* pressure, the area-averaged pressure is given by

$$\bar{P}_t = \frac{\int P_t dA}{\int dA} \sim \frac{\Sigma P_{t_1} \Delta A_1 + \cdots P_{t_n} \Delta A_n}{A} .$$

For the case of equal increments of ΔA,

$$P_t \sim \frac{\Delta A}{A} \Sigma(P_{t_1} + \cdots P_{t_n}) = \frac{1}{n} \Sigma(P_{t_1} + \cdots P_{t_n}) .$$

Using the error propagation method, the pressure area averaged precision error, S_p, is

$$S_p = \left[\left(\frac{1}{n}\right)^2 (S_p)^2 * n\right]^{1/2} = \sqrt{\frac{1}{n}} (S_p)$$

where S_p is the precision error for the individual measurements. The pressure area averaged bias error is equal to the bias error (B_p) of the individual measurements because the average of numerous measurements having the same bias does not reduce the bias error of the averaged value. The measurement uncertainty for the area-averaged pressure (for equal increments of area) is given by

$$\pm U_p = \pm \left[B_p + \sqrt{\frac{1}{n}} (t_{95} S_p) \right] .$$

Similarly, the measurement uncertainty for a mass flow-averaged pressure or for any calculated parameter can be defined providing the bias and precision error of the elements are estimated and that the influence coefficient matrix for the dependent elements is evaluated. The influence coefficient matrix can be developed by using the differential equations which interrelate the various dependent and independent variables; or by using the engine data reduction program and perturbating each independent variable, in turn, by 1 percent about the measured value to determine the percentage change in each dependent parameter.

Gas turbine influence matrices are also a major diagnostic tool used by engine manufacturers and test centers to estimate the sensitivity of various parameters on component and system performance (Refs 2.39 and 2.61). Table 2.V is an example from Reference 2.62 of an influence coefficient matrix for sea-level operation of a gas turbine engine having a compressor pressure ratio of 10.0 and a turbine inlet temperature of 2160°R. The boxes within each column contain parameters immediately obtainable from knowledge of the compressor pressure ratio and turbine inlet temperature and quantify how each parameter varies with the independent variable. Therefore, the first column shows the sensitivity of an error in turbine inlet temperature for all other conditions held constant to the various engine parameters, the second column the sensitivity of compressor rotor speed, and so forth. Nominal measurement uncertainties for some of the measurement systems used to derive component and system flow-averaged performance parameters are presented in Table 2.VI. The measurement uncertainty levels are based on using the Abernethy-Thompson model with all measurements traceable to the National Bureau of Standards. The type of information in Tables 2.V and 2.VI is used to make both pretest and posttest performance measurement uncertainty evaluations and to determine whether proposed flow measurement systems and averaging procedures are adequate to establish performance limits.

Sampling Error

Flow-averaging sampling error is related to the measured property distortion pattern and the number of flow measurements for a given spatial area. Due to the ability to make detailed measurement surveys, sampling error generally is minimal for isolated component testing; however, because of measurement space limitations, it is an important consideration in most engine system experiments. The practices for estimating probe sampling error are not as exacting as those of measurement uncertainty and are best discussed by example. Figure 2.4 shows a representative inlet distortion pattern for a low bypass turbofan high-pressure compressor operating at a cruise power setting. The max-min distortion levels for both pressure and temperature are 4 percent; wall boundary layers are not included in the flow distortion patterns. A reference flow average value for pressure and temperature is determined by area integration of the distortion patterns, and Figure 2.5 shows the local percent deviation from this reference value as a function of circumferential position. The derivation of Figure 2.5 is based on using a single five-probe rake with elements on equal area and illustrates that for this case, the maximum sampling error possible is nominally ±1 percent for temperature and ±0.6 percent for pressure. The sampling errors can be propagated through an influence coefficient matrix to estimate the effect of sampling error on component and engine performance. For example, using the engine operating conditions corresponding to Table 2.V, a 1-percent bias error in compressor inlet temperature corresponds to a 2.16-percent error in engine net thrust and a 0.16-percent error in specific fuel consumption. Figure 2.5 also illustrates the percentage difference, for this case, in area-weighted and mass flow-weighted flow averaging.

In practice, isolated component distortion flow patterns from test rigs are assumed to be representative of the component flow patterns that will be encountered in engine system tests. Therefore, the component flow patterns are used to judiciously locate engine instrumentation and to develop engine flow correction factors. For engine flow patterns with high distortion levels where sampling errors are more of a problem, flowpath average properties are determined, if possible, using work and energy balances based on single valued measurements such as mass flow, power, and thrust. Although there are means for estimating sampling errors in highly distorted flow fields, this is still considered an area requiring further development.

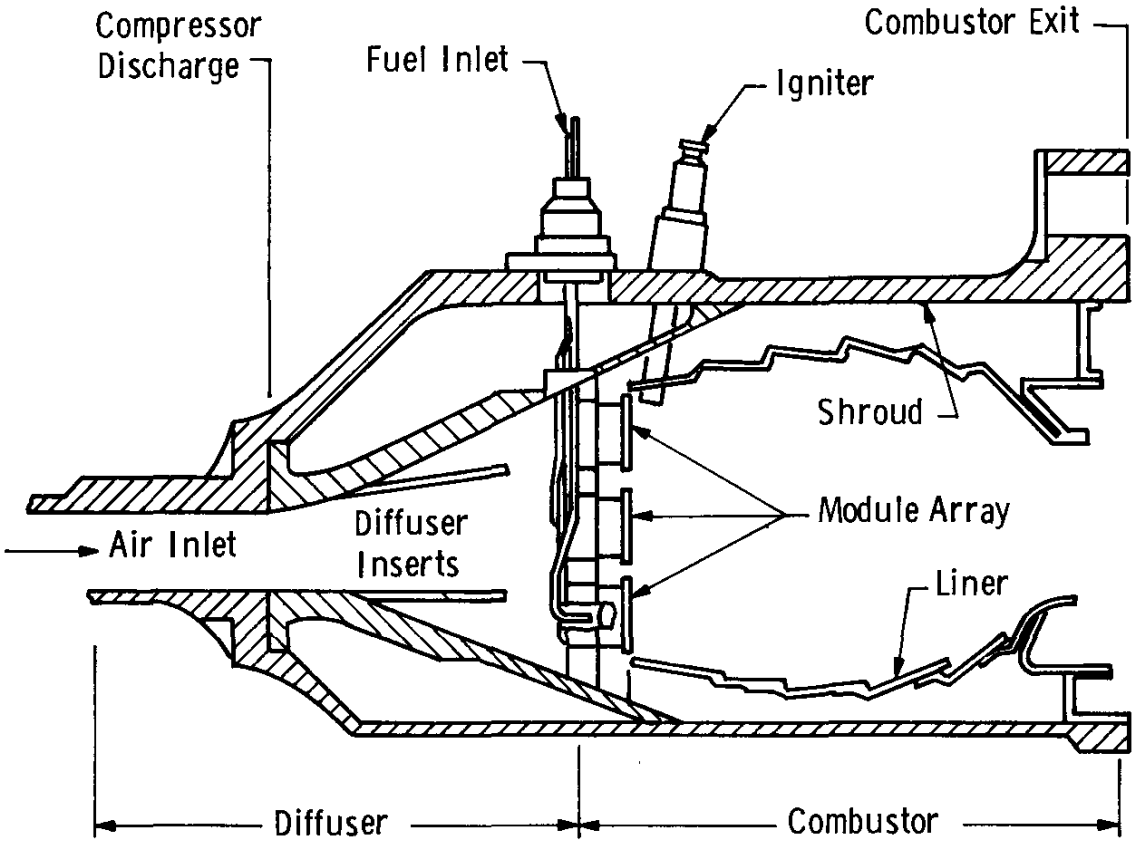

Fig.2.1 Annular swirl-can combustor

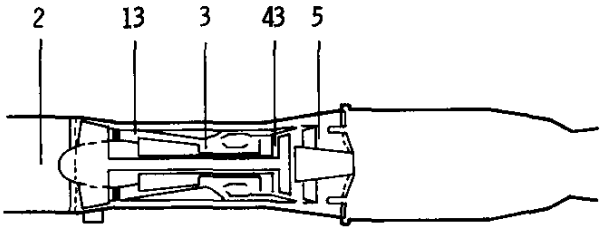

2 Engine Inlet
13 Bypass Duct Inlet
3 HP Engine Compressor Discharge
43 LP Turbine Inlet
5 LP Turbine Discharge

Station	2	13	3	43	5
Total Pressure	6	22	15		27
Stream Static Pressure	6	2			
Wall Static Pressure	4				

○ Total Pressure
● Static Pressure
○● Pitot-Static Pressure Probe
× Total Temperature
△ Manifold Hot-Cold Stream Total Pressures

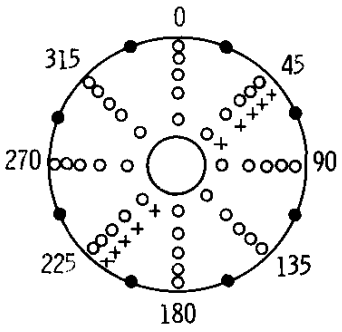

Station 2

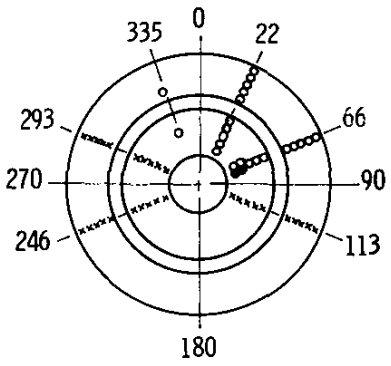

Station 13

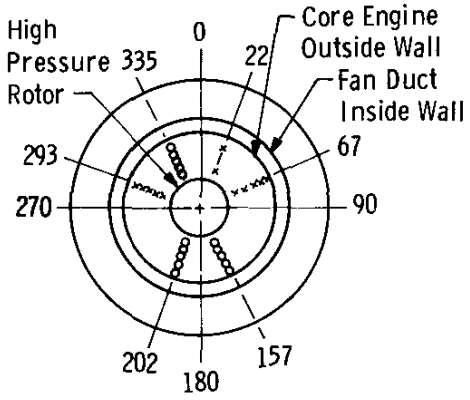

Station 3

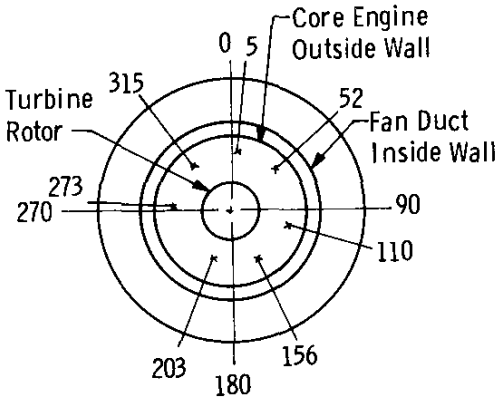

Station 43

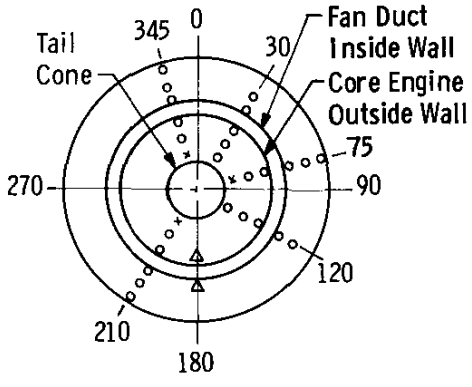

Station 5

Angular Positions in Degrees

Fig.2.2 Single-stream turbofan engine schematic and station designation

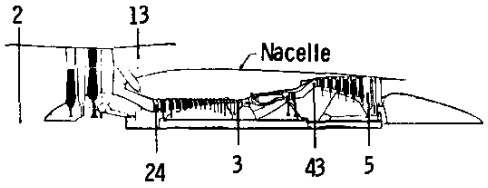

2	Engine Inlet	3	HP Engine Compressor Discharge
13	Bypass Duct Inlet	43	LP Turbine Inlet
24	HP Compressor Inlet	5	LP Turbine Discharge

Engine Station	2	13	24	3	43	5	Nacelle
Total Pressure	24	40	25	20	1	25	0
Static Pressure	16	0	5	5	0	0	90
Stress Temperature	24	20	20	25	1	25	0

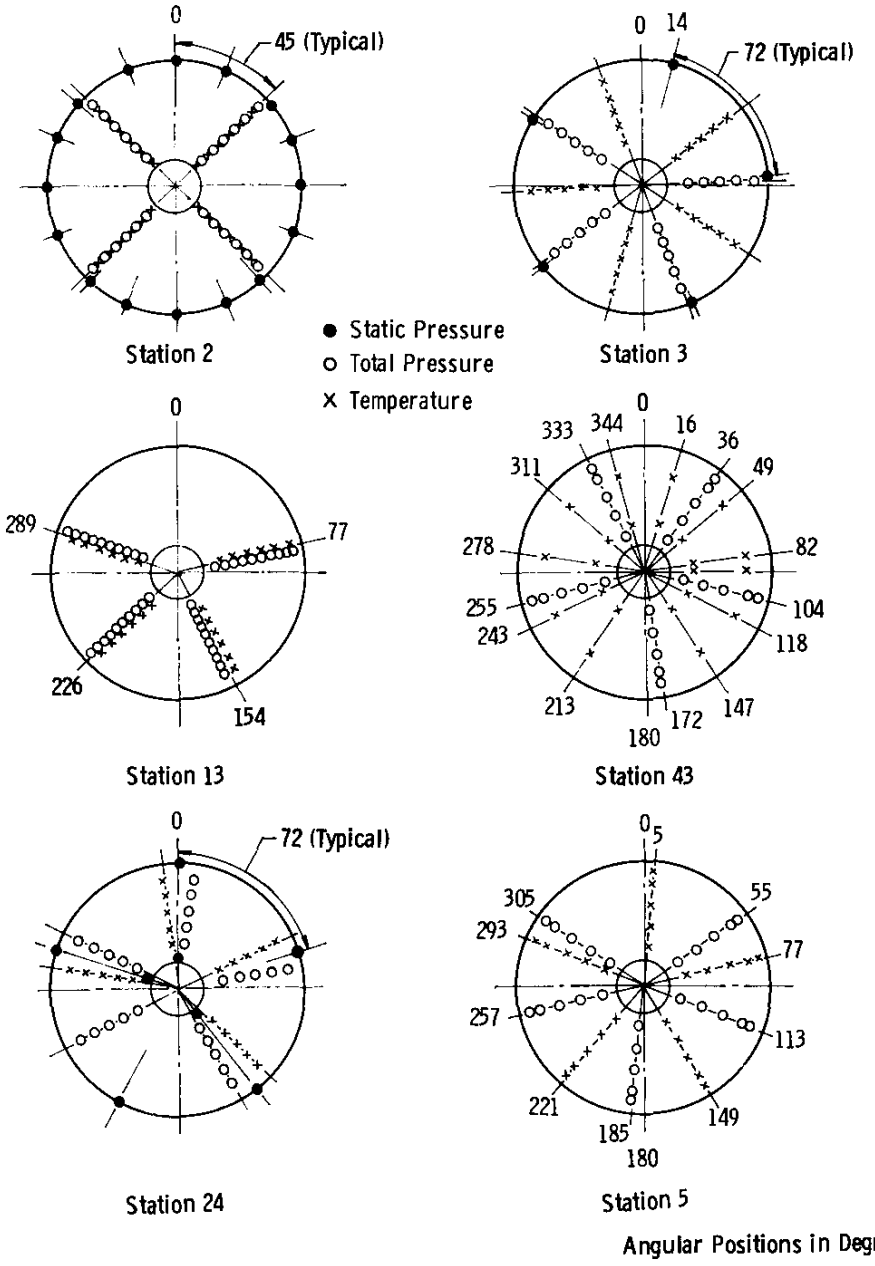

Fig.2.3 Dual-stream turbofan engine schematic and station designation

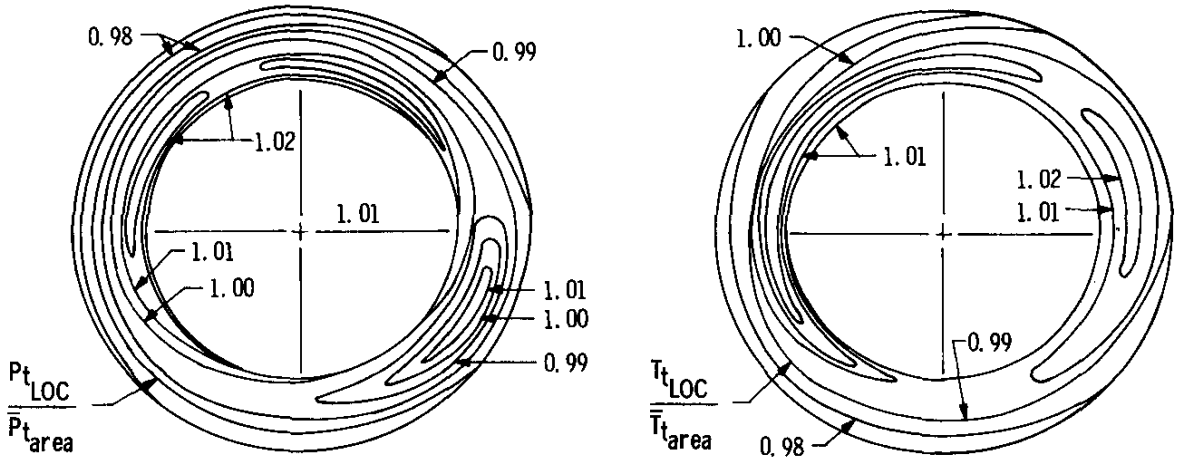

Fig.2.4 Representative high pressure compressor inlet total pressure and total temperature distributions (Ref.2.63)

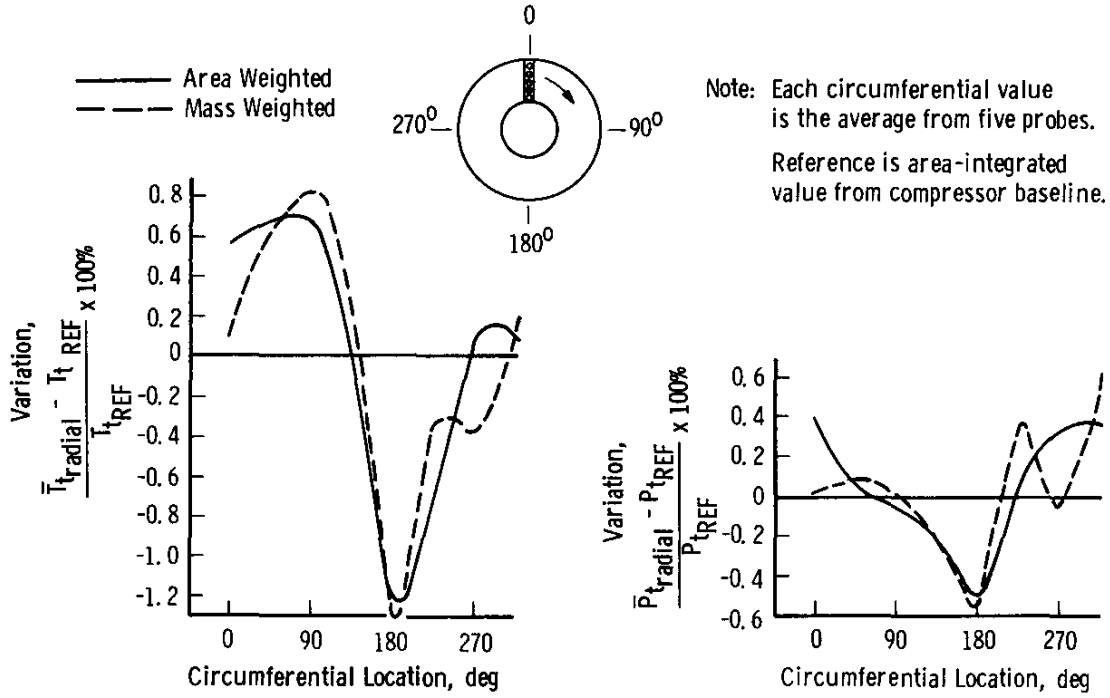

Fig.2.5 Circumferential variation of compressor inlet flow averaged properties (Ref.2.63)

TABLE 2.I Compressor Flowpath-Averaging Practices

Organization	Performance Parameters	Inlet Parameters		Outlet Parameters	
		Measured	Averaged	Measured	Averaged
Arnold Engineering Development Center		Not Currently Engaged in Compressor Component Testing			
Centre d'Essais des Propulseurs	Efficiency Pressure Ratio Temperature Ratio	P_t T_t Airflow	$\bar{P}_t$, $\bar{T}_t$ } Area AVG	P_t T_t	$\bar{P}_t$, $\bar{T}_t$ } Area AVG
Deutsche Forschungs-und Versuchsanstalt für Luft-und Raumfahrt	Efficiency Pressure Ratio Temperature Ratio	P_t T_t P_s (wall) Airflow	$\bar{T}_t$, $\bar{T}_s$, $\bar{S}$ } Mass AVG $\bar{P}_s$ } f($\bar{T}_s$, $\bar{S}$) (1*) $\bar{P}_t$ } f($\bar{P}_s$, $\bar{T}_s$, $\bar{T}_t$) (2)	P_t T_t P_s (wall)	Circumferential Direction: All Quantities Area Weighted Radial Direction: $\bar{\bar{T}}_t$, $\bar{\bar{T}}_s$, $\bar{\bar{S}}$ } Mass AVG $\bar{\bar{P}}_s$ } f($\bar{\bar{T}}_s$, $\bar{\bar{S}}$) (1) $\bar{\bar{P}}_t$ } f($\bar{\bar{P}}_s$, $\bar{\bar{T}}_s$, $\bar{\bar{T}}_t$) (2)
National Gas Turbine Establishment	Efficiency Pressure Ratio Temperature Ratio Inlet Distortion	P_t T_t P_s (wall) Airflow Torque	$\bar{P}_t$, $\bar{T}_t$ } Area AVG $\bar{P}_s$ } Numeric AVG	P_t T_t P_s (wall) α	$\bar{P}_t$, $\bar{T}_t$ } Mass AVG $\bar{P}_s$ } Area AVG
National Aeronautics and Space Administration (Lewis Research Center)	Distortion Efficiency Pressure Ratio Temperature Ratio	P_s (wall) P_t T_t Airflow	$\bar{P}_s$ } Numeric AVG $\bar{P}_t$ } (3) $\bar{T}_t$ } (4)	P_s (wall) P_t T_t	$\bar{P}_s$ } Numeric AVG $\bar{P}_t$ } (3) $\bar{T}_t$ } (4)

*Numbers in parentheses refer to numbered footnotes following Table 2.IV.

TABLE 2.II Turbine Flowpath-Averaging Practices

Organization	Performance Parameters	Inlet Parameters		Outlet Parameters	
		Measured	Averaged	Measured	Averaged
Arnold Engineering Development Center		Not Currently Engaged in Turbine Component Testing			
Centre d'Essais des Propulseurs	Efficiency Pressure Ratio Temperature Ratio	P_t T_t	$\bar{P}_t$, $\bar{T}_t$ } Area AVG	P_t T_t	$\bar{P}_t$, $\bar{T}_t$ } Area AVG
Deutsche Forschungs-und Versuchsanstalt für Luft-und Raumfahrt	Efficiency Pressure Ratio Temperature Ratio Loss Coefficient	P_t T_t P_s (wall) Airflow	Option (OP.) 1. Circumferential Direction: All Quantities Area Avg Radial Direction: $\bar{\bar{T}}_t$, $\bar{\bar{T}}_s$, $\bar{\bar{S}}$ } Mass AVG $\bar{\bar{P}}_s$ } f($\bar{\bar{T}}_s$, $\bar{\bar{S}}$) (1)* $\bar{\bar{P}}_t$ } f($\bar{\bar{P}}_s$, $\bar{\bar{T}}_s$, $\bar{\bar{T}}_t$) (2) OP. 2. "DZUNG Method"	P_t T_t P_s (wall) α	OP. 1. Circumferential Direction: All Quantities Area Avg Radial Direction: $\bar{\bar{T}}_t$, $\bar{\bar{T}}_s$, $\bar{\bar{S}}$, $\bar{\bar{\alpha}}$ } Mass AVG $\bar{\bar{P}}_s$ } f($\bar{\bar{T}}_s$, $\bar{\bar{S}}$) (1) $\bar{\bar{P}}_t$ } f($\bar{\bar{P}}_s$, $\bar{\bar{T}}_s$, $\bar{\bar{T}}_t$) (2) OP. 2. "DZUNG Method"
National Gas Turbine Establishment	Efficiency Pressure Ratio Temperature Ratio	P_t T_t Airflow P_s (wall)	$\bar{P}_t$, $\bar{T}_t$ } Area AVG $\bar{P}_s$ Numeric AVG	P_t T_t P_s (wall) α Torque	$\bar{T}_t$ } (17) $\bar{P}_t$ } (18)
National Aeronautics and Space Administration (Lewis Research Center)	Total Pressure Ratio Static Pressure Ratio Efficiency	Airflow T_t P_s (wall)	$\bar{P}_s$ } Numeric AVG $\bar{T}_t$ } Area AVG $\bar{P}_t$ } (16)	Airflow α T_t P_s (wall) Rotor Speed Torque	$\bar{P}_s$ } Numeric AVG $\bar{T}_t$ } (17) or (21) $\bar{P}_t$ } (18) $\bar{\alpha}$ } (19)

*Numbers in parentheses refer to numbered footnotes following Table 2.IV.

TABLE 2.III Combustor Flowpath-Averaging Practices

Organization	Performance Parameters	Inlet Parameters		Outlet Parameters	
		Measured	Averaged	Measured	Averaged
Arnold Engineering Development Center	Efficiency Pressure Loss Temperature Rise	P_t T_t Airflow Fuel Flow	$\bar{P}_t$, $\bar{T}_t$ } Mass AVG	P_t P_s (wall) Gas Analysis	$\bar{P}_t$, $\bar{h}_t$ } (5)* $\bar{\eta}(\bar{\alpha})$ } Mass AVG $\bar{P}_s$ } Numeric AVG $\bar{T}_t$ } (6)
Centre d'Essais des Propulseurs	Efficiency Pressure Loss Temperature Rise	P_t T_t Airflow Fuel Flow	$\bar{P}_t$ } Area AVG $\bar{T}_t$ } Numeric AVG	P_t T_t Gas Analysis	$\bar{P}_t$ } Area AVG $\bar{T}_t$ } Numeric AVG
** Deutsche Forschungs-und Versuchsanstalt für Luft-und Raumfahrt	Efficiency Smoke Exhaust Emission Outlet Distortion	P_t T_t P_s (wall) Airflow Fuel Flow	$\bar{P}_t$, $\bar{T}_t$ } Area AVG	P_t T_t Smoke Gas Analysis	$\bar{P}_t$, $\bar{T}_t$ (12) } Area AVG
National Gas Turbine Establishment	Efficiency Pressure Loss Outlet Distortion	P_t T_t Airflow Fuel Flow	$\bar{P}_t$ } Area AVG $\bar{T}_t$ } Numeric AVG	P_t T_t P_s (wall) Gas Analysis	$\bar{P}_t$ } Area AVG $\bar{T}_t$ } Numeric AVG
National Aeronautics and Space Administration (Lewis Research Center)	Efficiency Pressure Loss Distortion Patterns	P_t T_t P_s (wall) Airflow Fuel Flow	$\bar{P}_t$, $\bar{T}_t$ } Mass AVG $\bar{P}_s$ } Numeric AVG $\bar{T}_t$(Distortion) } Nonweighted	P_t T_t P_s (wall) Gas Analysis	$\bar{P}_t$, $\bar{T}_t$ } Area AVG $\bar{P}_s$ } Numeric AVG $\bar{T}_t$(Distortion) } Nonweighted $\bar{T}_t$(Option) } Gas Analysis of Unburned Hydrocarbons

* Numbers in parentheses refer to numbered footnotes following Table 2.IV.
**Combustor testing done at Motoren-und Turbinen-Union.

TABLE 2.IV Engine System Flowpath-Averaging Practices

a. Compressor

Organization	Performance Parameters	Inlet Parameters		Outlet Parameters	
		Measured	Averaged	Measured	Averaged
Arnold Engineering Development Center	Efficiency Pressure Ratio Temperature Ratio	P_t T_t P_s (wall) Airflow	$\bar{P}_t$, $\bar{T}_t$ } Area AVG $\bar{P}_s$ } Numeric AVG	P_t T_t P_s (wall)	$\bar{P}_t$, $\bar{T}_t$ } Area AVG $\bar{P}_s$ } Numeric AVG
Centre d'Essais des Propulseurs	Efficiency Pressure Ratio Temperature Ratio	P_t T_t Airflow	$\bar{P}_t$ } Area AVG $\bar{T}_t$ } Enthalpy Mass AVG	P_t T_t	$\bar{P}_t$ } Area AVG $\bar{T}_t$ } Enthalpy Mass AVG
Deutsche Forschungs-und Versuchsanstalt für Luft-und Raumfahrt	Not Currently Engaged in Engine System Testing				
National Gas Turbine Establishment	Efficiency Pressure Ratio Temperature Ratio	P_t T_t P_s (wall) Airflow	$\bar{P}_t$ } Area AVG $\bar{T}_t$, $\bar{P}_s$ } Numeric AVG	P_t T_t P_s (wall)	$\bar{P}_t$ } Area AVG $\bar{T}_t$, $\bar{P}_s$ } Numeric AVG
National Aeronautics and Space Administration (Lewis Research Center)	Efficiency Pressure Ratio Temperature Ratio	P_t T_t Airflow P_s (wall)	$\bar{P}_t$, $\bar{T}_t$ } Mass AVG $\bar{P}_s$ } Numeric AVG	P_t T_t P_s (wall)	$\bar{P}_t$, $\bar{T}_t$ } Area AVG $\bar{P}_s$ } Numeric AVG

TABLE 2.IV Continued

b. Combustor

Organization	Performance Parameters	Inlet Parameters		Outlet Parameters	
		Measured	Averaged	Measured	Averaged
Arnold Engineering Development Center	Efficiency Burner Loss	P_t T_t P_s (wall) Airflow (15)* Fuel Flow	$\bar{P}_t$, $\bar{T}_t$ } Area AVG $\bar{P}_s$ } Numeric AVG		$\bar{P}_t$, $\bar{h}_t$ } (5) $\bar{T}_t$ } f($\bar{h}_t$, $\bar{P}_t$, FAR) (6)
Centre d'Essais des Propulseurs	Outlet Gas Temperature	P_t T_t P_s (wall) Airflow (15) Fuel Flow	$\bar{P}_t$, $\bar{T}_t$ } Area AVG $\bar{P}_s$ } Numeric AVG		$\bar{T}_t$ } (5) & (6)
Deutsche Forschungs-und Versuchsanstalt für Luft-und Raumfahrt		Not Currently Engaged in Engine System Testing			
National Gas Turbine Establishment	Outlet Gas Temperature	P_t P_s (wall) Airflow } (15) Fuel Flow	$\bar{P}_t$ } Area AVG $\bar{P}_s$ } Numeric AVG		$\bar{P}_t$, $\bar{T}_t$ } (7)
National Aeronautics and Space Administration (Lewis Research Center)	Efficiency Burner Loss Effective Temperature Rise	P_t T_t Airflow } (15) Fuel Flow P_s (wall)	$\bar{P}_t$, $\bar{T}_t$ } Area AVG $\bar{P}_s$ } Numeric AVG		$\bar{T}_t$ } (5) & (6)

*Numbers in parentheses refer to numbered footnotes following Table 2.IV

c. Turbine

Organization	Performance Parameters		Inlet Parameters		Outlet Parameters	
			Measured	Averaged	Measured	Averaged
Arnold Engineering Development Center	Efficiency Pressure Ratio Temperature Ratio	High Pressure		$\bar{P}_t$, $\bar{h}_t$ } (5)* $\bar{T}_t$ } f($\bar{h}_t$, $\bar{P}_t$, FAR) (6)	T_t P_t P_s (wall)	$\bar{T}_t$, $\bar{P}_t$ } Area AVG $\bar{P}_s$ } Numeric AVG
		Low Pressure	T_t P_t P_s (wall)	$\bar{T}_t$, $\bar{P}_t$ } Area AVG $\bar{P}_s$ } Numeric AVG	P_t T_t	$\bar{T}_t$, $\bar{P}_t$ } Area AVG
Centre d'Essais des Propulseurs	Efficiency Pressure Ratio Temperature Ratio		P_t T_t	$\bar{P}_t$ } Area AVG $\bar{T}_t$ } Enthalpy Mass AVG	P_t T_t	$\bar{P}_t$ } Area AVG $\bar{T}_t$ } Enthalpy Mass AVG
Deutsche Forschungs-und Versuchsanstalt für Luft-und Raumfahrt			Not Currently Engaged in Engine System Testing			
National Gas Turbine Establishment	Efficiency Pressure Ratio Temperature Ratio	High Pressure		$\bar{P}_t$, $\bar{T}_t$ } (7)	P_t T_t P_s (wall)	$\bar{P}_t$ } Area AVG $\bar{T}_t$, $\bar{P}_s$ } Numeric AVG
		Low Pressure	P_t T_t P_s (wall)	$\bar{P}_t$ } Area AVG $\bar{T}_t$, $\bar{P}_s$ } Numeric AVG	P_t T_t P_s (wall)	$\bar{P}_t$ } Area AVG $\bar{T}_t$, $\bar{P}_s$ } Numeric AVG
National Aeronautics and Space Administration (Lewis Research Center)	Efficiency Pressure Ratio Temperature Ratio	High Pressure		$\bar{P}_t$, $\bar{T}_t$ } (7)	P_t T_t	$\bar{P}_t$, $\bar{T}_t$ } Area AVG
		Low Pressure	P_t T_t	$\bar{P}_t$, $\bar{T}_t$ } Area AVG	P_t T_t	$\bar{P}_t$, $\bar{T}_t$ } Area AVG

*Numbers in parentheses refer to numbered footnotes following Table 2.IV

TABLE 2.IV Concluded

d. Afterburner

Organization	Performance Parameters		Inlet Parameters		Outlet Parameters	
			Measured	Averaged	Measured	Averaged
Arnold Engineering Development Center	Efficiency Burner Loss	Core	P_t T_t	$\bar{P}_t$, $\bar{T}_t$ } Area AVG	P_s (wall) P_t (no reheat) Thrust	$\bar{P}_s$ } Numeric AVG $\bar{P}_t$ (no reheat) } Area AVG $\bar{P}_t$ (reheat) } (9) $\bar{T}_t$ } (10) or (11) & (6)
		Bypass	P_t T_t	$\bar{P}_t$, $\bar{T}_t$ } Area AVG		
		Mixed	Fuel Flow	$\bar{P}_t$, $\bar{h}_t$ } (8)* $\bar{T}_t$ } f($\bar{P}_t$, $\bar{h}_t$, FAR) (6)		
Centre d'Essais des Propulseurs	Efficiency Burner Loss Outlet Gas Temperature	Core	P_t T_t Fuel Flow	$\bar{P}_t$ } Numeric AVG $\bar{T}_t$ } Area AVG		
		Bypass	P_t	$\bar{P}_t$ } Numeric AVG		
		Mixed	Fuel Flow			
Deutsche Forschungs-und Versuchsanstalt für Luft-und Raumfahrt	Not Currently Engaged in Engine System Testing					
National Gas Turbine Establishment	Efficiency Outlet Gas Temperature	Core	P_t T_t P_s (wall) Fuel Flow	$\bar{P}_t$, $\bar{T}_t$, $\bar{P}_s$ } Numeric AVG	P_s (wall) P_t T_t	$\bar{P}_s$ } Numeric AVG $\bar{T}_t$ } (13) or (14) $\bar{P}_t$ } Area AVG or (18)
		Bypass	P_t T_t P_s (wall)	$\bar{P}_t$, $\bar{T}_t$, $\bar{P}_s$ } Numeric AVG		
		Mixed	P_t T_t	$\bar{P}_t$, $\bar{T}_t$ } (7)		
National Aeronautics and Space Administration (Lewis Research Center)	Burner Loss Efficiency Effective Temperature Rise Mach (Inlet) Exhaust Emission		Airflow Fuel Flow T_t P_t PS (wall)	$\bar{T}_t$, $\bar{P}_t$ } Area AVG $\bar{P}_s$ } Numeric AVG	P_t Thrust Exhaust Gas Analysis	$\bar{P}_t$ } Area AVG $\bar{T}_t$ } (20)

*Numbers in parentheses refer to numbered footnotes following Table 2.IV.

e. Nozzle

Organization	Performance Parameters	Inlet Parameters		Outlet Parameters	
		Measured	Averaged	Measured	Averaged
Arnold Engineering Development Center	Flow Coefficient Thrust Coefficient	P_s (wall) P_t (no reheat)	$\bar{P}_s$ } Numeric AVG $\bar{P}_t$ } Area AVG $\bar{T}_t$ } (10) or (11) & (6)*	P_s (atmos) Thrust	$\bar{P}_s$ } Numeric AVG
Centre d'Essais des Propulseurs	Thrust Coefficient			Thrust	
Deutsche Forschungs-und Versuchsanstalt für Luft-und Raumfahrt	Not Currently Engaged in Engine System Testing				
National Gas Turbine Establishment	Flow Coefficient Thrust Coefficient	P_s (wall)	$\bar{P}_s$ } Numeric AVG	P_s (atmos) Thrust	$\bar{P}_s$ } Numeric AVG
National Aeronautics and Space Administration (Lewis Research Center)	Flow Coefficient Thrust Coefficient	P_s (wall) P_t (no reheat)	$\bar{P}_s$ } Numeric AVG $\bar{P}_t$ } Area AVG $\bar{T}_t$ } (10) or (11) & (6)	P_s (atmos) Thrust	$\bar{P}_s$ } Numeric AVG

*Numbers in parentheses refer to numbered footnotes following Table 2.IV.

(1) $\bar{P}_s = P_0 \left(\frac{\bar{T}_s}{\bar{T}_0}\right) \cdot \exp\left(-\frac{\bar{s}}{R}\right)$

(Index o → reference)

(2) $\bar{P}_t = P_{t_0} \left(\bar{T}_t / \bar{T}_s\right)^{\frac{\gamma}{\gamma-1}}$

(3) Area-averaged circumferentially, then radial mass-averaged.

(4) Area-averaged circumferentially, then radial energy-balanced.

(5) Combustor pressure is estimated using a numeric average of combustor chamber static pressure and estimated burner Mach number.

Combustor enthalpy is estimated using compressor mass flow minus turbine cooling and leakage, compressor discharge enthalpy, measured fuel flow, and combustion efficiency.

(6) Temperature obtained from thermodynamic tables for specified enthalpy, pressure, and fuel-air ratio.

(7) Calculated using air flow, fuel flow, and combustion efficiency.

(8) $\bar{P}_t = \left\{\dot{m}_A(5) \cdot P(5) + \dot{m}_A(16) \cdot P_t(16)\right\} / \dot{m}_t$

$\bar{h}_t = \left\{\dot{m}_A(5) \cdot h_t(5) + \dot{m}_A(16) \cdot \dot{m}(16)\right\} / \dot{m}_t$

(9) $\bar{P}_{t(\text{reheat})} = \bar{P}_{t(\text{reheat})} \left[\left\{\frac{P_{t(\text{reheat})}}{P_{t(\text{no reheat})}}\right\}_{CAL} - \Delta P_{t(\text{drag})}\right]$ where $\left\{\frac{P_{t(\text{reheat})}}{P_{t(\text{no reheat})}}\right\}_{CAL}$ is evaluated using Rayleigh line heat addition.

(10) $\bar{T}_t = [V(7)]^2 / (2\gamma R/1 - \gamma) \left\{1 - \frac{\bar{P}_{t(\text{reheat})}^{\frac{\gamma-1}{\gamma}}}{\bar{P}_s}\right\}$

Next, calculate thrust based on $\bar{T}_t$; continue iteration until set tolerance for difference in measured and calculated thrust is not exceeded.

(11) Afterburner Energy Balance:

$\dot{m}(7) \cdot h_t(7) \cdot \dot{m}(62) \cdot h_t(7) + \dot{m}_F(6)\left\{(h_t)_F(6) + \eta_i(6) \cdot FHV\right\}$

(12) A theoretical heat balance model is used to correct each individual measured temperature for pressure, air-fuel ratio, radiation, heat conduction, and recovery factor prior to averaging.

(13) Calculated using thrust and mass flow.

(14) Calculated using area-averaged measured total pressure, flow area, and mass flow.

(15) Core flow is calculated using a high-pressure turbine flow function or from a compressor-turbine work balance.

(16) $\bar{P}_t$ is calculated using averaged inlet total temperature, inlet static pressure, and measured airflow.

(17) $\bar{T}_t$ used to calculate turbine exit average total pressure is calculated using an area-averaged turbine inlet temperature, specific enthalpy drop obtained from measured torque, rotor speed, and air flow.

(18) $\bar{P}_t$ is calculated using torque-derived $\bar{T}_t$ (17), numeric-averaged $\bar{P}_s$, energy-averaged exit flow angle (21), and measured air flow.

(19) $\bar{\alpha}$ is the area-averaged flow angle.

(20) $\bar{T}_t$ is calculated using measured thrust, exit total pressure, measured airflow, and measured fuel flow.

(21) $\bar{T}_t$ is used to calculate an energy-averaged turbine exit flow angle and is calculated using a mass enthalpy average.

Footnotes Pertaining to Tables 2.I Through 2.IV

TABLE 2.V Influence Coefficient Chart (Ref. 2.62)

(Compressor Pressure Ratio = 10, Burner Inlet Temperature = 2160°R, Flight Altitude = 0 ft, Flight Mach No. = 0)										
Parameter	Turbine Inlet Temperature	Compressor Speed	Compressor Inlet Temperature	Compressor Inlet Pressure	Ambient Pressure	Compressor Bleed	Compressor Flow	Compressor Adiabatic Efficiency	Relative Burner Pressure Loss (ΔP/P)	Turbine Inlet Nozzle Area
Turbine Inlet Temperature	1	0	0	0	0	0	0	0	0	0
Compressor Speed	0	1	0	0	0	0	0	0	0	0
Compressor Flow	0	2	-1.5	1	1	0	1	0	0	0
Compressor Exit Temperature	0.17	0.67	0.53	0	0	0.33	0.33	-0.55	0.34	-0.33
Compressor Exit Pressure	0.5	2.0	-1.5	1	1	1	1	0	1.04	-1
Fuel Flow	1.81	1.36	-2	1	1	0.68	0.68	0.53	-0.33	0.32
Turbine Flow	0	2	-1.5	1	1	1	1	0	0	0
Turbine Exit Temperature	1.25	-0.43	-0.04	0	0	0.14	-0.21	0.36	-0.22	0.21
Turbine Exit Pressure	1.5	0.28	-1.64	1	1	1.5	0.14	1.43	-0.86	-0.14
Engine Exhaust Nozzle Area	-0.86	1.5	0.12	0	0	-0.5	0.75	-1.25	0.80	0.25
Net Thrust	1.19	1.89	-2.16	1.38	1	1.65	0.95	0.72	-0.43	0.05
Turbine Power	2.38	1.79	-2.77	1.75	1	2.32	0.89	1.43	-0.86	0.11
Specific Fuel Consumption	0.62	-0.53	0.16	-0.38	0	-0.97	-0.27	-0.19	0.1	0.27

TABLE 2.VI Typical Measurement Uncertainties for Parameters Used in Turbine Engine Flow Averaging

Parameter	Steady-State Uncertainty (Percent of Reading, Unless Units Are Designated)
Scale Force	0.5
Torque	0.5
Air Flow	0.5 to 2 (Venturis and Metering Nozzles) 2 to 5 (Uncalibrated Orifices)
Core Flow (Turbofan Engine)	2 to 4
Fuel Flow	0.5 to 1
Pressure	0.3 to 1
Temperature	2°F Plus 0.3 Percent of Reading
Rotor Speed	0.3 to 0.5
Exhaust Nozzle Area	1
Flow Angles	1 Degree

Chapter 3

THEORETICAL CONSIDERATIONS ON AVERAGING

SUMMARY

In Section 3.1 the physical contents of averaging procedures are discussed in great detail.

Two groups of averaging methods:

- averaging methods based on "Integral System Effects" and
- averaging methods based on "Complete Equilibrium"

are considered, which differ in principle.

The second group is practical only for swirl-free channel flow with constant cross section and for two-dimensional cascade flow. Additionally Dzung's "Consistent Averaging Method", which can be added neither to the first nor to the second group, is treated.

After considerable discussion of the suggestion of W.Traupel in the first group and the method of L.S.Dzung for averaging in turbomachinery flow, from the theoretical point of view Dzung's procedure needs no correction factors. It is identical to the averaging method based on "Complete Equilibrium" when applied to swirl-free channel flow with constant cross section as well as to two-dimensional cascade flow.

In Section 3.2 a method is proposed which leads to averaged quantities intended to represent the *usefulness* or the *function* of the engine component located downstream of the nonuniform flow considered. First the general method is discussed which uses the concept of a uniform flow "equivalent" to the real flow.

The method is based on the following principles:–

(a) take into account the specific character of each component of a turbojet/fan.
(b) ensure coherence between the various components of an engine.

For application to an engine it is necessary to choose for each component a significant performance parameter or parameters.

The method is then described in detail for the different turbine engine components: exhaust nozzle, turbine, compressor or fan, combustor, after burner channel, diffuser, and air inlet. Simplified formulae applicable to a calorifically perfect gas are also presented.

In the following chapters the method presented here is usually called Pianko's Method.

3.1 REPRESENTATION OF SYSTEM ACTION BY AVERAGED QUANTITIES

Nomenclature

The notation in this section is consistent with the general nomenclature provided at the beginning of this report. In addition the following symbols and indices are used:

a^*_S	critical velocity of sound
B	non-dimensional momentum function
C_{fl}	specific heat capacity of an incompressible fluid
C_v	specific heat capacity at constant volume†
$\dot{D}$	swirl flow

† In addition to the meaning given in the general nomenclature.

e	unit tensor
e_{an}	specific "anergy"
$\dot{E}$	energy flux
$\dot{E}_{Rot}$	energy flux in rotating relative system
$\dot{E}_{ex}$	"exergy" flow
$\dot{E}_{an}$	"anergy" flow
f	body force
F_1, F_2	abbreviation for certain integrals in Equations (128) and (129)
h_{Rot}	specific rothalpy
$\dot{I}$	momentum flux
k	isentropic exponent
M*	critical Mach number
p	cascade spacing
P_{mech}	mechanical power
$\dot{Q}$	added or removed heat energy per unit time
u	specific internal energy
U	internal energy
v	specific volume
v	volume
$\dot{W}$	added or removed mechanical work per unit time
x, y, z	Cartesian coordinates
r, Θ, z	Cylindrical coordinates
z	real gas factor
α, ϵ, ζ	correction factors
μ	shear viscosity
$\hat{\mu}$	volume viscosity
λ	heat conductivity coefficient
ν	hub to tip ratio
ν	exponent in Equation (6)
π_s	isentropic pressure function
σ	stress tensor
ϕ	non-dimensional flow function
ψ	specific dissipation

Indices

Ax	in axial direction
B	hub
C	based on continuity
D	based on swirl
E	based on energy
H	outer casing
I	based on momentum
n	normal
p	at constant pressure
r	in radial direction
is	at constant entropy

t tangential to the cascade front*

T at constant temperature

Symbols

($\bar{\ }$) average value†

( )* non-dimensional value

($\vec{\ }$) vector

($\underline{\ }$) tensor

General

In order to be able to treat the aerodynamic and thermodynamic processes in a fluid flow with the aid of elementary stream tube theory, it is necessary to establish representative average values for the surfaces of a fixed control volume. These average values describe correctly the integral effect of the fluid flowing through this control volume. This problem arises not only in the interpretation of test results, but also during the aerodynamic design of components.

Although each theoretical treatise for the formation of physically sensible average values starts from the idea that the non-homogeneous flow conditions in the control surface are fully known, this condition often presents considerable difficulties in practical test rigs. The arguments resulting therefrom, which are more concerned with practical matters in the formulation of rules for averaging, are not examined at this point. Thus, the following arguments always assume that the non-homogeneous flow conditions are known accurately.

The averaging methods given in the literature can be divided in principle into two groups.

The first group relies only on averaging definitions which represent, qualitatively and accurately, the "Integral System Effects" of interest. Here an attempt is made to satisfy an additional condition, namely, to establish basic equations by means of average values with as few correction factors as possible.

In the second group, the non-homogeneous flow state in the measurement or calculation plane is converted into a state of "Complete Equilibrium" with the aid of the conservation laws for mass, momentum and energy. This condition should be attained asymptotically in an infinitely long settling channel, because of the viscosity of the fluid, if the fluid does not stick to the wall but moves along without friction.

3.1.1 Averaging Method Based on "Integral System Effects"

In this method of averaging, the attempt is made primarily to represent the "Integral System Effects" of interest by representative average values. As a reasonable additional condition, the requirement is made to use as few correction factors as possible in the formulation of the conservation laws by means of the defined average values.

The suggestions contained in the literature which belong to the first group of averaging methods limit themselves almost exclusively to swirl-free channel flow and to three-dimensional turbomachine flow. Since two-dimensional cascade flow can be considered as a special case of three-dimensional turbomachine flow, it will not be treated specially in this presentation.

In the following discussions it is assumed that the thermodynamic behaviour of the fluid is always known. For that reason, the most important equations of state for the two idealizations incompressible fluid and ideal gas, with consideration of the temperature dependency of the specific heats have been assembled in Table 3.1.I with the help of the so-called thermodynamic functions. Taking into account the temperature dependencies of the specific heats by means of average values, it should be pointed out, in contrast to Reference 3.1.1 that these average value formulations are not a part of the problem area of the averaging methods.

In order to point out clearly the problems encountered in averaging methods based on "Integral System Effects", the discussion will centre, as far as possible, on swirl-free channel flow. Then, in the presentation of the three-dimensional turbomachine flow, only additions, (i.e. problems specific to turbomachines) will be discussed.

3.1.1.1 Swirl-Free Channel Flow

In connection with the multitude of experimental investigations of channel flows, the literature contains almost as many suggestions for averaging methods. Table 3.1.II shows a comparison between the three different suggestions according to References 3.1.2 to 3.1.5 which clearly show the problems encountered in the choice of primary average values, as they result from averaging specifications as well as from the problems with the average values thus derived, including the necessary correction factors.

---

* In addition to meaning according to general nomenclature.

† Contrary to the general nomenclature a single bar denotes all average values.

Since it is desired to describe correctly the "Integral System Effects" by means of "representative" average values, it makes sense to start the discussion with the three conservation laws for mass, momentum and energy in integral form. If one neglects the normal and tangential stresses in the inlet and exit plane of the control volume resulting from fluid viscosity, the three basic equations take the following forms for the steady channel flow shown in Figure 3.1.1:

continuity equation

$$\int_{A_e} \rho_{se} V_e \, dA_e - \int_{A_i} \rho_{si} V_i dA_i = 0 , \tag{1}$$

momentum equation

$$\int_{A_e} (P_{se} + \rho_{se} V_e^2) dA_e - \int_{A_i} (P_{si} + \rho_{si} V_i^2) dA_i = \Sigma F , \tag{2}$$

energy equation

$$\int_{A_e} \left(h_{se} + \frac{V_e^2}{2}\right) \rho_{se} V_e \, dA_e - \int_{A_i} \left(h_{si} + \frac{V_i^2}{2}\right) \rho_{si} V_i dA_i = \dot{Q}_{i-e} . \tag{3}$$

Without limiting the general validity, the effect of the thermodynamic pressure in the inlet and exit plane has been included in the surface integrals for both the momentum and energy equations. Thus the enthalpy term appears in Equation (3).

For swirl-free one-dimensional channel flow of a chemically homogeneous fluid, three averaging specifications are sufficient to determine two average values of internal state values in addition to the value of the average velocity, the only external state value. All other static as well as total state values can be calculated as derived average values with the help of the thermodynamic relations. The following averaging specifications can be deduced from the conservation laws according to Equations (1) to (3):

average static pressure

$$\bar{P}_s := \frac{1}{A} \int_A P_s \, dA , \tag{4}$$

average static enthalpy

$$\bar{h}_s := \frac{\int_A h_s \rho_s V \, dA}{\int_A \rho_s V \, dA} , \tag{5}$$

average velocity

$$\bar{V} := \sqrt[\nu]{\frac{\int_A \rho_s V^\nu \, dA}{\bar{\rho}_s A}} . \tag{6}$$

Thus the average density

$$\bar{\rho}_s = \bar{\rho}_s(\bar{h}_s, \bar{P}_s) \tag{7}$$

is a derived average value. Depending on the choice of the exponent $\nu = 1, 2$, or 3, the average velocity is either a continuity, momentum, or energy average value. Independent of the chosen averaging specification for the average velocity, two correction factors are needed in order to represent correctly the velocity integrals in the conservation laws by means of the velocity average value. While the suggestions compared in Table 3.1.II use, in a further sense, only average continuity values for the average velocity, whereby only the suggestion of J.L.Livesey and T.Hugh according to Reference 3.1.3 satisfies exactly Equation (6) for $\nu = 1$, the conservation laws are shown in Table 3.1.III with the aid of an average velocity based on continuity, momentum and energy including the necessary correction factors.

As far as the average value definitions for the two internal state values are concerned, in Table 3.1.II the three authors use the averaging specification given in Equation (5) for the average static enthalpy. However, there are differences in the choice of a second average state value to be defined. Thus A.J.W.Smith in Reference 3.1.2 and, by implication also R.D.Tyler in Reference 3.1.5, employ an area-averaged static pressure according to Equation (4), provided that the assumption $\bar{P}_s = P_s$ = constant made by R.D.Tyler is a result from Equation (4). The average density, unnecessarily defined by A.J.W.Smith and R.D.Tyler as a third internal state value, leads to additional correction factors being needed in both suggestions, as shown in Table 3.1.II.

The averaging method suggested by W.Traupel in Reference 3.1.6 (2nd edition) for turbomachine flow also uses the average static pressure and the average static enthalpy as primary average values for the internal state. Applied to swirl-free channel flow, the averaging specifications given by W.Traupel for P_s and h_s are identical to those in Equations (4) and (5). In place of the continuity average value for the average velocity, W.Traupel (Reference 3.1.3, 2nd edition) prefers the momentum average values for the average velocity vectors, in consideration of the kinematic relationship between absolute and relative flow, which is relevant for turbomachine flow. According to Equation (6), $\nu = 2$ corresponds to one-dimensional channel flow.

Deviating from the area-averaging static pressure as a result of the momentum equation, H.E.Rosslenbroich gives the following averaging specification for P_s in Reference 3.2.1.

$$\bar{P}_s := \frac{\frac{1}{A}\int_A r P_s \, d\dot{m}}{\sqrt{\frac{1}{\dot{m}}\int_{\dot{m}} r^2 \, d\dot{m}}} \quad . \tag{8}$$

This averaging suggestion, obviously deduced from the moment of momentum equation has no practical significance for turbomachines.

In contrast, Table 3.1.II contains the suggestion of J.L.Livesey and T.Hugh (Ref.3.1.3) which uses the mass-averaged static entropy $\bar{s}$ in place of the area-averaged static pressure $\bar{P}_s$

$$\bar{s} := \frac{\int_A s \rho_s V \, dA}{\int_A \rho_s V \, dA} \tag{9}$$

as a second internal state value. Then all other average thermodynamic state values are functions of $\bar{h}_s$ and $\bar{s}$. This is valid especially for the average static pressure $\bar{P}_s = \bar{P}_s(\bar{h}_s, \bar{s})$. In the formulation of the momentum law according to Equation (2) using $\bar{P}_s = P_s(\bar{h}_s, \bar{s})$ the correction factor α becomes necessary, see Table 3.1.II.

This procedure is also used by W.Traupel (Reference 3.1.6, 2nd edition) as a method for average value formation for the internal state. Beyond that, in reference 3.1.6 (3rd edition) it is suggested that the mass average of the specific volume v_s be utilized as an extensive state value. For the simple case of swirl-free channel flow, the averaging specification becomes

$$\bar{v}_s := \frac{\int_A V \, dA}{\int_A \rho_s V \, dA} \quad . \tag{10}$$

Because $v_s = 1/\rho_s$, Equation (10) is identical to the averaging specification for the average density $\bar{\rho}_s$ of A.J.W.Smith in Reference 3.1.2, see Table 3.1.II.

Because the simultaneous use of the average values defined in Reference 3.1.6 (3rd edition) – $\bar{P}_s$ from Equation (4), $\bar{h}_s$ from Equation (5), $\bar{s}$ from Equation (9), and $\bar{v}_s$ from Equation (10) – would require additional correction factors in the thermodynamic equations of state, W.Traupel recommends the following three methods:

(a) $\bar{P}_s$ from Equation (4) and $\bar{h}_s$ from Equation (5)
$\rightarrow \bar{v}_s = v_s(\bar{P}_s, \bar{h}_s)$, $\bar{s} = \bar{s}(\bar{P}_s, \bar{h}_s)$

(b) $\bar{h}_s$ from Equation (5) and $\bar{s}$ from Equation (9)
$\rightarrow v_s = \bar{v}_s(\bar{h}_s, \bar{s})$, $\bar{P}_s = \bar{P}_s(\bar{h}_s, \bar{s})$

(c) $\bar{v}_s$ from Equation (10) and $\bar{h}_s$ from Equation (5)
$\rightarrow \bar{P}_s = \bar{P}_s(\bar{h}_s, \bar{v}_s)$, $\bar{s} = \bar{s}(\bar{h}_s, \bar{v}_s)$

for the determination of the average internal state. The fact that the two derived average state values do not satisfy the averaging rules that belong to them is demonstrated in Reference 3.1.6 (3rd edition) in the following idealized example.

Two equal mass flows, with different temperatures and thus with different static enthalpies $\bar{h}_{s1}$ and $\bar{h}_{s2}$, flow through a cross section in which the static pressure is constant. Figure 3.1.2 shows the qualitative result for the average internal state resulting from the three methods.

Especially noticeable is the difference in the average entropy values between methods a and b. If it is imagined that the mixing process again occurs in a surface of discontinuity, method b includes no irreversible mixing losses, because the averaging rule for the static entropy can be interpreted as a conservation law for the surface of discontinuity. On the

other hand, the entropy difference between points A and B only represents an irreversible increase in entropy of the real mixing process if the kinetic energies in the two side streams are neglected. Since the differences in the average internal state are very small for this idealized example and in most cases they lie below the tolerance of measurements, W.Traupel (Reference 3.1.6, 3rd edition) recommends procedure a, which excels in its practical utilization.

Normally the evaluation of the aerodynamic quality of a system rests with the second law of thermodynamics. Here it must be checked which quantitative statement with regard to the irreversibilities arising within a system is possible, using the mass-averaged entropy from Equation (9) directly for the determination of the internal state.

The mechanical work ψ_{i-e}

$$\psi_{i-e} = \int_{s_i}^{s_e} T_s Ds - q_{i-e} \tag{11}$$

dissipated into internal energy along a stream line depends, as does the irreversible portion of the path-dependent integral $\int_i^e T_s\, Ds$, on the conditions between inlet and exit of the system. Thus the "representative" average value of the dissipation ψ_{i-e} cannot be accurately described quantitatively with the aid of the entropy flows.

Even in the case of an incompressible fluid, the relation for specific dissipation becomes

$$\psi_{i-e} = -\frac{P_{te} - P_{ti}}{\rho} \; . \tag{12}$$

This is valid only for adiabatic isoenergetic flow along the individual stream lines and a completely homogeneous inlet state. Only in that case is it possible to follow the individual fluid elements along their stream lines. Assuming a homogeneous inlet state for a compressible fluid, such as is often the case in rig tests of single components, an additional approximation to the real changes in state becomes necessary. The approximation may be a polytropic change in state along the stream lines. Because of the additional limiting condition of homogeneous inlet conditions and because the information from two measuring or calculation planes is needed, this method of average value formation will not be treated within this section.

On the other hand, the entropy flow only appears in the "exergetic" and the "anergetic" portion of the energy flow. In contrast to the physical interpretation of the mass-averaged specific entropy with the aid of the "exergy" flow, as given by J.L.Livesey and T.Hugh in Reference 3.1.3, here we prefer the "anergy" flow. The reason is that, according to the second law of thermodynamics, which limits energy conversion, the "anergetic" portion of the energy flow can no longer be converted to mechanical energy and thus must be considered as a real loss. According to Reference 3.1.7, where H.J.Baehr describes the quantitative formulation of the second law by means of the terms "exergy" and "anergy", the exergetic portion of the energy flow for swirl-free channel flow becomes

$$\dot{E}_{ex} := \int_A \left\{ \frac{V^2}{2} + [h_s - h_0 - T_0(s - s_0)] \right\} \rho_s V dA \; . \tag{13}$$

h_0 and s_0 are determined by the ambient pressure p_0 and the ambient temperature T_0. The kinetic energy represents pure "exergy" and the expression in the square brackets is the "exergetic" portion of the specific static enthalpy. The "anergetic" portion of the energy flow is given by the difference between energy and "exergy" flow

$$\dot{E}_{an} := \int_A [h_0 + T_0(s - s_0)] \rho_s V dA \; . \tag{14}$$

With the mass flow

$$\dot{m} = \int_A \rho_s V dA \tag{15}$$

Equation (14) becomes

$$\dot{E}_{an} = h_0 \dot{m} + T_0 \int_A s \rho_s V dA - T_0 s_0 \dot{m} \; . \tag{16}$$

If we introduce the average specific entropy $\bar{s}$ from Equation (9) into Equation (16), then we can represent the "anergy" flow

$$\dot{E}_{an} = [h_0 + T_0(\bar{s} - s_0)] \dot{m} \tag{17}$$

by means of average values. Thus with the average specific entropy it is possible to determine only the "anergy" increase, or the "exergy" decrease. Thus, for the only possible "anergy" increase between inlet and exit of the system, we get

$$\Delta \dot{E}_{an} = T_0(\bar{s}_e - \bar{s}_i)\dot{m} \geqslant 0 . \tag{18}$$

In Figure 3.1.3, for adiabatic flow, the specific dissipation ψ_{i-e}

$$\psi_{i-e} = \int_{s_i}^{s_e} T_s \, Ds_{irr} \tag{19}$$

as well as the increase in "anergy" Δe_{an}

$$\Delta e_{an} = T_0(s_e - s_i) \tag{20}$$

are shown along a stream line in the T,s diagram. Here it is very noticeable that the irreversible increase in "anergy" decreases with increasing temperature level where the energy dissipation takes place.

Hence, it follows that no quantitative statement about the mechanical work dissipated into internal energy can be made as a result of the "anergy" increase.

In conjunction with Reference 3.3.3, the practical application of the mass-averaged specific entropy will be explained with the aid of the thermodynamic functions shown in Table 3.1.I for an incompressible fluid and for an ideal gas; the temperature dependency of the specific heats will be taken into consideration.

Assuming that during a change in state of the system under consideration the fluid composition does not change, then the integration constant s_0 for an arbitrary reference state can be set equal to zero in the equation of state for the specific entropy (Table 3.1.I):

incompressible fluid	$s_0(T_0) = 0$,
ideal gas	$s_0(p_0, T_0) = 0$.

Then, the rule for averaging for the incompressible fluid, using Equation (15) becomes

$$s^*(T) = \frac{1}{\dot{m}} \int_A s^*(T)\rho_s V \, dA . \tag{21}$$

For the ideal gas we get

$$\frac{\bar{s}}{R} = \ln\left(\frac{\pi_s(T_s)}{\bar{P}_s/P_0}\right) = \frac{1}{\dot{m}} \int_A \ln\left(\frac{\pi_s(T_s)}{P_s/P_0}\right)\rho_s V dA . \tag{22}$$

Since the ratio of the total state to the static state is isentropic, we get the following equation

$$\frac{\bar{s}}{R} = \ln\left(\frac{\pi_s(\bar{T}_t)}{\bar{P}_t/P_0}\right) = \frac{1}{\dot{m}} \int_A \ln\left(\frac{\pi_s(T_t)}{P_t/P_0}\right)\rho_s V dA . \tag{23}$$

Equations (22) and (23) can be used optionally if, for the determination of $\bar{T}_t$, either the energetic average value of the velocity or the particular necessary correction factor is taken into account from Tables 3.1.II or 3.1.III.

Since in the majority of experimental investigations, for swirl-free channel flow, either the static pressure P_s or the total temperature T_t is to be considered as constant across the cross section within the accuracy of measurements, the numerical evaluation of Equations (22) and (23) is simplified.

For P_s = constant Equation (22) simplifies to

$$s_p^*(\bar{T}_s) - \ln\left(\frac{\bar{P}_s}{P_0}\right) = \frac{1}{\dot{m}} \int s_p^*(T_s)\rho_s V dA - \ln\left(\frac{P_s}{P_0}\right) . \tag{24}$$

Because of the small differences in static temperature across the cross section, one can set

$$s_p^*(\bar{T}_s) \approx \frac{1}{\dot{m}} \int_A s_p^*(T_s)\rho_s V dA \tag{25}$$

where the average temperature $\bar{T}_s$ has already been fixed by the average specific enthalpy according to Equation (5). From the approximation according to Equation (25) it follows that $\bar{P}_s \approx P_s$ = constant. Thus, the numerical evaluation of the entropy-averaging rule for P_s = constant can often be ignored.

For T_t = constant, from Equation (23) and in agreement with References 3.1.3 and 3.1.5 we get an averaging rule for the total pressure

$$\ln \bar{P}_t = \frac{1}{\dot{m}} \int_A \ln P_t \, \rho_s \, V \, dA \, . \tag{26}$$

If, within the limits of accuracy of the measurements, the static pressure P_s as well as the total temperature T_t can be considered as constant, then because

$$\bar{P}_s \approx P_s = \text{constant} \, , \text{ and} \tag{27}$$

$$\bar{T}_t \approx T_t = \text{constant} \tag{28}$$

one requires only a single additional averaging rule or other condition in order to determine the average state uniquely. For this apparently simple case, because $\bar{P}_s$ and $\bar{T}_t$ are obtained directly from measurements, test engineers prefer to use simple averaging methods. The "continuity" and "total pressure" methods fall into this category, for example.

For the continuity method only the following three directly measured quantities are used:

- the constant static pressure P_s by means of wall taps,
- the constant total temperature T_t by means of thermocouples,
- mass flow $\dot{m}$ by means of probes or an orifice.

All other average state values are determined from iterative solutions of the continuity equation. Approximating the thermodynamic behaviour of the fluid by a calorically ideal gas with C_p = constant, it is recommended to utilize the gas-dynamic functions of the non-dimensional mass flow in the form of

$$\phi := \frac{\dot{m}\sqrt{R\bar{T}_t}}{A P_s} \, . \tag{29}$$

Since for this method, which is also contained in the VDI compressor specifications according to Reference 3.1.8, only directly measured values are used, it often seems that the average problem is not really touched on, or is avoided in an elegant fashion. Neither is true.

In the "total pressure" method, in addition to Equations (27) and (28) the average total pressure $\bar{P}_t$, as area averaged,

$$\bar{P}_t := \frac{1}{A} \int_A P_t \, dA \tag{30}$$

or, as mass-averaged,

$$\bar{P}_t := \frac{1}{\dot{m}} \int_A P_t \, \rho_s V \, dA \tag{31}$$

is used. In the case of a circular cross section, for a simple numerical evaluation of Equation (30), the total pressure probes are positioned at equal-area radii. Then the measured total pressures can be averaged arithmetically. Unfortunately, test engineers use this method also in cases where P_s and T_t are not constant across the cross section. For the average static pressure $\bar{P}_s$ they use the arithmetic mean of the values obtained from the hub and from the outer casing and obtain the average total temperature $\bar{T}_t$ from arithmetically averaged equal-area values. An extensive discussion of the "continuity" and the "total pressure" method, as compared to the averaging technique based on "Complete Equilibrium", is contained in Reference 3.1.10 for swirl-free channel flows.

3.1.1.2 Three-Dimensional Turbomachine Flow

In contrast to the one-dimensional channel flow, where continuity considerations predominate for determining average velocity according to Section 3.1.1.1, it is to be expected that the energetic velocity averages will predominate for turbomachine flow.

If we use a cylindrical coordinate system with the three coordinates r, Θ, and z, where the z axis coincides with the axis of the machine, the energy averaging rules for the three components of the absolute velocity V are as follows:–

$$\bar{V}^2_{rE} := \frac{1}{\dot{m}} \int_A V_r^2 \, \rho_s V_n \, dA \, , \tag{32a}$$

$$\bar{V}^2_{\theta E} := \frac{1}{\dot{m}} \int_A V_\theta^2 \, \rho_s V_n \, dA \, , \tag{32b}$$

$$\bar{V}_{zE}^2 := \frac{1}{\dot{m}} \int_A V_z^2 \rho_s V_n \, dA \, . \tag{32c}$$

Here for the mass flow $\dot{m}$

$$\dot{m} = \int_A \rho_s V_n \, dA \tag{33}$$

if, according to Figure 3.1.4 the velocity component V_n is normal to area A.

Because it may be necessary to represent all the relations relevant to the problem by means of average values without using correction factors, it must be checked if the average velocity values based on energy satisfy the vectorial kinematic condition

$$\underline{V} = \underline{\omega} \times \underline{r} + \underline{W} \, . \tag{34}$$

According to Reference 3.1.6 (2nd edition) and Reference 3.1.9, this is not true for the expression valid circumferentially

$$V_\theta = \omega r + W_\theta \, , \tag{35}$$

if the averaging rule from Equation (32) for the circumferential velocity $U = \omega r$, or because ω = constant, for the radius r in the form

$$\bar{r}_E^2 = \frac{1}{\dot{m}} \int_A r^2 \rho_s V_n \, dA \tag{36}$$

is used. From Equation (35) we get two expressions for

$$\bar{V}_{\theta E}^2 = \frac{1}{\dot{m}} \int_A V_\theta^2 \rho_s V_n \, dA = \frac{1}{\dot{m}} \int_A (\omega r + W_\theta)^2 \rho_s V_n \, dA$$

$$\bar{V}_{\theta E}^2 = \omega^2 \bar{r}_E^2 + \frac{2\omega}{\dot{m}} \int_A r W_\theta \rho_s V_n \, dA + \bar{W}_{\theta E}^2 \tag{37}$$

and

$$\bar{V}_{\theta E}^2 = \omega^2 \bar{r}_E^2 + 2\omega \bar{r}_E \bar{W}_{\theta E} + \bar{W}_{\theta E}^2$$

$$\bar{V}_{\theta E}^2 = \omega^2 \bar{r}_E^2 + \frac{2\omega}{\dot{m}} \sqrt{\int_A r^2 \rho_s V_n \, dA} \sqrt{\int_A W_\theta^2 \rho_s V_n \, dA} + \bar{W}_{\theta E}^2 \, . \tag{38}$$

The above expressions are not identical.

On the other hand, Equation (35) is satisfied by average velocity values on a momentum basis

$$\bar{V}_{rI} := \frac{1}{\dot{m}} \int_A V_r \rho_s V_n \, dA \tag{39a}$$

$$\bar{V}_{\theta I} := \frac{1}{\dot{m}} \int_A V_\theta \rho_s V_n \, dA \tag{39b}$$

$$\bar{V}_{zI} := \frac{1}{\dot{m}} \int_A V_z \rho_s V_n \, dA \tag{39c}$$

according to Reference 3.1.6 (2nd edition), if one averages the circumferential velocity $U = \omega r$ or the radius r

$$\bar{r}_I := \frac{1}{\dot{m}} \int_A r \rho_s V_n \, dA \tag{40}$$

on a momentum basis according to Equation (39). From Equation (35) we get

$$\bar{V}_{\theta I} = \frac{1}{\dot{m}} \int_A V_\theta \rho_s V_n \, dA = \frac{1}{\dot{m}} \int_A (\omega r + W_\theta) \rho_s V_n \, dA$$

$$\bar{V}_{\theta I} = \omega \bar{r}_I + \bar{W}_{\theta I} \, . \tag{41}$$

For the stationary relative flow in a turbomachine rotor rotating with constant angular velocity, the energy equation is

$$\int_{A_e} h_{Rot\,e}\rho_{se}V_{ne}\,dA_e - \int_{A_i} h_{Rot\,i}\rho_{si}V_{ni}\,dA_i = \dot{W}_{Fi-e} + \dot{Q}_{i-e} \ . \tag{42}$$

Here $\dot{Q}_{i-e}$ denotes the heat conducted in or out per unit time and $\dot{W}_{Fi-e}$ the mechanical power of the friction forces which, according to Figure 3.1.4, arise in the co-rotating control volume in the relative system. If the relative velocity $\underline{w}$ in the rothalpy term appearing in Equation (42)

$$h_{Rot} := h_s + \frac{W^2}{2} - \frac{(\omega r)^2}{2} \tag{43}$$

is replaced by the absolute velocity $\underline{V}$, with the aid of the kinematic condition in Equation (34), with

$$h_{Rot} = h_s + \frac{V^2}{2} - \omega r V_\theta \tag{44}$$

we can write the following expression for the energy equation

$$\int_{A_e}\left(h_{se} + \frac{V_e^2}{2}\right)\rho_{se}V_{ne}\,dA_e - \int_{A_i}\left(h_{si} + \frac{V_i^2}{2}\right)\rho_{si}\,V_{ni}\,dA_i =$$

$$= \omega\left\{\int_{A_e} r_e V_{\theta e}\rho_{se}V_{ne}\,dA_e - \int_{A_i} r_i V_{\theta i}\rho_{si}V_{ni}\,dA_i\right\} + \dot{W}_{Fi-e\,rel} + \dot{Q}_{i-e\,rel} \ . \tag{45}$$

The subscript "rel" in $\dot{W}_{Fi-e}$ and $\dot{Q}_{i-e}$ emphasizes that Equation (45) is still valid for the relative system in spite of the transformation. Assuming adiabatic flow and neglecting the mechanical power of the frictional forces arising at the boundaries of the co-rotating control volume, Equation (45) simplifies to

$$P_{mech} = \int_{A_e}\left(h_{se} + \frac{V_e^2}{2}\right)\rho_{se}V_{ne}\,dA_e - \int_{A_i}\left(h_{si} + \frac{V_i^2}{2}\right)\rho_{si}V_{ni}\,dA_i =$$

$$= \omega\left\{\int_{A_e} r_e V_{\theta e}\rho_{se}V_{ne}\,dA_e - \int_{A_i} r_i V_{\theta i}\rho_{si}V_{ni}\,dA_i\right\} \ , \tag{46}$$

where P_{mech} denotes the mechanical power transferred by the rotor and referred to the absolute system. The second part of Equation (46), which is known as Euler's turbomachine equation, represents a central relationship in turbomachine theory because of its kinematic content together with energy transfer.

To represent the swirl flows in Euler's turbomachine equation by the momentum-averaged circumferential components $\bar{V}_{\theta I}$ according to Equation (39), it is necessary to define a reference radius r_{REF}

$$\bar{r}_{REF} := \frac{\int_A r V_\theta \rho_s V_n\,dA}{\bar{V}_{\theta I}} \tag{47}$$

With r_{REF} we express the second part of Equation (46) by

$$P_{mech} = \omega\{(\bar{r}_{REF}\bar{V}_{\theta I})_e - (\bar{r}_{REF}\bar{V}_{\theta I})_i\}\dot{m} \ . \tag{48}$$

According to Reference 3.1.6 (2nd edition) a noticeable difference may exist between $\bar{U}_I = \omega\bar{r}_I$ and $\bar{U}_{REF} = \omega\bar{r}_{REF}$ depending on swirl distribution. In order to eliminate this problem, the suggestion is made in Reference 3.1.14, Reference 3.1.6 (3rd edition) and in Reference 3.1.9 to use swirl averaging instead of momentum averaging, both for the circumferential components of the absolute and relative velocity

$$\bar{r}_D\bar{V}_{\theta D} := \frac{1}{\dot{m}}\int_A r V_\theta \rho_s V_n\,dA \ , \tag{49}$$

$$\bar{r}_D\bar{W}_{\theta D} := \frac{1}{\dot{m}}\int_A r W_\theta \rho_s V_n\,dA \tag{50}$$

and for the circumferential velocity and radius

$$\bar{r}_D^2 := \frac{1}{\dot{m}}\int_A r^2\rho_s V_n\,dA \ . \tag{51}$$

momentum equation

$$\dot{I} = \int_A (\rho_s V^2 + P_s) dA = (\bar{\rho}_s \bar{V}^2 + \bar{P}_s) A \ , \tag{65}$$

energy equation

$$\dot{E} = \int_A \left(h_s + \frac{V^2}{2}\right) \rho_s V dA = \left(\bar{h}_s + \frac{\bar{V}^2}{2}\right) \bar{\rho}_s \bar{V} A \ . \tag{66}$$

In addition to the caloric equation of state

$$\bar{h}_s = \bar{h}_s(\bar{P}_s, \bar{\rho}_s) \tag{67}$$

four equations are available for determining the four unknowns $\bar{P}_s$, $\bar{\rho}_s$, $\bar{h}_s$ and $\bar{V}$.

For a real fluid, a closed solution of Equations (64) to (67) is not possible. The necessary iteration can, for example, be carried out in the following sequence:

(1) assumption of $\bar{V}$,

(2) $\bar{\rho} = \dfrac{\dot{m}}{\bar{V} A}$, continuity equation

(3) $\bar{P}_s = \dfrac{\dot{I} - \dot{m}\bar{V}}{A}$ momentum equation

(4) $\bar{h}_{sS} = \bar{h}_s(\bar{P}_s, \bar{\rho}_s)$, caloric equation of state

(5) $h_{sE} = \dfrac{\dot{E}}{\dot{m}} - \dfrac{\bar{V}^2}{2}$, energy equation

(6) $F: = \left| 1 - \dfrac{\bar{h}_{ss}}{\bar{h}_{sE}} \right| \leqslant \epsilon$. convergence condition

If the temperature dependency of the specific heats for an ideal gas are to be considered, then an iterative solution is also necessary.

A trivial exception is found for the incompressible fluid, where $\bar{\rho} = \rho$ = constant, whose caloric equation of state is as follows for the specific enthalpy

$$h_s = h_{REF} + \int_{T_{REF}}^{T} C_{fl}(T) DT + \frac{P_s - P_{REF}}{\rho} \ . \tag{68}$$

For this special case, all unknowns can be determined in sequence from Equations (64) to (66)

$$\bar{V} = \frac{\dot{m}}{\rho A} \ , \tag{69}$$

$$\bar{P}_s = \frac{\dot{I} - \dot{m} V}{A} \ , \tag{70}$$

$$\bar{h}_s = \frac{\dot{E}}{\dot{m}} - \frac{\bar{V}^2}{2} \ . \tag{71}$$

If, according to Reference 3.1.6, a compressible fluid can be approximated by an ideal vapour with constant isentropic exponent k†, then, with the aid of the caloric equation of state for the specific enthalpy

$$h_s = \frac{k}{k-1} \frac{P_s}{\rho_s} \tag{72}$$

† The generally valid relation for the isentropic exponent k is as follows

$$k: = \frac{\rho_s}{P_s} \left(\frac{\partial P_s}{\partial \rho_s}\right)_{is} = \frac{\rho_s}{P_s} \left(\frac{\partial P_s}{\partial \rho_s}\right)_T \frac{C_p}{C_v} \ ,$$

so that for an ideal gas based on the Boyle-Mariotte law the following is valid

$$k = \gamma = \frac{C_p(T)}{C_v(T)} \ .$$

and the thermal equation of state

$$\frac{P_s}{\rho_s} = z R T_s \ , \tag{73}$$

a closed solution is possible. Here in Equation (72) the constant of integration of the specific enthalpy has already been taken into account and the factor for a real gas in Equation (73) depends only on the entropy $z = z(s)$.

From Equations (64) to (66) and Equation (72) we get

$$\frac{\bar{P}_s}{\rho_s} = \frac{\dot{I}}{\dot{m}} \bar{V} - \bar{V}^2 = \frac{k-1}{k}\left\{\frac{\dot{E}}{\dot{m}} - \frac{\bar{V}^2}{2}\right\}$$

and thus

$$\bar{V}^2 - \frac{2k}{k-1}\frac{\dot{I}}{\dot{m}}\bar{V} + 2\frac{k-1}{k+1}\frac{\dot{E}}{\dot{m}} = 0 \ . \tag{74}$$

Equation (74) has two solutions

$$\bar{V}_{1/2} = \frac{k}{k+1}\frac{\dot{I}}{\dot{m}} \pm \sqrt{\left(\frac{k}{k+1}\frac{\dot{I}}{\dot{m}}\right)^2 - 2\frac{k-1}{k+1}\frac{\dot{E}}{\dot{m}}} \ . \tag{75}$$

If we consider the critical velocity of sound a_s^* which, for an ideal vapour, has the following expression

$$\bar{a}_s^{*2} = 2\frac{k-1}{k+1}\bar{h}_t = 2\frac{k-1}{k+1}\frac{\dot{E}}{\dot{m}} \tag{76}$$

then, because

$$\bar{V}_1 \bar{V}_2 = 2\frac{k-1}{k+1}\frac{\dot{E}}{\dot{m}} = \bar{a}_s^{*2} \tag{77}$$

we get the (+) sign in front of the radical representing the compression solution of the shock and the (−) sign representing the expansion solution.

For subsonic flow, the (+)-sign in front of the radical contradicts the second law of thermodynamics. Thus, for the average velocity $\bar{V}$, the following is valid

$$\bar{V} = \frac{k}{k+1}\frac{\dot{I}}{\dot{m}} - \sqrt{\left(\frac{k}{k+1}\frac{\dot{I}}{\dot{m}}\right)^2 - 2\frac{k-1}{k+1}\frac{\dot{E}}{\dot{m}}} \ . \tag{78}$$

All other state values can be determined successively from Equations (64) to (66).

Using the isentropic exponent equal to the ratio of specific heat capacities $k = \gamma = C_p/C_v$ in Equation (72), and the real gas factor $z = 1$ in Equation (73), the closed solution is also valid for a calorically ideal gas with C_p = constant.

Under the assumption that in the measurement or the calculation plane the total temperature and the static pressure are constant, M.D.Wyatt has presented this averaging method in Reference 3.1.10 for a calorically ideal gas employing the gas-dynamic functions.

Taking a calorically ideal gas with C_p = constant, then, on the basis of the following assumptions:

$$T_t = \text{constant} = \bar{T}_t \quad \text{and}$$

$$P_s = \text{constant} \neq \bar{P}_s$$

the continuity as well as the momentum equation can be described in the following form with the aid of both gas-dynamic functions

flow rate

$$\phi: = \frac{\dot{m}\sqrt{RT_t}}{AP_s} = \rho_s V \frac{\sqrt{RT_t}}{P_s} \quad \text{and} \tag{79}$$

momentum

$$B: = \frac{\dot{I}}{AP_s} = \frac{\rho_s V^2 + P_s}{P_s} \tag{80}$$

as follows:

Using this averaging definition based on swirl, which because of

$$\bar{r}_D V_{\theta D} = \frac{1}{\dot{m}} \int_A r V_\theta \rho_s V_n \, dA = \frac{1}{\dot{m}} \int_A r(\omega r + W_\theta) \rho_s V_n \, dA$$

$$\bar{r}_D \bar{V}_{\theta D} = \omega \bar{r}_D^2 + \bar{r}_D \bar{W}_{\theta D} \tag{52}$$

satisfies the kinematic condition in a circumferential direction in Equation (34), Euler's turbomachinery equation becomes

$$P_{mech} = \omega \{ (\bar{r}_D \bar{V}_{\theta D})_e - (\bar{r}_D \bar{V}_{\theta D})_i \} \dot{m} \tag{53}$$

instead of Equation (48).

Using swirl averaging according to Equations (49) to (51), only the second part of Equation (46) can be expressed simply by average values. If one formulates the first part of Equation (46) in terms of average values, this is possible without using correction factors only when, besides the mass-averaged static enthalpy

$$h_s := \frac{1}{\dot{m}} \int_A h_s \rho_s V_n \, dA \tag{54}$$

average energy values for the velocity components according to Equation (32) are used. Energetic average velocity values appear in all definitions for total efficiencies, too. This is opposed by the fact that energy-based average velocity values do not satisfy the kinematic condition posed by Equation (35).

To avoid introducing correction factors in the energy relations, W.Traupel (Ref.3.1.6) defines an "ideal" static enthalpy $\tilde{h}_s$

$$\tilde{h}_s + \frac{\bar{V}_I^2}{2} := \bar{h}_s + \frac{\bar{V}_E^2}{2} \tag{55}$$

with

$$\bar{V}_I^2 := \bar{V}_{rI}^2 + \bar{V}_{\theta I}^2 + \bar{V}_{zI}^2 \tag{56}$$

for the channel flow and

$$\bar{V}_I^2 := \bar{V}_{rI}^2 + \bar{V}_{\theta D}^2 + \bar{V}_{zI}^2 \tag{57}$$

for the turbomachine flow according to Reference 3.1.6 (3rd edition).

For Traupel's proposal a in Section 3.1.1.1, where the average internal state is determined by the area-averaged static pressure $\bar{P}_s$ and the mass-averaged static enthalpy $\bar{h}_s$, we obtain an "ideal" static entropy $\tilde{s}$

$$\tilde{s} := \tilde{s}(\bar{h}_s, \bar{P}_s) \tag{58}$$

and an ideal static density $\tilde{\rho}_s$

$$\tilde{\rho}_s := \tilde{\rho}(\bar{h}_s, \bar{P}_s) , \tag{59}$$

for example.

It is now easy to prove that $\bar{V}_I \leqslant \bar{V}_E$. Hence, it follows that always $\tilde{h}_s \geqslant \bar{h}_s$ and $\tilde{s} \geqslant \bar{s}$. Figure 3.1.5 shows the change in state in a turbomachine rotor in the h, s diagram. The plotted difference between the average energy-based change of state and the "ideal" average change of state has only a qualitative character.

The error introduced into the continuity equation by the use of the "ideal" static density $\tilde{\rho}_s$ is taken into account by the correction factors ϵ_{CI} and $\tilde{\epsilon}_{CI}$, as dictated by the use of $\bar{V}_{nI}$

$$V_{nI} := \frac{1}{\dot{m}} \int_A \rho_s V_n^2 \, dA . \tag{60}$$

From the continuity equation formulated from average values

$$\dot{m} = \int_A \rho_s V_n \, dA = \bar{\rho}_s \epsilon_{CI} \bar{V}_{nI} A = \tilde{\rho}_s \tilde{\epsilon}_{CI} V_{nI} A \tag{61}$$

we obtain for the two correction factors ϵ_{CI} and $\tilde{\epsilon}_{CI}$

$$\epsilon_{CI} := \frac{\int_A \rho_s V_n \, dA}{\bar{\rho}_s(\bar{h}_s, \bar{s}) V_{nI} A} \tag{62}$$

and

$$\tilde{\epsilon}_{CI} := \frac{\int_A \rho_s V_n \, dA}{\tilde{\rho}_s(\tilde{h}_s, \tilde{s}) \bar{V}_{nI} A} \tag{63}$$

The introduction of these ideal state values eliminates only the need for correction factors in the energy equation. It is still necessary either to introduce correction factors or to use different average value definitions for the velocity components in the continuity and the momentum equations.

3.1.2 Averaging Method Based on "Complete Equilibrium"

Using this method of averaging, the non-homogeneous flow condition in the measurement or calculation plane is converted into a state of "Complete Equilibrium" by means of the conservation laws for mass, momentum, and energy. This is the method used in nearly all two-dimensional cascade experiments today.

The condition of "Complete Equilibrium" is characterized by the fact that the viscous fluid is in a state of equilibrium, both mechanically and thermally. This means that neither momentum nor energy exchange takes place between the individual fluid particles. If, for instance, the fluid has a swirl component, then only pressure forces normal to the velocity vector are allowable which effect the required change in direction of the circumferential component of the velocity vector. In order to avoid the normal and tangential stresses arising from viscosity, it is necessary that the fluid behaves as a solid body. As a condition for thermal equilibrium, the static temperature has to be constant. Then no heat transfer as a result of conduction or radiation takes place.

For the three types of flow

- swirl-free channel flow with constant cross section
- two-dimensional cascade flow and
- co-axial swirl flow

treated more extensively below, the conditions arranged in Table 3.1.IV result. Inserting these flow conditions into the constitutive equations given in Appendix 2 for cartesian and cylindrical coordinates, all viscosity-dependent stresses disappear and no heat transfer takes place.

In order to describe the effects of a system in whose exit plane the averaging method is used quantitatively accurately by the state values of "Complete Equilibrium", the integrals of the conservation quantities – mass, momentum, swirl and energy – have to be equal at the inlet and exit of the control volume in which the irreversible mixing process occurs. Considering that the irreversible mixing process occurs in a real settling channel of infinite length, then the condition of "Complete Equilibrium" will not be reached, because of wall boundary layers. Thus, as a matter of definition, the no-slip condition existing on a real wall should be neglected, without limiting the effect of viscosity necessary for an irreversible mixing process.

In order to make this abstraction clearer, according to L.S.Dzung in Reference 3.1.14, one should simply imagine that the mixing process occurs in a discontinuity plane similar to a compression shock. Thus, the additional condition that the inlet and exit plane areas of the control volume are equal is satisfied automatically. The fact that the system of equations resulting from the conservation laws produces two solutions underlines the analogy to the compression shock. For subsonic flow, one solution contradicts the second law of thermodynamics and, for supersonic flow, a strong and a weak solution arise with respect to the irreversible entropy increase.

The following treatment of the individual flow conditions always starts with the assumption that the mixing process occurs within a discontinuity plane.

3.1.2.1 Swirl-Free Channel Flow with Constant Cross Section

The conservation laws for a discontinuity plane within the swirl-free channel flow with constant cross section attain the following state values of "Complete Equilibrium":

continuity equation

$$\dot{m} = \int_A \rho_s V \, dA = \bar{\rho}_s \bar{V} A \, , \tag{64}$$

continuity equation

$$\dot{m} = \int_A \rho_s V dA = \frac{P_s}{\sqrt{RT_t}} \int_A \phi dA = \frac{AP_s}{\sqrt{R\bar{T}_t}} \bar{\phi} \ , \tag{81}$$

momentum equation

$$\dot{I} = \int_A (\rho_s V^2 + P_s) dA = P_s \int_A B dA = A \bar{P}_s \bar{B} \ . \tag{82}$$

The numerical evaluation of the energy equation results from the first assumption.

For the numerical evaluation of the two integrals in Equations (81) and (82), it is only necessary to determine the total pressure profile and the static pressure by means of wall tappings for

$$\phi = \frac{\sqrt{\frac{2\gamma}{\gamma-1}\left\{1-\left(\frac{P_s}{P_t}\right)^{(\gamma-1)/\gamma}\right\}}}{\left(\frac{P_s}{P_t}\right)^{(\gamma-1)/\gamma}} \tag{83}$$

and

$$B = 1 + \frac{2\gamma}{\gamma-1}\left\{\left(\frac{P_t}{P_s}\right)^{(\gamma-1)/\gamma} - 1\right\} \ . \tag{84}$$

Using the critical Mach number dependency of these two gas-dynamic functions

$$\phi = \frac{\sqrt{\frac{2\gamma}{\gamma+1}}\, M^*}{1-\frac{\gamma-1}{\gamma+1} M^{*2}} \tag{85}$$

and

$$B = \frac{1+M^{*2}}{1-\frac{\gamma-1}{\gamma+1} M^{*2}} \tag{86}$$

then, in contrast to Reference 3.1.10, a closed solution is possible for the average critical Mach number M^*

$$\frac{1+\bar{M}^{*2}}{\sqrt{\frac{2\gamma}{\gamma+1}}\, \bar{M}^*} = \frac{\bar{B}}{\bar{\phi}} = \frac{\dot{I}}{\dot{m}\sqrt{R\bar{T}_t}}$$

$$\bar{M}^*_{1/2} = \sqrt{\frac{\gamma}{2(\gamma+1)R\bar{T}_t}} \frac{\dot{I}}{\dot{m}} \pm \sqrt{\frac{\gamma}{2(\gamma+1)R\bar{T}_t}\left(\frac{\dot{I}}{\dot{m}}\right)^2 - 1} \ . \tag{87}$$

Because $M^*_1 M^*_2 = 1$ for subsonic channel flow, only the (—) sign in front of the radical is compatible with the second law of thermodynamics.

The following relation exists between the constant static pressure P_s in the measuring plane and the average value of the static pressure $\bar{P}_s$

$$\frac{\bar{P}_s}{P_s} = \frac{1}{A} \int_A B dA = \frac{1-\frac{\gamma-1}{\gamma+1}\bar{M}^{*2}}{1+\bar{M}^{*2}} \leqslant 1 \ . \tag{88}$$

3.1.2.2 Two-Dimensional Cascade Flow

The strictly two-dimensional cascade flow is an instructive example for the philosophy of the averaging method based on "Complete Equilibrium". Because of the periodicity condition and the infinite extent of the flow plane normal to the flow, one may indeed imagine that the condition of "Complete Equilibrium" will be attained after an infinitely long run. N.Scholz first presents this averaging method for the two-dimensional incompressible cascade flow in Reference 3.1.11 and J.Amecke first published a closed solution for the two-dimensional compressible cascade flow of

a calorically ideal gas in References 3.1.12 and 3.1.13. As shown in Figure 3.1.6, they both utilize a finite two-dimensional control volume K1 to generate this averaging method for the evaluation of two-dimensional cascade experiments.

For the purpose of uniform presentation, the derivation of an averaging method for two-dimensional cascade flow utilizes a differential control volume in the form of a discontinuity plane, as mentioned above.

Applying the laws of conservation to the discontinuity surface, we obtain the following four equations:

continuity equation

$$\dot{m} = \int_t^{t+p} \rho_{se} V_e \sin\alpha_e \, dt = \bar{\rho}_{se} \bar{V}_e \sin\bar{\alpha}_e \, p \tag{89}$$

momentum equation normal to the cascade front

$$\dot{I}_n = \int_t^{t+p} (\rho_{se} V_e^2 \sin^2\alpha_e + P_{se}) dt = (\bar{\rho}_{se} \bar{V}_e^2 \sin^2\bar{\alpha}_e + \bar{P}_{se}) p \tag{90}$$

momentum equation tangential to the cascade front

$$\dot{I}_t = \int_t^{t+p} \rho_{se} V_e^2 \cos\alpha_e \sin\alpha_e \, dt = \bar{\rho}_{se} \bar{V}_e^2 \cos\bar{\alpha}_e \sin\bar{\alpha}_e \, p \tag{91}$$

energy equation

$$\dot{E} = \int_t^{t+p} \left(h_{se} + \frac{V_e^2}{2}\right) \rho_{se} V_e \sin\alpha_e \, dt = \left(\bar{h}_{se} + \frac{\bar{V}_e^2}{2}\right) \bar{\rho}_{se} \bar{V}_e \sin\bar{\alpha}_e \, p \, . \tag{92}$$

Together with the caloric equation of state according to Equation (67), we again have five equations for the determination of the five unknowns: $\bar{P}_{se}$, $\bar{\rho}_{se}$, $\bar{h}_{se}$, $\bar{V}_e$ and $\bar{\alpha}_e$.

For a real fluid, as well as for an ideal gas taking account of the temperature dependency of the specific heats, this system of equations must also be solved iteratively:

(1) assumption of $(\bar{V}_e \sin\bar{\alpha}_e)$,

(2) $\bar{\rho}_{se} = \dfrac{\dot{m}}{(\bar{V}_e \sin\bar{\alpha}_e) p}$, continuity equation

(3) $\bar{P}_{se} = \dfrac{\dot{I}_n - \dot{m}(\bar{V}_e \sin\bar{\alpha}_e)}{P}$, momentum equation normal to cascade front

(4) $\bar{h}_{seS} = \bar{h}_s(\bar{P}_{se}, \bar{\rho}_{se})$, caloric equation of state

(5) $\bar{V}_e \cos\bar{\alpha}_e = \dfrac{\dot{I}_t}{\dot{m}}$, momentum equation tangential to cascade front

(6) $\bar{h}_{seE} = \dfrac{\dot{E}}{\dot{m}} - \dfrac{\bar{V}_e^2}{2}$, energy equation

(7) $F = \left| 1 - \dfrac{\bar{h}_{seS}}{\bar{h}_{seE}} \right| \leqslant \epsilon$. convergence condition

For an incompressible fluid the four unknowns: $\bar{P}_{se}$, $\bar{h}_{se}$, $\bar{V}_e$ and $\bar{\alpha}_e$ can be determined one after another from Equations (89) to (92)

$$\bar{P}_{se} = \frac{\dot{I}_n}{P} - \frac{1}{\rho}\left(\frac{\dot{m}}{P}\right)^2 , \tag{93}$$

$$\bar{V}_e = \sqrt{\left(\frac{\dot{m}}{\rho p}\right)^2 + \left(\frac{\dot{I}_t}{\dot{m}}\right)^2} , \tag{94}$$

$$\bar{\alpha}_e = \operatorname{arc\,cot}\left(\rho p \frac{\dot{I}_t}{\dot{m}^2}\right), \tag{95}$$

$$\bar{h}_{se} = \frac{\dot{E}}{\dot{m}} - \frac{\bar{V}_e^2}{2}. \tag{96}$$

For a real fluid approximated by an ideal vapour, it follows from Equation (72) as well as from Equations (89) to (92), that a quadratic equation can be obtained for the normal component $(\bar{V}_e \sin \bar{\alpha}_e)$

$$(\bar{V}_e \sin \bar{\alpha}_e)^2 - \frac{2k}{k+1} \frac{\dot{I}_n}{\dot{m}} (\bar{V}_e \sin \bar{\alpha}_e) + 2 \frac{k-1}{k+1} \left\{ \frac{\dot{E}}{\dot{m}} - \frac{1}{2} \left(\frac{\dot{I}_t}{\dot{m}} \right)^2 \right\} = 0 \tag{97}$$

with the two solutions

$$(\bar{V}_e \sin \bar{\alpha}_e)_{1/2} = \frac{k}{k+1} \frac{\dot{I}_n}{\dot{m}} \pm \sqrt{\left(\frac{k}{k+1} \frac{\dot{I}_n}{\dot{m}} \right)^2 - 2 \frac{k-1}{k+1} \left\{ \frac{\dot{E}}{\dot{m}} - \frac{1}{2} \left(\frac{\dot{I}_t}{\dot{m}} \right)^2 \right\}}. \tag{98}$$

In the subsonic region, the (+) sign in front of the radical contradicts the second law of thermodynamics and in the supersonic region the thermodynamic probability is very low.

If we reduce the total enthalpy $\bar{h}_{te}$ by the kinetic energy of the tangential component $(V_e \cos \bar{\alpha}_e)$

$$\bar{h}_{te-n} := \bar{h}_{te} - \frac{(V_e \cos \bar{\alpha}_e)^2}{2} \tag{99}$$

and if we form the critical velocity of sound a^*_{Se-n}, associated with it, analogous to Equation (76)

$$a^{*2}_{Se-n} := 2 \frac{k-1}{k+1} \bar{h}_{te-n} \tag{100}$$

we get the following equation

$$(\bar{V}_e \sin \bar{\alpha}_e)_1 (\bar{V}_e \sin \bar{\alpha}_e)_2 = a^{*2}_{Se-n} \tag{101}$$

analogous to the oblique compression shock.

If the flow towards the cascade in Figure 3.1.6 can be considered homogeneous within the accuracy of measurements and if it is assumed that the cascade flow proceeds adiabatically on the whole, then, because

$$\frac{\dot{E}}{\dot{m}} = \bar{h}_{te} - h_{ti} \tag{102}$$

the numerical evaluation of the energy equation can be omitted. This is true for both incompressible and compressible fluids.

Besides the assumption that the cascade flow proceeds adiabatically on the whole, J.Amecke, in References 3.1.12 and 3.1.13, also neglects the energy exchange between the individual stream lines resulting from friction forces. Then the energy balance for a calorically ideal gas is simplified for $\bar{T}_{te} = T_{te} = \text{constant}$. For this reason, J.Amecke does not use the energy balance as an independent equation in the solution of the system of equations. With the aid of the formulation of the continuity equation, normalized with the gas-dynamic functions, as well as with the two momentum equations, he determines the three unknowns appearing therein, namely $(\bar{P}_{te}/P_{ti})$, $\bar{\alpha}_e$ and $\bar{M}^*_e$. The closed solution consists of a bi-quadratic equation for the average value of the critical Mach number $\bar{M}^*_e$.

N.Scholz also ignores the energy balance in deriving averaging requirements for an incompressible fluid (see Reference 3.1.11). This means that for an incompressible fluid the path-independent dissipation

$$\psi_{i-\bar{e}} = \int_{s_i}^{\bar{s}_e} T \, Ds_{irr} = \int_{T_i}^{\bar{T}_e} C_{fl}(T) \, DT \tag{103}$$

with the aid of the total pressures

$$\psi_{i-\bar{e}} = -\frac{\bar{P}_{te} - P_{ti}}{\rho} \tag{104}$$

can be determined only under the assumption that the flow proceeds adiabatically and isoenergetically.

3.1.2.3 Swirl Flow in a Parallel Annulus

Although swirl flow in a parallel annulus with constant hub and tip radius is not very representative of the general area of turbomachinery flow, it still represents the only possible form of swirl flow which can be treated with averaging methods based on "Complete Equilibrium".

If all the state values of the "Complete Equilibrium" are referenced to the values for the outer casing $\bar{x}^* = \bar{x}/\bar{x}_H$, the total equilibrium state of a given swirl flow in a coaxial annular volume can be characterized by the following five radial distributions:–

Velocity components

radial component $$\bar{V}_r^* = 0\,, \tag{105}$$

circumferential component $$\bar{V}_\theta^* = r^*\,, \tag{106}$$

axial component $$\bar{V}_{Ax}^* = 1\,, \tag{107}$$

Static state

temperature $$\bar{T}^* = 1\,, \tag{108}$$

pressure $$\frac{d\bar{P}_s^*}{dr^*} = \frac{\bar{V}_{\theta H}^2}{\bar{P}_{sH}/\bar{\rho}_{sH}}\rho_s^* r^*\,. \tag{109}$$

Equation (109) results from the simple radial equilibrium valid for $\bar{V}_r^* = 0$.

For $\bar{V}_r^* = 0$ the four starting values $\bar{V}_{\theta H}$, $\bar{V}_{AxH}$, $\bar{T}_{sH}$ and $\bar{P}_{sH}$ of the radial distributions still must be determined for the outer casing. For that purpose the four conservation laws of mass, axial momentum, swirl and energy, applied to the discontinuity surface, are available:

continuity equation

$$\dot{m} = 2\pi\int_{r_B}^{r_H}\rho_s V_{Ax}\,r\,dr = 2\pi\bar{\rho}_{sH}\bar{V}_{AxH}r_H^2\int_\nu^1\bar{\rho}_s^* r^*\,dr^*\,, \tag{110}$$

momentum equation in axial direction

$$\dot{I}_{Ax} = 2\pi\int_{r_B}^{r_H}(\rho_s V_{Ax}^2 + P_s)r\,dr =$$

$$= 2\pi r_H^2\left\{\bar{\rho}_{sH}\bar{V}_{AxH}^2\int_\nu^1\bar{\rho}_s^* r^*\,dr^* + \bar{P}_{sH}\int_\nu^1\bar{P}_s^* r^*\,dr^*\right\}, \tag{111}$$

swirl equation

$$\dot{D} = 2\pi\int_{r_B}^{r_H}\rho_s V_\theta V_{Ax}\,r^2\,dr = 2\pi\bar{\rho}_{sH}\bar{V}_{\theta H}\bar{V}_{AxH}r_H^3\int_\nu^1\bar{\rho}_s^*\bar{V}_\theta^* r^{*2}\,dr^*\,, \tag{112}$$

energy equation

$$\dot{E} = 2\pi\int_{r_B}^{r_H}\rho_s V_{Ax}\left\{h_s + \frac{V_r^2}{2} + \frac{V_\theta^2}{2} + \frac{V_{Ax}^2}{2}\right\}r\,dr =$$

$$= 2\pi\bar{\rho}_{sH}\bar{V}_{AxH}r_H^2\left\{\bar{h}_{sH}\int_\nu^1\bar{\rho}_s^*\bar{h}_s^* r^*\,dr^* + \right.$$

$$\left. + \frac{\bar{V}_{AxH}^2}{2}\int_\nu^1\bar{\rho}_s^* r^*\,dr^* + \frac{\bar{V}_{\theta H}^2}{2}\int_\nu^1\bar{\rho}_s^*\bar{V}_\theta^{2*} r^*\,dr^*\right\}\,. \tag{113}$$

With the thermal equation of state $\rho_s = \rho_s(P_s, T_s)$ and a caloric equation of state, e.g. $h_s = h_s(P_s, \rho_s)$, the system of equations for a real fluid can be solved iteratively. If an incompressible fluid with

$$h_s = u_s(T) + \frac{P_s}{\rho} \tag{114}$$

is treated, the simple radial equilibrium according to Equation (109) yields

$$\bar{P}_s^* = 1 + \rho \frac{\bar{V}_{\theta H}^2}{P_{sH}} \frac{r^{*2} - 1}{2} \quad . \tag{115}$$

In this way, the four starting values of the radial distributions at the outer casing of "Complete Equilibrium" can be determined in succession from the conservation laws in the following order:

continuity equation

$$\dot{m} = 2\pi\rho \bar{V}_{AxH} r_H^2 \int_\nu^1 r^* \, dr^*$$

$$\bar{V}_{AxH} = \frac{\dot{m}}{\pi r_H^2 (1 - \nu^2)\rho} \quad , \tag{116}$$

swirl equation

$$\dot{D} = 2\pi\rho \bar{V}_{AxH} \bar{V}_{\theta H} r_H^3 \int_\nu^1 r^{*3} dr^*$$

$$\bar{V}_{\theta H} = \frac{2\dot{D}}{\pi\rho \bar{V}_{AxH} r_H^3 (1 - \nu^4)} \quad , \tag{117}$$

momentum equation in axial direction

$$\dot{I}_{Ax} = \dot{m} \bar{V}_{AxH} + 2\pi \bar{P}_{sH} r_H^2 \int_\nu^1 \bar{P}_s^* r^* dr^*$$

$$\bar{P}_{sH} = \frac{\dot{I}_{Ax} - \dot{m} \bar{V}_{AxH}}{\pi r_H^2 (1 - \nu^2)} + \rho \bar{V}_{\theta H} \frac{1 - \nu^4}{4} \quad , \tag{118}$$

energy equation

$$\dot{E} = 2\pi\rho \bar{V}_{AxH} r_H^2 \left\{ \bar{u}_{sH} \int_\nu^1 r^* dr^* + \frac{\bar{P}_{sH}}{\rho} \int_\nu^1 \bar{P}_s^* r^* dr^* + \right.$$

$$\left. + \frac{\bar{V}_{AxH}^2}{2} \int_\nu^1 r^* dr^* + \frac{\bar{V}_{\theta H}^2}{2} \int_\nu^1 r^{*3} dr^* \right\}$$

$$\bar{u}_{sH} = \frac{\dot{E} - \dot{I}_{Ax} \bar{V}_{AxH} - \frac{\dot{D} \bar{V}_{\theta H}}{2 r_H}}{\dot{m}} + \frac{\bar{V}^2_{AxH}}{2} \quad . \tag{119}$$

The radiation distributions of all relevant state values of an incompressible fluid are presented in Table 3.1.V. Since the entropy of an incompressible fluid

$$s = s_{REF} + \int_{T_{REF}}^{T} C_{fl}(T) \frac{DT}{T} \tag{120}$$

depends only on the temperature, the specific entropy as well as the total temperature are constant, owing to the constant static temperature.

If a real fluid can be approximated by an ideal gas, from the thermal equation of state

$$\bar{\rho}_s^* = \frac{\bar{P}_s^*}{\bar{T}_s^*} \tag{121}$$

together with Equations (108) and (109), we obtain the same radial distribution for the static density and for the static pressure

$$\bar{\rho}_s^* = \bar{P}_s^* = \exp\left\{ \frac{\bar{V}_{\theta H}^2}{R \bar{T}_{sH}} \frac{r^{*2} - 1}{2} \right\} \quad . \tag{122}$$

Taking into account that for an ideal gas the specific enthalpy

$$h = h_{REF} + \int_{T_{REF}}^{T} C_p(T)\,DT \tag{123}$$

is only a function of temperature, the conservation laws according to Equations (110) to (113) take the following forms:

continuity equation

$$\frac{\dot{m}}{2\pi r_H^2} = \bar{\rho}_{sH}\,V_{AxH} \int_{\nu}^{1} \bar{\rho}_s^* r^* dr^* , \tag{124}$$

momentum equation in axial direction

$$\frac{\dot{I}_{Ax}}{2\pi r_H^2} = \left\{\bar{V}_{AxH} + \frac{R\bar{T}_{sH}}{\bar{V}_{AxH}}\right\}\left\{\bar{\rho}_{sH}\,\bar{V}_{AxH} \int_{\nu}^{1} \bar{\rho}_s^* r^* dr^*\right\} , \tag{125}$$

swirl equation

$$\frac{\dot{D}}{2\pi r_H^2} = r_H\,\bar{V}_{\theta H}\,\bar{\rho}_{sH}\,\bar{V}_{AxH} \int_{\nu}^{1} \bar{\rho}_s^* r^{*3} dr^* , \tag{126}$$

energy equation

$$\frac{\dot{E}}{2\pi r_H^2} = \left\{\bar{h}_{sH} + \frac{\bar{V}_{AxH}^2}{2}\right\}\bar{\rho}_{sH}\,\bar{V}_{AxH} \int_{\nu}^{1} \bar{\rho}_s^* r^* dr^* + \\ + \frac{\bar{V}_{\theta H}^2}{2}\,\bar{\rho}_{sH}\,\bar{V}_{AxH} \int_{\nu}^{1} \bar{\rho}_s^* r^{*3} dr^* , \tag{127}$$

This formulation of the conservation laws allows easier recognition of the iterative solution method. With the closed solution of the two integrals (see Appendix 3)

$$F_1 := \int_{\nu}^{1} \bar{\rho}_s^* r^* dr^*$$

$$F_1 = \frac{R\bar{T}_{sH}}{\bar{V}_{\theta H}^2}\left\{1 - \exp\left[\frac{\bar{V}_{\theta H}^2}{R\bar{T}_{sH}}\,\frac{\nu^2 - 1}{2}\right]\right\} \tag{128}$$

$$F_2 := \int_{\nu}^{1} \bar{\rho}_s^* r^{*3} dr^*$$

$$F_2 = \frac{R\bar{T}_{sH}}{\bar{V}_{\theta H}^2}\left\{1 - \nu^2 \exp\left[\frac{\bar{V}_{\theta H}^2}{R\bar{T}_{sH}}\,\frac{\nu^2 - 1}{2}\right] - 2F_1\right\} \tag{129}$$

the system of equations can be solved iteratively in the following way:

(1) assumption of $\bar{V}_{AxH}$

(2) $\bar{T}_{sH} = \frac{\bar{V}_{AxH}}{R}\left\{\frac{\dot{I}_{Ax}}{\dot{m}} - \bar{V}_{AxH}\right\}$ moment equation in axial direction

(3) $\bar{h}_{sH} = \bar{h}(\bar{T}_{sH})$ caloric equation of state

(4) $\bar{V}_{\theta H} = 2\frac{r_H}{\dot{D}}\left\{\dot{E} - \left(\bar{h}_{sH} + \frac{\bar{V}_{AxH}^2}{2}\right)\dot{m}\right\}$ energy equation

(5) $(\bar{\rho}_{sH}\,\bar{V}_{AxH})_C = \frac{\dot{m}}{2\pi r_H^2 F_1}$ continuity equation

(6) $(\bar{\rho}_{sH}\,\bar{V}_{AxH})_D = \frac{\dot{D}}{2\pi r_H^3 \bar{V}_{\theta H} F_2}$ swirl equation

$$(7)\quad F = \left| 1 - \frac{(\rho_{sH} V_{AxH})_D}{(\bar{\rho}_{sH} V_{AxH})_C} \right| \leqslant \epsilon \qquad \text{convergence condition}$$

The radial distributions of the state values for constant specific heat capacities are presented in Table 3.1.V.

This demonstrates that the averaging method based on "Complete Equilibrium" has only little practical importance for a given swirl flow in a coaxial annular volume in the light of one-dimensional evaluation of test results.

The utility of the averaging method based on "Complete Equilibrium" for turbomachines is limited to a very great extent by the fact that a stress-free state in the rotationally symmetric flow of a viscous fluid occurs only when the fluid moves as an inelastic body, i.e. without radial velocity components. For this reason, this method of averaging cannot be employed for turbomachines with diagonal or radial flows.

3.1.3 The "Consistent Averaging Method" by L.S.Dzung

The averaging method presented by L.S.Dzung in Reference 3.1.14 for three-dimensional turbomachine flow can be placed in the second group of averaging methods based on "Complete Equilibrium", because the system of equations results from the conservation laws.

However, since the average state does not correspond to the state of "Complete Equilibrium", if the radial and the circumferential components of the absolute velocity are not equal to zero, the method designated by L.S.Dzung as "consistent" is placed in the first group of averaging methods based on "Integral System Effects". The main advantage of Dzung's "Consistent Averaging Method", in contrast to the first group is that correction factors are not required.

L.S.Dzung formulates the following conservation equations for the rotating relative system for the discontinuity surface shown in Figure 3.1.7:

continuity equation

$$\dot{m} = \int_A \rho_s W_m \, dA = \bar{\rho}_s \bar{W}_m A \,, \tag{130}$$

momentum equation in direction of meridian

$$I_m = \int_A (\rho_s W_m^2 + P_s) dA = (\bar{\rho}_s \bar{W}_m^2 + \bar{P}_s) A \,, \tag{131}$$

swirl equation

$$\dot{D} = \int_A r(\omega r + W_\theta) \rho_s W_m \, dA = \bar{r}(\omega \bar{r} + \bar{W}_\theta) \bar{\rho}_s \bar{W}_m A \,, \tag{132}$$

energy equation

$$\dot{E}_{Rot} = \int_A \left(h_s + \frac{W^2}{2} - \frac{(\omega r)^2}{2} \right) \rho_s W_m \, dA = \left(\bar{h}_s + \frac{\bar{W}^2}{2} - \frac{(\omega \bar{r})^2}{2} \right) \bar{\rho}_s \bar{W}_m A \,. \tag{133}$$

The bar above the symbol again denotes the "representative" average state. If we set $\omega = 0$ and formally write V in place of W, Equations (130) to (133) are also valid for the absolute system. It must also be noted that only the meridian and circumferential components of the relative or absolute velocity appear in the conservation equations. L.S.Dzung explains this by the fact that the position of the discontinuity surface A must be chosen in this way so that the integral for the component W_A in the direction of the straight line trace of the discontinuity surface A must become zero

$$\int_A \rho_s W_A \, dA \approx 0 \,. \tag{134}$$

Together with the caloric equation of state according to (67) $\bar{h}_s = \bar{h}_s(\bar{\rho}_s, \bar{P}_s)$ there are available only five equations for the six unknowns $\bar{P}_s$, $\bar{\rho}_s$, $\bar{h}_s$, $\bar{W}_m$, $\bar{W}_\theta$ and $\bar{r}$. In order to obtain a solution L.S.Dzung postulates that all terms of the kinematic condition in a circumferential direction according to Equation (35) should be averaged on a swirl basis. This means the same as the additional requirement that in Equation (132) the corresponding terms on both sides are equal, i.e. that

$$\int_A r W_\theta \rho_s W_m \, dA = \bar{r} \bar{W}_\theta \bar{\rho}_s \bar{W}_m A \tag{135}$$

and

$$\int_A \omega r^2 \rho_s W_m \, dA = \omega \bar{r}^2 \bar{\rho}_s W_m A \ . \tag{136}$$

Equations (135) and (136) do not follow from the swirl equations and thus contain an arbitrary factor. Using the average radius $\bar{r}$ defined in this manner from Equation (136) which corresponds to Equation (51), the conservation equations result in:

$$\bar{\rho}_s W_m = \frac{\dot{m}}{A} \ , \tag{137}$$

$$\rho W_m^2 + \bar{P}_s = \frac{\dot{I}_m}{A} \ , \tag{138}$$

$$\rho_s \bar{W}_m \bar{W}_\theta = \frac{1}{A}\left\{\frac{\dot{D}}{\bar{r}} - \omega \bar{r} \dot{m}\right\} \ , \tag{139}$$

$$\bar{\rho} \bar{W}_m \left\{h_s + \frac{\bar{W}^2}{2}\right\} = \frac{1}{A}\left\{\dot{E}_{Rot} + \frac{(\omega \bar{r})^2}{2} \dot{m}\right\} \ . \tag{140}$$

The solution of this system of equations corresponds to that for the two-dimensional cascade flow shown in Section 3.1.2.2. For an ideal vapour the closed solution becomes

$$W_{m1/2} = \frac{k}{k+1} \frac{\dot{I}_m}{\dot{m}} \pm \sqrt{\left(\frac{k}{k+1} \frac{\dot{I}_m}{\dot{m}}\right)^2 - 2 \frac{k-1}{k+1}\left[\frac{\dot{E}_{Rot}}{\dot{m}} + \frac{(\omega \bar{r})^2}{2} - \frac{\bar{W}_\theta^2}{2}\right]} \ . \tag{141}$$

Here again the (+) sign in front of the radical contradicts the second law of thermodynamics in the subsonic region and possesses little thermodynamic reality in the supersonic region.

The solution methodology analogous to that for the two-dimensional cascade flow does not mean that the average flow conditions automatically satisfy thermal and mechanical equilibrium. Only the swirl-free channel flow with constant cross section treated in Section 3.1.2.1 and the two-dimensional cascade flow shown in Section 3.1.2.2 are included as special cases in the averaging method of L.S.Dzung. Having a flow with radial or circumferential component for the absolute velocity in a cylindrical coordinate system, the average state defined by Equations (137) to (140) gives quantitatively correct answers for the "Integral System Effect" of the values subject to conservation principles. In these cases, the entropy increase occurring in the discontinuity surface cannot be interpreted as a real mixing loss.

Applying the averaging method of L.S.Dzung to a turbomachine stage with nearly swirl-free inflow and outflow, the flow condition in the blade-free plane between guide vane and impeller is distorted by the use of average values depending on swirl distribution, because the mixing losses are charged to the particular system under consideration.

TABLE 3.1.I

Equations of State of the Idealizations; Incompressible Fluid and Ideal Gas

	Incompressible fluid	*Ideal gas*
Thermal equation of state	$\rho = \text{const}$	$\rho = \dfrac{P}{RT}$
Caloric equation of state		
Spec. internal energy	$u = u_{REF} + u^*(T);\ u^*(T): = \int_{T_{REF}}^{T} C_{fl}(T)DT$	$u = u_{REF} + u^*(T);\ u^*(T): = \int_{T_{REF}}^{T} C_v(T)DT$
Spec. enthalpy	$h = h_{REF} + u^*(T) + \dfrac{P - P_{REF}}{\rho}$	$h = h_{REF} + h^*(T);\ h^*(T): = \int_{T_{REF}}^{T} C_p(T)DT$
Spec. entropy	$s = s_{REF} + s^*(T);\ s^*(T): = \int_{T_{REF}}^{T} C_{fl}(T)\,\dfrac{DT}{T}$	$s = s_{REF} + R\left\{s_p^*(T) - \ln\dfrac{P}{P_{REF}}\right\};\ s_p^*(T): = \int_{T_{REF}}^{T} \dfrac{C_p(T)}{R}\,\dfrac{DT}{T}$
		$s = s_{REF} + R\ln\left\{\dfrac{\pi_s(T)}{P/P_{REF}}\right\}$
Isentropic pressure function		$\pi_s := \exp\left\{\int_{T_{REF}}^{T} \dfrac{C_p(T)}{R}\,\dfrac{DT}{T}\right\}$

TABLE 3.1.II

Comparison of the Averaging Suggestions for Swirl-free Steady Channel Flow According to References 3.1.2 to 3.1.5

Definition and basic equation	*Suggestions of A.J.W.Smith in Reference 3.1.2*	*Suggestions of J.L.Livesey/T.Hugh in References 3.1.3 and 3.1.4*	*Suggestions of R.D.Tyler in Reference 3.1.5*
Thermal equation of state	$\frac{\bar{P}}{R\bar{\rho}\bar{T}} := \zeta$ $\zeta = 1$ for $P = \text{const}^{\dagger}$	$\frac{\bar{P}}{R\bar{\rho}\bar{T}} = 1$	$\frac{\bar{P}}{R\bar{\rho}\bar{T}} = 1$
Average static pressure	$\bar{P}_s := \frac{1}{A}\int_A P_s dA$	$\bar{P}_s = \bar{P}_s(h_s, s)^{\triangle}$	$\bar{P}_s := P_s = \text{const}^{\square}$
Average static density	$\bar{\rho}_s := \frac{\int_A \rho_s V dA}{\int_A V dA}$	$\bar{\rho}_s = \bar{\rho}_s(\bar{h}_s, \bar{s})$	$\bar{\rho}_s := \frac{1}{A}\int_A \rho_s dA$
Average static temperature	$\bar{T}_s = \bar{T}_s(\bar{h}_s)$	$\bar{T}_s = \bar{T}_s(\bar{h}_s)$	$\bar{T}_s = \frac{\bar{P}_s}{R\bar{\rho}_s}$ $\frac{1}{\bar{T}_s} = \frac{1}{A}\int_A \frac{1}{T_s} dA^{\circ}$
Average static spec. enthalpy	$\bar{h}_s := \frac{\int_A h_s \rho_s V dA}{\int_A \rho_s V dA}$	$\bar{h}_s := \frac{\int_A h_s \rho_s V dA}{\int_A \rho_s V dA}$	$\bar{h}_s := \frac{\int_A h_s \rho_s V dA}{\int_A \rho_s V dA}$
Average spec. entropy	No statement	$s := \frac{\int_A s \rho_s V dA}{\int_A \rho_s V dA}$	No statement

† with $h = C_p T$ and the gas equation it follows for the correcting factor ζ

$$\zeta := \frac{\bar{P}_s}{R\bar{\rho}_s\bar{T}_s} = \frac{\frac{1}{A}\int_A P_s dA \int_A V dA}{R\int_A T_s \rho_s V dA} = \frac{\int_A P_s dA \int_A V dA}{A\int_A P_s V dA}$$

△ $\bar{P}_s = \bar{P}_t\left(\frac{\bar{T}_s}{\bar{T}_t}\right)^{\gamma/(\gamma-1)}$ for caloric ideal gas with $C_p = \text{const}$

□ R.D.Tyler assumes that the static pressure is constant in the channel cross section concerned

○ the additional definition of average temperature follows from the gas equation together with the definition for $\bar{P}_s$ and it does not agree with the so-called mixing rule contained in the definition of $\bar{h}_s$. Therefore, an additional correction factor $\bar{h}_s = \bar{h}_s(\epsilon_T \bar{T}_s)$ is needed for $\bar{T}_s$ and $\bar{h}_s$.

TABLE 3.1.II (continued)

Comparison of the Averaging Suggestions for Swirl-free Steady Channel Flow According to References 3.1.2 to 3.1.5

Definition and basic equations	*Suggestions of A.J.W.Smith in Reference 3.1.2*	*Suggestions of J.L.Livesey/T.Hugh in References 3.1.3 and 3.1.4*	*Suggestions of R.D.Tyler in Reference 3.1.5*
Average velocity	$\bar{V}: = \frac{1}{A}\int V dA$	$V: = \frac{1}{\bar{\rho}_s A}\int_A \rho_s V dA$	$\bar{V}: = \frac{\int_A \rho_s V dA}{\int_A \rho_s dA}$
Continuity equation $\dot{m}_e - \dot{m}_i = 0$	$\frac{\dot{m}}{A} = \bar{\rho}_s \bar{V}$	$\frac{\dot{m}}{A} = \bar{\rho}_s \bar{V}$	$\frac{\dot{m}}{A} = \bar{\rho}_s \bar{V}$
Momentum equation $\dot{I}_e - \dot{I}_i = \Sigma F$	$\frac{\dot{I}}{A} = \bar{P}_s + \bar{\rho}_s \epsilon_I \bar{V}^2$ $\epsilon_I: = \frac{\int_A \rho_s V^2 dA}{\bar{\rho}_s \bar{V}^2 A}$	$\frac{\dot{I}}{A} = \alpha_I P_s + \bar{\rho}_s \epsilon_I \bar{V}^2$ $\epsilon_I: = \frac{\int_A \rho_s V^2 dA}{\bar{\rho}_s \bar{V}^2 A}$ $\alpha_I: = \frac{1}{\bar{P}_s A}\int_A P_s dA$	$\frac{\dot{I}}{A} = \bar{P}_s + \bar{\rho}_s \epsilon_I \bar{V}^2$ $\epsilon_I: = \frac{\int_A \rho_s V^2 dA}{\bar{\rho} \bar{V}^2 A}$
Energy equation $\dot{E}_e - E_i = \dot{W}_{i-e} + \dot{Q}_{i-e}$	$\frac{\dot{E}}{A} = \bar{\rho}_s \bar{V} \bar{h}_s + \frac{\bar{\rho}_s}{2} \epsilon_E \bar{V}^3$ $\epsilon_E: = \frac{\int_A \rho_s V^3 dA}{\bar{\rho}_s \bar{V}^3 A}$	$\frac{\dot{E}}{A} = \bar{\rho}_s \bar{V} \bar{h}_s + \frac{\bar{\rho}_s}{2} \epsilon_E \bar{V}^3$ $\epsilon_E: = \frac{\int_A \rho_s V^3 dA}{\bar{\rho}_s \bar{V}^3 A}$	$\frac{\dot{E}}{A} = \bar{\rho}_s \bar{V} \bar{h} + \frac{\bar{\rho}_s}{2} \epsilon_E \bar{V}^3$ $\epsilon_E: = \frac{\int_A \rho_s V^3 dA}{\bar{\rho}_s \bar{V}^3 A}$
Average spec. total enthalpy	$\bar{h}_t = \bar{h}_s + \epsilon_E \frac{\bar{V}^2}{2}$	$\bar{h}_t = \bar{h}_s + \epsilon_E \frac{V^2}{2}$	$h_t = h_s + \epsilon_E \frac{V^2}{2}$
Average Mach number	$\bar{M}: = \sqrt{\frac{\bar{V}^2}{\gamma R \bar{T}_s}}$	$\bar{M}: = \sqrt{\frac{\epsilon_E \bar{V}^2}{\gamma R \bar{T}_s}}$	$\bar{M}: = \sqrt{\frac{\epsilon_E \bar{V}^2}{\gamma R \bar{T}_s}}$
Average total temperature	$\bar{T}_t = \bar{T}_t(\bar{h}_t)$	$\bar{T}_t = \bar{T}_t(\bar{h}_t)$	$\bar{T}_t = \bar{T}_t(\bar{h}_t)$
Average total pressure	$\bar{P}_t: = \bar{P}_s\left(\frac{\bar{T}_t}{\bar{T}_s}\right)^{\gamma/(\gamma-1)}$	$\ln \bar{P}_t: = \frac{\int_A \ln P_t \rho_s V dA}{\int_A \rho_s V dA}$	$\ln \bar{P}_t: = \frac{\int \ln P_t \rho_s V dA}{\int \rho_s V dA}$ ◇

◇ for T_t = constant and P_s = constant it follows from the definition of $\bar{T}_s$:

$$\bar{P}_t^{(\gamma-1)/\gamma} = \frac{1}{A}\int_A P_t^{(\gamma-1)/\gamma} dA \ .$$

TABLE 3.1.III

Representation of Conservation Laws for Swirl-free Steady Channel flow According to Equations (1) to (3), with the Aid of Average Values from Equations (4) to (7)

Law of conservation	*Mean velocity* $\bar{V}_C$ *based on continuity*	*Mean velocity* $\bar{V}_I$ *based on momentum*	*Mean velocity* $\bar{V}_E$ *based on energy*
Continuity equation $\dot{m}_e - \dot{m}_i = 0$	$\frac{\dot{m}}{A} = \bar{\rho}_s \bar{V}_C$ $\bar{V}_C := \frac{\int_A \rho_s V \, dA}{\bar{\rho}_s A}$	$\frac{\dot{m}}{A} = \bar{\rho}_s \epsilon_{CI} \bar{V}_I$ $\epsilon_{CI} := \frac{\int_A \rho_s V \, dA}{\bar{\rho}_s \bar{V}_I A}$	$\frac{\dot{m}}{A} = \bar{\rho}_s \epsilon_{CE} \bar{V}_E$ $\epsilon_{CE} := \frac{\int_A \rho_s V \, dA}{\bar{\rho}_s \bar{V}_E A}$
Momentum equation $\dot{I}_e - \dot{I}_i = \Sigma F$	$\frac{\dot{I}}{A} = \bar{P}_s + \bar{\rho}_s \epsilon_{IC} \bar{V}_C^2$ $\epsilon_{IC} := \frac{\int_A \rho_s V^2 \, dA}{\bar{\rho}_s \bar{V}_C^2 A}$	$\frac{\dot{I}}{A} = \bar{P}_s + \bar{\rho}_s \bar{V}_I^2$ $\bar{V}_I := \sqrt{\frac{\int_A \rho_s V^2 \, dA}{\bar{\rho}_s A}}$	$\frac{\dot{I}}{A} = \bar{P}_s + \bar{\rho}_s \epsilon_{IE} \bar{V}_E^2$ $\epsilon_{IE} := \frac{\int_A \rho_s V^2 \, dA}{\bar{\rho}_s \bar{V}_E^2 A}$
Energy equation $\dot{E}_e - \dot{E}_i = \dot{Q}_{i-e}$	$\frac{\dot{E}}{A} = \bar{\rho}_s \bar{V}_C \bar{h}_s + \frac{\bar{\rho}_s}{2} \epsilon_{EC} \bar{V}_C^3$ $\epsilon_{EG} := \frac{\int_A \rho_s V^3 \, dA}{\bar{\rho}_s \bar{V}_C^3 A}$	$\frac{\dot{E}}{A} = \bar{\rho}_s \epsilon_{CI} \bar{V}_I \bar{h}_s + \frac{\bar{\rho}_s}{2} \epsilon_{EI} \bar{V}_I^3$ $\epsilon_{EI} := \frac{\int_A \rho_s V^3 \, dA}{\bar{\rho}_s \bar{V}_I^3 A}$	$\frac{\dot{E}}{A} = \bar{\rho}_s \epsilon_{CE} \bar{V}_E \bar{h}_s + \frac{\bar{\rho}_s}{2} V_E^3$ $\bar{V}_E := \sqrt[3]{\frac{\int_A \rho_s V^3 \, dA}{\bar{\rho}_s A}}$

TABLE 3.1.IV

Condition for "Complete Equilibrium"

Type of flow	*Thermal equilibrium average static temperature* T	*Mechanical equilibrium average velocity* V
Swirl free channel flow with constant cross section	T_s = const	V = const
Two-dimensional cascade flow	$\bar{T}_s$ = const	$\bar{V}_n$ = const (normal) $\bar{V}_t$ = const (tangential)
Coaxial swirl flow	$\bar{T}_s$ = const	$\bar{V}_r$ = const (radial) $\bar{V}_\theta/r$ = const (circumf.) $\bar{V}_{Ax}$ = const (axial)

TABLE 3.1.V

Radial Distributions of State Values of "Complete Equilibrium" of a Coaxial Swirl Flow

Values of state	*Incompressible fluid:* ρ = const	*Caloric ideal gas:* $\rho = \frac{P}{RT}$ (C_p = const)
Velocity		
Radial component	$\bar{V}_r^* = 0$	$\bar{V}_r^* = 0$
Circumf. component	$\bar{V}_\theta^* = r^*$	$\bar{V}_\theta^* = r^*$
Axial component	$\bar{V}_{Ax}^* = 1$	$\bar{V}_{Ax} = 1$
Static state		
Temperature	$T_s^* = 1$	$T_s^* = 1$
Pressure (resp. density)	$\bar{P}_s^* = 1 + \frac{\rho \bar{V}_{\theta H}^2}{2P_{sH}}(r^{*2} - 1)$	$P_s^* = \bar{\rho}_s^* = \exp\left\{\frac{\bar{V}_{\theta H}^2}{2R\bar{T}_{sH}}(r^{*2} - 1)\right\}$
Spec. enthalpy	$\bar{h}_s^* = 1 + \frac{\bar{V}_{\theta H}^2}{2\bar{h}_{sH}}(r^{*2} - 1)$	$h_s^* = 1$
Spec. entropy	$s^* = 1$	$\bar{s}^* = 1 + \frac{\bar{V}_{\theta H}^2}{2T_{sH}\bar{s}_H}(r^{*2} - 1)$
Total state		
Temperature	$T_t^* = 1; (T_{tH} = T_{sH})$	$\bar{T}_t^* = 1 + \frac{V_{\theta H}^2}{2C_p\bar{T}_{tH}}(r^{*2} - 1)$
Pressure	$P_t^* = 1 + \frac{\rho \bar{V}_{\theta H}^2}{\bar{P}_{tH}}(r^{*2} - 1)$	$P_t^* = \bar{P}_s^*\left\{1 + \frac{\bar{V}_{\theta H}^2}{2C_p\bar{T}_{tH}}(r^{*2} - 1)\right\}^{\gamma/(\gamma-1)}$
Spec. enthalpy	$h_t^* = 1 + \frac{V_{\theta H}^2}{\bar{h}_{tH}}(r^{*2} - 1)$	$\bar{h}_t^* = 1 + \frac{\bar{V}_{\theta H}^2}{2\bar{h}_{tH}}(r^{*2} - 1)$

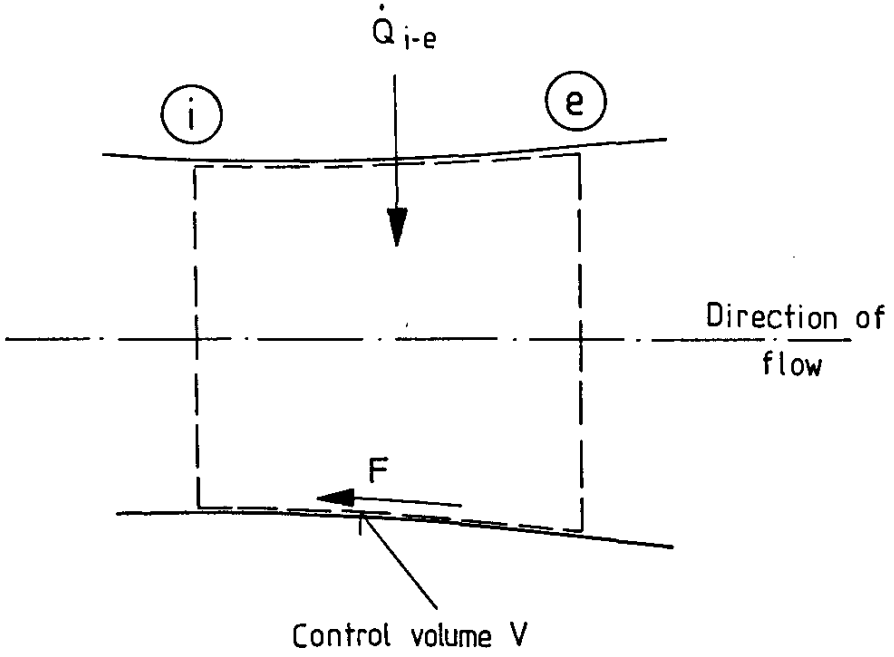

Fig.3.1.1 Swirl-free channel flow

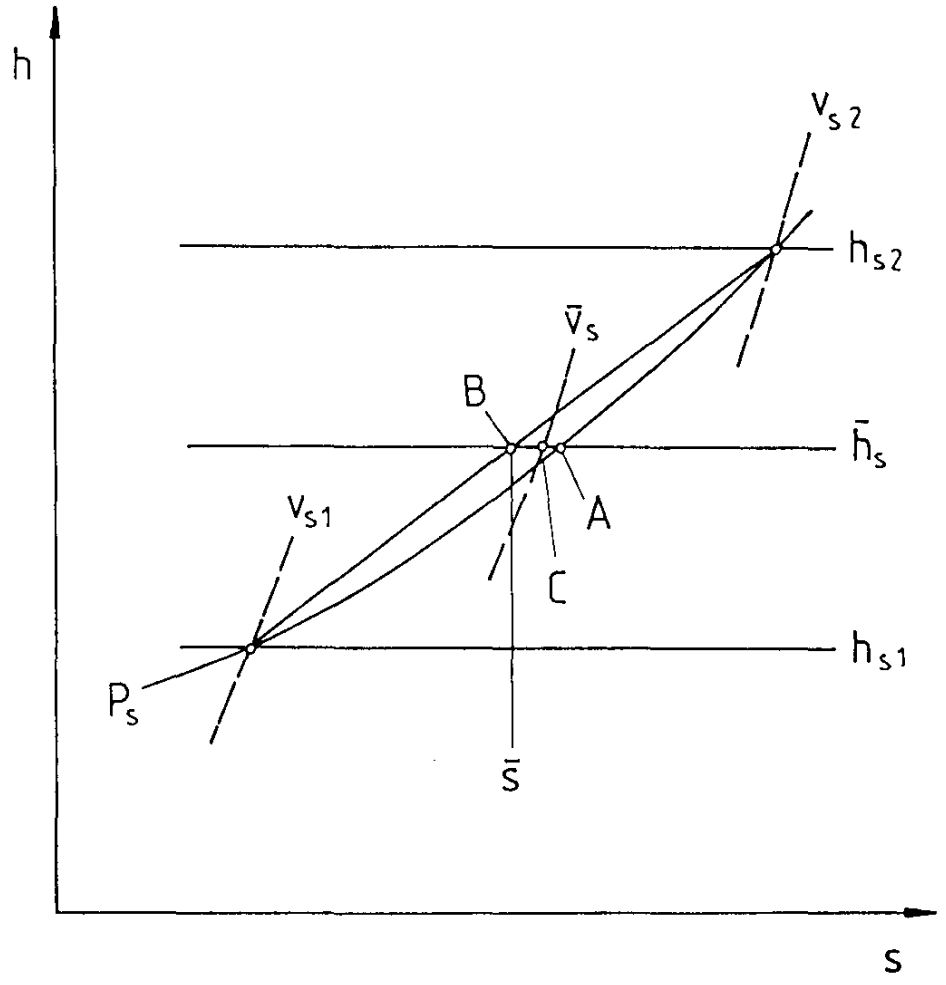

Fig.3.1.2 h, s diagram for comparison of the averaging method for the internal state as given by W.Traupel in Reference 3.1.6 (3rd edition)

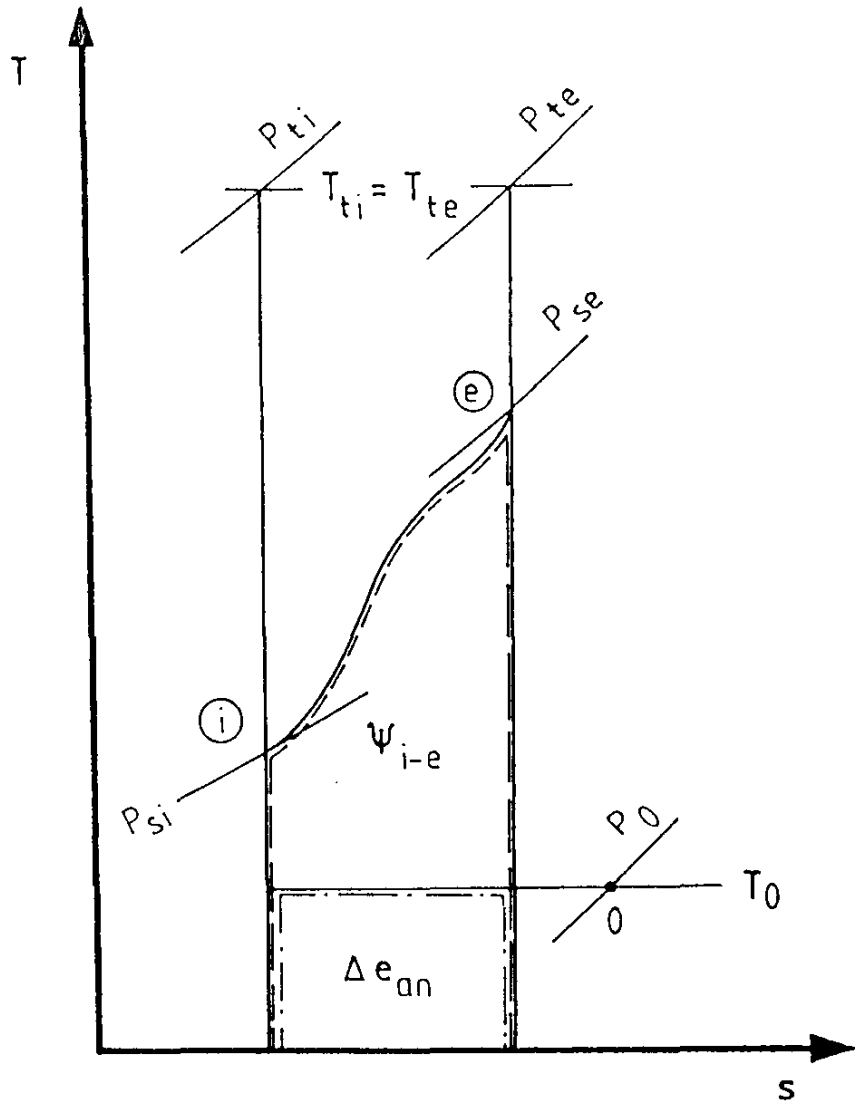

$$\psi_{i-e} = \int_{s_i}^{s_e} T_s \, D\, s$$

$$\Delta e_{an} = T_0 \, (s_e - s_i)$$

Fig.3.1.3 Representation of the specific dissipation ψ_{i-e} and the specific "anergy" increase Δe_{an} for an adiabatic change of state

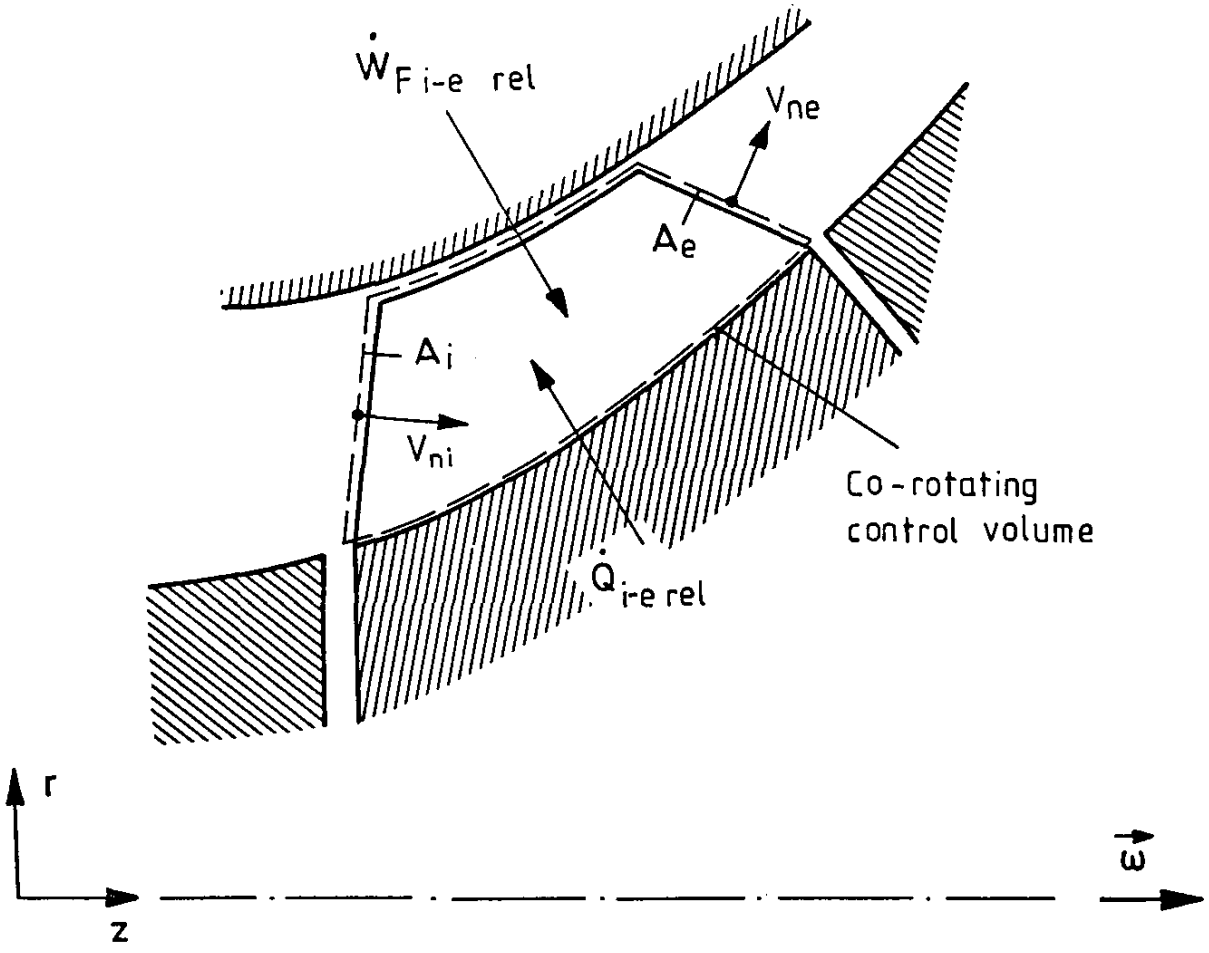

Fig.3.1.4 Co-rotating control volume for a turbomachine rotor

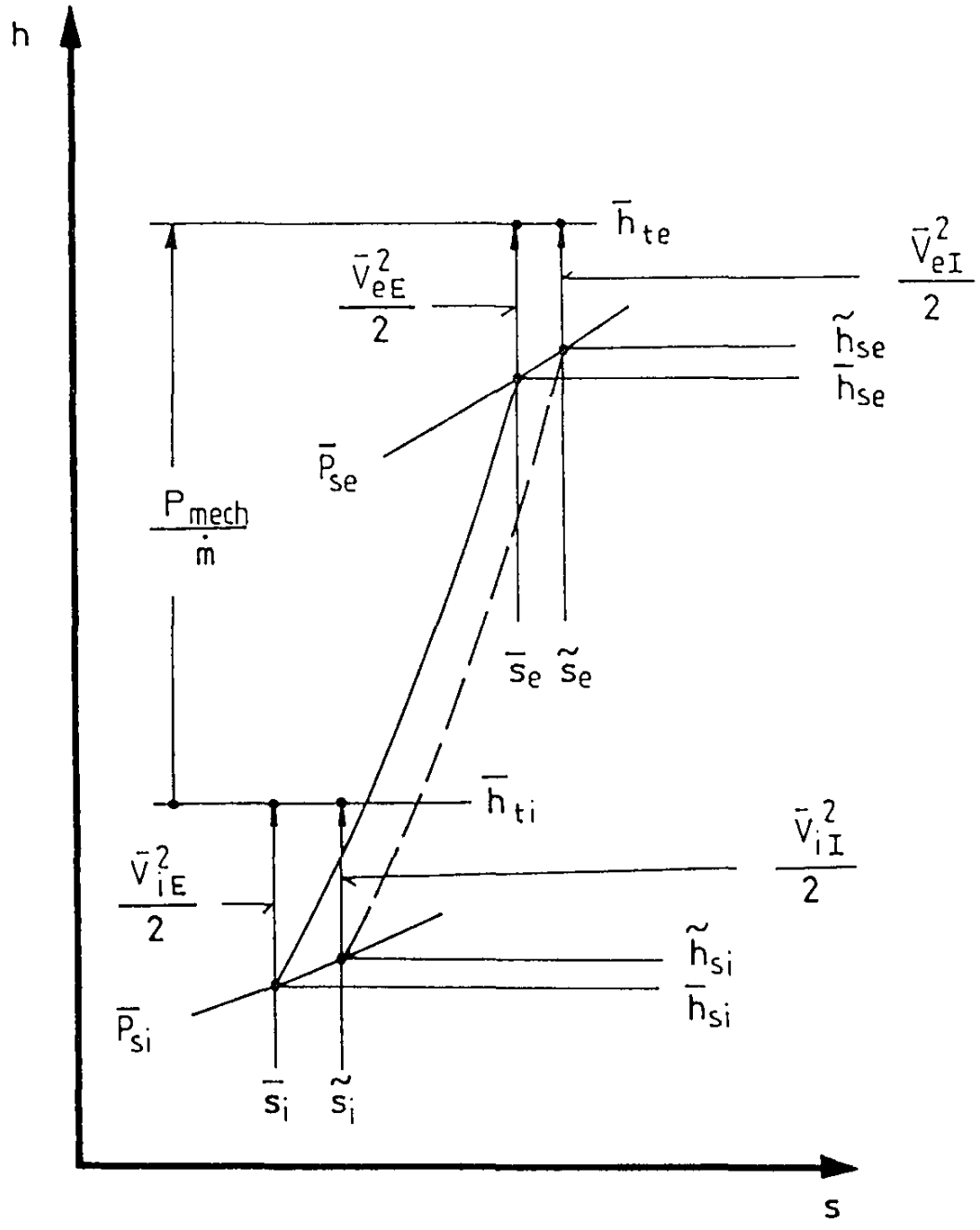

Fig.3.1.5 Representation of state changes in a turbomachine rotor by means of average values

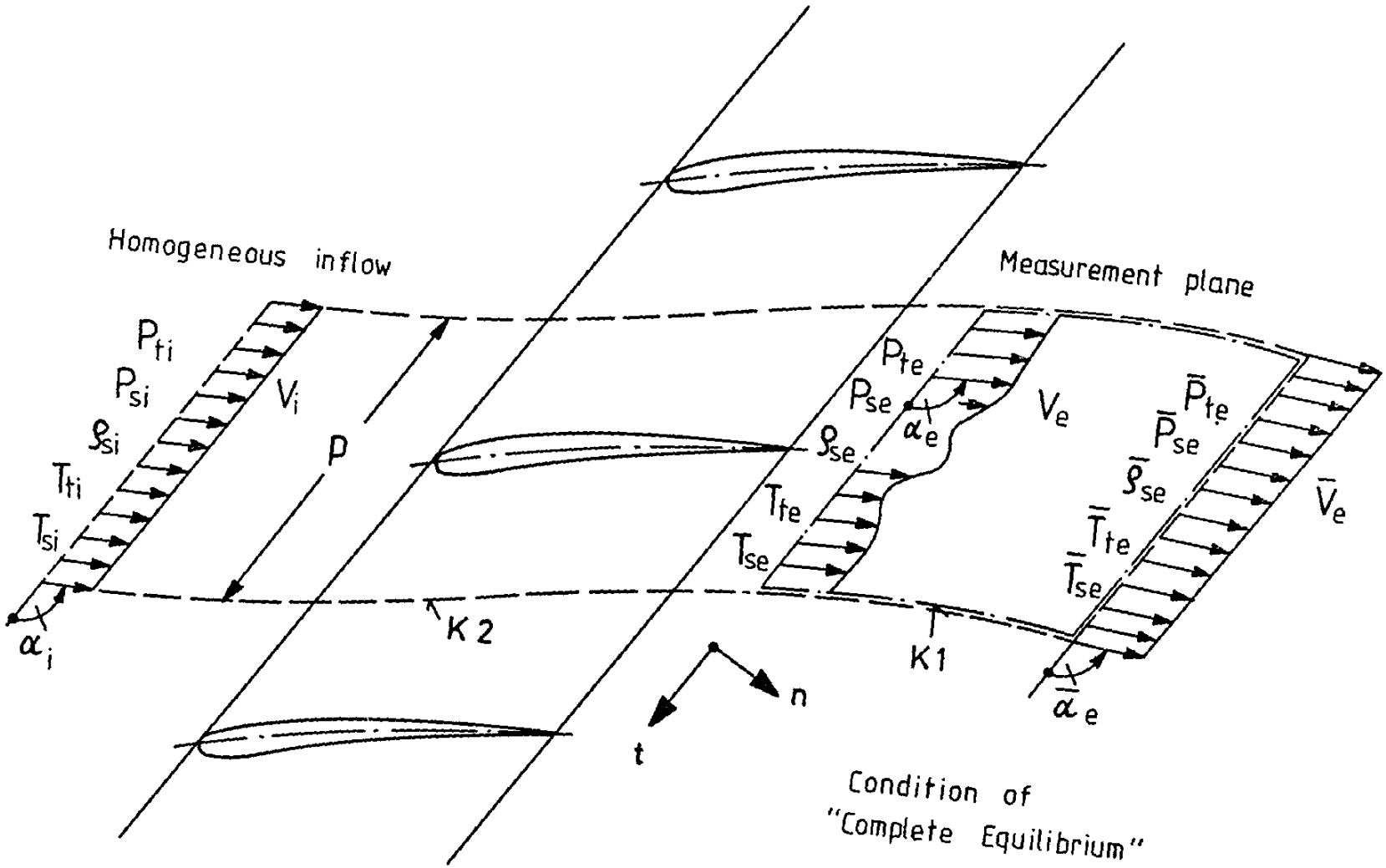

Fig.3.1.6 Two-dimensional cascade flow

2.1 Cartesian Coordinates

$$\begin{bmatrix} q_x \\ q_y \\ q_z \end{bmatrix} = \lambda \begin{bmatrix} \frac{\partial T_s}{\partial x} \\ \frac{\partial T_s}{\partial y} \\ \frac{\partial T_s}{\partial z} \end{bmatrix} \tag{5}$$

2.2 Cylindrical Coordinates

$$\begin{bmatrix} q_r \\ q_\theta \\ q_z \end{bmatrix} = \lambda \begin{bmatrix} \frac{\partial T_s}{\partial r} \\ \frac{1}{r}\frac{\partial T_s}{\partial \theta} \\ \frac{\partial T_s}{\partial z} \end{bmatrix} \tag{6}$$

Appendix 2

CLOSED SOLUTION OF THE DEFINITE INTEGRALS ACCORDING TO EQUATIONS (128) and (129)

1. $$F_1 := \int_\nu^1 \rho_s^* r^* dr^* = \int_\nu^1 \exp\left\{\frac{\bar{V}_{\theta H}^2}{2R\bar{T}_{sH}}(r^{*2}-1)\right\} r^* dr^* \tag{1}$$

substitution:
$$x := \frac{\bar{V}_{\theta H}^2}{2R\bar{T}_{sH}}(r^{*2}-1) \tag{2}$$

$$dx = \frac{\bar{V}_{\theta H}^2}{RT_{sH}} r^* dr^*$$

$$F_1 = \frac{R\bar{T}_{sH}}{\bar{V}_{\theta H}^2}\int_{x_B}^0 \exp(x)\,dx = \frac{RT_{sH}}{\bar{V}_{\theta H}^2}\exp(x)\Big|_{x_B}^0$$

$$F_1 = \frac{RT_{sH}}{\bar{V}_{\theta H}^2}\left\{1-\exp\left[\frac{\bar{V}_{\theta H}^2}{2R\bar{T}_{sH}}(\nu^2-1)\right]\right\} \tag{3}$$

2. $$F_2 := \int_\nu^1 \rho_s r^{*3} dr^* = \int_\nu^1 \exp\left\{\frac{\bar{V}_{\theta H}^2}{2R\bar{T}_{sH}}(r^{*2}-1)\right\} r^{*3} dr^* \tag{4}$$

partial integration $\int u\,dv = uv - \int v\,du$

$$u := \frac{RT_{sH}}{\bar{V}_{\theta H}^2} r^{*2} \longrightarrow du = \frac{2R\bar{T}_{sH}}{\bar{V}_{\theta H}^2} r^* dr^* \tag{5}$$

$$dv := \exp\left\{\frac{\bar{V}_{\theta H}^2}{2R\bar{T}_{sH}}(r^{*2}-1)\right\}\frac{\bar{V}_{\theta H}^2}{RT_{sH}} r^* dr^* \tag{6}$$

$$v = \exp\left\{\frac{\bar{V}_{\theta H}^2}{2R\bar{T}_{sH}}(r^{*2}-1)\right\}$$

$$F_2 = \frac{R\bar{T}_{sH}}{\bar{V}_{\theta H}^2}\left\{1-\nu^2\exp\left[\frac{\bar{V}_{\theta H}^2}{2R\bar{T}_{sH}}(\nu^2-1)\right]\right\} - \frac{2R\bar{T}_{sH}}{\bar{V}_{\theta H}^2}\int_\nu^1 \exp\left\{\frac{\bar{V}_{\theta H}^2}{2RT_{sH}}(r^*-1)\right\} r^* dr^*$$

$$F_2 = \frac{R\bar{T}_{sH}}{\bar{V}_{\theta H}^2}\left\{1-\nu^2\exp\left[\frac{\bar{V}_{\theta H}^2}{2R\bar{T}_{sH}}(\nu^2-1)\right]-2F_1\right\} \quad . \tag{7}$$

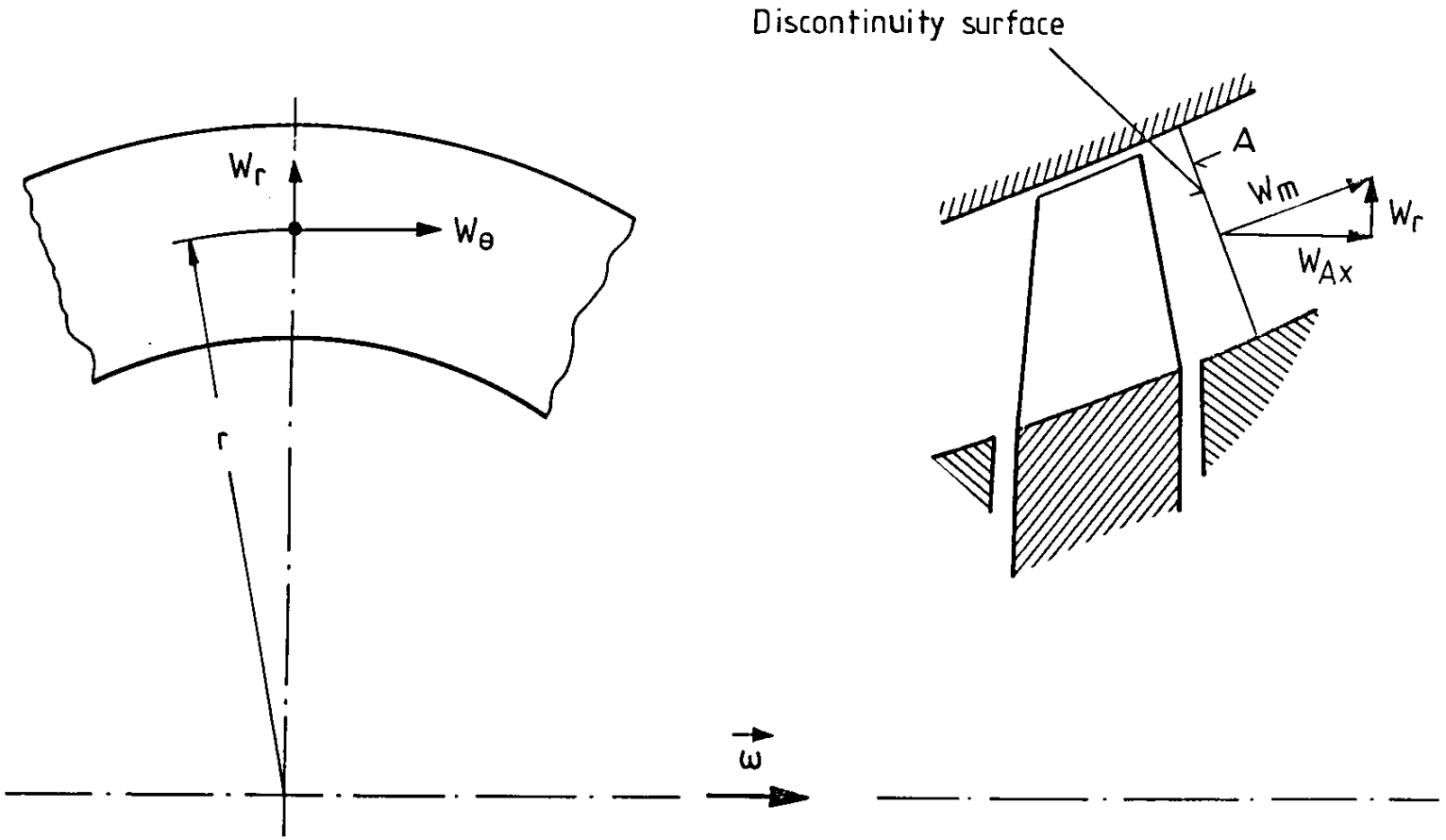

Fig.3.1.7 Discontinuity surface after a turbomachine rotor

Appendix 1

CONSTITUTIVE EQUATIONS FOR STRESS (NAVIER-STOKES) AND HEAT CONDUCTIVITY (FOURIER)

1. CONSTITUTIVE EQUATIONS FOR STRESS (NAVIER-STOKES)

$$\underline{\underline{\sigma}} = -P_s\underline{\underline{e}} + 2\mu\underline{\underline{d}} + \hat{\mu}d_1\underline{\underline{e}} \tag{1}$$

$$|\underline{\underline{\sigma}}| = -P_s|\underline{\underline{e}}| + 2\mu|\underline{\underline{d}}| + \hat{\mu}d_1|\underline{\underline{e}}| \tag{1a}$$

1.1 Cartesian Coordinates

$$\begin{bmatrix} \sigma_{xx} & \sigma_{xy} & \sigma_{xz} \\ & \sigma_{yy} & \sigma_{yz} \\ \text{SYM} & & \sigma_{zz} \end{bmatrix} = -P_s\begin{bmatrix} 1 & 0 & 0 \\ 0 & 1 & 0 \\ 0 & 0 & 1 \end{bmatrix} + 2\mu\begin{bmatrix} \frac{\partial V_x}{\partial x} & \frac{1}{2}\left(\frac{\partial V_x}{\partial y} + \frac{\partial V_y}{\partial x}\right) & \frac{1}{2}\left(\frac{\partial V_x}{\partial z} + \frac{\partial V_z}{\partial x}\right) \\ & \frac{\partial V_y}{\partial y} & \frac{1}{2}\left(\frac{\partial V_y}{\partial z} + \frac{\partial V_z}{\partial y}\right) \\ \text{SYM} & & \frac{\partial V_z}{\partial z} \end{bmatrix} + \hat{\mu}\left(\frac{\partial V_x}{\partial x} + \frac{\partial V_y}{\partial y} + \frac{\partial V_z}{\partial z}\right)\begin{bmatrix} 1 & 0 & 0 \\ 0 & 1 & 0 \\ 0 & 0 & 1 \end{bmatrix} \tag{2}$$

1.2 Cylindrical Coordinates

$$\begin{bmatrix} \sigma_{rr} & \sigma_{r\theta} & \sigma_{rz} \\ & \sigma_{\theta\theta} & \sigma_{\theta z} \\ \text{SYM} & & \sigma_{zz} \end{bmatrix} = -P_s\begin{bmatrix} 1 & 0 & 0 \\ 0 & 1 & 0 \\ 0 & 0 & 1 \end{bmatrix} + 2\mu\begin{bmatrix} \frac{\partial W_r}{\partial r} & \frac{1}{2}\left[\frac{\partial W_\theta}{\partial r} + \frac{1}{r}\left(\frac{\partial W_r}{\partial \theta} - W_\theta\right)\right] & \frac{1}{2}\left(\frac{\partial W_z}{\partial r} + \frac{\partial W_r}{\partial z}\right) \\ & \frac{1}{r}\left(\frac{\partial W_\theta}{\partial \theta} + W_r\right) & \frac{1}{2}\left(\frac{1}{r}\frac{\partial W_z}{\partial \theta} + \frac{\partial W_\theta}{\partial z}\right) \\ \text{SYM} & & \frac{\partial W_z}{\partial z} \end{bmatrix} + \hat{\mu}\left(\frac{\partial W_r}{\partial r} + \frac{1}{r}\frac{\partial W_\theta}{\partial \theta} + \frac{\partial W_z}{\partial z} + \frac{W_r}{r}\right)\begin{bmatrix} 1 & 0 & 0 \\ 0 & 1 & 0 \\ 0 & 0 & 1 \end{bmatrix} \tag{3}$$

2. CONSTITUTIVE EQUATION FOR HEAT CONDUCTIVITY (FOURIER)

$$\underline{q} = \lambda\underline{\nabla}T_s \tag{4}$$

$$|\underline{q}| = \lambda|\underline{\nabla}T_s| \tag{4a}$$

3.2 DEFINITION OF A HOMOGENEOUS FLOW CHARACTERIZING THE PERFORMANCE OF A GAS TURBINE COMPONENT

Nomenclature

The notation used in this section is consistent with the general nomenclature provided at the beginning of this report, with the exception of the following differences adopted for the sake of simplification:

F: gross thrust (instead of F_G)

The subscript - is used instead of = to designate an average in the whole section.

In addition, the following notation, specific to this section, is used:

(/): typical ideal evolution of the fluid in the reheat channel
(D): typical ideal evolution of the fluid in the exhaust nozzle
(E): given heterogeneous flow
($\bar{E}$): homogeneous flow equivalent to (E)
K: characteristic quantity
(Pf): typical ideal evolution in the combustion chamber
(Γ): typical ideal evolution of the fluid in a compressor, turbine or fan
J: steam force or dynalpy $= Ps(1 + \gamma M^2)A$

3.2.0 Introduction

The need for representing an actual heterogeneous flow by a homogeneous one (that means one-dimensional) is particularly strong during the research and development of a turbojet (or turbofan). The engine manufacturer may utilise such an averaged flow in different ways:

- First, the process allows an easy comparison with the simple one-dimensional model, often used to predict the performance of the engine components or the complete engine.
- Moreover, an averaging procedure is necessary for characterizing an engine component quality by a limited number of figures.

For example, the compressor is characterized by its efficiency (isentropic or polytropic) and its pressure ratio, the combustor by the total pressure loss, etc. when these components have been tested on a rig test simulating some flight conditions. Having so characterized the engine components, it is then possible to predict the complete engine performance in other flight conditions than those tested.

A similar problem arises when a complete engine is tested. It is then important to attribute to each component the efficiency which correctly represents that component input to the engine overall performance in order to undertake further research on the component which may and must be improved. A poor judgment of the different components' merits may lead to very costly research or incorrect technical conclusions.

Consequently, since the use of averaged values is needed for the purpose of characterization of an engine component (in which the flow is heterogeneous during an actual test) it is important that the averaging method used be appropriate to the component considered. That's the reason for the averaging method presented here, in which the basic criterion is the specific function of each engine component with a view to obtaining an assessment of the various components as representative as possible of their influence on the final output which is the engine thrust and the engine specific fuel consumption. It is also intended to ensure a coherent analysis of the test results and accurate prediction of the engine performance.

As a result, in the following sections different averaging methods are described, each of them being matched to a particular engine component, while all the presented methods are based on the same general principles. One of the typical features of the methods described is that they lead sometimes to average values which are not intrinsic, i.e. which do not depend only on the data describing the heterogeneous flow but also on the conditions downstream of the component considered. For example the average total pressure at the inlet to a compressor (or turbine) depends on the exit total pressure of the compressor (or turbine). The average total pressure at the inlet to an exhaust nozzle depends on the atmospheric pressure and the expansion ratio across the nozzle.

However, the non-intrinsic character that some people might not like is in practice insignificant. It may be noticed, in Section 4.4 where the method is applied to all components of a turbojet, that the influence of the downstream conditions on the average total pressure is in most cases very small ($\simeq 0.1\%$) and often insignificant ($< 0.01\%$).

Moreover when the computation upstream of a compressor (or a turbine) is made with γ = cte, the method gives a total pressure fully independent of the downstream conditions. In that case, the average total pressure is given by a simple algebraic formula which is identical to those applicable in a combustor inlet. This formula is utilised by NASA (Ref.3.2.1) and by ONERA.

The method presented here, called "Pianko's Method" in the following chapters, has been applied and compared with other methods in the numerical examples of Chapter 4.

3.2.1 General Method for Defining a Flow ($\bar{E}$) Equivalent to the Real Flow (E)

The method for obtaining average values of a given heterogeneous flow (E), which is described in the present section, uses, as an intermediate stage, the concept of the uniform flow ($\bar{E}$) assumed to be "equivalent" to the real flow (E). The aerothermodynamic values of ($\bar{E}$) will be regarded as average values of the given real flow. In the analysis and definition of this equivalent flow, the following principles have been applied:

(a) take into account the specific character of each component of a turbojet/fan and be able, through a simple calculation, to predict from ($\bar{E}$) the most representative values of the functional characteristics of the component considered;

(b) ensure global coherence between the various components of an engine, to predict its overall performance (essentially thrust and specific consumption).

The following general assumptions have been adopted:

(1) (E) and ($\bar{E}$) consist of the same divariant fluid, that is to say a fluid whose thermodynamic properties are represented by the same Mollier diagram (h, s). The expressions obtained for a calorifically perfect gas (γ and C_p constant) are given in Section 3.2.7.

(2) The steady one dimensional calculation method has been essentially used. Note that the method derives the average value at INLET to a component. To find the average value at the outlet plane, the outlet flow must be treated as the inlet to the next component in the engine.

Each component will be defined by:

A_i: the inlet area

A_e: the exit area

K: one or several characteristic functional quantities, that is those which represent the function or usefulness of the component;

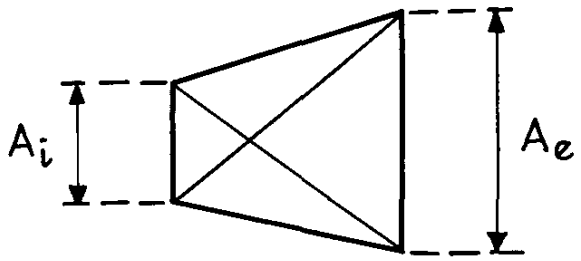

It is assumed that all the aerothermodynamic quantities of the flow (E) in the area A_i (velocity distribution, densities, temperatures, etc.) are given.

In order to define the equivalent flow ($\bar{E}$), the general method consists of going through the following steps for each component:

(1) define a *typical ideal evolution* allowing the calculation of one or several characteristic quantities K of this component. The same calculation will be used, whether the flow (E) or the flow ($\bar{E}$) passes through the component;

(2) evaluate one or several quantities K resulting from the passing of the real flow (E) through the component considered;

(3) define ($\bar{E}$) as being a uniform flow which leads to the same quantity – or quantities – $\bar{K}$ when ($\bar{E}$) passes through the component considered.

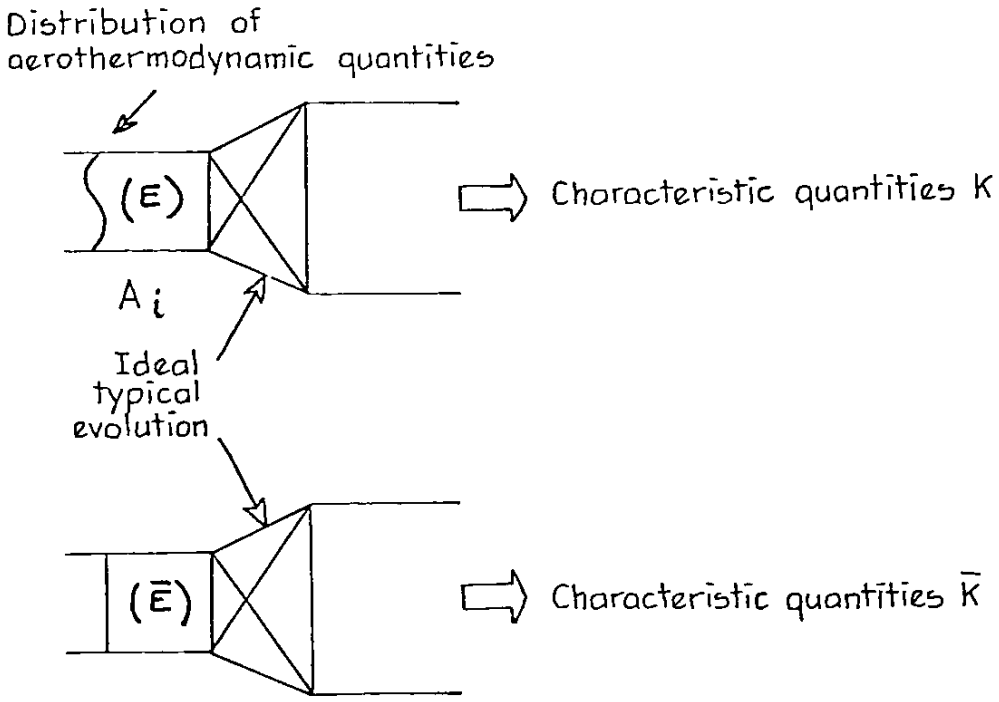

Conditions of equivalence

$$K = \bar{K}$$

We can see that the definition of the flow $(\bar{E})$ depends on the component under consideration, through the characteristic quantities K: this means that the average quantities, calculated by the proposed method, are not, in principle, intrinsic quantities related only to the aerothermodynamic data in the plane A_i. As these quantities are intended to represent the *usefulness* or the *function* of the component, their values depend on how the gas flow which passes through the component is used.

Generally speaking, when we try to define a homogeneous flow equivalent to a given heterogeneous flow, we are necessarily led to introduce a degree of arbitrariness and to lose some useful items of information. As four independent integral quantities entirely define a homogeneous one-dimensional flow, it is impossible to maintain simultaneously the mass flow, the enthalpy, the entropy, the momentum, the area and the thrust. In an intrinsic method (the results of which depend only on local conditions), the selection of the parameters used is arbitrary, whereas in the method proposed here, the selection is made in such a manner that the result is the most representative of the component function.

The general method described above will be applied successively, for the sake of example, to the following components:

1 – exhaust nozzle
2 – turbine, compressor or fan
3 – combustion chamber
4 – after-burner channel
5 – diffusor and air inlet

Remark:

In all the cases dealt with below, it has been implicitly assumed that the velocity is normal to the section A with no swirling velocity. The mass flow is then calculated by

$$d\dot{m} = \rho V dA .$$

If the flow is not normal to A the more general formula:

$$d\dot{m} = \rho V_x dA$$

is used, V_x being the component of V normal to the section A.

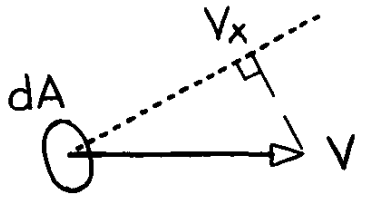

3.2.2 Exhaust Nozzle

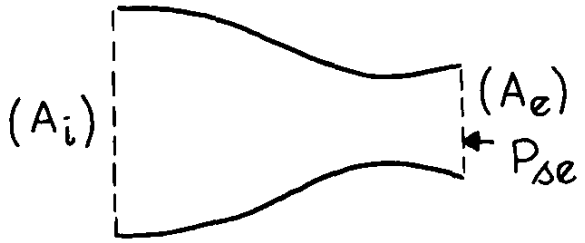

3.2.2.1 The Typical Ideal Evolution (D)

The typical ideal evolution (D) is an isentropic expansion which is adiabatic up to a given uniform pressure Pse (possibly different from the ambient pressure Po). This ideal evolution (D) is compatible with an assumption that the tangential velocities in the section Ai are small and can be neglected.

3.2.2.2 The Characteristic Quantities K *are the following:*

- the thrust F
- the mass flow rate $\dot{m}$
- the total enthalpy flow rate H_t

3.2.2.3 Calculation of the Characteristic Quantities Resulting from the Flow (E):

- the data of (E) in A_i make it possible to calculate:
  - the total mass flow rate:

$$\dot{m} = \int_{A_i} \rho_i V_i \, dA_i$$

  - and the total enthalpy flow rate:

$$H_{ti} = \int_{A_i} h_{ti} \, d\dot{m}_i = \int_{A_i} h_{ti} \rho_i V_i \, dA_i \, .$$

We assume that each streamlet of (E), issuing from the elementary area dA_i, and whose mass flow rate is $d\dot{m}_i$ undergoes the isentropic adiabatic expansion (D) from A_i to the pressure Pse. After this expansion, the density and the velocity become ρ_e and V_e, these values depending on elementary streamlet considered. When the flow (E) undergoes, from A_i, the evolution (D), we find as a result, an exhaust area A'_e which is not necessarily equal to the given real area A_e. The conservation of the mass flow rate between A_i and A'_e makes it possible to calculate A'_e.

$$A'_e = \int_{A_i} \frac{d\dot{m}_i}{\rho_e V_e} = \int_{A_i} \frac{\rho_i V_i}{\rho_e V_e} \, dA_i \, .$$

We can now calculate the ideal thrust F which is delivered when the flow E is subjected to expansion (D).

$$F = (P_{se} - P_o) A'_e + \int_{A'_e} V_e \, d\dot{m}_e \, .$$

3.2.2.4 Determination of the Equivalent Flow (E)

We shall attempt to determine $(\bar{E})$ so that after the evolution (D), we have not only $\bar{P}_{se} = P_{se}$ but also the following relations

$$\dot{\bar{m}}_i = \dot{m}_i$$
$$\bar{H}_{ti} = H_{ti}$$
$$\bar{F} = F \ .$$

As a result:

$$\bar{h}_t = \bar{h}_{te} = \bar{h}_t = \frac{H_{ti}}{\dot{m}_i} \tag{1}$$

$$\frac{\bar{F}}{\dot{m}} = \frac{(P_{se} - P_o)}{\bar{\rho}_e \bar{V}_e} + \bar{V}_e = \frac{F}{\dot{m}} \ . \tag{2}$$

The two Equations (1) and (2) and the state equation enable us to locate, in the Mollier diagram, the point $\bar{i}$ representing the stagnation state of the flow.

Equation (1) gives $\bar{h}_t$ directly. We calculate s such that, taking the value of $\bar{h}_t$ into account, Equation (2) is satisfied. Then we know the stagnation state $(\bar{h}_t, \bar{s})$ of $(\bar{E})$.

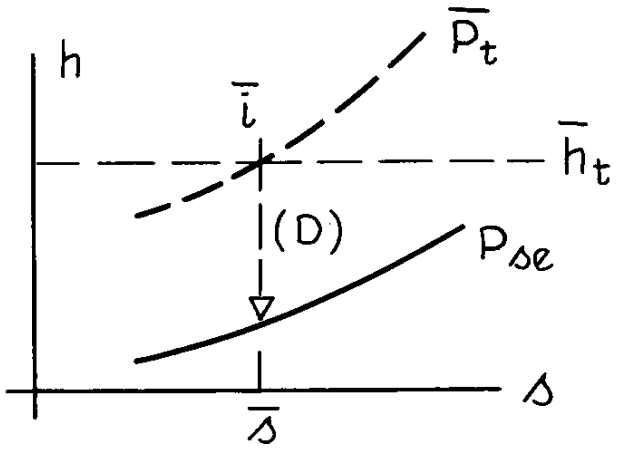

If we wish to define accurately the local state of $(\bar{E})$ in $\bar{A}_i$, one (and only one) additional condition is required to locate this point along the isentropic line $\bar{s}$.

For example, we can take $\bar{A}_i = A_i$ or the condition $\bar{P}_{si} = P_{si}$ defining thus a flow coefficient for the inlet section.

3.2.2.5 Comments and Remarks

- We note that the calculation by the method described of the average values at the entrance of the nozzle $(\bar{h}_t, \bar{s})$, from which the total pressure and the total temperature can be derived, does not at all necessitate measuring the thrust delivered by the nozzle. On the contrary, the method makes it necessary to calculate the thrust F delivered by the nozzle when the latter is the site of the typical ideal evolution (D) (that is to say an isentropic adiabatic expansion up to a given uniform pressure Pse). It is quite possible, and even likely, that this calculated thrust is different from the measured thrust F_m (when this measurement is carried out). The causes of the possible difference noticed between F and F_m may be the following:

  - measurement errors
  - nozzle defects (frictions, separations, etc.)

  It may even happen that the calculated thrust F is *lower* than the measured thrust F_m. This could happen in a good quality nozzle where the heterogeneous flow provided in the entrance undergoes a homogenization by a mixing with moderate losses. In this case, the thrust calculated for a heterogeneous flow may be lower than the real thrust delivered by a homogenized flow.

  In the method described above, we use the mass flow rate through the nozzle. Two values of the mass flow rate can be used:

the mass flow rate calculated in the area A_i, using the measured local aerothermodynamic values

$$\dot{m}_i = \int_{A_i} \rho_i V_i dA_i$$

or the total measured mass flow rate measured by means of a conventional calibrated device.

It should be pointed out that, even if we are sure of the accuracy of the measured mass flow rate, *it is the calculated mass flow which must be used.* As a matter of fact, the total enthalpy H_{ti} is obtained through a calculation which uses the aerothermodynamic values in the area A_i

$$H_{ti} = \int h_{ti} \rho_i V_i dA_i .$$

This being so, we must use the same aerothermodynamic values (ρ_i, V_i), that is to say use the calculated mass flow rate to calculate the enthalpy per unit mass.

$$\bar{h}_{ti} = \frac{H_{ti}}{\dot{m}_i} .$$

Should we use the measured mass flow rate, different from the calculated one, we would not find again *the* total temperature of a homogeneous flow.

- It should also be noted that there are three different values for the nozzle exit area:
  - the real, geometric, measured area A_e
  - the calculated area A'_e for the typical ideal evolution (D) of the heterogeneous flow (E)
  - the calculated area $\bar{A}_e$ for the uniform flow ($\bar{E}$) undergoing the typical ideal evolution (D).

A similar method is described in Reference 4.2.4.

Important remark:

To calculate the thrust $\bar{F}$ corresponding to ($\bar{E}$), it is first necessary to calculate $\bar{A}_e$, for example by using the mass flow rate conservation equation. In fact, the relations:

$$\bar{P}_{se} = P_{se}$$
$$\bar{\dot{m}} = \dot{m}$$
$$\bar{H}_{ti} = H_{ti}$$
$$\bar{F} = F$$

imply that, when (E) is not uniform, $\bar{A}_e$ is different from A_e.

This means that, when we calculate the thrust of a nozzle from the average flow within its inlet plane, it is necessary (among other corrections) to apply a coefficient C_A to the exit area Ae, that is to take $\bar{A}_e = C_A A_e$. If we do wish to have $\bar{A}_e = A_e$, we must give up one of the relations used, and, for example, accept $\bar{\dot{m}} \neq \dot{m}$.

- The average total pressure $\bar{P}_t$, which will be calculated by applying the method described above, is not an intrinsic quantity related to the given heterogeneous flow, since it depends on the value of the static pressure P_{se} chosen in the exit plane of the nozzle, and on the value of the ambient pressure P_o. The calculation examples given in Chapter 4 make it possible to know the order of magnitude of the influence of P_{se} and P_o on the value of P_t.

3.2.2.6 Application

At section A_i, entrance to a nozzle, the flow is supposed described by the distribution of the total pressure, total temperature, static pressure and fuel/air ratio. That means that to each elementary area ΔA_i is associated a value of P_{ti}, T_{ti}, P_{si} and FAR_i. It is also assumed that the tangential velocities may be neglected.

For the development of the calculation, we assume that the values of the following integrals are tabulated:

$$h = \int_{T_o}^{T} C_p(T) dT$$

and

$$\Phi = \frac{1}{R} \int_{T_o}^{T} \frac{C_p(T)}{T} dT$$

with an arbitrary origin T_o, as a function of the temperature and air/fuel ratio.

This allows the calculation of entropy per unit mass $s = R[\Phi - \ln P]$.

By writing that the entropy calculated with total values (pressure and temperature) is equal to the entropy calculated with static values, we can calculate in each point of the area A_i, the value of $\Phi(T_{si})$

$$\Phi(T_{si}) = R \ln \frac{P_{si}}{P_{ti}} + \Phi(T_{ti})$$

which yields the static temperature T_{si}.

Then, the latter gives $h(T_{si})$ and the velocity is obtained by

$$V_i = \sqrt{2[h(T_{ti}) - h(T_{si})]} \ .$$

The static pressure P_{si}, the static temperature T_{si} and the equation of state give the density

$$\rho_i = \frac{P_{si}}{R T_{si}}$$

hence the local flow rate

$$d\dot{m}_i = \rho_i V_i dA_i$$

and the total enthalpy

$$dH_{ti} = h(T_{ti}) d\dot{m}_i \ .$$

The main assumption is that each streamlet undergoes an isentropic expansion down to the area dA' where the static pressure is P_{se}. As we also know $P_{te} = P_{ti}$ and $T_{te} = T_{ti}$, we can calculate by the method used above:

$$T_{se}, V_e, \rho_e \text{ and } dA'_e = \frac{d\dot{m}_i}{\rho_e V_e} \ .$$

Then, we calculate the thrust delivered by the mass flow rate $d\dot{m}_i$

$$dF = (P_{se} - P_o) dA'_e + V_e d\dot{m}_i \ .$$

From the values computed at each area ΔA_i, by summing we obtain

– mass flow rate: $\dot{m}_i = \Sigma d\dot{m}_i$

– enthalpy: $H_{ti} = \Sigma h(T_{ti}) d\dot{m}_i$

– ideal thrust: $F = \Sigma dF$

– the enthalpy per unit mass is: $\bar{h}_{ti} = \frac{H_{ti}}{\dot{m}_i}$.

This corresponds to a temperature $\bar{T}_{ti}$ such as

$$\bar{h}_{ti} = h(\bar{T}_{ti}) \ .$$

By writing that $\bar{F} = F$ or else $\frac{\bar{F}}{\dot{m}} = \frac{F}{\dot{m}}$, we obtain the equation

$$\frac{(P_{se} - P_o)}{\bar{\rho}_e \bar{V}_e} + \bar{V}_e = \frac{F}{\dot{m}} \ .$$

If we take into account the state equation $\frac{P_{se}}{\bar{\rho}_e} = R\bar{T}_{se}$, this equation can also be expressed as follows:

$$\frac{(P_{se} - P_o)}{P_{se} \bar{V}_e} R\bar{T}_{se} + \bar{V}_e = \frac{F}{\dot{m}}$$

which, with the equation

$$\bar{h}_{ti} = \bar{h}_{te} = h(\bar{T}_{se}) + \frac{\bar{V}_e^2}{2}$$

makes up a system of two equations with two unknown quantities $\bar{T}_{se}$ and $\bar{V}_e$.

By solving these two equations we know the values of $\bar{V}_e$ and $\bar{T}_{se}$. From the latter we obtain $\bar{\Phi}_{se} = \Phi(\bar{T}_{se})$.

We calculate the total pressure which we are trying to define $\bar{P}_t$ by writing that

$$\Phi(\bar{T}_t) - \ln \bar{P}_t = \Phi(\bar{T}_{se}) - \ln P_{se}$$

from which we derive

$$\ln \frac{\bar{P}_t}{P_{se}} = \Phi(\bar{T}_t) - \Phi(\bar{T}_{se})$$

therefore

$$\boxed{\bar{P}_t = P_{se} \exp[\Phi(\bar{T}_t) - \Phi(\bar{T}_{se})] \ .}$$

The quantities characterizing the homogeneous flow $(\bar{E})$ are therefore known: $\bar{T}_t$ and $\bar{P}_t$.

The local values (static temperature, static pressure, velocity) of the homogeneous flow $(\bar{E})$ may be calculated by assuming a value for the area $\bar{A}_i$.

3.2.3 Turbine, or Compressor, or Fan

3.2.3.1 The Typical Ideal Evolution (Γ)

The typical ideal evolution (Γ) is an isentropic expansion (or compression), which is adiabatic up to a fixed stagnation pressure P_{te}.

3.2.3.2 The Characteristic Quantities K

The characteristic quantities K which have been selected are:

- ΔH_t the variation of the total enthalpy flow during (Γ)
- the mass flow rate $\dot{m}$
- the total enthalpy flow H_{ti} at the entrance of the component.

3.2.3.3 Calculation of the Characteristic Quantities Resulting from the Flow (E)

- As in the case of the nozzle, we calculate the total mass flow within the section A_i:

$$\dot{m}_i = \int_{A_i} \rho_i V_i \, dA_i$$

and the total enthalpy flow:

$$H_{ti} = \int_{A_i} h_{ti} \, d\dot{m}_i = \int_{A_i} h_{ti} \rho_i V_i \, dA_i$$

- The evolution (Γ) applied to each streamlet $d\dot{m}_i$ from the initial state (h_{ti}, s_i) to P_{te}, determines the variation of the enthalpy per unit mass Δh_t, from which we deduce the value of

$$\Delta H_t = \int_{A_i} \Delta h_t \, d\dot{m}_i \ .$$

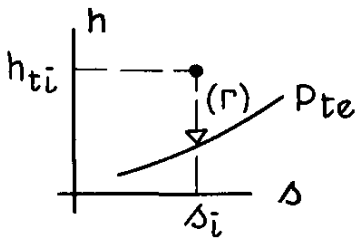

3.2.3.4 Determination of the Equivalent Flow (E)

– We wish to determine $(\bar{E})$ which has the same total enthalpy flow at the inlet, that is $H_{ti} = H_{ti}$, the same mass flow rate $\dot{m} = \dot{m}$ and such that after the evolution (Γ) we have $\Delta\bar{H}_t = \Delta H_t$ which leads to:

$$\Delta h_t = \frac{\Delta H_t}{\dot{m}_i} \tag{3}$$

$$h_{ti} = \frac{H_{ti}}{\dot{m}_i}. \tag{4}$$

The two Equations (3) and (4) make it possible to locate the point $\bar{i}$ of the flow $(\bar{E})$ in the Mollier diagram. In fact, as $\bar{h}_{ti}$ is known, it suffices to define, on the enthalpy line $\bar{h}_{ti}$, a point $\bar{i}$ such that through the transformation (Γ) we may have:

$$\Delta\bar{h}_t = \frac{\Delta H_t}{\dot{m}_i}.$$

Then we know the stagnation state $(\bar{E})\Gamma: \bar{h}_{ti}, \bar{s}_i$

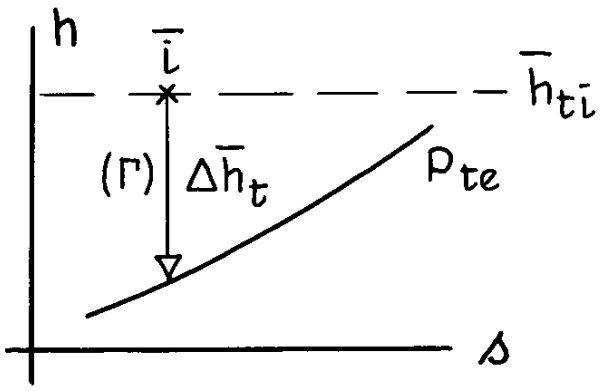

3.2.3.5 Comments and Remarks

– As in the case of the nozzle, the mass flow to be used is that calculated in the area A_i, and not the measured mass flow.

– In the case of a fan or compressor, the assumption of a calorifically perfect gas (γ = const.) is quite realistic. In this case, as shown in Section 3.2.7 the total pressure of the homogeneous flow $(\bar{E})$

$$\bar{P}_{ti} = \left[\frac{\int_{A_i} T_{ti}\, d\dot{m}_i}{\int_{A_i} \frac{T_{ti}}{P_{ti}^{(\gamma-1)/\gamma}}\, d\dot{m}_i} \right]^{\gamma/(\gamma-1)}$$

is independent of the pressure ratio.

3.2.3.6 Application

We shall deal here with two cases of calculation related to a compressor (or fan) (with the assumption γ = const) and to a turbine.

Example of a compressor (or fan)

The formula applicable when γ = const. gives

$$P_{ti} = \left[\frac{\int_{A_i} T_{ti} d\dot{m}_i}{\int_{A_i} \frac{T_{ti}}{P_{ti}^{(\gamma-1)/\gamma}} d\dot{m}_i} \right]^{\gamma/(\gamma-1)}$$

The calculation of the mass flow $d\dot{m}_i$ at each ΔA_i is elementary when the values of P_{ti}, T_{ti} and the static pressure P_{si} are known.

The total temperature T_{ti} is given by

$$\bar{T}_{ti} = \frac{\int T_{ti} d\dot{m}_i}{\dot{m}_i} .$$

Example of a turbine

The flow entering a turbine is usually rather heterogeneous and, taking into account the temperature level, the use of a constant value of γ cannot be justified.

We regard as known the functions

$$h(T) = \int^T C_p(T) dT$$

and

$$\Phi(T) = \frac{1}{R} \int \frac{C_p(T)}{T} dT$$

as a function of T and the fuel/air ratio.

For each streamlet with inlet area ΔA_i, we calculate, as in the case of the nozzle, the static temperature T_{si}, the velocity V_i and the density ρ_i. These quantities give the elementary mass flow

$$d\dot{m}_i = \rho_i V_i dA_i .$$

Knowing T_{ti}, we have $h(T_{ti})$; as this streamlet undergoes an isentropic expansion to P_{te}, we have, writing that $s_i = s_e$:

$$\Phi(T_{ti}) - \ln P_{ti} = \Phi(T_{te}) - \ln P_{te}$$

therefore

$$\Phi(T_{te}) = \ln \frac{P_{te}}{P_{ti}} + \Phi(T_{ti}) .$$

From the function $\Phi(T_{te})$ we obtain T_{te}, from which we derive h_{te}. Then, we know the enthalpy at the inlet H_{ti} and at the exit, H_{te}.

$$H_{ti} = \int h_{ti} d\dot{m}_i$$

$$H_{te} = \int h_{te} dm_i .$$

Now, we know the enthalpy per unit mass at the inlet:

$$\bar{h}_{ti} = \frac{H_{ti}}{\dot{m}_i}$$

to which corresponds the temperature $\bar{T}_{ti}$.

Likewise, we calculate the enthalpy per unit mass at the exit:

$$\bar{h}_{te} = \frac{H_{te}}{\dot{m}_i}$$

to which corresponds the temperature $\bar{T}_{te}$.

Then, we calculate the total pressure $\bar{P}_{ti}$, writing that the flow $(\bar{E})$ undergoes an isentropic expansion between the areas A_i and A_e, that is:

$$\Phi(T_{te}) - \ln P_{te} = \Phi(\bar{T}_{ti}) - \ln \bar{P}_{ti}$$

from which:

$$\ln \frac{\bar{P}_{ti}}{P_{te}} = \Phi(\bar{T}_{ti}) - \Phi(T_{te}) \ .$$

Hence

$$\boxed{\bar{P}_{ti} = P_{te} \exp[\Phi(\bar{T}_{ti}) - \Phi(\bar{T}_{te})] \ .}$$

The quantities generating the homogeneous flow $(\bar{E})$ are therefore known: $\bar{T}_{ti}$ and $\bar{P}_{ti}$.

The local values (static temperature, static pressure, velocity) of the homogeneous flow $(\bar{E})$ may be calculated by assuming a value for the area $\bar{A}_i$.

The average total pressure $\bar{P}_{ti}$ thus calculated is not an intrinsic quantity since it depends on the value of P_{te} taken at the turbine exit. The influence of P_{te} on the value of $\bar{P}_{ti}$ is examined in Section 4.4.

3.2.4 Combustion Chamber

3.2.4.1 The Typical Ideal Evolution

The typical ideal evolution is a given increase of the total enthalpy flow ΔH_t, without any thermal losses and with as few pressure losses as possible. For this purpose, we shall take a constant pressure combustion (P_f) a given pressure P_{si} and a fixed fuel/air ratio FAR.

It is realistic to assume that at the inlet to the combustor, in the area A_i, the pressure is uniform $(P_{si} = \text{const.})$. This pressure will be assumed for the constant pressure combustion.

When the static pressure in the plane A_i is not uniform, the method described here can nevertheless be applied, as explained in the remark at the end of this section.

With the ideal evolution chosen, there is no velocity variation between the areas A_i and A_e, that is:

$$\Delta h_t = \Delta h_s$$

or

$$E_{ce} = (1 + FAR)E_{ci} \ .$$

3.2.4.2 The Characteristic Quantities K

The characteristic quantities K are:

- the total enthalpy flow H_{te} at the exit
- the entropy flow S_e at the exit
- the mass flow $\dot{m}$
- the kinetic energy flow Ec_e at the exit

3.2.4.3 Computation of the Characteristic Quantities Resulting from the Flow (E)

- As previously, we calculate the mass flow in the area A_i:

$$\dot{m}_i = \int_{A_i} \rho_i V_i \, dA_i$$

the total enthalpy flow

$$H_{ti} = \int_{A_i} h_{ti} \, d\dot{m}_i = \int_{A_i} \rho_i V_i h_{ti} \, dA_i$$

and the static enthalpy flow:

$$H = \int_{A_i} h_{si} \, d\dot{m}_i = \int_{A_i} \rho_i V_i h_{si} \, dA_i \ .$$

In a similar way, we calculate the kinetic energy flow

$$E_{ci} = \frac{1}{2}\int_{A_i} V_i^2\, d\dot{m}_i = \frac{1}{2}\int_{A_i} \rho_i V_i^3\, dA_i$$

and the entropy flow rate

$$S_i = \int_{A_i} s_i\, d\dot{m}_i = \int_{A_i} s_i \rho_i V_i\, dA_i \ .$$

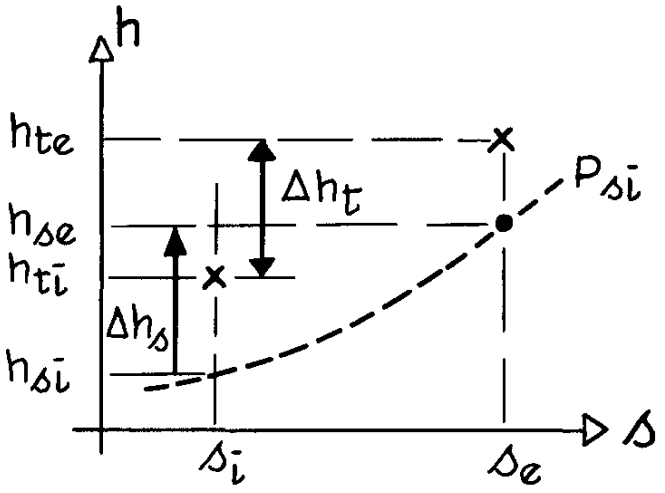

– The evolution (P_f) determines for each element $d\dot{m}_i$ of (E) the increase of enthalpy per unit mass:

$$\Delta h_t = (1 + FAR)h_{te} - h_{ti} = (FAR)(FHV)$$

(FHV being the heating value of the fuel).

The increase of the total enthalpy flow is:

$$\Delta H_t = \int_{A_i} \Delta h_t\, d\dot{m}_i = (FAR)(FHV)\dot{m}_i$$

hence:

$$H_{te} = H_{ti} + \Delta H_t = H_{ti} + (FAR)(FHV)\dot{m}_i \ .$$

Since a constant pressure evolution is assumed, therefore no change in velocity is expected. We have

$$H_{se} = H_{si} + (FAR)(FHV)\dot{m}_i \ .$$

Therefore, we know the enthalpies per unit mass

$$\frac{H_{ti}}{\dot{m}_i}, \frac{H_{si}}{\dot{m}_i}, \frac{H_{te}}{\dot{m}_e} \text{ and } \frac{H_{se}}{\dot{m}_e} \ .$$

On Mollier's diagram, the entropy s_e at the exit is therefore determined, and we can calculate:

$$S_e = (1 + FAR)\int_{A_i} s_e\, d\dot{m}_i \ .$$

3.2.4.4 Determination of the Equivalent Flow $(\bar{E})$

– This flow must be such that:

$$\bar{H}_{te} = H_{te} = H_{ti} + (FAR)(FHV)\dot{m}_i$$
$$\bar{S}_e = S_e$$

$$\dot{m}_i = \dot{m}_i$$

$$\bar{E}_{ce} = E_{ce}$$

Now, the elevation (P_f) applied to $(\bar{E})$ determines

$$\bar{H}_{te} = \bar{H}_{ti} + (FAR)(FHV)\dot{m}_i$$

which leads to:

$$\bar{H}_{ti} = H_{ti}$$

hence:

$$\boxed{\bar{h}_{ti} = \frac{1}{\dot{m}_i} \int_{A_i} h_{ti} d\dot{m}_i \ .}$$

In addition, since the velocity is invariant in the constant pressure evolution, we have:

$$\bar{H}_{te} - \bar{H}_{se} = (1 + FAR)[\bar{H}_{ti} - \bar{H}_{si}]$$

$$H_{te} - H_{se} = (1 + FAR)[H_{ti} - H_{si}]$$

which, with the equivalence $E_{ce} = \bar{E}_{ce}$ leads to: $\bar{H}_{si} = H_{si}$ that is:

$$\boxed{\bar{h}_{si} = \frac{1}{\dot{m}_i} \int_{A_i} h_{si} d\dot{m}_i \ .}$$

Knowing $\bar{h}_{si}$, $\bar{h}_{ti}$ and the pressure P_{si} we can entirely determine the flow $(\bar{E})$ whose stagnation state and local state we now know.

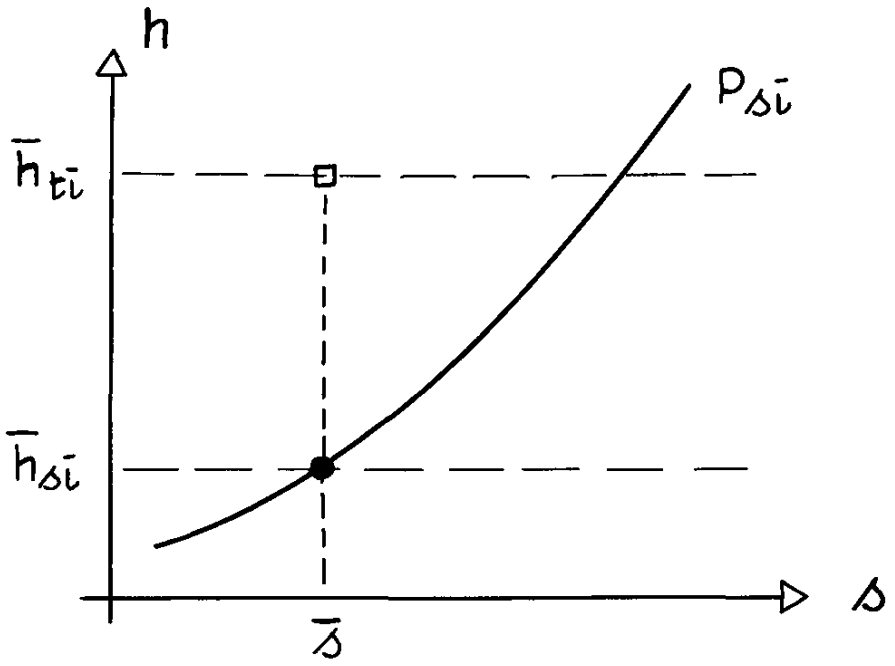

We note that the flow $(\bar{E})$ has been defined without resorting to the condition

$$\bar{S}_e = S_e \ .$$

However, the above relation is verified if the flow distortion is small enough to permit the linearization of the relation s(h, P) in the area A. In fact, if we can write:

$$s_e = \bar{s}_e + \bar{s}_e'(h_{se} - \bar{h}_{se})$$

then, we obtain

$$S_e = \int (1 + FAR) s_e \, d\dot{m}_i = \dot{m}_i (1 + FAR) \bar{s}_e = \bar{S}_e$$

provided that the relation $\int h_{se} \, d\dot{m}_i = \dot{m}_i \bar{h}_{se}$ is verified. This relation which can also be written $H_{se} = \bar{H}_{se}$ is obvious since

$$H_{se} = H_{te} - E_{ce}$$

and

$$\bar{H}_{se} = \bar{H}_{te} - \bar{E}_{ce} \ .$$

Now, we do have, by definition

$$H_{te} = \bar{H}_{te}$$

and

$$E_{ce} = \bar{E}_{ce} \ .$$

3.2.4.5 Comments and Remarks

As in the other cases dealt with previously, the mass flow to be used is that calculated in the area A_i and not that measured.

We notice that the stagnation state of $(\bar{E})$ at the combustor inlet is independent of the fuel/air ratio. This is why, although in principle, the assumption of $\gamma = \text{const.}$ is not realistic for a combustion, we can nevertheless carry out the corresponding calculations and calculate the average values, as these are not influenced by combustion. It is shown in the Annex that

$$\bar{P}_{ti} = \left[\frac{\int_{A_i} T_{ti} \, d\dot{m}_i}{\int_{A_i} \frac{T_{ti}}{P_{ti}^{(\gamma-1)/\gamma}} \, d\dot{m}_i} \right]^{\gamma/(\gamma-1)}$$

We recognize the formula which was obtained for the compressor (or fan or turbine).

- In the assumption of a calorifically perfect gas ($C_p = \text{const.}$), ΔS is determined by ΔH in a constant pressure transformation, so that the evolution (P_f) applied to (E) will ensure:

$$\Delta \bar{S} = \Delta S$$

which implies, since $\bar{S}_e = S_e$

$$\bar{S}_i = S_i \ .$$

- In principle, the above calculations use a Mollier diagram corresponding to the pure air for the state at the combustor inlet (area A_i) and to the burnt gases with the fuel/air ratio equal to FAR for the combustor exit (area A_e)

Important remark

Case when the static pressure in the plane A_i is not constant

The knowledge of $\bar{h}_{ti}$, $\bar{h}_{si}$ and of the mean static pressure $\bar{P}_{si}$ is required to calculate the stagnation state and local state of $(\bar{E})$. In what precedes, it has been assumed that the static pressure of the flow (E) was constant in the section $A_i (P_{si} = \text{const.})$ and, in this case, it has been assumed that the static pressure of $(\bar{E})$ was of equal value.

When P_{si} is not constant, it is always possible to use the general method to calculate:

$$\bar{h}_{ti} = \frac{1}{\dot{m}_i} \int_{A_i} h_{ti} \, d\dot{m}_i$$

and

$$\bar{h}_{si} = \frac{1}{\dot{m}_i} \int_{A_i} h_{si} \, d\dot{m}_i$$

however, it is necessary to know the mean static pressure $\bar{P}_{si}$ prior to defining $(\bar{E})$.

It is possible, of course, to calculate a mean pressure of the P_{si}'s in a purely arbitrary manner (area averaged mean value is often used).

– However, there is also a more rational method for calculating a static pressure $\bar{P}_{si}$ of (E). When the flow (E) is

– homogeneous in total pressure (P_{ti} = const.)

– homogeneous in total temperature (T_{ti} = const.)

– non homogeneous in static pressure (P_{si} variable in A_i)

then it is easy to demonstrate that there is a single value of $\bar{P}_{si}$, such that, by applying the general method, we find:

$$\bar{P}_{ti} = P_{ti} \ .$$

Based on the calculations carried out in Section 3.2.7, it is easily demonstrated that for a calorifically perfect gas (γ = const) this value of $\bar{P}_{si}$ is given by

$$\bar{P}_{si} = \left[\frac{\int_{A_i} (P_{si})^{(\gamma-1)/\gamma} \, d\dot{m}_i}{\int_{A_i} d\dot{m}_i} \right]^{\gamma/(\gamma-1)}$$

It is recommended to resort to this formula to deal with all the cases when the static pressure of the flow (E) is not constant within A_i.

3.2.4.6 Application

– Applying the same methods as those used previously, we calculate

$$\dot{m}_i = \int_{A_i} d\dot{m}_i \ ; \quad H_{ti} = \int_{A_i} h_{ti} d\dot{m}_i$$

and

$$H_{si} = \int_{A_i} h_{si} d\dot{m}_i \ .$$

Then, we know

$$\bar{h}_{ti} = \frac{\bar{H}_{ti}}{\dot{m}_i} \quad \text{hence} \quad \bar{T}_{ti}$$

and

$$\bar{h}_{si} = \frac{H_{si}}{\dot{m}_i} \quad \text{hence} \quad \bar{T}_{si} \ .$$

The entropy per unit mass is given by

$$\bar{s}_i = R[\Phi(\bar{T}_{si}) - \ln P_{si}]$$

P_{ti} is then given by

$$\Phi(\bar{T}_{si}) - \ln \bar{P}_{si} = \Phi(\bar{T}_{ti}) - \ln \bar{P}_{ti}$$

that is

$$\boxed{\bar{P}_{ti} = \bar{P}_{si} \exp[\Phi(\bar{T}_{ti}) - \Phi(\bar{T}_{si})] \ .}$$

We know the quantities generating the homogeneous flow (E), $\bar{T}_{ti}$, $\bar{P}_{ti}$ and static pressure $\bar{P}_s$. All other static values may be then calculated.

3.2.5 Afterburner Channel

3.2.5.1 The typical ideal evolution (/) will be combustion in a constant section, without any thermal losses nor wall friction, with a given fuel/air ratio FAR. We shall note that the evolution (/) necessarily retains the momentum dynalpy or stream force of the flow:

$$J_i = J_e \ .$$

3.2.5.2 The Characteristic Quantities K

The characteristic quantities K are:

– the mass flow $\dot{m}$

the total enthalpy flow at the exit of the afterburner channel H_{te}

the stream force or dynalpy at the exit of the afterburner channel J_e.

3.2.5.3 Calculation of the Characteristic Quantities Resulting from the Flow (E)

– As previously, we calculate the mass flow in the area A_i

$$\dot{m}_i = \int_{A_i} \rho_i V_i \, dA_i \ .$$

The mass flow at the exit is $(1 + FAR)\dot{m}_i$.

We calculate the total enthalpy flow in the area A

$$H_{ti} = \int_{A_i} h_{ti} \, d\dot{m}_i = \int_{A_i} h_{ti} \rho_i V_i \, dA_i$$

then the total enthalpy flow at the exit:

$$H_{te} = H_{ti} + (FAR)(FHV)\dot{m}_i \ .$$

Finally, the dynalpy at the exit J_e:

$$J_e = J_i = \int_{A_i} (P_{si} + \rho_i V_i^2) dA_i \ .$$

3.2.5.4 Determination of the Equivalent Flow ($\bar{E}$)

– ($\bar{E}$) must satisfy the following relations

$$\begin{cases} \bar{\dot{m}}_i = \dot{m}_i \\ \bar{H}_{te} = H_{te} \\ \bar{J}_e = J_e \ . \end{cases}$$

Now the transformation ($\mathcal{J}$) applied to ($\bar{E}$) gives:

$$H_{te} = \bar{H}_{ti} + (FAR)(FHV)\dot{m}_i$$

which leads to

$$\bar{H}_{ti} = H_{ti} \ .$$

In addition, ($\mathcal{A}$) applied to ($\bar{E}$) leads also to:

$$J_e = \bar{J}_i$$

($\bar{E}$) is therefore such that

$$\begin{cases} \bar{\dot{m}}_i = \dot{m}_i \\ \bar{H}_{ti} = H_{ti} \\ \bar{J}_i = J_i \ . \end{cases}$$

These relations can also be written as follows:

$$\begin{cases} \bar{\rho}_i \bar{V}_i = \dfrac{\dot{m}_i}{A_i} \\ \bar{h}_{ti} = \bar{h}_{si} + \dfrac{\bar{V}_i^2}{2} = \dfrac{H_{ti}}{\dot{m}_i} \\ \bar{P}_{si} + \bar{\rho}_i \bar{V}_i^2 = \dfrac{\bar{J}_i}{A_i} \ . \end{cases}$$

– The three previous equations include three main unknown quantities $\bar{\rho}_i$, $\bar{P}_{si}$, $\bar{V}_i$, since, by definition $h = h(P, \rho)$. The problem is therefore determined and we can calculate $\bar{\rho}_i$, $\bar{P}_{si}$, $\bar{V}_i$, which, with $\bar{h}_{ti}$, determine entirely the flow ($\bar{E}$) (stagnation and static states).

3.2.5.5 Comments and Remarks

– As in the other cases, the quantities which will be used to calculate the stagnation state of the homogeneous flow ($\bar{E}$) will be calculated and not measured ones (mass flow, momentum).

- It may be noted that the equations used to determine the flow (E) are independent of the fuel/air injected into the afterburner channel, and depend only on the state of the flow (E) in the area A_i. These three equations are identical to those which we would obtain by writing that the heterogeneous flow (E) homogenizes in the course of an adiabatic mixing process at a constant section, and without friction on the walls.

3.2.5.6 Application

The three equations given in Section 3.2.5.4 give the values of $\bar{\rho}_i$, $\bar{P}_{si}$, and $\bar{V}_i$. The value of the total enthalpy per unit mass $\bar{h}_{ti} = H_{ti}/\dot{m}_i$ gives the value of the total temperature $\bar{T}_{ti}$. The state equation gives the value of the static temperature $T_{si} = \bar{P}_{si}/R\bar{\rho}_i$. Then the total pressure is obtained by writing that the entropy computed with total values is equal to that computed with static values

$$\Phi(\bar{T}_{ti}) - \ln \bar{P}_{ti} = \Phi(\bar{T}_{si}) - \ln \bar{P}_{si}$$

and

$$\boxed{\bar{P}_{ti} = \bar{P}_{si} \exp[\Phi(\bar{T}_{ti}) - \Phi(\bar{T}_{si})] \ .}$$

3.2.6 Diffuser and Air Intake

If we try to apply the general method to the case of a diffuser (and the case of an air intake) considered per se as a component, we are confronted with a particular difficulty. As a matter of fact, the real component is usually adiabatic and has a constant flow rate; therefore, the normal assumptions used to define $(\bar{E})$ include the equalities:

$$\left.\begin{aligned} \bar{\dot{m}}_i &= \dot{m}_i \\ \bar{h}_{ti} &= \frac{1}{\dot{m}_i} \int_{A_i} h_{ti} d\dot{m}_i \end{aligned}\right\} \qquad (5)$$

But the *typical evolution* which should be an isentropic recompression without any external work cannot be achieved for the flow (E), as neither the boundary layers nor the low speed streamlets cannot undergo it. So, we have the choice of two avenues to solve this problem:

(a) either, consider the diffuser or air intake as being part and parcel of the preceding or the following component (for instance the compressor for the air intake, or the combustor for the diffuser) and apply, at the inlet and at the exit, the method defined for the complete component considered;

(b) or, develop a specific method different from the general one. This method may be for instance the definition of a homogeneous flow which possesses in the inlet area A_i a number of integral quantities calculated on the basis of the given heterogeneous flow. For the sake of example, three sets of integral quantities providing the means of defining a homogeneous flow are proposed below

(b1)	(b2)	(b3)
– mass flow	– mass flow	– mass flow
– enthalpy flow	– enthalpy flow	– enthalpy flow
– area	– area	– area
– static pressure	– dynalpy	– entropy flow

In procedure (b1), it is explicitly assumed that the given flow (E) has constant pressure in the section A_i.

The procedure (b2) amounts to considering a constant section mixing of (E).

3.2.7 Case of the Calorifically Perfect Gas

3.2.7.1 Exhaust Nozzle

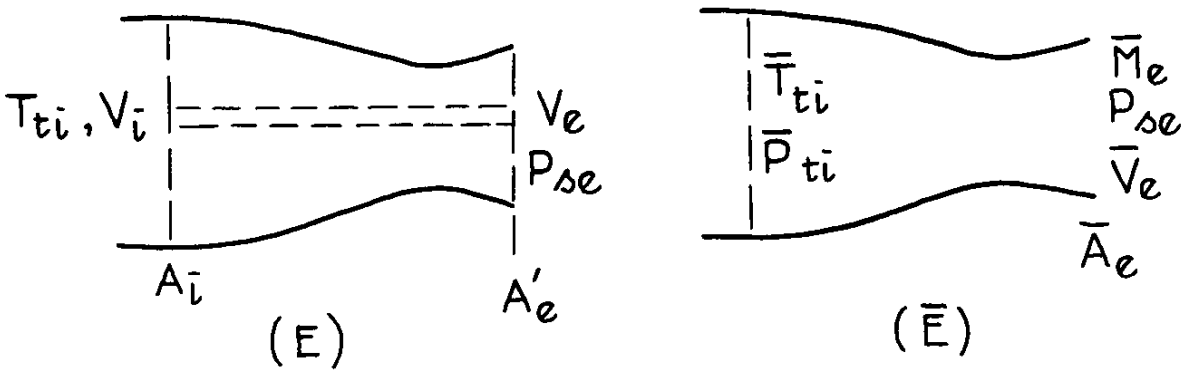

Here, the equality $\bar{h}_{ti} = \dfrac{H_{ti}}{\dot{m}_i}$ is written as follows:

$$\bar{T}_{ti} = \frac{1}{\dot{m}_i} \int_{A_i} T_{ti}\, d\dot{m}_i \,.$$

Each element $d\dot{m}_i$ of (E) delivers a thrust:

$$dF = V_e\, d\dot{m}_i + (P_{se} - P_o) dA'_e$$

that is

$$dF = V_e\, d\dot{m}_i + \frac{(P_{se} - P_o)}{\rho_e V_e} d\dot{m}_i \,.$$

The thrust F delivered by the flow (E) is therefore:

$$F = \int_{A_i} \left[V_e + \frac{(P_{se} - P_o)}{\rho_e V_e} \right] d\dot{m}_i \,.$$

The thrust delivered by the flow $(\bar{E})$ is:

$$\bar{F} = \bar{V}_e \bar{\dot{m}}_i + (P_{se} - P_o) \bar{A}_e$$

that is, after elementary transformation:

$$\bar{F} = \frac{\bar{\dot{m}}_i \sqrt{\gamma R \bar{T}_{te}} \left[\bar{M}_e + \dfrac{P_{se} - P_o}{P_{se}} \times \dfrac{1}{\gamma \bar{M}_e} \right]}{\sqrt{1 + \dfrac{\gamma - 1}{2} \bar{M}_e^2}}$$

where we know

$$\bar{\dot{m}}_i = \dot{m}_i$$

and

$$\bar{T}_{te} = \bar{T}_{ti} = \frac{1}{\dot{m}_i} \int_{A_i} T_{ti}\, d\dot{m}_i \,.$$

The fundamental equality $\bar{F} = F$ is therefore written as follows

$$\frac{\bar{M}_e + \dfrac{P_{se} - P_o}{P_{se}} \times \dfrac{1}{\gamma \bar{M}_e}}{\sqrt{1 + \dfrac{\gamma - 1}{2} \bar{M}_e^2}} = \frac{1}{\dot{m}_i \sqrt{\gamma R \bar{T}_{ti}}} \int_{A_i} \left[V_e + \frac{P_{se} - P_o}{\rho_e V_e} \right] d\dot{m}_i$$

whose solution gives $\bar{M}_e$. Then, we calculate:

$$\boxed{\bar{P}_{te} = \bar{P}_{ti} = P_{se} \left(1 + \frac{\gamma - 1}{2} \bar{M}_e^2 \right)^{\gamma/(\gamma-1)} \,.}$$

3.2.7.2 Turbine, or Compressor, or Fan

The isentropic expansion (or compression) of each streamlet $d\dot{m}_i$ of the flow (E) makes it possible to write:

$$\Delta H_t = \int_{A_i} \Delta h_t\, d\dot{m}_i = \int_{A_i} h_{te}\, d\dot{m}_i - H_{ti}$$

$$= Cp \int_{A_i} T_{te}\, d\dot{m}_i - H_{ti} = Cp \int_{A_i} T_{ti} \left(\frac{P_{te}}{P_{ti}} \right)^{(\gamma-1)/\gamma} d\dot{m}_i - H_{ti} \,.$$

The isentropic expansion or compression of the flow $(\bar{E})$ gives:

$$\Delta \bar{H}_t = Cp \bar{T}_{ti} \left(- \frac{P_{te}}{\bar{P}_{ti}} \right)^{(\gamma-1)/\gamma} \bar{\dot{m}}_i - \bar{H}_{ti} \,.$$

Taking into account the fact that $H_{ti} = H_{ti}$, we find that

$$Cp\,T_{ti}\left(\frac{P_{te}}{P_{ti}}\right)^{(\gamma-1)/\gamma} \dot{m} = Cp \int_{A_i} T_{ti}\left(\frac{P_{te}}{\bar{P}_{ti}}\right)^{(\gamma-1)/\gamma} d\dot{m}_i \ .$$

The total pressure $\bar{P}_{ti}$ of the flow (E) at the inlet to the component is given by:

$$\frac{\bar{T}_{ti}}{(\bar{P}_{ti})^{(\gamma-1)/\gamma}} = \frac{1}{\dot{m}_i} \int_{A_i} \frac{T_{ti}}{P_{ti}^{(\gamma-1)/\gamma}} d\dot{m}_i \ .$$

We note that $\bar{T}_{ti}/\bar{P}_{ti}^{(\gamma-1)/\gamma}$ is the value, averaged by the mass flow of $T_{ti}/P_{ti}^{(\gamma-1)/\gamma}$ whose logarithm is proportional to the entropy.

Taking into account the fact that $\bar{T}_{ti} = \frac{1}{\dot{m}_i} \int_{A_i} T_{ti} d\dot{m}_i$ we obtain:

$$\boxed{\bar{P}_{ti} = \left[\frac{\int_{A_i} T_{ti} d\dot{m}_i}{\int_{A_i} \frac{T_{ti}}{P_{ti}^{(\gamma-1)/\gamma}} d\dot{m}_i}\right]^{\gamma/(\gamma-1)}}$$

It should be pointed out that in the case of a calorifically perfect gas, $\bar{P}_{ti}$, the mean total pressure of the flow (E) at the inlet of the component is independent of P_{te}, that is to say independent of the pressure (or expansion) ratio.

3.2.7.3 Combustion Chamber

In the case of γ = const, the enthalpy per unit mass (total and static) is expressed by:

$$h_t = Cp\,T_t$$

$$h_s = Cp\,T_s = \frac{Cp\,T_t}{1 + \frac{\gamma-1}{2} M^2} = \frac{Cp\,T_t}{\left(\frac{P_t}{P_s}\right)^{(\gamma-1)/\gamma}}$$

and the entropy per unit mass is expressed by

$$s = R \ln \frac{T_t^{\gamma/(\gamma-1)}}{P_t} = R \ln \frac{T_s^{\gamma/(\gamma-1)}}{P_s} .$$

The equalities $\bar{h}_{ti} = \dfrac{\int_{A_i} h_{ti} d\dot{m}_i}{\dot{m}_i}$

and $\bar{h}_{si} = \dfrac{\int_{A_i} h_{si} d\dot{m}_i}{\dot{m}_i}$

are written

$$\bar{T}_{ti} = \frac{1}{\dot{m}_i} \times \int_{A_i} T_{ti} d\dot{m}_i$$

and

$$\bar{T}_{si} = \frac{1}{\dot{m}_i} \times \int_{A_i} \frac{T_{ti}}{\left(\frac{P_{ti}}{P_{si}}\right)^{(\gamma-1)/\gamma}} d\dot{m}_i \ .$$

The total pressure $\bar{P}_{ti}$ is calculated then by

$$\bar{P}_{ti} = P_{si} \times \left[\frac{\bar{T}_{ti}}{\bar{T}_{si}}\right]^{\gamma/(\gamma-1)}$$

hence

$$\bar{P}_{ti} = P_{si}\left[\frac{\int_{A_i} T_{ti}\,d\dot{m}_i}{\int_{A_i}\frac{T_{ti}}{\left(\frac{P_{ti}}{P_{si}}\right)^{(\gamma-1)/\gamma}}d\dot{m}_i}\right]^{\gamma/(\gamma-1)}$$

in the case where $P_{si} = \text{const}$, it follows:

$$\boxed{P_{ti} = \left[\frac{\int_{A_i} T_{ti}\,d\dot{m}_i}{\int_{A_i}\frac{T_{ti}}{P_{ti}^{(\gamma-1)/\gamma}}d\dot{m}_i}\right]^{\gamma/(\gamma-1)}}$$

It should be noted that this formula is identical to those of a turbine (or compressor or fan).

3.2.7.4 Afterburner Channel

In the case of $\gamma = \text{const}$ the three equations of Section 3.2.5.4 (conservation of the flow rate, total enthalpy and dynalpy) are written as follows:

$$\sqrt{\frac{\gamma}{R}}\frac{\bar{P}_{si}}{\sqrt{\bar{T}_{ti}}}A_i\bar{M}_i\sqrt{1+\frac{\gamma-1}{2}\bar{M}_i^2} = \dot{m}_i$$

$$\bar{T}_{ti} = \frac{\int_{A_i} T_{ti}\,d\dot{m}_i}{\dot{m}_i}$$

$$\bar{P}_{si}A_i(1+\gamma\bar{M}_i^2) = J_i\left[= \int_{A_i} P_{si}(1+\gamma M_i^2)\,dA_i\right] .$$

By dividing, side by side, the first equation by the third one, we obtain

$$\frac{\bar{M}_i\sqrt{1+\frac{\gamma-1}{2}\bar{M}_i^2}}{1+\gamma\bar{M}_i^2} = \frac{\dot{m}_i}{J_i}\sqrt{\bar{T}_{ti}}\sqrt{\frac{R}{\gamma}} = \xi$$

whose solution is

$$\bar{M}_i^2 = \frac{2\gamma\xi^2 - 1 + \sqrt{1-2\xi^2(1+\gamma)}}{\gamma - 1 - 2\gamma^2\xi^2} .$$

Knowing $\bar{M}_i$ we calculate

$$\bar{P}_{si} = \frac{J_i}{A_i(1+\gamma\bar{M}_i^2)}$$

and

$$\boxed{\bar{P}_{ti} = \bar{P}_{si}\left(1+\frac{\gamma-1}{2}\bar{M}_i^2\right)^{\gamma/(\gamma-1)}} .$$

Chapter 4

COMPARISON OF FLOW AVERAGING METHODS

SUMMARY

The intent of this chapter is to coalesce the material from the preceding chapters into numerical examples that illustrate the difference in results obtained from different flow averaging methods.

The analytical or experimental examples which include ducted flows, engine exhaust nozzle flows, turbomachinery component flows and engine system analyses are intended to illustrate the type of flow averaging problems encountered and the impact of the different flow averaging methods on engine component and engine system performance evaluation.

The objective of the section on ducted flows is to provide a systematic numerical illustration of basic single plane averaging methods for total pressure. A selection of other parameters is included. A broad and detailed parametric variation includes the effect of Mach number, 1/nth power laws and boundary layer thickness.

By means of experimental data from exhaust nozzle flows the problems of defining nozzle mean flow properties, flow coefficients and nozzle performance efficiency for nonuniform flowfields and the problems of relating uniform flow model data to full scale engine test results are discussed. Examples of different nozzle flowfield averaging methods using data from different bypass turbofan engine tests are presented.

One dimensional properties of turbomachinery flows are examined using analytical data for a single stage compressor and a two stage hot turbine. The axisymmetric flow fields are represented by one radial distribution of flow properties in each plane. To examine the magnitude of the differences likely to be found in practice, sample calculations have been done on actual test results from compressor inlets at different distortion conditions.

The final section contains an application of the Pianko method of averaging, described in section 3.2, to a set of coherent data representing the different sections of a turbojet, such as inlet of compressor, combustor, turbine, diffusor, reheat channel and nozzle. Comparison is made between the Pianko and the Dzung method.

4.1 DUCTED FLOW

A	Cross-sectional Area
$\dot{m}$	Mass flow rate
M	Mach number
M_0	Mainstream Mach number
P_s	Static pressure
P_t	Total pressure
R	Gas constant
R_0	Outer diameter in axial symmetry. Duct half-width two-dimensionally.
T_s	Static temperature
T_t	Total temperature
v	Local velocity
δ	Nominal boundary-layer thickness
ϵ_2	Momentum flux coefficient
ϵ_3	Energy flux coefficient
$-$	Over a character indicates a mean value of some form defined locally in the text.
1	Indicates an initial condition.

4.1.1 The objective of this section is to provide a systematic numerical illustration of averaging methods not confused by experimental error or traverse detail limitations. The five basic averaging methods for total pressure of Mass Weighting, Area Weighting, Mass Derivation, Constant Momentum Mixing in a constant area duct (Dzung) and Constant Entropy Flux (Livesey) are compared directly. A selection of other parameters is also presented, including momentum and energy flux coefficients, three forms of mean Mach Number, maximum to mean velocity ratio and the ratio of the mean static pressure to the static pressure (assumed constant in the non-uniform flow) for two methods of averaging.

Extensive comparative numerical tabulation is given for a wide variety of duct velocity profiles using 1/n power laws ($1 \leqslant n \leqslant 9$) boundary layer thicknesses ($0 \leqslant \delta/R_0 \leqslant 1$) and main stream Mach numbers ($0.2 \leqslant M_0 \leqslant 4.0$) and covering both axisymmetric and channel flows.

4.1.2 The assumed power law velocity profiles are shown in Figure 4.1.1. Power Law indices chosen are 1 (linear velocity profiles), $\frac{1}{3}, \frac{1}{5}, \frac{1}{7}$ (moderate to high R_e turbulent flow) and $\frac{1}{9}$. The boundary layer thickness δ/R_0 is varied incrementally by 0.1. Further assumptions include constant static pressure, constant total temperature, constant specific heats ($\gamma = 1.4$) which give a rational, simple model corresponding to Prandtl number equal to unity. The assumption of constant total temperature is of fundamental importance thermodynamically (see later). The constant static pressure corresponds to parallel flow and the absence of any turbulence which is formally excluded from the model. Detailed descriptions of the various averaging methods are to be found elsewhere in this volume (Chapters 2 and 3) but some repetition in summary is worthwhile here. The five different definitions of Mean Total Pressure, which may be computed directly from the assumed flows are as follows:

Mass Weighting

$$\bar{P}_t = \frac{\int_A P_t \times d\dot{m}}{\dot{m}}$$

may be found in isolation in relation to losses ($\Delta P_t/P_{tl}$) and, when associated with other mean variables, care is needed to distinguish whether these variables imply a mass derived assumption via $\dot{m}\sqrt{T_t}/AP_t$ for example or are obtained more simply via $\bar{P}_t/P_s$, ambiguity is common.

Area Weighting

$$\bar{P}_t = \frac{\int_A P_t \times dA}{A}$$

Similar comments apply as above.

Mass Derivation

$$\frac{\dot{m}\sqrt{T_t}}{AP_s} \rightarrow \frac{P_t}{P_s} \rightarrow P_t$$

Here a self consistent set of mean variables is implied via M, T_t/T_s, $v/\sqrt{T_t}$ etc.

Mixing at Constant Momentum, and in a Constant Area Duct (Dzung)

$$\dot{m}\frac{\sqrt{T_t}}{AP_s} = \left(\frac{\gamma}{R}\right)^{1/2} \bar{M} \left(1 + \frac{\gamma - 1}{2}\bar{M}^2\right)^{1/2}$$

$$\bar{P}_s = \frac{\int_A P_s(1 + \gamma \bar{M}^2)dA}{(1 + \gamma \bar{M}^2)A}$$

together imply an $\bar{M}$

Again a self consistent set of mean variables is implied as above. Here a total pressure mixing loss occurs together with a change in static pressure, usually a recovery. There are difficulties in interpretation for transonic flows dependent upon the assumption or otherwise of the occurrence of a normal shock wave with the mixing process and a contravention of the Second Law for supersonic solutions. See later discussion of results.

Constant Entropy Flux (Livesey), also called Entropy Weighting

$$\dot{m}\ln.\bar{P}_t = \int_A \ln P_t \times d\dot{m}$$

Again a self consistent set of mean variables is implied.

When constant T_t is assumed then no loss of total pressure is implied in this $\bar{P}_t$.

The mean static pressure is not equal to the assumed constant static pressure, although the difference can be ignored for $M_0 < 2$. Momentum flux is not conserved.

The above five mean total pressures have been computed for the assumed velocity profiles and in the tabular presentation have been normalised by division by the Constant Entropy Flux total pressure.

In order to be able to specify the independent flux contributions in the energy and momentum equations it is necessary to define energy and momentum flux coefficients ϵ_3 and ϵ_2 .

$$\epsilon_3 \times \dot{m}\bar{v}^2 = \int_A v^2 d\dot{m} \qquad \epsilon_2 \times \dot{m}\bar{v} = \int_A v d\dot{m}$$

Note that the Dzung method does not imply these two coefficients neither is it able to separately identify the independent flux contributions to the energy and momentum equations in the original non-uniform flow.

The energy and momentum flux coefficients are tabulated in the numerical results.

The integrations were performed using standard routines (NAGLIB, Mark 5, DOIGAF, Method of Gill and Miller) and 150 points within the boundary layer thickness. Comparable accuracy in a real data situation would only be obtainable by careful curve fitting of the sparse data (see later comments). Where six decimal places are quoted the fifth and sixth figures changed between 100 and 150 point representation of the profiles.

Integration at 400 point representation indicated that the fourth decimal place was accurate (at 150 point representation). For purposes of condensation of the presentation in the tables some magnitudes have been rounded to the third place of decimals and where six places are quoted these are the raw (150 point) figures for which the fourth place is accurate. These limiting accuracies are governed by the calculation of momentum mixed mean values (Dzung) where the equation solution procedures for mean Mach Number is demanding numerically. All data other than momentum mixed mean (Dzung) presented in the table are generally at slightly higher accuracy.

4.1.3 The eight pages of tabulation present numerically the results of the computations of the quantities described for the various velocity profiles. The first four pages are for the case of axisymmetrical flow, the last four pages are for two-dimensional flow. Each page carries the column headings once and covers two values of maximum Mach Number M_0 , one in the upper half page, the other in the lower half page. Within each half page are recognizable five blocks corresponding to the power law of the velocity profile, i.e.1, $\frac{1}{3}$, $\frac{1}{5}$, $\frac{1}{7}$, $\frac{1}{9}$. Within each of the power law blocks are ten rows corresponding to the boundary layer thickness δ/R_0 increments 0.1, 0.2, 0.3, 0.4, 0.5, 0.6, 0.7, 0.8, 0.9, 1.0. (R_0 is the outer diameter in axisymmetry and the duct half-width two-dimensionally).

The column headings are almost self explanatory. The first four columns are Mean Total Pressure values by different averaging methods, Mass Weighted, Area Weighted, Mass Derived and Momentum Mixed (Dzung) *all normalised by division by the Entropy Flux Mean Total Pressure (Livesey).* This normalisation gives the convenient indication of contravention of the Second Law of Thermodynamics in the Mean Total Pressure when the normalised value exceeds unity. (Note particularly here that this is always the case for Mass Weighting unless the Mach Number is zero i.e. incompressible flow). The mean velocity implied in the definitions of the energy flux and momentum flux coefficient in columns 5 and 6 and in the velocity ratio in column 10 is the Entropy Flux mean velocity (Livesey).

An asterisk (*) against a figure (see Tables for $M_0 \geqslant 2$) indicates that a subsonic result for Mixed Mean Mach Number (Dzung) is given together with the associated Mean Total Pressure and static pressure ratios but also that there does exist a Supersonic Mixed Mean Mach Number (Dzung) which does not contravene the Second Law of Thermodynamics. If of interest the Supersonic state values may be obtained by use of normal shock tables for the normal shock upstream Supersonic Mixed Mean Mach Number and the ratios of total pressure and static pressure across the shock with reference to the downstream Subsonic Mixed Mean Mach Number given in the table. Note that great care is needed in interpretation here. From the table ($M_0 \geqslant 2$) it will be seen that there exist conditions (without asterisk *) for which the Mixed Mean Mach Number *must* be subsonic. For these cases the state corresponding to the Supersonic Mixed Mean Mach Number will contravene the Second Law of Thermodynamics and is clearly inadmissible. The interpretation of the Supersonic Mixed Mean Mach Numbers which do not contravene the Second Law is difficult; it is unlikely that these states are realizable except under unusual circumstances, if at all.

As the solution procedures are carried out for the Mixed Mean Mach Number (Dzung) for progressively increasing $M_0 > 1.0$ it appears initially that subsonic Mixed Mean Mach Numbers occur naturally for all supersonic M_0 . It is also evident that one precise numerical interpretation of the achievement of this state is initial mixing to a Supersonic Mixed Mean Mach Number followed by the occurrence of a normal shock wave. However when entropy changes are investigated it is found that some of the Supersonic Mixed Mean Mach Number states contravene the Second Law indicating that the process of mixing and the occurrence of a normal shock can not be separated and the subsonic solution alone is tenable. The general progression to Subsonic Mixed Mean Mach Numbers is thus probably the preferred interpretation and is therefore the one quoted in the tables. The asterisk (*) distinguishes clearly where a supersonic result is available which does not contravene the Second Law and this supersonic state is readily calculated using normal shock tables. One objectionable feature of the Supersonic Mixed Mean Mach Numbers is that they can be greater (!) than the maximum Mach Number M_0 although eventually (for higher M_0) they are rationally less than M_0 . For a given profile there exists an M_0 for which $\bar{M}_{mixed} \equiv M_0$ for all δ/R_0 (in two dimensions) and this magnitude is closely $M_0 = 2.1$ for a linear profile. The same situation applies approximately for axisymmetrical flow.

4.1.4 In use the point of entry to the table could be determined from say M_0 , velocity ratio *or* power law index, and δ/R_0 (or some similar combination of variables relating to Mach Number level, profile shape and boundary layer thickness; many combinations are possible). An appropriate comparative profile and state is readily located for comparison

of the effect of different averaging methods for most arbitrary measured profiles which are likely to appear. The table then indicates clearly in the first four columns the significance of the variation of the Mean Total Pressure for the five principal methods of averaging together with the most useful other significant parameters which might be used in comparisons. It is therefore possible to estimate quickly, and with some accuracy, the differences implied by the different averaging methods from, for example, a rapidly determined first calculation by a simple method like Mass Derivation which might involve no traversing or integration if the mass flow is known.

Initial familiarisation with the table is probably best achieved by identification of already familiar velocity profiles and their averages. For example the linear profile ($n = 1$) which fills duct ($\delta/R_0 = 1.0$) at low Mach Number $M_0 = 0.2$ and which is therefore an effectively incompressible flow.

By inspection the following familiar results appear for this profile:

Mtm. Flux Coeff.	Energy Flux Coeff.	Vel. Ratio Max./Mean	
1.501	2.704	3.00	for axial symmetry
1.341	2.023	2.02	for two-dimensions

which are the accepted incompressible flow values modified very slightly by the effect of the slight compressibility implied by $M_0 = 0.2$. If the power law index is changed to $n = 1/7$ the results are again familiar:

1.023	1.063	1.226	for axial symmetry
1.022	1.058	1.150	for two-dimensions

Emphasis will be mostly concentrated on the first four columns, their magnitudes (i.e. relationship to the Entropy Flux Mean Total Pressure) and their differences. Note that the first column always exceeds unity in confirmation of the known fact that this Mean always contravenes the Second Law of Thermodynamics (for non-zero Mach Numbers). The discrepancy is small for Mach Numbers less than unity but above this the error increases dramatically and can imply a factor of 3.6 (!) for $n = 1$ when $M_0 = 4.0$. The Area Weighted Mean Total Pressure in column 2 also exceeds unity but to a much less extent at $M_0 = 3$ and 4.

Generally increasing M_0 increases the differences in Mean Total pressure magnitudes for the five different averaging methods. The following table summarizes the percentage differences from the Entropy Flux Mean Total Pressure.

M_0	Mass Weighted	Area Weighted	Mass Derived	Mtm. Mixed	
0.2	0%	− 1.0%	− 1.0%	− 0.6%	
1.0	+ 2.5%	−12.5%	−19.0%	− 9.0%	Axial Symmetry
4.0	+260.0%	−22.5%	−82.7%	−87.3% (44.9%)	
0.2	+0%	− 0.9%	− 0.9%	− 0.7%	
1.0	+ 2.2%	− 9.7%	−17.5%	− 7.7%	Two-dimensional
4.0	+151.0%	−17.6%	−76.9%	−86.9% (43.8%)	

These percentage differences are for the worst profiles, $n = 1$ and the magnitude of δ/R_0 which maximises the differences. Notice that the maximum differences occur generally for magnitudes of δ/R_0 intermediate between 0 and 1.0 (and not as might be expected for $\delta/R_0 = 1.0$). The figures in parentheses correspond to the interpretation (not given in the main tables) of the mixed flow which remains supersonic in average Mach Number. The differences are clearly magnified for axisymmetrical flow because a larger proportion of the flow is in a lower total pressure state in this case. Clearly as the velocity profile improves through $n = \frac{1}{3}, \frac{1}{5}, \frac{1}{7}, \frac{1}{9}$ the differences are progressively reduced. The differences are thus seen to be most strongly affected by non-uniformity (profile index n) and the level of the Mach Number with a very significant influence (within the profile shape effect) of the location of δ/R_0.

The dynamic influence on Total Pressure of the Mach Number level and hence the differences implied in averaging need emphasis. Nor should the indications of difference of 1% or 2% be made to appear trivial. A simple example will help here. Consider the case of subsonic diffuser of reasonably good recovery within which traverses are carried out at say a low area ratio of 1.5 and at some larger area ratio say 3.0 or 4.0. At the area ratio of 1.5 there will be significant distortion of the velocity profile combined with a high dynamic effect on the mean total pressure because of the still reasonably high mean velocity or Mach Number. At the higher area ratio although the velocity profile may be similarly (or often less) distorted the dynamic effect on mean total pressure will be almost negligible because of the large reduction in mean velocity or mean Mach Number. Given this situation the use of any of the last three averaging methods tabulated (Area Weighting, Mass Derivation or Momentum Mixing) will usually lead to a negative (!) loss coefficient, i.e. a rise in mean total pressure (averaged) between the two area ratio locations. This discrepancy arises because the

averages at the lower area ratio are significantly underestimated and those at the higher area ratio are much more precise although still underestimated. The author has demonstrated this effect on all the diffuser results in the literature which enable the comparison to be made. The effect is easily demonstrated at *both* low and high Mach Numbers. Mass Weighting does not give the effect because of the overestimation of mean total pressure at the lower area ratio.

In general the averaging method chosen will have significant effects on performance parameters; the possible influences should be investigated and this is facilitated by the tabulations presented. The two most soundly based averaging methods are Momentum Mixing (Dzung) and Constant Entropy Flux (Livesey), both have disadvantages. With the Dzung method an inevitable loss in total pressure is implied and this is well known to cause difficulties where turbo-machines are purpose designed to accept non-uniform distributions at entry. Here the Dzung method inevitably and unfairly debits the machine with a total pressure loss which does not occur. Additionally the difficulties of interpretation of the Dzung method, where mean Mach Numbers might be expected to be supersonic (see earlier discussion) and where the difficulties just mentioned are also amplified significantly mean that great care must be emphasized in interpretation of its use. With the Livesey method as presented it is only rigorous in its representation of mean total pressure for the assumption of uniform Total Temperature.

It would be wrong to leave this discussion at this point without mention of the two primary practical difficulties of averaging techniques. These are firstly the number of points of measurement within the profile and secondly the occurrence of separation. Rarely are sufficient points of measurement made available to allow precision to be achieved in averaging and the best that can be expected is consistency in the averaged values coupled with the acceptance of a significant departure from precision. These remarks apply particularly to measurement situations which do not cover adequately the boundary layer regions where the velocities tend to zero at the wall. The difficulties are magnified in the more practical axisymmetric situation where the bulk of the flow may be in the outer layers because of the greater area involved (2π r.dr). The useful comparisons achieved in the computation of the tables involved 150 points *in the boundary layer alone (!)*. Clearly therefore careful curve fitting is advised in situations of sparse data coupled with some representation of the approach of the velocity profile to zero wall velocity if more than mere consistency is required. Separation presents even greater difficulties but they are not insuperable. Successive integrations of the profile, for mass flow estimation, approaching nearer to the reversed flow each time will enable a point to be identified of positive (main flow direction) local velocity at which the integrated flow is equal to the known mass flow (say from a meter or a known machine condition). The point so identified separates the mainflow from the recirculating flow. The above discussion has been presented in two-dimensional terms for clarity, three-dimensionally the process is identical but involves contours of velocity rather than points on the velocity profile.

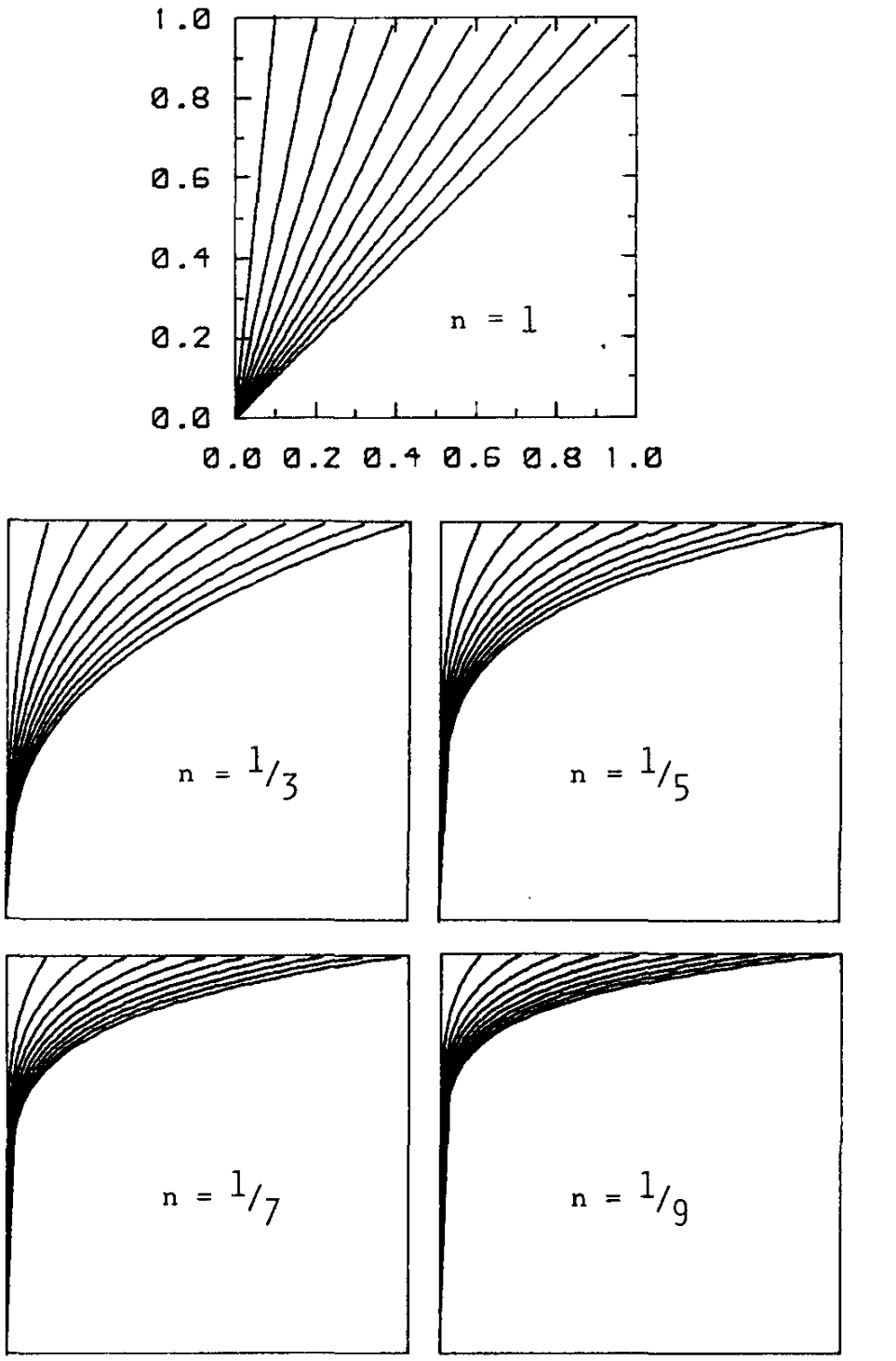

POWER LAW VELOCITY PROFILES

δ/R_0 = 0.1, 0.2, 0.3, 0.4, 0.5, 0.6, 0.7, 0.8, 0.9, 1.0

Figure 4.1.1

Description of the Twelve Column Tables

Column

1	Mass Weighted $\bar{P}_t$/Entropy Flux $\bar{P}_t$
2	Area Weighted $\bar{P}_t$/Entropy Flux $\bar{P}_t$
3	Mass Derived $\bar{P}_t$/Entropy Flux $\bar{P}_t$
4	Constant Momentum (Dzung) $\bar{P}_t$/Entropy Flux $\bar{P}_t$
5	Momentum Flux Coefficient ϵ_2
6	Energy Flux Coefficient ϵ_3
7	Mass Derived $\bar{M}$
8	Constant Momentum (Dzung) $\bar{M}$
9	Entropy Flux $\bar{M}$
10	Velocity Ratio Maximum/Mean
11	Entropy Flux $\bar{P}_s$/Defined, Constant P_s
12	Constant Momentum (Dzung) $\bar{P}_s$/Defined, Constant P_s

First four pages are for axisymmetrical flow. Last four pages are for two-dimensional flow.

Each page has the column headings once and covers two values of the Maximum Mach Number M_0, one in the upper half page, the other in the lower half page.

The five blocks in each half page correspond to the power law of the velocity profile, i.e. $1, \frac{1}{3}, \frac{1}{5}, \frac{1}{7}, \frac{1}{9}$.

Within each power law block are ten rows corresponding to boundary layer thickness δ/R_0 of 0.1, 0.2, 0.3, 0.4, 0.5, 0.6, 0.7, 0.8, 0.9, 1.0.

The mean velocity implied in the definitions of ϵ_2, ϵ_3 (columns 5 and 6) and in the velocity ratio (column 10) is the Entropy Flux mean velocity (Livesey).

TABLE 4.1.I

	Mass Weighted	Area Weighted	Mass Derived	Mtm. Mixed	Mtm. Flux Coeff	Energy Flux Coeff	Mach Number Mass Derived	Mach Number Mtm. Mixed	Mach Number Entropy Flux	Velocity Ratio Max/ Mean	Static p Ratio Entropy/ Wall	Static p Ratio Mixed/ Wall	n
	1.000013	0.997010	0.996334	0.998517	1.069	1.164	0.181	0.180	0.195	1.108	1.000004	1.002299	
	1.000024	0.994630	0.993619	0.997111	1.141	1.351	0.162	0.162	0.189	1.232	1.000007	1.003639	
	1.000034	0.992870	0.991784	0.995898	1.214	1.562	0.146	0.145	0.182	1.374	1.000010	1.004263	
	1.000042	0.991735	0.990733	0.994982	1.286	1.792	0.130	0.130	0.174	1.536	1.000012	1.004390	
	1.000047	0.991222	0.990389	0.994419	1.352	2.032	0.116	0.116	0.165	1.722	1.000014	1.004154	1
	1.000049	0.991311	0.990623	0.994281	1.411	2.265	0.104	0.103	0.156	1.932	1.000014	1.003748	
	1.000046	0.991962	0.991351	0.994592	1.457	2.470	0.092	0.092	0.145	2.168	1.000013	1.003315	
	1.000039	0.993097	0.992401	0.995337	1.487	2.618	0.082	0.082	0.133	2.429	1.000011	1.002984	
	1.000030	0.994596	0.993615	0.996448	1.500	2.691	0.074	0.074	0.121	2.709	1.000008	1.002870	
	1.000021	0.996274	0.994751	0.997794	1.501	2.704	0.067	0.066	0.109	3.000	1.000006	1.003070	
	1.000009	0.998357	0.998743	0.998814	1.020	1.051	0.190	0.190	0.195	1.052	1.000003	1.000078	
	1.000016	0.997075	0.997784	0.997864	1.038	1.099	0.181	0.181	0.189	1.106	1.000005	1.000083	
	1.000022	0.996144	0.997095	0.997161	1.054	1.142	0.172	0.172	0.184	1.162	1.000006	1.000059	
	1.000025	0.995553	0.996672	0.996710	1.067	1.180	0.164	0.164	0.178	1.219	1.000007	1.000046	
	1.000027	0.995287	0.996444	0.996513	1.077	1.210	0.157	0.157	0.172	1.277	1.000008	1.000083	1/3
	1.000028	0.995326	0.996388	0.996550	1.084	1.233	0.150	0.150	0.166	1.335	1.000008	1.000166	
	1.000027	0.995650	0.996465	0.996853	1.088	1.249	0.143	0.143	0.160	1.393	1.000008	1.000410	
	1.000025	0.996234	0.996637	0.997375	1.090	1.256	0.138	0.138	0.154	1.450	1.000007	1.000769	
	1.000022	0.997051	0.996853	0.998121	1.091	1.258	0.133	0.133	0.149	1.505	1.000006	1.001310	
	1.000019	0.998072	0.997069	0.999074	1.090	1.257	0.128	0.128	0.144	1.556	1.000005	1.002057	
$M_0 = .2$	1.000006	0.998716	0.999337	0.998927	1.010	1.026	0.193	0.193	0.196	1.035	1.000002	0.999556	
	1.000010	0.997715	0.998840	0.998101	1.019	1.049	0.187	0.187	0.191	1.069	1.000003	0.999228	
	1.000014	0.996991	0.998470	0.997499	1.026	1.068	0.181	0.181	0.187	1.104	1.000004	0.998985	
	1.000016	0.996535	0.998218	0.997122	1.031	1.084	0.176	0.176	0.183	1.138	1.000005	0.998847	
	1.000018	0.996338	0.998075	0.996967	1.035	1.096	0.171	0.171	0.178	1.172	1.000005	0.998831	1/5
	1.000018	0.996391	0.998031	0.997034	1.038	1.104	0.166	0.166	0.174	1.205	1.000005	0.998955	
	1.000018	0.996681	0.998034	0.997338	1.039	1.109	0.162	0.162	0.170	1.237	1.000005	0.999277	
	1.000017	0.997198	0.998101	0.997834	1.040	1.111	0.158	0.158	0.166	1.267	1.000005	0.999725	
	1.000016	0.997931	0.998186	0.998556	1.040	1.111	0.154	0.154	0.163	1.295	1.000004	1.000396	
	1.000014	0.998867	0.998286	0.999459	1.039	1.109	0.151	0.151	0.159	1.321	1.000004	1.001219	
	1.000004	0.998863	0.999599	0.998980	1.006	1.016	0.195	0.195	0.196	1.026	1.000001	0.999352	
	1.000007	0.997978	0.999269	0.998197	1.012	1.030	0.190	0.190	0.193	1.052	1.000002	0.998873	
	1.000010	0.997338	0.999029	0.997652	1.016	1.042	0.186	0.186	0.189	1.077	1.000003	0.998571	
	1.000011	0.996939	0.998848	0.997296	1.019	1.051	0.181	0.182	0.186	1.102	1.000003	0.998361	
	1.000012	0.996774	0.998772	0.997151	1.021	1.057	0.178	0.178	0.183	1.125	1.000003	0.998301	1/7
	1.000013	0.996837	0.998723	0.997239	1.023	1.061	0.174	0.174	0.179	1.148	1.000004	0.998449	
	1.000012	0.997122	0.998723	0.997535	1.024	1.064	0.171	0.171	0.176	1.170	1.000004	0.998765	
	1.000012	0.997623	0.998744	0.998035	1.024	1.065	0.168	0.168	0.173	1.190	1.000003	0.999259	
	1.000011	0.998332	0.998787	0.998736	1.023	1.064	0.165	0.165	0.170	1.209	1.000003	0.999937	
	1.000011	0.999243	0.998849	0.999636	1.023	1.063	0.163	0.163	0.168	1.226	1.000003	1.000806	
	1.000003	0.998938	0.999705	0.999012	1.004	1.012	0.196	0.196	0.197	1.021	1.000001	0.999261	
	1.000005	0.998111	0.999473	0.998267	1.008	1.021	0.192	0.192	0.194	1.041	1.000002	0.998736	
	1.000007	0.997514	0.999301	0.997715	1.011	1.029	0.188	0.189	0.191	1.061	1.000002	0.998331	
	1.000008	0.997144	0.999186	0.997380	1.013	1.035	0.185	0.185	0.188	1.081	1.000002	0.998104	
	1.000009	0.996996	0.999099	0.997260	1.015	1.040	0.182	0.182	0.185	1.099	1.000003	0.998060	1/9
	1.000009	0.997066	0.999063	0.997354	1.016	1.042	0.179	0.179	0.183	1.116	1.000003	0.998206	
	1.000009	0.997351	0.999076	0.997638	1.017	1.044	0.177	0.177	0.180	1.133	1.000003	0.998501	
	1.000009	0.997845	0.999088	0.998133	1.017	1.044	0.174	0.174	0.178	1.148	1.000003	0.998997	
	1.000009	0.998545	0.999123	0.998836	1.016	1.043	0.172	0.172	0.176	1.162	1.000002	0.999698	
	1.000008	0.999446	0.999179	0.999745	1.016	1.042	0.170	0.170	0.174	1.175	1.000002	1.000609	

	Mass Weighted	Area Weighted	Mass Derived	Mtm. Mixed	Mtm. Flux Coeff	Energy Flux Coeff	Mach Number Mass Derived	Mach Number Mtm. Mixed	Mach Number Entropy Flux	Velocity Ratio Max/ Mean	Static p Ratio Entropy/ Wall	Static p Ratio Mixed/ Wall	n
	1.000190	0.991153	0.985817	0.996722	1.070	1.165	0.361	0.357	0.389	1.108	1.000056	1.013335	
	1.000368	0.984023	0.975361	0.993177	1.143	1.354	0.325	0.319	0.377	1.232	1.000108	1.021280	
	1.000526	0.978657	0.968229	0.989784	1.216	1.566	0.292	0.285	0.363	1.374	1.000153	1.025149	
	1.000652	0.975088	0.964089	0.986966	1.289	1.798	0.261	0.254	0.348	1.537	1.000189	1.026123	
	1.000733	0.973319	0.962650	0.985034	1.356	2.041	0.233	0.227	0.330	1.722	1.000212	1.025100	1
	1.000759	0.973299	0.963489	0.984219	1.416	2.277	0.207	0.202	0.310	1.932	1.000218	1.022842	
	1.000720	0.974888	0.966210	0.984627	1.462	2.484	0.184	0.180	0.289	2.169	1.000205	1.019985	
	1.000617	0.977809	0.970283	0.986176	1.491	2.633	0.164	0.161	0.265	2.429	1.000175	1.017009	
	1.000469	0.981594	0.975007	0.988582	1.504	2.703	0.147	0.145	0.240	2.710	1.000133	1.014353	
	1.000322	0.985537	0.979466	0.991317	1.505	2.715	0.132	0.131	0.217	3.000	1.000091	1.012403	
	1.000137	0.996270	0.995061	0.997960	1.021	1.052	0.380	0.379	0.390	1.052	1.000040	1.003587	
	1.000249	0.993341	0.991293	0.996288	1.039	1.100	0.361	0.359	0.379	1.106	1.000073	1.006087	
	1.000336	0.991183	0.988674	0.994947	1.055	1.144	0.344	0.342	0.367	1.162	1.000098	1.007566	
	1.000396	0.989754	0.986957	0.994000	1.068	1.182	0.328	0.325	0.356	1.219	1.000114	1.008340	
	1.000428	0.989001	0.986051	0.993500	1.078	1.213	0.313	0.310	0.344	1.277	1.000123	1.008709	
	1.000434	0.988857	0.985823	0.993389	1.086	1.237	0.299	0.296	0.331	1.335	1.000125	1.008727	1/3
	1.000418	0.989243	0.986115	0.993663	1.090	1.252	0.286	0.284	0.319	1.393	1.000120	1.008597	
	1.000384	0.990067	0.986785	0.994301	1.092	1.260	0.275	0.272	0.308	1.450	1.000110	1.008505	
	1.000342	0.991224	0.987631	0.995210	1.092	1.262	0.265	0.262	0.296	1.505	1.000098	1.008489	
	1.000299	0.992602	0.988480	0.996376	1.092	1.260	0.256	0.253	0.286	1.556	1.000086	1.008779	
$M_0 = .4$	1.000090	0.997634	0.997391	0.998463	1.010	1.026	0.387	0.386	0.391	1.035	1.000026	1.001340	
	1.000163	0.995784	0.995433	0.997224	1.019	1.049	0.374	0.373	0.383	1.069	1.000047	1.002245	
	1.000217	0.994424	0.993975	0.996275	1.026	1.069	0.362	0.361	0.374	1.104	1.000063	1.002787	
	1.000254	0.993525	0.993027	0.995673	1.032	1.085	0.351	0.350	0.365	1.138	1.000073	1.003199	
	1.000275	0.993052	0.992457	0.995367	1.036	1.097	0.341	0.339	0.356	1.172	1.000079	1.003461	1/5
	1.000281	0.992970	0.992235	0.995374	1.039	1.106	0.331	0.330	0.348	1.205	1.000081	1.003713	
	1.000276	0.993237	0.992288	0.995636	1.040	1.111	0.322	0.321	0.339	1.237	1.000079	1.003931	
	1.000262	0.993810	0.992509	0.996163	1.041	1.113	0.315	0.313	0.331	1.267	1.000075	1.004248	
	1.000244	0.994644	0.992841	0.996926	1.041	1.112	0.308	0.306	0.324	1.295	1.000070	1.004710	
	1.000225	0.995694	0.993193	0.997929	1.040	1.111	0.301	0.300	0.317	1.321	1.000064	1.005434	
	1.000063	0.998196	0.998368	0.998663	1.006	1.017	0.390	0.390	0.393	1.026	1.000018	1.000384	
	1.000113	0.996787	0.997067	0.997629	1.012	1.031	0.380	0.380	0.386	1.052	1.000033	1.000687	
	1.000150	0.995752	0.996121	0.996891	1.016	1.042	0.371	0.371	0.379	1.077	1.000043	1.000947	
	1.000176	0.995073	0.995507	0.996401	1.019	1.051	0.363	0.362	0.372	1.102	1.000051	1.001117	
	1.000190	0.994727	0.995111	0.996150	1.022	1.058	0.355	0.354	0.365	1.125	1.000055	1.001236	1/7
	1.000196	0.994691	0.994963	0.996195	1.023	1.063	0.348	0.347	0.358	1.148	1.000056	1.001504	
	1.000195	0.994940	0.994959	0.996453	1.024	1.065	0.341	0.340	0.352	1.170	1.000056	1.001789	
	1.000188	0.995450	0.995043	0.996977	1.024	1.066	0.335	0.334	0.346	1.190	1.000054	1.002281	
	1.000178	0.996196	0.995255	0.997717	1.024	1.065	0.330	0.329	0.340	1.209	1.000051	1.002927	
	1.000168	0.997152	0.995456	0.998624	1.023	1.064	0.325	0.324	0.335	1.226	1.000048	1.003675	
	1.000046	0.998482	0.998836	0.998806	1.005	1.012	0.392	0.392	0.394	1.021	1.000013	0.999993	
	1.000083	0.997295	0.997924	0.997872	1.008	1.022	0.384	0.384	0.388	1.041	1.000024	0.999975	
	1.000110	0.996426	0.997245	0.997192	1.011	1.030	0.377	0.377	0.382	1.061	1.000032	0.999972	
	1.000128	0.995859	0.996739	0.996759	1.014	1.036	0.370	0.370	0.376	1.081	1.000037	1.000010	
	1.000139	0.995580	0.996493	0.996564	1.015	1.040	0.363	0.363	0.370	1.099	1.000040	1.000112	
	1.000144	0.995573	0.996350	0.996635	1.016	1.043	0.358	0.357	0.365	1.116	1.000042	1.000386	1/9
	1.000144	0.995821	0.996306	0.996891	1.017	1.045	0.352	0.352	0.360	1.133	1.000041	1.000685	
	1.000141	0.996309	0.996400	0.997393	1.017	1.045	0.347	0.347	0.355	1.148	1.000040	1.001195	
	1.000135	0.997020	0.996537	0.998131	1.017	1.044	0.343	0.342	0.350	1.162	1.000039	1.001932	
	1.000129	0.997938	0.996713	0.999026	1.016	1.043	0.339	0.338	0.346	1.175	1.000037	1.002751	

AXISYMMETRICAL

TABLE 4.1.II

Mass Weighted	Area Weighted	Mass Derived	Mtm. Mixed	Mtm. Flux Coeff	Energy Flux Coeff	Mach Number Mass Derived	Mach Number Mtm. Mixed	Mach Number Entropy Flux	Velocity Ratio Max/ Mean	Static p Ratio Entropy/ Wall	Static p Ratio Mixed/ Wall	n
$M_0 = .6$												
1.000887	0.982617	0.969913	0.993533	1.071	1.167	0.543	0.524	0.584	1.108	1.000271	1.038142	
1.001730	0.968440	0.947584	0.986078	1.145	1.359	0.489	0.463	0.565	1.233	1.000524	1.057801	
1.002489	0.957595	0.932213	0.978905	1.220	1.575	0.438	0.412	0.544	1.375	1.000745	1.066064	
1.003112	0.950191	0.923194	0.972960	1.294	1.811	0.392	0.368	0.521	1.538	1.000920	1.067066	
1.003536	0.946286	0.919762	0.968879	1.363	2.058	0.349	0.329	0.494	1.723	1.001032	1.063381	1
1.003694	0.945838	0.921282	0.967108	1.424	2.299	0.310	0.294	0.464	1.934	1.001064	1.056917	
1.003532	0.948621	0.926885	0.967804	1.470	2.509	0.275	0.262	0.431	2.170	1.001005	1.049061	
1.003043	0.954113	0.935543	0.970825	1.500	2.659	0.245	0.235	0.395	2.431	1.000857	1.041026	
1.002313	0.961346	0.945699	0.975498	1.512	2.730	0.218	0.211	0.358	2.711	1.000648	1.033672	
1.001579	0.968783	0.955381	0.980647	1.511	2.735	0.196	0.191	0.323	3.002	1.000443	1.027891	
1.000847	0.993218	0.989346	0.996505	1.021	1.053	0.570	0.564	0.584	1.052	1.000195	1.012085	
1.001190	0.987844	0.981237	0.993490	1.060	1.103	0.542	0.532	0.567	1.107	1.000355	1.019705	
1.001614	0.983828	0.975420	0.991051	1.057	1.148	0.515	0.504	0.550	1.162	1.000478	1.024042	
1.001910	0.981100	0.971668	0.989286	1.070	1.187	0.491	0.479	0.532	1.220	1.000561	1.026091	
1.002076	0.979562	0.969647	0.988218	1.081	1.219	0.468	0.456	0.514	1.278	1.000605	1.026526	1/3
1.002114	0.979089	0.969112	0.987874	1.089	1.243	0.446	0.436	0.495	1.336	1.000612	1.026006	
1.002040	0.979522	0.969720	0.988163	1.093	1.258	0.427	0.417	0.477	1.394	1.000587	1.024877	
1.001879	0.980673	0.971161	0.988974	1.095	1.266	0.410	0.401	0.459	1.451	1.000539	1.023472	
1.001669	0.982323	0.973001	0.990249	1.095	1.267	0.394	0.386	0.442	1.505	1.000477	1.022287	
1.001458	0.984229	0.974852	0.991730	1.094	1.265	0.380	0.373	0.426	1.557	1.000417	1.021340	
1.000432	0.996048	0.994350	0.997606	1.011	1.027	0.580	0.577	0.587	1.035	1.000129	1.005600	
1.000783	0.992937	0.990048	0.995673	1.020	1.051	0.560	0.555	0.573	1.069	1.000232	1.009396	
1.001049	0.990619	0.986841	0.994171	1.027	1.071	0.542	0.536	0.560	1.104	1.000309	1.011717	
1.001233	0.989039	0.984781	0.993125	1.033	1.088	0.525	0.519	0.546	1.139	1.000361	1.013004	
1.001338	0.988134	0.983517	0.992566	1.038	1.100	0.510	0.503	0.533	1.172	1.000390	1.013687	1/5
1.001373	0.987830	0.983048	0.992423	1.040	1.109	0.495	0.488	0.520	1.205	1.000398	1.013882	
1.001349	0.988044	0.983122	0.992659	1.042	1.114	0.482	0.475	0.507	1.237	1.000390	1.013800	
1.001282	0.988687	0.983570	0.993271	1.043	1.116	0.470	0.463	0.495	1.267	1.000370	1.013746	
1.001191	0.989665	0.984296	0.994146	1.042	1.116	0.459	0.453	0.483	1.296	1.000343	1.013716	
1.001097	0.990880	0.985094	0.995241	1.041	1.114	0.449	0.443	0.473	1.322	1.000316	1.013897	
1.000304	0.997216	0.996377	0.998136	1.007	1.017	0.584	0.583	0.589	1.026	1.000090	1.003058	
1.000547	0.995028	0.993591	0.996649	1.012	1.032	0.570	0.567	0.578	1.052	1.000161	1.005169	
1.000730	0.993401	0.991578	0.995518	1.017	1.044	0.556	0.552	0.567	1.077	1.000214	1.006511	
1.000856	0.992295	0.990152	0.994799	1.020	1.053	0.543	0.539	0.556	1.102	1.000250	1.007476	
1.000931	0.991669	0.989274	0.994409	1.023	1.060	0.531	0.527	0.546	1.126	1.000271	1.008024	1/7
1.000961	0.991474	0.988909	0.994339	1.024	1.065	0.520	0.516	0.535	1.148	1.000279	1.008329	
1.000954	0.991661	0.988895	0.994578	1.025	1.067	0.510	0.506	0.526	1.170	1.000276	1.008558	
1.000922	0.992179	0.989144	0.995118	1.025	1.068	0.501	0.496	0.516	1.191	1.000266	1.008871	
1.000874	0.992974	0.989573	0.995914	1.025	1.067	0.492	0.488	0.508	1.209	1.000252	1.009323	
1.000823	0.993994	0.990044	0.996887	1.024	1.066	0.485	0.480	0.500	1.226	1.000237	1.009861	
1.000224	0.997810	0.997440	0.998420	1.005	1.012	0.587	0.586	0.591	1.021	1.000066	1.001780	
1.000402	0.996089	0.995434	0.997164	1.009	1.022	0.575	0.574	0.581	1.042	1.000118	1.003006	
1.000535	0.994811	0.993940	0.996264	1.012	1.031	0.564	0.562	0.572	1.061	1.000157	1.003943	
1.000628	0.993948	0.992861	0.995653	1.014	1.037	0.554	0.551	0.563	1.081	1.000183	1.004531	
1.000684	0.993467	0.992244	0.995370	1.016	1.042	0.544	0.541	0.554	1.099	1.000199	1.005028	
1.000709	0.993339	0.991928	0.995348	1.017	1.045	0.535	0.532	0.546	1.117	1.000206	1.005372	1/9
1.000709	0.993528	0.991897	0.995592	1.018	1.046	0.527	0.524	0.538	1.133	1.000205	1.005711	
1.000691	0.994002	0.992068	0.996108	1.018	1.046	0.519	0.516	0.530	1.148	1.000200	1.006186	
1.000663	0.994727	0.992366	0.996867	1.017	1.046	0.513	0.509	0.524	1.162	1.000191	1.006832	
1.000632	0.995668	0.992717	0.997806	1.017	1.044	0.507	0.503	0.517	1.175	1.000182	1.007577	
												n
1.002508	0.972806	0.950421	0.988275	1.073	1.170	0.725	0.667	0.778	1.109	1.000806	1.094655	
1.004943	0.950324	0.913381	0.974693	1.149	1.366	0.653	0.583	0.753	1.234	1.001560	1.128885	
1.007191	0.932805	0.887676	0.962101	1.226	1.588	0.586	0.518	0.725	1.377	1.002227	1.138668	
1.009096	0.920495	0.872206	0.951980	1.303	1.830	0.523	0.463	0.693	1.540	1.002760	1.135309	
1.010463	0.913588	0.865898	0.945252	1.374	2.085	0.465	0.416	0.656	1.727	1.003105	1.124370	1
1.011064	0.912147	0.867777	0.942462	1.436	2.333	0.413	0.373	0.616	1.938	1.003210	1.109182	
1.010697	0.915957	0.876615	0.943901	1.484	2.568	0.365	0.335	0.571	2.175	1.003037	1.092410	
1.009287	0.924305	0.890809	0.949239	1.513	2.699	0.324	0.301	0.522	2.435	1.002589	1.075906	
1.007063	0.935678	0.907880	0.957349	1.523	2.766	0.288	0.272	0.472	2.715	1.001950	1.061177	
1.004774	0.947474	0.924342	0.966054	1.520	2.764	0.258	0.246	0.424	3.004	1.001322	1.049543	
1.001873	0.989711	0.982067	0.994281	1.022	1.055	0.760	0.737	0.778	1.053	1.000587	1.035149	
1.003471	0.981461	0.968283	0.989156	1.043	1.107	0.722	0.689	0.755	1.107	1.001071	1.052291	
1.004747	0.975201	0.958391	0.985018	1.060	1.154	0.686	0.650	0.732	1.164	1.001443	1.060172	
1.005663	0.970848	0.951922	0.981999	1.074	1.195	0.653	0.617	0.707	1.221	1.001696	1.062441	
1.006197	0.968275	0.948380	0.980203	1.085	1.228	0.621	0.587	0.682	1.279	1.001831	1.061448	1/3
1.006347	0.967305	0.947380	0.979541	1.093	1.252	0.592	0.562	0.657	1.338	1.001853	1.058389	
1.006148	0.967706	0.948351	0.979888	1.098	1.268	0.566	0.538	0.631	1.396	1.001777	1.054224	
1.005670	0.969183	0.950704	0.981114	1.100	1.276	0.542	0.518	0.607	1.452	1.001628	1.049882	
1.005029	0.971382	0.953832	0.982928	1.099	1.276	0.521	0.499	0.584	1.507	1.001439	1.045823	
1.004379	0.973899	0.957122	0.985008	1.098	1.274	0.502	0.483	0.563	1.558	1.001252	1.042481	
$M_0 = .8$												
1.001269	0.994223	0.990439	0.996337	1.011	1.029	0.772	0.760	0.782	1.035	1.000391	1.018182	
1.002311	0.989632	0.982933	0.993280	1.021	1.054	0.746	0.727	0.764	1.070	1.000705	1.028289	
1.003117	0.986167	0.977574	0.990895	1.029	1.075	0.722	0.700	0.745	1.105	1.000940	1.033555	
1.003683	0.983753	0.973857	0.989251	1.036	1.092	0.698	0.676	0.726	1.140	1.001099	1.035962	
1.004015	0.982297	0.971738	0.988276	1.040	1.105	0.677	0.655	0.708	1.173	1.001187	1.036366	1/5
1.004134	0.981689	0.970850	0.987948	1.043	1.114	0.657	0.636	0.690	1.206	1.001212	1.035633	
1.004070	0.981806	0.971010	0.988188	1.045	1.119	0.639	0.619	0.672	1.238	1.001186	1.034277	
1.003869	0.982504	0.971820	0.988893	1.045	1.121	0.622	0.604	0.655	1.268	1.001123	1.032688	
1.003590	0.983633	0.973060	0.989969	1.045	1.121	0.607	0.590	0.640	1.297	1.001039	1.031246	
1.003300	0.985029	0.974454	0.991292	1.044	1.119	0.594	0.578	0.626	1.322	1.000954	1.030205	
1.000901	0.996066	0.993819	0.997295	1.007	1.018	0.779	0.771	0.785	1.026	1.000275	1.010986	
1.001629	0.992987	0.989070	0.995116	1.013	1.033	0.759	0.747	0.770	1.052	1.000493	1.017632	
1.002185	0.990654	0.985466	0.993468	1.018	1.046	0.740	0.725	0.755	1.078	1.000655	1.021472	
1.002574	0.989032	0.983112	0.992524	1.022	1.056	0.722	0.707	0.740	1.102	1.000765	1.023392	
1.002808	0.988055	0.981584	0.991690	1.025	1.063	0.705	0.690	0.725	1.126	1.000829	1.024182	1/7
1.002904	0.987653	0.980913	0.991497	1.026	1.068	0.690	0.675	0.711	1.149	1.000852	1.024170	
1.002888	0.987750	0.980879	0.991721	1.027	1.071	0.676	0.662	0.697	1.171	1.000844	1.023796	
1.002788	0.988262	0.981272	0.992289	1.027	1.071	0.664	0.650	0.684	1.191	1.000812	1.023269	
1.002641	0.989105	0.981980	0.993165	1.027	1.071	0.652	0.639	0.673	1.210	1.000768	1.022900	
1.002484	0.990191	0.982897	0.994261	1.026	1.069	0.642	0.629	0.662	1.227	1.000722	1.022771	
1.000670	0.997035	0.995583	0.997823	1.005	1.013	0.783	0.778	0.787	1.021	1.000203	1.007294	
1.001206	0.994691	0.992119	0.996109	1.010	1.024	0.766	0.758	0.774	1.042	1.000362	1.012009	
1.001612	0.992928	0.989536	0.994823	1.013	1.032	0.751	0.741	0.761	1.062	1.000481	1.014875	
1.001897	0.991706	0.987788	0.993957	1.016	1.039	0.736	0.725	0.749	1.081	1.000562	1.016525	
1.002072	0.990978	0.986655	0.993463	1.017	1.044	0.723	0.712	0.737	1.100	1.000610	1.017251	1/9
1.002151	0.990696	0.986102	0.993382	1.018	1.047	0.711	0.699	0.725	1.117	1.000631	1.017697	
1.002152	0.990806	0.986097	0.993591	1.019	1.049	0.699	0.688	0.714	1.134	1.000629	1.017693	
1.002097	0.991255	0.986358	0.994127	1.019	1.049	0.689	0.678	0.704	1.149	1.000611	1.017758	
1.002010	0.991988	0.986867	0.994930	1.019	1.048	0.680	0.669	0.694	1.163	1.000585	1.017949	
1.001914	0.992952	0.987442	0.995940	1.018	1.047	0.672	0.661	0.686	1.175	1.000557	1.018314	

TABLE 4.1.III

Mass Weighted	Area Weighted	Mass Derived	Mtm. Mixed	Mtm. Flux Coeff	Energy Flux Coeff	Mach Number Mass Derived	Mach Number Mtm. Mixed	Mach Number Entropy Flux	Velocity Ratio Max/ Mean	Static p Ratio Entropy/ Wall	Static p Ratio Mixed/ Wall	n
1.005353	0.963042	0.928962	0.978571	1.076	1.175	0.908	0.752	0.972	1.110	1.001823	1.234586	
1.010673	0.932041	0.875803	0.956450	1.155	1.377	0.819	0.661	0.940	1.236	1.003545	1.265576	
1.015728	0.907399	0.838503	0.937288	1.235	1.607	0.735	0.592	0.904	1.381	1.005080	1.262182	
1.020179	0.888547	0.815442	0.922535	1.315	1.859	0.655	0.534	0.863	1.546	1.006321	1.242719	
1.023560	0.878898	0.805429	0.913187	1.389	2.124	0.582	0.483	0.817	1.734	1.007139	1.215191	
1.025296	0.875738	0.807094	0.909847	1.453	2.382	0.514	0.437	0.765	1.946	1.007405	1.183988	1
1.024802	0.880015	0.819002	0.912751	1.502	2.604	0.454	0.396	0.708	2.183	1.007020	1.152272	
1.021748	0.890982	0.839064	0.921505	1.530	2.756	0.401	0.358	0.646	2.443	1.005981	1.122727	
1.016554	0.906662	0.863956	0.934338	1.538	2.815	0.355	0.325	0.581	2.722	1.004483	1.097064	
1.011053	0.923254	0.888308	0.947856	1.531	2.803	0.318	0.295	0.521	3.009	1.003006	1.077130	
1.004106	0.986253	0.973586	0.990496	1.024	1.058	0.950	0.854	0.972	1.053	1.001347	1.129095	
1.007687	0.975088	0.953277	0.982191	1.046	1.113	0.902	0.798	0.943	1.109	1.002466	1.147861	
1.010620	0.966474	0.938524	0.975666	1.065	1.163	0.856	0.756	0.912	1.166	1.003331	1.149109	
1.012791	0.960341	0.928770	0.971104	1.080	1.206	0.813	0.721	0.881	1.224	1.003925	1.142714	
1.014116	0.956559	0.923342	0.968448	1.092	1.241	0.773	0.690	0.848	1.282	1.004243	1.132350	1/3
1.014563	0.954927	0.921708	0.967558	1.100	1.267	0.736	0.663	0.815	1.341	1.004296	1.120130	
1.014174	0.955156	0.923044	0.968269	1.104	1.283	0.702	0.638	0.783	1.399	1.004118	1.107735	
1.013097	0.956861	0.926583	0.970202	1.106	1.289	0.671	0.616	0.751	1.456	1.003764	1.095925	
1.011596	0.959556	0.931298	0.972917	1.105	1.289	0.644	0.596	0.721	1.510	1.003315	1.085432	
1.010054	0.962666	0.936164	0.975921	1.103	1.285	0.620	0.578	0.694	1.561	1.002872	1.076951	
1.002827	0.992435	0.985655	0.994248	1.013	1.031	0.965	0.895	0.977	1.035	1.000907	1.089888	
1.005193	0.986360	0.974600	0.989459	1.023	1.058	0.931	0.854	0.953	1.071	1.001637	1.103201	
1.007056	0.981712	0.966453	0.985824	1.032	1.080	0.900	0.823	0.929	1.106	1.002187	1.104969	
1.008392	0.978407	0.960896	0.983295	1.039	1.099	0.870	0.798	0.905	1.141	1.002560	1.101380	
1.009202	0.976334	0.957634	0.981838	1.044	1.113	0.842	0.776	0.881	1.175	1.002767	1.095340	
1.009514	0.975358	0.956300	0.981346	1.047	1.122	0.816	0.756	0.857	1.208	1.002825	1.088236	1/5
1.009391	0.975318	0.956458	0.981651	1.049	1.127	0.793	0.739	0.834	1.240	1.002761	1.080812	
1.008933	0.976024	0.957701	0.982606	1.049	1.129	0.771	0.723	0.812	1.270	1.002609	1.073794	
1.008277	0.977268	0.959557	0.984043	1.048	1.128	0.752	0.708	0.792	1.298	1.002409	1.067761	
1.007587	0.978822	0.961673	0.985724	1.047	1.126	0.735	0.695	0.774	1.324	1.002205	1.062907	
1.002032	0.994984	0.990737	0.995979	1.008	1.020	0.973	0.917	0.980	1.027	1.000642	1.069733	
1.003698	0.990978	0.983512	0.992696	1.015	1.036	0.947	0.885	0.961	1.053	1.001152	1.080169	
1.004989	0.987926	0.978170	0.990225	1.020	1.050	0.922	0.861	0.941	1.079	1.001533	1.081801	
1.005908	0.985761	0.974489	0.988543	1.024	1.061	0.899	0.841	0.921	1.103	1.001792	1.079647	
1.006471	0.984403	0.972266	0.987564	1.027	1.068	0.878	0.823	0.902	1.128	1.001942	1.075461	1/7
1.006713	0.983762	0.971209	0.987250	1.029	1.073	0.858	0.808	0.884	1.150	1.001996	1.070631	
1.006686	0.983737	0.971140	0.987475	1.030	1.076	0.840	0.794	0.866	1.172	1.001974	1.065541	
1.006457	0.984217	0.971797	0.988183	1.030	1.076	0.824	0.781	0.850	1.192	1.001897	1.060937	
1.006108	0.985086	0.972835	0.989211	1.029	1.076	0.809	0.770	0.834	1.211	1.001790	1.056814	
1.005734	0.986222	0.974115	0.990506	1.028	1.074	0.796	0.759	0.820	1.228	1.001678	1.053769	
1.001524	0.996281	0.993332	0.996916	1.006	1.014	0.978	0.931	0.983	1.021	1.000476	1.057419	
1.002760	0.993319	0.988098	0.994437	1.011	1.026	0.956	0.904	0.966	1.042	1.000851	1.066289	
1.003708	0.991068	0.984297	0.992571	1.014	1.035	0.937	0.884	0.950	1.063	1.001131	1.067819	
1.004381	0.989475	0.981537	0.991308	1.017	1.042	0.918	0.867	0.933	1.082	1.001323	1.066327	
1.004800	0.988483	0.979866	0.990611	1.019	1.047	0.900	0.853	0.918	1.101	1.001436	1.063499	1/9
1.004993	0.988028	0.979121	0.990396	1.020	1.051	0.884	0.840	0.902	1.118	1.001483	1.059918	
1.005002	0.988040	0.978949	0.990619	1.021	1.052	0.870	0.828	0.888	1.135	1.001477	1.056289	
1.004875	0.988448	0.979311	0.991211	1.021	1.052	0.856	0.818	0.875	1.150	1.001434	1.052939	
1.004666	0.989176	0.980074	0.992091	1.020	1.052	0.844	0.808	0.862	1.164	1.001370	1.050066	
1.004438	0.990149	0.981108	0.993207	1.020	1.050	0.834	0.799	0.851	1.176	1.001302	1.047984	

$M_0 = 1.0$

1.035477	0.935124	0.826621	0.687092*	1.101	1.226	1.824	0.576*	1.937	1.127	1.017461	3.959211*	
1.075569	0.877760	0.697826	0.659627*	1.210	1.500	1.651	0.573*	1.865	1.275	1.034927	3.468455*	
1.120153	0.828587	0.605601	0.639423*	1.325	1.826	1.481	0.569*	1.784	1.445	1.051571	3.026921*	
1.168129	0.788517	0.544199	0.627842*	1.441	2.198	1.315	0.562*	1.692	1.638	1.066154	2.634784*	
1.216423	0.758754	0.510043	0.626641*	1.549	2.594	1.157	0.552*	1.588	1.856	1.076963	2.291408*	1
1.258371	0.740828	0.501336	0.638063	1.639	2.971	1.008	0.538	1.471	2.090	1.081896	1.996479	
1.281834	0.736486	0.517955	0.664473	1.696	3.261	0.871	0.521	1.342	2.339	1.078903	1.749107	
1.269549	0.747142	0.559694	0.707255	1.710	3.389	0.750	0.499	1.202	2.592	1.067057	1.548715	
1.209481	0.772213	0.622674	0.763588	1.680	3.324	0.647	0.473	1.059	2.841	1.048388	1.394501	
1.126446	0.805399	0.691785	0.820571	1.631	3.152	0.565	0.444	0.927	3.090	1.029891	1.286115	
1.032061	0.978839	0.923577	0.720889*	1.043	1.095	1.891	0.586*	1.933	1.067	1.014121	4.084494*	
1.064013	0.961037	0.864181	0.724630*	1.082	1.188	1.784	0.596*	1.863	1.135	1.026450	3.699275*	
1.094472	0.946578	0.819980	0.732319*	1.117	1.274	1.682	0.607*	1.789	1.204	1.036478	3.344255*	
1.121540	0.935381	0.789537	0.744090*	1.145	1.347	1.584	0.620*	1.713	1.272	1.043736	3.019266*	
1.142835	0.927289	0.771653	0.759956*	1.165	1.404	1.491	0.633*	1.635	1.338	1.047875	2.724672*	1/3
1.155739	0.922054	0.765070	0.779643*	1.176	1.441	1.404	0.647*	1.557	1.400	1.048762	2.460515*	
1.157992	0.919337	0.768158	0.802454*	1.179	1.455	1.323	0.662*	1.478	1.458	1.046589	2.226798*	
1.148780	0.918727	0.778873	0.827182*	1.175	1.450	1.250	0.677*	1.402	1.511	1.041963	2.024326*	
1.130232	0.919765	0.794458	0.851875*	1.167	1.431	1.186	0.692*	1.331	1.559	1.035957	1.853680*	
1.108822	0.921955	0.811087	0.873892*	1.156	1.407	1.130	0.704*	1.268	1.603	1.030072	1.716262*	
1.024420	0.989797	0.954775	0.728779*	1.026	1.056	1.918	0.587*	1.942	1.045	1.010092	4.168552*	
1.047304	0.981451	0.919314	0.739143*	1.048	1.107	1.840	0.596*	1.882	1.089	1.018517	3.859493*	
1.067699	0.974838	0.892848	0.751901*	1.066	1.150	1.764	0.607*	1.822	1.132	1.025084	3.572053*	
1.084550	0.969797	0.874564	0.766912*	1.080	1.184	1.693	0.619*	1.762	1.172	1.029674	3.305926*	
1.096810	0.966137	0.863385	0.783999*	1.089	1.208	1.625	0.631*	1.702	1.210	1.032267	3.062147*	1/5
1.103631	0.963650	0.858695	0.802685*	1.094	1.222	1.562	0.645*	1.643	1.245	1.032968	2.839770*	
1.104629	0.962124	0.859152	0.822399*	1.095	1.226	1.503	0.658*	1.585	1.276	1.032032	2.639412*	
1.100202	0.961369	0.863768	0.842343*	1.093	1.223	1.450	0.672*	1.531	1.305	1.029864	2.461634*	
1.091845	0.961237	0.870767	0.861436*	1.089	1.214	1.403	0.686*	1.481	1.330	1.027017	2.306408*	
1.082314	0.961628	0.878543	0.878455*	1.084	1.204	1.362	0.700*	1.437	1.353	1.024159	2.174512*	
1.018883	0.994006	0.969337	0.731088*	1.018	1.038	1.934	0.586*	1.949	1.034	1.007461	4.224519*	
1.035937	0.989178	0.945212	0.742986*	1.032	1.071	1.871	0.594*	1.899	1.066	1.013557	3.966636*	
1.050567	0.985398	0.927107	0.756464*	1.044	1.098	1.811	0.604*	1.848	1.097	1.018225	3.726301*	
1.062206	0.982536	0.914514	0.771323*	1.053	1.119	1.754	0.614*	1.798	1.125	1.021462	3.502996*	
1.070386	0.980455	0.906831	0.787319*	1.058	1.133	1.700	0.624*	1.749	1.152	1.023324	3.296967*	
1.074840	0.979022	0.903219	0.804105*	1.061	1.141	1.650	0.635*	1.702	1.176	1.023943	3.108326*	1/7
1.075622	0.978118	0.903110	0.821269*	1.062	1.143	1.604	0.646*	1.657	1.197	1.023524	2.937719*	
1.073218	0.977649	0.905531	0.838203*	1.061	1.141	1.562	0.656*	1.614	1.217	1.022343	2.784637*	
1.068624	0.977556	0.909617	0.854283*	1.058	1.136	1.524	0.667*	1.575	1.234	1.020740	2.649754*	
1.063362	0.977815	0.914348	0.868775*	1.055	1.130	1.491	0.677*	1.540	1.250	1.019096	2.533259*	
1.014989	0.995990	0.977342	0.731616*	1.013	1.028	1.945	0.585*	1.956	1.027	1.005724	4.263953*	
1.028194	0.992783	0.959529	0.743565*	1.024	1.052	1.892	0.592*	1.912	1.052	1.010341	4.042719*	
1.039248	0.990285	0.946196	0.756597*	1.032	1.071	1.841	0.600*	1.868	1.076	1.013846	3.836187*	
1.047842	0.988401	0.936818	0.770507*	1.038	1.085	1.794	0.609*	1.826	1.098	1.016273	3.643791*	
1.053774	0.987035	0.931033	0.785106*	1.042	1.095	1.749	0.617*	1.784	1.118	1.017697	3.466156*	
1.056997	0.986103	0.928214	0.800090*	1.044	1.100	1.707	0.626*	1.745	1.137	1.018236	3.303016*	1/9
1.057681	0.985533	0.927872	0.815136*	1.045	1.102	1.669	0.635*	1.707	1.153	1.018052	3.154787*	
1.056251	0.985277	0.929378	0.829857*	1.044	1.101	1.634	0.644*	1.672	1.168	1.017344	3.021764*	
1.053413	0.985308	0.932225	0.843759*	1.043	1.097	1.603	0.652*	1.639	1.181	1.016342	2.903499*	
1.050134	0.985624	0.935495	0.856410*	1.041	1.093	1.575	0.660*	1.610	1.193	1.015296	2.800820*	

$M_0 = 2.0$

AXISYMMETRICAL

TABLE 4.1.IV

$M_0 = 3.0$

Mass Weighted	Area Weighted	Mass Derived	Mtm. Mixed	Mtm. Flux Coeff	Energy Flux Coeff	Mach Number Mass Derived	Mach Number Mtm. Mixed	Mach Number Entropy Flux	Velocity Ratio Max/ Mean	Static p Ratio Entropy/ Wall	Static p Ratio Mixed/ Wall	n
1.068261	0.931971	0.751451	0.315048*	1.143	1.316	2.738	0.479*	2.894	1.162	1.048837	8.842876*	
1.153209	0.872280	0.573421	0.305690*	1.306	1.736	2.476	0.482*	2.774	1.357	1.101304	7.488930*	
1.259657	0.821698	0.448774	0.301287*	1.489	2.282	2.217	0.487*	2.638	1.588	1.155613	6.269918*	
1.396035	0.781183	0.365345	0.303460*	1.684	2.961	1.961	0.491*	2.485	1.856	1.208147	5.185979*	
1.560537	0.751797	0.314836	0.314828*	1.876	3.736	1.710	0.496*	2.311	2.156	1.252546	4.238566*	1
1.756532	0.734362	0.293295	0.339529*	2.034	4.486	1.469	0.501*	2.115	2.471	1.279116	3.426431*	
1.952845	0.728515	0.301316	0.384088*	2.117	4.985	1.243	0.504*	1.898	2.766	1.275948	2.750767*	
2.056801	0.731057	0.344359	0.457149*	2.089	4.978	1.040	0.500*	1.663	2.998	1.234362	2.211493*	
1.885107	0.736205	0.428371	0.563673	1.949	4.429	0.867	0.501	1.422	3.144	1.160474	1.808711	
1.457452	0.747026	0.536826	0.681694	1.783	3.740	0.733	0.489	1.207	3.264	1.087778	1.541785	
1.072099	0.984508	0.870714	0.336459*	1.079	1.169	2.818	0.482*	2.881	1.098	1.043267	9.189072*	
1.153251	0.973915	0.771343	0.348764*	1.155	1.348	2.639	0.490*	2.756	1.199	1.083748	8.133541*	
1.242474	0.968025	0.697536	0.366167*	1.224	1.524	2.465	0.500*	2.625	1.300	1.119125	7.165737*	
1.336543	0.966223	0.646175	0.389768*	1.283	1.682	2.297	0.511*	2.489	1.398	1.146769	6.285795*	
1.428454	0.967240	0.615029	0.420772*	1.324	1.804	2.136	0.524*	2.350	1.487	1.164090	5.493198*	1/3
1.505705	0.968951	0.602454	0.460314*	1.345	1.872	1.984	0.539*	2.209	1.561	1.169139	4.788449*	
1.549801	0.968421	0.606941	0.508933*	1.343	1.878	1.843	0.556*	2.068	1.618	1.161409	4.170920*	
1.540433	0.962697	0.626418	0.565706*	1.322	1.826	1.714	0.573*	1.932	1.657	1.142677	3.640590*	
1.469781	0.950921	0.656635	0.626951*	1.288	1.737	1.601	0.595*	1.806	1.682	1.117535	3.198981*	
1.368575	0.937543	0.689783	0.684755*	1.252	1.645	1.506	0.615*	1.696	1.701	1.093264	2.847543*	
1.060498	0.997057	0.916171	0.341572*	1.053	1.112	2.856	0.482*	2.892	1.068	1.032789	9.399094*	
1.124165	0.996859	0.850709	0.358289*	1.100	1.218	2.716	0.489*	2.782	1.135	1.061740	8.532024*	
1.188807	0.998869	0.801651	0.379002*	1.140	1.313	2.581	0.498*	2.671	1.198	1.085563	7.731812*	
1.250836	1.002247	0.767430	0.404199*	1.172	1.390	2.451	0.507*	2.558	1.256	1.103089	6.998170*	
1.305006	1.005824	0.746645	0.434262*	1.192	1.443	2.328	0.517*	2.446	1.305	1.113473	6.330724*	1/5
1.344574	1.008163	0.737946	0.469328*	1.201	1.469	2.212	0.529*	2.336	1.345	1.116431	5.730151*	
1.362398	1.007811	0.739953	0.509019*	1.199	1.468	2.105	0.541*	2.229	1.376	1.112471	5.196525*	
1.353624	1.003824	0.750423	0.552107*	1.189	1.444	2.008	0.554*	2.129	1.397	1.103039	4.729368*	
1.320216	0.996580	0.766374	0.596237*	1.173	1.407	1.921	0.567*	2.036	1.412	1.090540	4.329581*	
1.276200	0.988482	0.783830	0.637690*	1.157	1.368	1.847	0.580*	1.956	1.425	1.078180	3.998425*	
1.050200	1.001220	0.939714	0.342900*	1.038	1.081	2.880	0.481*	2.904	1.052	1.025338	9.539728*	
1.100634	1.003957	0.892386	0.360246*	1.072	1.154	2.763	0.488*	2.807	1.101	1.047007	8.801218*	
1.149242	1.007668	0.856832	0.380612*	1.099	1.216	2.651	0.495*	2.711	1.146	1.064312	8.116148*	
1.193253	1.011645	0.831993	0.404213*	1.120	1.264	2.544	0.502*	2.615	1.186	1.076737	7.486264*	
1.229279	1.015053	0.816847	0.431070*	1.133	1.296	2.443	0.511*	2.521	1.220	1.084041	6.909854*	1/7
1.253698	1.017024	0.810207	0.461046*	1.138	1.311	2.349	0.519*	2.430	1.247	1.086355	6.388728*	
1.263490	1.016847	0.810977	0.493591*	1.138	1.310	2.261	0.529*	2.343	1.268	1.084257	5.921514*	
1.257581	1.014248	0.817418	0.527737*	1.132	1.297	2.182	0.538*	2.262	1.284	1.078793	5.509172*	
1.238578	1.009719	0.827389	0.561908*	1.123	1.277	2.111	0.547*	2.188	1.295	1.071450	5.151575*	
1.214291	1.004767	0.838410	0.593959*	1.113	1.255	2.049	0.556*	2.122	1.305	1.064050	4.849848*	
1.042107	1.002712	0.953804	0.342975*	1.030	1.062	2.896	0.481*	2.914	1.041	1.020135	9.640900*	
1.082997	1.006239	0.917502	0.359834*	1.055	1.116	2.796	0.486*	2.828	1.080	1.037009	8.995592*	
1.120982	1.010114	0.890146	0.379017*	1.075	1.161	2.700	0.492*	2.743	1.115	1.050253	8.396317*	
1.154046	1.013792	0.871071	0.400539*	1.090	1.195	2.608	0.499*	2.660	1.145	1.059653	7.842152*	
1.180003	1.016697	0.859411	0.424353*	1.099	1.217	2.522	0.506*	2.579	1.171	1.065202	7.335250*	1/9
1.196834	1.018301	0.854062	0.450162*	1.104	1.227	2.442	0.513*	2.501	1.191	1.067145	6.873603*	
1.203215	1.018252	0.854264	0.477505*	1.103	1.227	2.367	0.520*	2.427	1.208	1.065994	6.458792*	
1.199233	1.016519	0.858497	0.505598*	1.099	1.219	2.300	0.527*	2.358	1.220	1.062530	6.090619*	
1.187140	1.013551	0.865343	0.533326*	1.094	1.206	2.239	0.534*	2.296	1.229	1.057770	5.768765*	
1.171885	1.010363	0.873210	0.559307*	1.087	1.192	2.186	0.541*	2.240	1.237	1.052898	5.494454*	

$M_0 = 4.0$

Mass Weighted	Area Weighted	Mass Derived	Mtm. Mixed	Mtm. Flux Coeff	Energy Flux Coeff	Mach Number Mass Derived	Mach Number Mtm. Mixed	Mach Number Entropy Flux	Velocity Ratio Max/ Mean	Static p Ratio Entropy/ Wall	Static p Ratio Mixed/ Wall	n
1.087522	0.930366	0.698016	0.132875*	1.189	1.423	3.646	0.438*	3.846	1.204	1.086739	15.622955*	
1.202933	0.871024	0.490209	0.129003*	1.422	2.046	3.292	0.442*	3.672	1.462	1.186586	13.012280*	
1.359245	0.823544	0.350124	0.127826*	1.701	2.955	2.939	0.446*	3.476	1.784	1.298713	10.670233*	
1.576994	0.790184	0.258651	0.130503*	2.024	4.232	2.588	0.451*	3.253	2.179	1.418375	8.595615*	
1.888025	0.774052	0.202673	0.139151*	2.369	5.879	2.242	0.458*	3.000	2.639	1.533109	6.787580*	1
2.336265	0.778700	0.174694	0.157858*	2.675	7.641	1.904	0.467*	2.716	3.126	1.617799	5.247146*	
2.951949	0.805043	0.173427	0.194827*	2.837	8.804	1.581	0.476*	2.399	3.541	1.633068	3.974634*	
3.601184	0.839318	0.206822	0.266146*	2.735	8.412	1.285	0.488*	2.055	3.741	1.540372	2.969881*	
3.546648	0.829569	0.294275	0.395438*	2.360	6.435	1.034	0.497*	1.703	3.654	1.348608	2.234926*	
2.098543	0.752577	0.432598	0.568290	1.960	4.498	0.846	0.499	1.398	3.492	1.164014	1.770705	
1.104642	0.989691	0.821269	0.143672*	1.124	1.269	3.734	0.440*	3.819	1.139	1.083060	16.199551*	
1.233408	0.988090	0.686861	0.151469*	1.254	1.584	3.471	0.446*	3.628	1.291	1.166795	14.086958*	
1.391305	0.995949	0.588415	0.163158*	1.380	1.930	3.215	0.454*	3.428	1.448	1.246047	12.161221*	
1.581861	1.013459	0.520220	0.180206*	1.493	2.271	2.965	0.463*	3.221	1.601	1.313600	10.423273*	
1.802755	1.039341	0.478049	0.204690*	1.579	2.552	2.724	0.473*	3.007	1.738	1.360683	8.871246*	1/3
2.036465	1.069703	0.459792	0.239441*	1.622	2.709	2.495	0.487*	2.790	1.841	1.378689	7.505003*	
2.234606	1.093314	0.464503	0.287852*	1.613	2.695	2.280	0.502*	2.574	1.898	1.362402	6.324744*	
2.305408	1.095922	0.491556	0.352671*	1.555	2.516	2.085	0.521*	2.365	1.906	1.314128	5.329906*	
2.149163	1.063045	0.537294	0.432612*	1.466	2.243	1.915	0.542*	2.172	1.876	1.246741	4.522050*	
1.826652	1.008227	0.589588	0.515964*	1.378	1.987	1.775	0.563*	2.008	1.841	1.183180	3.902734*	
1.093027	1.005061	0.874962	0.146765*	1.090	1.191	3.780	0.440*	3.831	1.103	1.066126	16.559696*	
1.204951	1.016149	0.778411	0.157543*	1.176	1.391	3.565	0.446*	3.657	1.207	1.128431	14.768463*	
1.329642	1.032936	0.706637	0.171866*	1.254	1.585	3.356	0.452*	3.481	1.306	1.183159	13.126070*	
1.466044	1.054283	0.656587	0.190705*	1.317	1.753	3.155	0.460*	3.303	1.396	1.226144	11.628937*	
1.605690	1.077721	0.626035	0.215271*	1.360	1.874	2.963	0.468*	3.125	1.469	1.253449	10.280823*	1/5
1.731550	1.098914	0.613305	0.246832*	1.378	1.929	2.781	0.478*	2.950	1.521	1.262347	9.078279*	
1.816128	1.111586	0.617092	0.286473*	1.370	1.912	2.613	0.489*	2.780	1.549	1.252496	8.024216*	
1.826213	1.108973	0.634952	0.334294*	1.341	1.835	2.460	0.501*	2.621	1.554	1.226936	7.117270*	
1.743760	1.088335	0.663034	0.388220*	1.300	1.724	2.325	0.514*	2.475	1.544	1.192457	6.357802*	
1.607952	1.058653	0.693683	0.442520*	1.258	1.616	2.211	0.527*	2.351	1.531	1.159004	5.747968*	
1.083572	1.010182	0.905328	0.147813*	1.069	1.145	3.811	0.439*	3.845	1.080	1.053043	16.811638*	
1.175752	1.024324	0.831538	0.159301*	1.133	1.287	3.626	0.445*	3.690	1.158	1.101011	15.246124*	
1.274546	1.041659	0.776343	0.173768*	1.187	1.416	3.449	0.450*	3.533	1.229	1.141430	13.805550*	
1.375571	1.060763	0.737714	0.191816*	1.229	1.521	3.278	0.456*	3.378	1.291	1.171930	12.486345*	
1.471018	1.079358	0.714338	0.214107*	1.256	1.591	3.116	0.463*	3.225	1.340	1.190657	11.291395*	1/7
1.549001	1.094261	0.704595	0.241184*	1.267	1.622	2.963	0.471*	3.077	1.374	1.196768	10.218273*	
1.594479	1.101765	0.706926	0.273306*	1.263	1.612	2.822	0.479*	2.935	1.393	1.190899	9.269424*	
1.593769	1.098837	0.719328	0.310001*	1.246	1.570	2.694	0.488*	2.803	1.399	1.175461	8.443342*	
1.544612	1.085410	0.738201	0.349620*	1.221	1.510	2.580	0.497*	2.683	1.396	1.154643	7.741299*	
1.470629	1.067281	0.758855	0.388813*	1.196	1.449	2.483	0.505*	2.580	1.390	1.134038	7.163390*	
1.073390	1.011816	0.924748	0.148092*	1.055	1.115	3.833	0.439*	3.859	1.065	1.043440	16.998638*	
1.151374	1.026164	0.865889	0.159521*	1.105	1.223	3.671	0.444*	3.718	1.126	1.081654	15.604010*	
1.231443	1.042162	0.821684	0.173412*	1.145	1.317	3.515	0.448*	3.578	1.181	1.113018	14.316257*	
1.309396	1.058464	0.790860	0.190140*	1.176	1.391	3.366	0.454*	3.440	1.228	1.136154	13.134075*	
1.379018	1.073217	0.772055	0.210052*	1.196	1.439	3.224	0.460*	3.305	1.264	1.150179	12.058655*	1/9
1.432259	1.084183	0.764143	0.233349*	1.204	1.459	3.092	0.466*	3.176	1.289	1.154964	11.088379*	
1.460507	1.089129	0.765491	0.259970*	1.201	1.453	2.969	0.472*	3.053	1.304	1.151337	10.224733*	
1.457683	1.086649	0.774387	0.289366*	1.190	1.427	2.858	0.479*	2.940	1.310	1.141175	9.468376*	
1.425431	1.077391	0.788117	0.320255*	1.174	1.389	2.759	0.486*	2.837	1.310	1.127340	8.818439*	
1.379141	1.065331	0.803111	0.350466*	1.157	1.351	2.674	0.492*	2.747	1.308	1.113438	8.275459*	

AXISYMMETRICAL

TABLE 4.1.V

Mass Weighted	Area Weighted	Mass Derived	Mtm. Mixed	Mtm. Flux Coeff	Energy Flux Coeff	Mach Number Mass Derived	Mach Number Mtm. Mixed	Mach Number Entropy Flux	Velocity Ratio Max/ Mean	Static p Ratio Entropy/ Wall	Static p Ratio Mixed/ Wall	n
1.000006	0.998390	0.998028	0.999219	1.035	1.080	0.190	0.190	0.197	1.053	1.000002	1.001264	
1.000013	0.996859	0.996242	0.998395	1.071	1.169	0.180	0.179	0.194	1.112	1.000004	1.002359	
1.000020	0.995422	0.994715	0.997518	1.109	1.267	0.170	0.169	0.191	1.179	1.000006	1.002936	
1.000026	0.994097	0.993439	0.996627	1.149	1.374	0.160	0.159	0.187	1.253	1.000008	1.003340	
1.000032	0.992907	0.992432	0.995723	1.189	1.492	0.150	0.149	0.182	1.338	1.000009	1.003426	1
1.000038	0.991881	0.991732	0.994854	1.230	1.617	0.140	0.139	0.177	1.435	1.000011	1.003236	
1.000042	0.991059	0.991386	0.994057	1.269	1.747	0.129	0.129	0.171	1.547	1.000012	1.002767	
1.000043	0.990493	0.991436	0.993366	1.304	1.873	0.119	0.119	0.163	1.678	1.000012	1.001984	
1.000041	0.990256	0.991962	0.992886	1.330	1.977	0.109	0.109	0.153	1.833	1.000012	1.000951	
1.000032	0.990451	0.993062	0.992686	1.341	2.023	0.099	0.099	0.141	2.020	1.000009	0.999606	
1.000005	0.999104	0.999332	0.999351	1.010	1.026	0.195	0.195	0.197	1.026	1.000001	1.000030	
1.000009	0.998246	0.998718	0.998709	1.021	1.052	0.190	0.190	0.195	1.054	1.000003	0.999992	
1.000013	0.997427	0.998183	0.998075	1.030	1.078	0.185	0.185	0.192	1.083	1.000004	0.999885	
1.000017	0.996651	0.997722	0.997452	1.040	1.103	0.180	0.180	0.188	1.114	1.000005	0.999708	
1.000020	0.995923	0.997359	0.996865	1.048	1.126	0.175	0.175	0.185	1.146	1.000006	0.999461	1/3
1.000022	0.995247	0.997066	0.996257	1.056	1.148	0.169	0.170	0.181	1.181	1.000006	0.999143	
1.000024	0.994627	0.996886	0.995692	1.062	1.167	0.164	0.164	0.177	1.217	1.000007	0.998755	
1.000024	0.994070	0.996813	0.995157	1.068	1.183	0.159	0.159	0.173	1.256	1.000007	0.998295	
1.000024	0.993581	0.996821	0.994636	1.071	1.194	0.154	0.154	0.168	1.298	1.000007	0.997723	
1.000021	0.993169	0.996965	0.994178	1.073	1.198	0.149	0.149	0.163	1.342	1.000006	0.997120	
1.000003	0.999295	0.999650	0.999399	1.005	1.013	0.197	0.197	0.198	1.018	1.000001	0.999723	
1.000006	0.998611	0.999338	0.998828	1.010	1.026	0.193	0.193	0.196	1.036	1.000002	0.999467	
1.000009	0.997948	0.999035	0.998263	1.015	1.039	0.190	0.190	0.193	1.054	1.000002	0.999178	
1.000011	0.997307	0.998794	0.997706	1.019	1.050	0.186	0.186	0.191	1.074	1.000003	0.998857	
1.000013	0.996689	0.998611	0.997136	1.023	1.061	0.183	0.183	0.188	1.094	1.000004	0.998457	1/5
1.000014	0.996097	0.998435	0.996598	1.027	1.071	0.179	0.180	0.185	1.115	1.000004	0.998072	
1.000015	0.995531	0.998316	0.996072	1.030	1.079	0.176	0.176	0.183	1.137	1.000004	0.997655	
1.000015	0.994993	0.998250	0.995538	1.032	1.086	0.172	0.173	0.180	1.160	1.000004	0.997160	
1.000015	0.994486	0.998236	0.995040	1.034	1.090	0.169	0.170	0.176	1.183	1.000004	0.996678	
1.000014	0.994010	0.998248	0.994559	1.035	1.093	0.165	0.166	0.173	1.208	1.000004	0.996163	
1.000002	0.999374	0.999783	0.999445	1.003	1.009	0.197	0.197	0.198	1.013	1.000001	0.999652	
1.000004	0.998761	0.999573	0.998893	1.006	1.017	0.195	0.195	0.196	1.027	1.000001	0.999286	
1.000006	0.998160	0.999394	0.998347	1.009	1.024	0.192	0.192	0.194	1.041	1.000002	0.998902	
1.000007	0.997574	0.999245	0.997806	1.012	1.031	0.190	0.190	0.192	1.055	1.000002	0.998500	
1.000009	0.997001	0.999100	0.997271	1.015	1.038	0.187	0.187	0.190	1.070	1.000002	0.998080	1/7
1.000010	0.996443	0.998985	0.996742	1.017	1.044	0.184	0.185	0.188	1.085	1.000003	0.997641	
1.000010	0.995901	0.998898	0.996220	1.019	1.049	0.182	0.182	0.186	1.101	1.000003	0.997184	
1.000011	0.995374	0.998839	0.995706	1.020	1.053	0.179	0.180	0.184	1.117	1.000003	0.996709	
1.000011	0.994865	0.998806	0.995200	1.021	1.056	0.176	0.177	0.181	1.133	1.000003	0.996215	
1.000010	0.994373	0.998799	0.994703	1.022	1.058	0.174	0.175	0.179	1.150	1.000003	0.995703	
1.000002	0.999414	0.999837	0.999441	1.002	1.006	0.198	0.198	0.198	1.011	1.000000	0.999559	
1.000003	0.998837	0.999705	0.998909	1.005	1.012	0.196	0.196	0.197	1.022	1.000001	0.999158	
1.000004	0.998268	0.999575	0.998381	1.007	1.017	0.194	0.194	0.195	1.033	1.000001	0.998745	
1.000005	0.997709	0.999448	0.997857	1.009	1.022	0.192	0.192	0.194	1.044	1.000002	0.998320	
1.000006	0.997159	0.999350	0.997336	1.010	1.027	0.189	0.190	0.192	1.056	1.000002	0.997883	1/9
1.000007	0.996618	0.999254	0.996820	1.012	1.031	0.187	0.188	0.190	1.068	1.000002	0.997434	
1.000008	0.996088	0.999186	0.996308	1.014	1.035	0.185	0.186	0.188	1.080	1.000002	0.996972	
1.000008	0.995568	0.999144	0.995801	1.015	1.038	0.183	0.184	0.186	1.092	1.000002	0.996499	
1.000008	0.995060	0.999104	0.995299	1.016	1.040	0.181	0.182	0.184	1.105	1.000002	0.996013	
1.000008	0.994562	0.999089	0.994803	1.016	1.042	0.179	0.180	0.182	1.118	1.000002	0.995515	

$M_o = .2$

Mass Weighted	Area Weighted	Mass Derived	Mtm. Mixed	Mtm. Flux Coeff	Energy Flux Coeff	Mach Number Mass Derived	Mach Number Mtm. Mixed	Mach Number Entropy Flux	Velocity Ratio Max/ Mean	Static p Ratio Entropy/ Wall	Static p Ratio Mixed/ Wall	n
1.000098	0.995285	0.992334	0.998385	1.035	1.081	0.380	0.377	0.395	1.053	1.000029	1.007519	
1.000199	0.990858	0.985506	0.996546	1.072	1.170	0.360	0.355	0.389	1.112	1.000059	1.013527	
1.000301	0.986774	0.979588	0.994510	1.111	1.269	0.340	0.334	0.382	1.179	1.000088	1.018014	
1.000401	0.983101	0.974605	0.992388	1.150	1.377	0.320	0.313	0.374	1.253	1.000117	1.021138	
1.000496	0.979927	0.970667	0.990249	1.191	1.496	0.299	0.293	0.365	1.338	1.000145	1.022893	1
1.000580	0.977368	0.967947	0.988284	1.232	1.622	0.279	0.273	0.354	1.435	1.000169	1.023493	
1.000644	0.975576	0.966524	0.986563	1.272	1.754	0.259	0.253	0.341	1.547	1.000186	1.022785	
1.000671	0.974762	0.966671	0.985364	1.307	1.881	0.238	0.233	0.325	1.678	1.000193	1.020962	
1.000637	0.975216	0.968641	0.984955	1.334	1.986	0.218	0.214	0.305	1.833	1.000183	1.018005	
1.000496	0.977364	0.972950	0.985731	1.344	2.031	0.197	0.195	0.280	2.020	1.000142	1.013898	
1.000072	0.997995	0.997375	0.998918	1.011	1.026	0.390	0.389	0.395	1.026	1.000021	1.001972	
1.000140	0.996125	0.994965	0.997867	1.021	1.053	0.380	0.378	0.389	1.054	1.000041	1.003616	
1.000203	0.994404	0.992908	0.996819	1.031	1.079	0.369	0.368	0.383	1.083	1.000059	1.004845	
1.000259	0.992846	0.991097	0.995819	1.040	1.104	0.359	0.357	0.377	1.114	1.000075	1.005743	
1.000306	0.991465	0.989666	0.994878	1.049	1.128	0.349	0.347	0.370	1.146	1.000089	1.006307	1/3
1.000344	0.990279	0.988555	0.994012	1.057	1.150	0.338	0.336	0.362	1.181	1.000100	1.006536	
1.000369	0.989309	0.987841	0.993201	1.064	1.170	0.328	0.326	0.354	1.218	1.000107	1.006349	
1.000378	0.988577	0.987463	0.992567	1.069	1.185	0.318	0.316	0.345	1.257	1.000109	1.005981	
1.000368	0.988110	0.987569	0.992032	1.073	1.197	0.307	0.306	0.335	1.298	1.000106	1.005196	
1.000334	0.987938	0.988090	0.991687	1.074	1.201	0.297	0.296	0.325	1.343	1.000096	1.004145	
1.000048	0.998720	0.998622	0.999139	1.005	1.014	0.393	0.393	0.396	1.018	1.000014	1.000648	
1.000092	0.997515	0.997341	0.998320	1.010	1.027	0.386	0.386	0.391	1.036	1.000027	1.001186	
1.000132	0.996389	0.996252	0.997546	1.015	1.039	0.379	0.379	0.386	1.054	1.000038	1.001612	
1.000167	0.995347	0.995299	0.996785	1.020	1.051	0.372	0.372	0.381	1.074	1.000048	1.001839	
1.000196	0.994395	0.994479	0.996075	1.024	1.062	0.365	0.365	0.376	1.094	1.000057	1.001952	1/5
1.000219	0.993537	0.993884	0.995387	1.027	1.072	0.358	0.358	0.371	1.115	1.000063	1.001865	
1.000234	0.992780	0.993411	0.994760	1.030	1.080	0.351	0.351	0.365	1.137	1.000068	1.001663	
1.000241	0.992132	0.993105	0.994165	1.033	1.087	0.344	0.344	0.359	1.160	1.000070	1.001261	
1.000239	0.991598	0.993047	0.993643	1.035	1.092	0.337	0.337	0.352	1.183	1.000069	1.000742	
1.000226	0.991189	0.993140	0.993201	1.035	1.094	0.330	0.330	0.345	1.208	1.000065	1.000104	
1.000033	0.999020	0.999146	0.999249	1.003	1.009	0.395	0.395	0.396	1.013	1.000010	1.000142	
1.000064	0.998086	0.998317	0.998563	1.007	1.017	0.389	0.389	0.393	1.027	1.000019	1.000310	
1.000091	0.997201	0.997611	0.997905	1.010	1.025	0.384	0.384	0.389	1.041	1.000027	1.000412	
1.000115	0.996368	0.996974	0.997241	1.012	1.032	0.379	0.379	0.385	1.055	1.000033	1.000362	
1.000135	0.995588	0.996434	0.996574	1.015	1.039	0.374	0.374	0.380	1.070	1.000039	1.000160	1/7
1.000151	0.994865	0.995999	0.995978	1.017	1.044	0.368	0.368	0.376	1.085	1.000044	0.999978	
1.000161	0.994200	0.995656	0.995382	1.019	1.050	0.363	0.363	0.372	1.101	1.000047	0.999645	
1.000167	0.993597	0.995422	0.994860	1.021	1.054	0.358	0.358	0.367	1.117	1.000048	0.999329	
1.000167	0.993059	0.995294	0.994310	1.022	1.057	0.352	0.353	0.362	1.133	1.000048	0.998779	
1.000160	0.992589	0.995314	0.993838	1.023	1.058	0.347	0.348	0.357	1.150	1.000046	0.998244	
1.000025	0.999172	0.999357	0.999319	1.002	1.006	0.396	0.396	0.397	1.011	1.000007	0.999916	
1.000047	0.998376	0.998784	0.998693	1.005	1.012	0.391	0.392	0.394	1.022	1.000014	0.999880	
1.000067	0.997613	0.998274	0.998087	1.007	1.018	0.387	0.387	0.390	1.033	1.000019	0.999800	
1.000084	0.996884	0.997826	0.997466	1.009	1.023	0.383	0.383	0.387	1.044	1.000024	0.999590	
1.000098	0.996192	0.997388	0.996867	1.011	1.027	0.379	0.379	0.384	1.056	1.000028	0.999337	
1.000110	0.995536	0.997060	0.996291	1.012	1.032	0.374	0.375	0.380	1.068	1.000032	0.999041	1/9
1.000118	0.994919	0.996791	0.995739	1.014	1.035	0.370	0.370	0.376	1.080	1.000034	0.998702	
1.000122	0.994343	0.996626	0.995212	1.015	1.038	0.366	0.366	0.372	1.092	1.000035	0.998319	
1.000123	0.993808	0.996468	0.994677	1.016	1.041	0.361	0.362	0.368	1.105	1.000035	0.997807	
1.000119	0.993316	0.996417	0.994204	1.017	1.042	0.357	0.358	0.364	1.118	1.000034	0.997335	

$M_o = .4$

TABLE 4.1.VI

Mass Weighted	Area Weighted	Mass Derived	Mtm. Mixed	Mtm. Flux Coeff	Energy Flux Coeff	Mach Number Mass Derived	Mach Number Mtm. Mixed	Mach Number Entropy Flux	Velocity Ratio Max/ Mean	Static p Ratio Entropy/ Wall	Static p Ratio Mixed/ Wall	n
1.000457	0.990776	0.983755	0.996946	1.036	1.082	0.571	0.559	0.592	1.053	1.000140	1.022346	
1.000929	0.982109	0.969201	0.993229	1.073	1.172	0.541	0.522	0.583	1.113	1.000284	1.038693	
1.001409	0.974107	0.956553	0.989092	1.112	1.272	0.511	0.487	0.572	1.179	1.000428	1.050205	
1.001888	0.966913	0.945884	0.984798	1.153	1.382	0.481	0.455	0.560	1.254	1.000569	1.057734	
1.002349	0.960710	0.937442	0.980569	1.195	1.503	0.450	0.425	0.546	1.339	1.000703	1.061727	1
1.002766	0.955743	0.931447	0.976697	1.237	1.632	0.419	0.395	0.530	1.436	1.000821	1.062578	
1.003091	0.952343	0.928212	0.973514	1.277	1.766	0.388	0.367	0.510	1.548	1.000908	1.060504	
1.003248	0.950970	0.928261	0.971542	1.313	1.896	0.357	0.339	0.486	1.679	1.000944	1.055854	
1.003104	0.952288	0.932353	0.971371	1.340	2.003	0.326	0.311	0.456	1.835	1.000892	1.048629	
1.002418	0.957279	0.941501	0.973941	1.350	2.046	0.294	0.284	0.417	2.022	1.000691	1.038927	
1.000340	0.996378	0.994260	0.998183	1.011	1.027	0.585	0.581	0.592	1.026	1.000103	1.006796	
1.000664	0.993025	0.989135	0.996355	1.022	1.054	0.569	0.563	0.583	1.054	1.000200	1.012146	
1.000965	0.989967	0.984596	0.994598	1.032	1.081	0.554	0.545	0.574	1.083	1.000289	1.016332	
1.001236	0.987235	0.980767	0.992938	1.042	1.107	0.538	0.528	0.564	1.114	1.000368	1.019418	
1.001470	0.984864	0.977623	0.991376	1.051	1.131	0.523	0.512	0.554	1.147	1.000436	1.021379	1/3
1.001657	0.982892	0.975208	0.990001	1.059	1.154	0.507	0.496	0.542	1.181	1.000488	1.022419	
1.001783	0.981366	0.973560	0.988880	1.066	1.174	0.491	0.481	0.530	1.218	1.000523	1.022654	
1.001833	0.980339	0.972771	0.987992	1.071	1.190	0.475	0.465	0.516	1.257	1.000535	1.021921	
1.001788	0.979871	0.972921	0.987481	1.075	1.201	0.459	0.450	0.501	1.299	1.000519	1.020495	
1.001623	0.980036	0.974076	0.987336	1.076	1.206	0.443	0.436	0.485	1.343	1.000470	1.018198	
1.000229	0.997879	0.996977	0.998702	1.006	1.014	0.590	0.588	0.593	1.018	1.000069	1.003013	
1.000441	0.995908	0.994278	0.997498	1.011	1.028	0.579	0.576	0.586	1.036	1.000132	1.005618	
1.000634	0.994096	0.991812	0.996303	1.016	1.041	0.568	0.564	0.579	1.055	1.000188	1.007529	
1.000804	0.992455	0.989718	0.995194	1.021	1.053	0.558	0.553	0.571	1.074	1.000238	1.008991	
1.000947	0.990997	0.987985	0.994185	1.025	1.064	0.547	0.542	0.563	1.094	1.000280	1.010031	
1.001061	0.989734	0.986603	0.993259	1.028	1.074	0.537	0.531	0.555	1.115	1.000312	1.010577	1/5
1.001139	0.988681	0.985561	0.992437	1.032	1.083	0.526	0.520	0.546	1.137	1.000333	1.010671	
1.001175	0.987854	0.984983	0.991744	1.034	1.090	0.515	0.510	0.536	1.160	1.000343	1.010356	
1.001165	0.987271	0.984785	0.991172	1.036	1.094	0.504	0.500	0.526	1.184	1.000339	1.009582	
1.001099	0.986951	0.985018	0.990794	1.037	1.097	0.494	0.490	0.515	1.208	1.000319	1.008511	
1.000161	0.998500	0.998048	0.998981	1.004	1.009	0.592	0.591	0.594	1.013	1.000048	1.001616	
1.000309	0.997094	0.996303	0.998023	1.007	1.018	0.584	0.582	0.589	1.027	1.000092	1.002998	
1.000442	0.995788	0.994751	0.997104	1.010	1.026	0.576	0.574	0.583	1.041	1.000131	1.004066	
1.000558	0.994586	0.993386	0.996228	1.013	1.033	0.568	0.565	0.576	1.055	1.000165	1.004833	
1.000656	0.993495	0.992205	0.995403	1.016	1.040	0.560	0.557	0.570	1.070	1.000193	1.005315	1/7
1.000733	0.992520	0.991275	0.994636	1.018	1.046	0.552	0.549	0.563	1.085	1.000215	1.005528	
1.000788	0.991667	0.990520	0.993937	1.020	1.051	0.543	0.541	0.556	1.101	1.000230	1.005488	
1.000816	0.990944	0.990004	0.993316	1.022	1.055	0.535	0.533	0.549	1.117	1.000238	1.005218	
1.000815	0.990358	0.989788	0.992784	1.023	1.058	0.527	0.525	0.541	1.133	1.000237	1.004737	
1.000783	0.989917	0.989731	0.992321	1.024	1.060	0.519	0.517	0.533	1.150	1.000228	1.003966	
1.000119	0.998815	0.998663	0.999134	1.003	1.006	0.594	0.593	0.595	1.011	1.000035	1.000926	
1.000228	0.997696	0.997366	0.998310	1.005	1.012	0.587	0.586	0.590	1.022	1.000067	1.001698	
1.000325	0.996645	0.996244	0.997503	1.007	1.018	0.580	0.579	0.585	1.033	1.000096	1.002231	
1.000409	0.995664	0.995221	0.996749	1.009	1.023	0.574	0.572	0.580	1.044	1.000120	1.002641	
1.000480	0.994758	0.994368	0.996054	1.011	1.028	0.567	0.566	0.575	1.056	1.000141	1.002935	1/9
1.000536	0.993928	0.993610	0.995353	1.013	1.033	0.561	0.559	0.569	1.068	1.000157	1.002909	
1.000576	0.993179	0.993016	0.994719	1.014	1.036	0.554	0.553	0.563	1.080	1.000168	1.002786	
1.000598	0.992515	0.992583	0.994158	1.016	1.039	0.547	0.546	0.557	1.093	1.000174	1.002575	
1.000601	0.991938	0.992308	0.993606	1.017	1.042	0.541	0.540	0.551	1.105	1.000175	1.002077	
1.000583	0.991453	0.992185	0.993140	1.017	1.043	0.534	0.533	0.545	1.118	1.000169	1.001515	

$M_0 = .6$

Mass Weighted	Area Weighted	Mass Derived	Mtm. Mixed	Mtm. Flux Coeff	Energy Flux Coeff	Mach Number Mass Derived	Mach Number Mtm. Mixed	Mach Number Entropy Flux	Velocity Ratio Max/ Mean	Static p Ratio Entropy/ Wall	Static p Ratio Mixed/ Wall	n
1.001288	0.985621	0.973248	0.994556	1.037	1.083	0.761	0.722	0.789	1.054	1.000417	1.060595	
1.002631	0.972046	0.949264	0.987751	1.075	1.175	0.722	0.664	0.776	1.113	1.000843	1.095557	
1.004015	0.959445	0.928275	0.980308	1.116	1.278	0.682	0.616	0.762	1.180	1.001274	1.116496	
1.005417	0.948039	0.910492	0.972706	1.158	1.391	0.642	0.574	0.746	1.255	1.001699	1.127794	
1.006792	0.938122	0.896257	0.965478	1.201	1.515	0.601	0.535	0.727	1.341	1.002103	1.132017	1
1.008064	0.930091	0.885953	0.959047	1.244	1.647	0.560	0.498	0.705	1.438	1.002460	1.130244	
1.009099	0.924497	0.880200	0.954014	1.285	1.785	0.518	0.464	0.678	1.551	1.002730	1.123346	
1.009661	0.922129	0.879828	0.951188	1.323	1.919	0.476	0.430	0.645	1.683	1.002844	1.111934	
1.009320	0.924154	0.886221	0.951648	1.350	2.028	0.433	0.396	0.605	1.838	1.002691	1.096237	
1.007264	0.932373	0.901375	0.957181	1.359	2.069	0.390	0.363	0.551	2.024	1.002073	1.076726	
1.000981	0.994528	0.990360	0.997050	1.012	1.028	0.779	0.765	0.789	1.026	1.000309	1.020908	
1.001922	0.989459	0.981703	0.994081	1.023	1.056	0.759	0.735	0.777	1.054	1.000601	1.035373	
1.002808	0.984835	0.974071	0.991186	1.034	1.084	0.738	0.709	0.765	1.084	1.000871	1.045267	
1.003617	0.980707	0.967521	0.988473	1.044	1.111	0.717	0.684	0.751	1.115	1.001111	1.051764	
1.004324	0.977136	0.962107	0.986028	1.054	1.137	0.696	0.662	0.737	1.148	1.001316	1.055529	
1.004898	0.974190	0.957958	0.983914	1.062	1.160	0.674	0.641	0.721	1.182	1.001477	1.056921	1/3
1.005298	0.971948	0.955114	0.982243	1.069	1.181	0.653	0.620	0.704	1.219	1.001582	1.056347	
1.005472	0.970505	0.953687	0.981111	1.075	1.198	0.631	0.601	0.685	1.258	1.001619	1.054025	
1.005353	0.969974	0.953923	0.980591	1.079	1.209	0.609	0.582	0.665	1.300	1.001571	1.050000	
1.004855	0.970489	0.955896	0.980906	1.080	1.213	0.587	0.564	0.642	1.344	1.001418	1.044732	
1.000669	0.996915	0.994896	0.998045	1.006	1.015	0.786	0.779	0.791	1.018	1.000208	1.010360	
1.001294	0.994057	0.990251	0.996188	1.012	1.029	0.772	0.759	0.781	1.036	1.000399	1.018224	
1.001867	0.991444	0.986036	0.994400	1.017	1.043	0.757	0.741	0.771	1.055	1.000572	1.023828	
1.002378	0.989094	0.982515	0.992748	1.022	1.056	0.743	0.724	0.761	1.075	1.000723	1.027763	
1.002814	0.987029	0.979491	0.991261	1.026	1.067	0.728	0.709	0.750	1.095	1.000850	1.030289	
1.003162	0.985272	0.977128	0.989959	1.030	1.078	0.714	0.694	0.738	1.116	1.000948	1.031565	1/5
1.003405	0.983848	0.975322	0.988877	1.034	1.087	0.699	0.679	0.725	1.138	1.001015	1.031761	
1.003524	0.982788	0.974311	0.988034	1.036	1.094	0.684	0.665	0.712	1.161	1.001044	1.030943	
1.003497	0.982122	0.973988	0.987459	1.038	1.099	0.669	0.652	0.698	1.184	1.001031	1.029189	
1.003297	0.981887	0.974332	0.987220	1.039	1.101	0.655	0.639	0.684	1.209	1.000969	1.026707	
1.000476	0.997902	0.996668	0.998556	1.004	1.009	0.789	0.785	0.792	1.013	1.000146	1.006220	
1.000916	0.995950	0.993723	0.997171	1.007	1.018	0.778	0.770	0.784	1.027	1.000280	1.010991	
1.001315	0.994151	0.991043	0.995860	1.011	1.027	0.767	0.757	0.776	1.041	1.000399	1.014569	
1.001666	0.992516	0.988625	0.994650	1.014	1.035	0.756	0.744	0.767	1.056	1.000503	1.017192	
1.001964	0.991054	0.986647	0.993555	1.017	1.042	0.745	0.732	0.758	1.070	1.000590	1.018991	
1.002201	0.989775	0.985008	0.992547	1.019	1.048	0.734	0.721	0.749	1.086	1.000657	1.019868	1/7
1.002368	0.988691	0.983790	0.991675	1.021	1.054	0.723	0.709	0.739	1.101	1.000704	1.020079	
1.002458	0.987816	0.982898	0.990971	1.023	1.058	0.711	0.699	0.729	1.117	1.000727	1.019769	
1.002459	0.987161	0.982494	0.990392	1.024	1.061	0.700	0.688	0.719	1.134	1.000725	1.018739	
1.002359	0.986743	0.982484	0.990004	1.025	1.063	0.689	0.678	0.708	1.151	1.000694	1.017256	
1.000355	0.998406	0.997661	0.998826	1.003	1.007	0.791	0.788	0.793	1.011	1.000108	1.004056	
1.000680	0.996912	0.995487	0.997714	1.005	1.013	0.782	0.777	0.787	1.022	1.000206	1.007298	
1.000973	0.995525	0.993457	0.996654	1.008	1.019	0.773	0.766	0.780	1.033	1.000293	1.009753	
1.001229	0.994248	0.991755	0.995681	1.010	1.025	0.764	0.756	0.772	1.045	1.000369	1.011658	
1.001446	0.993088	0.990282	0.994769	1.012	1.030	0.755	0.746	0.765	1.056	1.000432	1.012905	
1.001618	0.992049	0.989036	0.993914	1.014	1.034	0.746	0.737	0.757	1.068	1.000481	1.013504	1/9
1.001742	0.991140	0.988011	0.993185	1.015	1.038	0.737	0.728	0.749	1.080	1.000516	1.013816	
1.001811	0.990365	0.987295	0.992513	1.017	1.041	0.728	0.719	0.741	1.093	1.000534	1.013508	
1.001821	0.989732	0.986880	0.991976	1.018	1.044	0.719	0.710	0.732	1.106	1.000536	1.012944	
1.001765	0.989249	0.986673	0.991529	1.018	1.045	0.709	0.702	0.724	1.119	1.000519	1.011910	

$M_0 = .8$

TABLE 4.1.VII

Mass Weighted	Area Weighted	Mass Derived	Mtm. Mixed	Mtm. Flux Coeff	Energy Flux Coeff	Mach Number Mass Derived	Mach Number Mtm. Mixed	Mach Number Entropy Flux	Velocity Ratio Max/ Mean	Static p Ratio Entropy/ Wall	Static p Ratio Mixed/ Wall	n
1.002735	0.980322	0.961634	0.989729	1.038	1.085	0.953	0.818	0.986	1.054	1.000942	1.188815	
1.005622	0.962025	0.927292	0.977762	1.078	1.180	0.904	0.749	0.970	1.114	1.001910	1.234834	
1.008642	0.944729	0.897061	0.965555	1.120	1.286	0.855	0.696	0.952	1.182	1.002893	1.254855	
1.011753	0.928928	0.871403	0.953711	1.164	1.403	0.804	0.651	0.931	1.258	1.003868	1.260018	
1.014871	0.915020	0.850636	0.942834	1.209	1.532	0.753	0.611	0.907	1.344	1.004800	1.254994	1
1.017841	0.903553	0.835311	0.933566	1.254	1.670	0.701	0.573	0.878	1.443	1.005632	1.242058	
1.020368	0.895310	0.826341	0.926657	1.297	1.814	0.648	0.537	0.844	1.556	1.006269	1.222239	
1.021902	0.891446	0.825104	0.923319	1.336	1.953	0.594	0.501	0.803	1.689	1.006550	1.196624	
1.021383	0.893732	0.833685	0.925261	1.364	2.064	0.539	0.465	0.750	1.845	1.006205	1.165663	
1.016681	0.905028	0.855472	0.935198	1.370	2.101	0.483	0.429	0.681	2.030	1.004752	1.129568	
1.002141	0.992717	0.985873	0.995125	1.013	1.030	0.974	0.894	0.986	1.027	1.000710	1.103640	
1.004219	0.985942	0.973146	0.990219	1.025	1.060	0.948	0.852	0.971	1.055	1.001381	1.128874	
1.006200	0.979738	0.961751	0.985568	1.036	1.089	0.921	0.821	0.955	1.085	1.002004	1.140349	
1.008036	0.974176	0.952061	0.981337	1.048	1.118	0.895	0.794	0.937	1.116	1.002562	1.144515	
1.009671	0.969344	0.944022	0.977638	1.058	1.145	0.868	0.770	0.918	1.150	1.003040	1.143725	1/3
1.011026	0.965340	0.937780	0.974568	1.067	1.170	0.841	0.748	0.898	1.185	1.003416	1.139103	
1.012001	0.962286	0.933473	0.972277	1.075	1.192	0.813	0.727	0.876	1.222	1.003663	1.131538	
1.012464	0.960326	0.931322	0.970942	1.081	1.209	0.785	0.707	0.852	1.261	1.003750	1.121659	
1.012239	0.959633	0.931619	0.970669	1.084	1.221	0.757	0.688	0.825	1.303	1.003637	1.109450	
1.011091	0.960422	0.934547	0.971740	1.085	1.224	0.728	0.670	0.796	1.347	1.003273	1.095525	
1.001485	0.995975	0.992412	0.996997	1.007	1.016	0.982	0.924	0.988	1.018	1.000481	1.072315	
1.002887	0.992244	0.985426	0.994069	1.013	1.031	0.964	0.894	0.976	1.037	1.000925	1.089656	
1.004185	0.988830	0.979222	0.991349	1.019	1.046	0.945	0.871	0.963	1.056	1.001328	1.097758	
1.005355	0.985761	0.973886	0.988892	1.024	1.060	0.927	0.852	0.949	1.076	1.001681	1.100911	
1.006367	0.983070	0.969400	0.986728	1.029	1.072	0.908	0.834	0.935	1.096	1.001978	1.100687	1/5
1.007186	0.980790	0.965747	0.984894	1.033	1.083	0.889	0.819	0.919	1.118	1.002209	1.097947	
1.007770	0.978961	0.963110	0.983465	1.037	1.093	0.870	0.804	0.903	1.140	1.002364	1.093441	
1.008069	0.977628	0.961566	0.982459	1.040	1.100	0.851	0.790	0.886	1.162	1.002432	1.087291	
1.008023	0.976841	0.960993	0.981946	1.041	1.105	0.832	0.777	0.868	1.186	1.002400	1.079872	
1.007558	0.976656	0.961751	0.981977	1.042	1.107	0.813	0.764	0.849	1.210	1.002251	1.071308	
1.001071	0.997322	0.995119	0.997871	1.004	1.010	0.986	0.941	0.990	1.014	1.000341	1.055948	
1.002069	0.994834	0.990509	0.995830	1.008	1.020	0.972	0.917	0.980	1.027	1.000653	1.069438	
1.002980	0.992547	0.986467	0.993927	1.012	1.029	0.958	0.899	0.969	1.042	1.000933	1.075684	
1.003790	0.990476	0.982982	0.992203	1.015	1.038	0.943	0.883	0.958	1.056	1.001176	1.078236	
1.004483	0.988635	0.979937	0.990660	1.018	1.045	0.929	0.870	0.946	1.071	1.001380	1.078165	1/7
1.005041	0.987041	0.977538	0.989347	1.021	1.052	0.915	0.857	0.934	1.087	1.001539	1.076447	
1.005441	0.985711	0.975667	0.988255	1.023	1.058	0.900	0.846	0.921	1.102	1.001649	1.073202	
1.005660	0.984664	0.974317	0.987415	1.025	1.062	0.885	0.835	0.908	1.119	1.001703	1.068800	
1.005669	0.983922	0.973683	0.986843	1.026	1.066	0.871	0.825	0.894	1.135	1.001696	1.063366	
1.005435	0.983508	0.973751	0.986577	1.027	1.067	0.856	0.815	0.880	1.152	1.001621	1.057147	
1.000806	0.998009	0.996440	0.998358	1.003	1.007	0.989	0.951	0.991	1.011	1.000253	1.046074	
1.001549	0.996150	0.993216	0.996787	1.006	1.014	0.977	0.931	0.982	1.022	1.000483	1.057186	
1.002223	0.994430	0.990292	0.995319	1.009	1.021	0.965	0.916	0.973	1.033	1.000689	1.062400	
1.002818	0.992858	0.987665	0.993982	1.011	1.027	0.954	0.903	0.964	1.045	1.000867	1.064658	
1.003324	0.991441	0.985439	0.992762	1.013	1.032	0.942	0.892	0.954	1.057	1.001016	1.064660	1/9
1.003731	0.990189	0.983503	0.991689	1.015	1.037	0.930	0.881	0.944	1.069	1.001132	1.063253	
1.004024	0.989110	0.982063	0.990780	1.017	1.041	0.918	0.872	0.934	1.081	1.001214	1.060802	
1.004192	0.988215	0.981009	0.990037	1.018	1.045	0.906	0.863	0.923	1.094	1.001258	1.057429	
1.004218	0.987516	0.980334	0.989470	1.019	1.047	0.895	0.854	0.912	1.107	1.001260	1.053256	
1.004085	0.987023	0.980033	0.989092	1.020	1.049	0.882	0.846	0.900	1.120	1.001217	1.048408	

$M_0 = 1.0$

Mass Weighted	Area Weighted	Mass Derived	Mtm. Mixed	Mtm. Flux Coeff	Energy Flux Coeff	Mach Number Mass Derived	Mach Number Mtm. Mixed	Mach Number Entropy Flux	Velocity Ratio Max/ Mean	Static p Ratio Entropy/ Wall	Static p Ratio Mixed/ Wall	n
1.017654	0.966208	0.905738	0.703107*	1.050	1.109	1.910	0.577*	1.968	1.063	1.008913	4.217080*	
1.037587	0.933426	0.821867	0.686698*	1.105	1.234	1.817	0.576*	1.932	1.133	1.018372	3.934246*	
1.060167	0.901930	0.748144	0.672067*	1.163	1.378	1.720	0.575*	1.892	1.212	1.028318	3.651828*	
1.085770	0.872101	0.684559	0.659739*	1.226	1.543	1.619	0.575*	1.844	1.302	1.038610	3.368920*	
1.114682	0.844489	0.631521	0.650626*	1.292	1.730	1.514	0.574*	1.789	1.403	1.048951	3.086515*	1
1.146837	0.819910	0.589914	0.645995*	1.359	1.936	1.403	0.572*	1.724	1.519	1.058773	2.803736*	
1.181079	0.799624	0.561376	0.648020*	1.424	2.153	1.288	0.571*	1.645	1.650	1.066994	2.521032*	
1.213058	0.785681	0.549486	0.660408*	1.479	2.357	1.166	0.569*	1.548	1.798	1.071563	2.238125*	
1.228659	0.781616	0.561519	0.690216*	1.510	2.494	1.037	0.567*	1.425	1.959	1.068533	1.955366*	
1.180663	0.794006	0.614363	0.752268	1.486	2.442	0.902	0.564	1.260	2.121	1.050109	1.672560	
1.016259	0.988895	0.959183	0.720552*	1.022	1.048	1.944	0.582*	1.966	1.034	1.007364	4.284519*	
1.033211	0.978467	0.921963	0.721485*	1.044	1.098	1.887	0.587*	1.930	1.069	1.014537	4.068770*	
1.050706	0.968802	0.888797	0.723879*	1.066	1.148	1.828	0.592*	1.891	1.106	1.021384	3.852272*	
1.068477	0.959998	0.859805	0.728053*	1.086	1.197	1.768	0.599*	1.849	1.145	1.027732	3.635478*	
1.086060	0.952165	0.835265	0.734368*	1.105	1.244	1.706	0.606*	1.803	1.184	1.033350	3.418096*	1/3
1.102672	0.945425	0.815849	0.743298*	1.122	1.287	1.643	0.614*	1.753	1.226	1.037936	3.200010*	
1.117009	0.939907	0.802037	0.755440*	1.135	1.323	1.578	0.624*	1.699	1.267	1.041093	2.980620*	
1.126892	0.935733	0.796769	0.771620*	1.144	1.349	1.511	0.636*	1.639	1.310	1.042296	2.759688*	
1.128637	0.932999	0.795493	0.792980*	1.147	1.359	1.443	0.650*	1.573	1.351	1.040854	2.537054*	
1.115913	0.931716	0.806058	0.821027*	1.141	1.348	1.372	0.667*	1.498	1.391	1.035851	2.311456*	
1.012524	0.994608	0.975955	0.724660*	1.013	1.029	1.958	0.582*	1.970	1.023	1.005305	4.328629*	
1.025101	0.989615	0.953844	0.729402*	1.026	1.058	1.916	0.587*	1.939	1.046	1.010321	4.156982*	
1.037557	0.985044	0.934119	0.735248*	1.038	1.085	1.872	0.592*	1.907	1.070	1.014965	3.985297*	
1.049844	0.980921	0.916890	0.742299*	1.049	1.111	1.828	0.598*	1.872	1.094	1.019138	3.812527*	
1.061011	0.977267	0.902279	0.750788*	1.059	1.134	1.783	0.605*	1.836	1.119	1.022720	3.639427*	1/5
1.071161	0.974097	0.890564	0.760919*	1.068	1.155	1.738	0.612*	1.797	1.144	1.025568	3.465544*	
1.079391	0.971417	0.881914	0.772973*	1.075	1.171	1.691	0.621*	1.756	1.168	1.027509	3.290925*	
1.084700	0.969216	0.876924	0.787255*	1.079	1.182	1.643	0.630*	1.712	1.192	1.028338	3.114998*	
1.085655	0.967455	0.875867	0.804209*	1.080	1.187	1.595	0.641*	1.665	1.216	1.027805	2.938061*	
1.080187	0.966053	0.879393	0.824281*	1.079	1.184	1.545	0.654*	1.615	1.239	1.025615	2.758940*	
1.009754	0.996815	0.983669	0.725885*	1.009	1.020	1.966	0.582*	1.974	1.017	1.003938	4.357598*	
1.019332	0.993876	0.968615	0.731653*	1.018	1.039	1.932	0.586*	1.948	1.035	1.007606	4.215426*	
1.028592	0.991188	0.955318	0.738221*	1.026	1.057	1.897	0.591*	1.920	1.052	1.010953	4.072704*	
1.037351	0.988756	0.943485	0.745695*	1.033	1.074	1.862	0.596*	1.891	1.070	1.013919	3.929611*	
1.045368	0.986580	0.933410	0.754169*	1.040	1.089	1.827	0.602*	1.861	1.087	1.016435	3.785895*	
1.052327	0.984655	0.925247	0.763785*	1.045	1.101	1.790	0.608*	1.829	1.105	1.018423	3.641769*	1/7
1.057818	0.982968	0.919027	0.774682*	1.050	1.111	1.754	0.614*	1.796	1.122	1.019792	3.497059*	
1.061300	0.981496	0.915202	0.787028*	1.052	1.118	1.716	0.622*	1.761	1.139	1.020439	3.351650*	
1.062060	0.980202	0.913703	0.801003*	1.054	1.122	1.678	0.630*	1.725	1.156	1.020246	3.205131*	
1.059153	0.979027	0.915026	0.816879*	1.053	1.121	1.640	0.639*	1.686	1.172	1.019076	3.057889*	
1.007780	0.997859	0.987999	0.726208*	1.007	1.015	1.972	0.581*	1.977	1.014	1.003028	4.378338*	
1.015306	0.995878	0.976803	0.732099*	1.013	1.029	1.943	0.585*	1.954	1.028	1.005823	4.256143*	
1.022468	0.994036	0.966908	0.738658*	1.019	1.042	1.914	0.589*	1.930	1.041	1.008352	4.134448*	
1.029131	0.992391	0.958167	0.745879*	1.025	1.054	1.884	0.594*	1.905	1.055	1.010576	4.011984*	
1.035128	0.990877	0.950591	0.753838*	1.029	1.064	1.855	0.599*	1.879	1.069	1.012453	3.888890*	
1.040248	0.989506	0.944480	0.762646*	1.033	1.073	1.825	0.604*	1.853	1.083	1.013934	3.765724*	1/9
1.044230	0.988264	0.939710	0.772377*	1.036	1.081	1.794	0.609*	1.825	1.096	1.014966	3.642194*	
1.046749	0.987132	0.936454	0.783119*	1.039	1.086	1.763	0.615*	1.796	1.109	1.015489	3.518056*	
1.047395	0.986080	0.934889	0.795001*	1.040	1.088	1.732	0.622*	1.766	1.122	1.015437	3.393493*	
1.046651	0.985071	0.935088	0.808124*	1.040	1.088	1.700	0.629*	1.735	1.135	1.014736	3.267963*	

$M_0 = 2.0$

TABLE 4.1.VIII

	Max. Weighted	Area Weighted	Mass Derived	Mtm. Mixed	Mtm. Flux Coeff	Energy Flux Coeff	Mach Number Mass Derived	Mach Number Mtm. Mixed	Mach Number Entropy Flux	Velocity Ratio Max/ Mean	Static p Ratio Entropy/ Wall	Static p Ratio Mixed/ Wall	n
	1.033314	0.964572	0.863494	0.321270*	1.070	1.149	2.866	0.477*	2.947	1.079	1.024555	9.554028*	
	1.072909	0.930476	0.743979	0.315246*	1.149	1.330	2.726	0.479*	2.887	1.170	1.051635	8.774866*	
	1.120620	0.898096	0.640565	0.310656*	1.237	1.550	2.579	0.481*	2.818	1.274	1.081395	7.996482*	
	1.178987	0.867972	0.552388	0.308041*	1.336	1.818	2.425	0.484*	2.738	1.396	1.113810	7.216672*	
	1.251536	0.840877	0.478871	0.308354*	1.444	2.141	2.261	0.488*	2.645	1.536	1.148463	6.437661*	1
	1.343033	0.817926	0.420071	0.313132*	1.561	2.523	2.087	0.493*	2.534	1.699	1.183933	5.657397*	
	1.459078	0.800710	0.377148	0.325296*	1.678	2.950	1.900	0.499*	2.399	1.882	1.216910	4.877112*	
	1.601668	0.791227	0.353655	0.350762*	1.779	3.357	1.698	0.508*	2.231	2.080	1.239530	4.095609*	
	1.740708	0.790080	0.360183	0.403594*	1.819	3.566	1.478	0.521*	2.014	2.262	1.233895	3.312287*	
	1.610868	0.780875	0.432256	0.525329	1.702	3.167	1.235	0.543	1.717	2.343	1.159570	2.525691	
	1.035650	0.991634	0.930505	0.332107*	1.040	1.084	2.907	0.479*	2.940	1.049	1.022232	9.738459*	
	1.075324	0.964584	0.867634	0.337340*	1.081	1.175	2.811	0.483*	2.875	1.101	1.044742	9.143965*	
	1.119455	0.979020	0.811627	0.344410*	1.123	1.270	2.711	0.487*	2.805	1.156	1.067144	8.548763*	
	1.168353	0.975107	0.762626	0.353848*	1.163	1.369	2.609	0.492*	2.729	1.213	1.088862	7.953056*	
	1.221983	0.972974	0.720962	0.366386*	1.202	1.467	2.503	0.498*	2.647	1.271	1.109042	7.356524*	1/3
	1.279466	0.972626	0.687527	0.383080*	1.237	1.559	2.392	0.506*	2.556	1.330	1.126437	6.758610*	
	1.337962	0.973765	0.663235	0.405520*	1.265	1.636	2.277	0.514*	2.456	1.387	1.139236	6.159431*	
	1.390092	0.975360	0.650312	0.436149*	1.282	1.686	2.157	0.525*	2.346	1.438	1.144827	5.558064*	
	1.417665	0.974627	0.652128	0.478929*	1.282	1.690	2.031	0.539*	2.221	1.479	1.139475	4.953391*	
	1.375362	0.964421	0.674862	0.540689*	1.256	1.626	1.899	0.557*	2.080	1.501	1.117913	4.344530*	
$M_o = 3.0$	1.030278	0.998197	0.955096	0.334739*	1.027	1.057	2.926	0.479*	2.945	1.035	1.017028	9.869003*	
	1.062662	0.997248	0.914293	0.342446*	1.054	1.114	2.851	0.482*	2.888	1.070	1.033661	9.364946*	
	1.097069	0.997178	0.877742	0.351734*	1.080	1.172	2.773	0.486*	2.827	1.107	1.049587	8.880632*	
	1.133209	0.997971	0.845659	0.362944*	1.104	1.228	2.694	0.491*	2.762	1.143	1.064399	8.394918*	
	1.170427	0.999565	0.818319	0.376568*	1.127	1.280	2.612	0.496*	2.694	1.179	1.077568	7.909407*	
	1.207421	1.001687	0.796329	0.393204*	1.146	1.326	2.528	0.502*	2.620	1.214	1.088414	7.422515*	1/5
	1.241740	1.003959	0.780301	0.413707*	1.160	1.362	2.442	0.508*	2.542	1.246	1.096058	6.934618*	
	1.268860	1.005515	0.771422	0.439253*	1.168	1.383	2.353	0.516*	2.458	1.275	1.099381	6.445613*	
	1.280427	1.004757	0.770981	0.471515*	1.168	1.385	2.260	0.525*	2.367	1.298	1.096959	5.955150*	
	1.260810	0.998692	0.781436	0.512908*	1.157	1.360	2.165	0.537*	2.269	1.313	1.087000	5.461719*	
	1.025350	1.000428	0.967766	0.335459*	1.020	1.042	2.938	0.478*	2.951	1.027	1.013240	9.922146*	
	1.051741	1.001383	0.938480	0.343696*	1.039	1.083	2.875	0.481*	2.900	1.053	1.025914	9.512383*	
	1.078945	1.002836	0.912104	0.353205*	1.058	1.122	2.811	0.485*	2.847	1.080	1.037799	9.100485*	
	1.106561	1.004719	0.888806	0.364275*	1.075	1.160	2.745	0.489*	2.791	1.106	1.048622	8.689625*	
	1.133921	1.006906	0.869182	0.377180*	1.090	1.194	2.678	0.493*	2.733	1.132	1.058049	8.277534*	1/7
	1.159938	1.009180	0.853215	0.392318*	1.102	1.223	2.610	0.498*	2.671	1.156	1.065674	7.864786*	
	1.184867	1.011181	0.841361	0.410203*	1.112	1.245	2.540	0.503*	2.607	1.179	1.071008	7.451947*	
	1.199912	1.012325	0.834439	0.431460*	1.117	1.258	2.468	0.509*	2.538	1.199	1.073459	7.037435*	
	1.206571	1.011661	0.833160	0.456992*	1.118	1.260	2.394	0.516*	2.466	1.215	1.072317	6.622848*	
	1.195523	1.007649	0.838601	0.487935*	1.112	1.248	2.318	0.524*	2.389	1.227	1.066737	6.206426*	
	1.021407	1.001257	0.975351	0.335544*	1.016	1.032	2.947	0.478*	2.956	1.021	1.010563	9.974936*	
	1.043258	1.002833	0.952850	0.343682*	1.030	1.063	2.892	0.481*	2.911	1.043	1.020544	9.617453*	
	1.065300	1.004681	0.932627	0.352892*	1.044	1.093	2.837	0.484*	2.864	1.064	1.029783	9.260015*	
	1.087148	1.006722	0.914859	0.363325*	1.057	1.120	2.781	0.487*	2.815	1.084	1.038089	8.901039*	
	1.108230	1.008835	0.899612	0.375222*	1.068	1.145	2.724	0.491*	2.764	1.104	1.045242	8.542637*	1/9
	1.127700	1.010834	0.887256	0.388823*	1.077	1.166	2.665	0.495*	2.711	1.122	1.050981	8.183353*	
	1.144313	1.012445	0.878069	0.404455*	1.084	1.181	2.606	0.499*	2.655	1.139	1.055001	7.823589*	
	1.156235	1.013258	0.872256	0.422530*	1.088	1.191	2.545	0.504*	2.597	1.155	1.056949	7.463738*	
	1.160745	1.012666	0.870631	0.443539*	1.089	1.193	2.483	0.509*	2.537	1.167	1.056415	7.102749*	
	1.153788	1.009765	0.873463	0.468136*	1.086	1.186	2.420	0.515*	2.473	1.177	1.052924	6.740527*	

													n
	1.042245	0.963590	0.832484	0.135607*	1.092	1.195	3.819	0.437*	3.923	1.098	1.042973	16.993690*	
	1.094062	0.929069	0.688466	0.133011*	1.199	1.446	3.629	0.438*	3.835	1.215	1.092127	15.488941*	
	1.158976	0.897078	0.565994	0.131177*	1.324	1.770	3.429	0.441*	3.735	1.354	1.148492	13.982571*	
	1.242386	0.868576	0.463461	0.130464*	1.471	2.195	3.217	0.443*	3.619	1.520	1.213057	12.476664*	
	1.352911	0.845048	0.379250	0.131469*	1.643	2.752	2.992	0.447*	3.482	1.721	1.286359	10.970171*	1
	1.504899	0.828877	0.312348	0.135296*	1.840	3.474	2.750	0.451*	3.319	1.962	1.367404	9.462797*	
	1.723027	0.823994	0.262568	0.144214*	2.053	4.366	2.486	0.458*	3.119	2.244	1.450792	7.954949*	
	2.048014	0.836632	0.232213	0.163596*	2.249	5.303	2.196	0.467*	2.869	2.549	1.519032	6.445982*	
	2.506873	0.871586	0.231478	0.209337*	2.324	5.754	1.870	0.483*	2.539	2.790	1.521899	4.932734*	
	2.356515	0.848838	0.312375	0.350190	2.006	4.362	1.495	0.514	2.075	2.680	1.326781	3.411458	
	1.050816	0.993922	0.903237	0.141017*	1.062	1.131	3.864	0.437*	3.908	1.069	1.041988	17.302673*	
	1.110146	0.990354	0.816517	0.144226*	1.129	1.279	3.722	0.440*	3.810	1.145	1.086280	16.104900*	
	1.179981	0.989821	0.739877	0.148693*	1.199	1.446	3.576	0.444*	3.702	1.226	1.132376	14.906525*	
	1.262785	0.992960	0.673223	0.154875*	1.271	1.630	3.423	0.448*	3.586	1.313	1.179312	13.707855*	
	1.361431	1.000492	0.616746	0.163471*	1.344	1.826	3.264	0.453*	3.458	1.405	1.225371	12.509647*	1/3
	1.478704	1.013104	0.571030	0.175574*	1.412	2.022	3.097	0.458*	3.317	1.497	1.267628	11.308714*	
	1.615365	1.031012	0.537531	0.193046*	1.469	2.195	2.922	0.466*	3.161	1.584	1.301234	10.106014*	
	1.763353	1.052532	0.519044	0.219226*	1.503	2.307	2.736	0.475*	2.985	1.656	1.318343	8.901203*	
	1.881414	1.069270	0.521704	0.260636*	1.497	2.296	2.538	0.487*	2.786	1.696	1.306586	7.693506*	
	1.798805	1.048322	0.558988	0.331476*	1.425	2.085	2.325	0.505*	2.556	1.675	1.247350	6.479356*	
$M_o = 4.0$	1.046637	1.001936	0.932815	0.142579*	1.046	1.095	3.887	0.437*	3.914	1.052	1.033853	17.492897*	
	1.099137	1.005835	0.871838	0.147349*	1.093	1.197	3.771	0.440*	3.823	1.106	1.068156	16.485664*	
	1.158292	1.011936	0.817563	0.153325*	1.140	1.304	3.652	0.443*	3.727	1.162	1.102294	15.477598*	
	1.224814	1.020451	0.769942	0.160875*	1.186	1.413	3.529	0.447*	3.624	1.219	1.135363	14.469791*	
	1.299055	1.031492	0.729486	0.170518*	1.229	1.521	3.401	0.451*	3.514	1.276	1.166058	13.462040*	1/5
	1.380364	1.044908	0.696782	0.183005*	1.267	1.619	3.269	0.456*	3.396	1.330	1.192515	12.452103*	
	1.465577	1.059916	0.673044	0.199492*	1.297	1.698	3.131	0.461*	3.269	1.378	1.212114	11.441053*	
	1.545419	1.074252	0.660062	0.221808*	1.313	1.743	2.988	0.468*	3.132	1.416	1.221220	10.429316*	
	1.595522	1.082150	0.661092	0.252963*	1.309	1.736	2.838	0.476*	2.982	1.437	1.214894	9.415260*	
	1.552548	1.069200	0.681908	0.298267*	1.277	1.654	2.680	0.487*	2.818	1.433	1.186610	8.398270*	
	1.041384	1.004716	0.949314	0.143128*	1.036	1.073	3.903	0.437*	3.921	1.041	1.027377	17.624466*	
	1.086716	1.010859	0.903127	0.148362*	1.071	1.149	3.803	0.440*	3.839	1.083	1.054441	16.749393*	
	1.136201	1.018498	0.861774	0.154664*	1.105	1.225	3.701	0.442*	3.753	1.125	1.080676	15.873711*	
	1.189816	1.027639	0.825501	0.162313*	1.138	1.300	3.597	0.445*	3.662	1.166	1.105389	14.998121*	
	1.247073	1.038152	0.794643	0.171678*	1.168	1.371	3.489	0.449*	3.566	1.206	1.127669	14.120632*	1/7
	1.306540	1.049652	0.769673	0.183293*	1.194	1.433	3.378	0.453*	3.465	1.244	1.146314	13.243696*	
	1.364924	1.061256	0.751600	0.197895*	1.213	1.481	3.263	0.457*	3.357	1.276	1.159768	12.365870*	
	1.415203	1.071119	0.741444	0.216575*	1.224	1.508	3.144	0.462*	3.243	1.302	1.166027	11.487455*	
	1.442756	1.075500	0.741205	0.240966*	1.222	1.505	3.021	0.469*	3.121	1.317	1.162558	10.607002*	
	1.416932	1.066796	0.753938	0.273647*	1.204	1.463	2.894	0.476*	2.990	1.318	1.146214	9.724970*	
	1.036608	1.005680	0.959741	0.143294*	1.029	1.059	3.914	0.437*	3.928	1.033	1.022547	17.722401*	
	1.075867	1.012377	0.923081	0.148596*	1.057	1.118	3.827	0.439*	3.853	1.067	1.044464	16.944542*	
	1.117698	1.020074	0.890172	0.154828*	1.083	1.176	3.737	0.442*	3.775	1.100	1.065343	16.166805*	
	1.161783	1.028682	0.861322	0.162205*	1.109	1.232	3.645	0.444*	3.694	1.133	1.084663	15.389608*	
	1.207380	1.037990	0.836671	0.171002*	1.131	1.283	3.551	0.447*	3.609	1.163	1.101774	14.611975*	1/9
	1.253000	1.047575	0.816801	0.181588*	1.150	1.327	3.455	0.451*	3.520	1.191	1.115862	13.833202*	
	1.295839	1.056651	0.802204	0.194466*	1.164	1.361	3.356	0.454*	3.426	1.216	1.125922	13.052874*	
	1.330753	1.063804	0.793804	0.210349*	1.172	1.380	3.254	0.459*	3.328	1.235	1.130718	12.273224*	
	1.348343	1.066507	0.792840	0.230226*	1.171	1.379	3.149	0.463*	3.224	1.247	1.128752	11.492859*	
	1.331295	1.060223	0.801040	0.255543*	1.160	1.354	3.041	0.469*	3.114	1.250	1.118235	10.710943*	

4.1.5 The calculations in the tables have been done assuming that the flow is fully-measured. In practice, many experiments are done in which the boundary layers are not traversed; the stagnation pressure is measured by a rake covering the free stream only. The total mass flow may be measured independently by a calibrated airmeter, however, and this extra information can be used to estimate a corrected mean stagnation pressure as follows:

Assume the flow in the duct is one of the family of ideal flows tabulated. Then the third column gives

$$\frac{P_{t1}}{\bar{P}_t} = \frac{\text{mass-derived stagnation pressure}}{\text{entropy-derived stagnation pressure}}$$

The seventh column gives M_1 = mass-derived Mach number from which (P_{t1}/P_s) follows. The free-stream Mach number M_0 gives

$$\frac{P_{tmax}}{P_s} = \frac{\text{mainstream stagnation pressure}}{\text{uniform static pressure}}$$

Hence the ratio

$$\left(\frac{\bar{P}_t}{P_{tmax}}\right) \text{ can be found as a function of } \left(\frac{P_{t1}}{P_{tmax}}\right).$$

Over the range of Mach numbers up to 0.8, and assuming boundary layers δ up to half the duct radius or width, and of profile exponent n between $\frac{1}{3}$ and $\frac{1}{9}$, both these ratios are quite near unity and to within about 1%

$$\frac{\bar{P}_t}{P_{tmax}} \simeq 1 - \frac{1}{K}\left(1 - \frac{P_{t1}}{P_{tmax}}\right)$$

where the constant K is 1.4.

This relationship can also be derived analytically if approximations are made. For the two-dimensional case

$$K = 1 + 3n$$

and for the axisymmetric case

$$K = 1 + 3n + \frac{3n\delta}{8R_0}(1 + 2n)$$

both results being independent of γ and M_0.

So it is possible to estimate a corrected mean stagnation pressure $\bar{P}_t$ from the free stream stagnation pressure P_{tmax} and the mass-derived stagnation pressure P_{t1}.

4.1.6 For purposes of comparison the method of Pianko (3.2) has been applied to a selection of the power law profiles. Note that necessarily there is an average quantity for each different system, e.g. compressor or turbine, combustion chamber, re-heat duct or jet nozzle and therefore space would not permit the presentation of every example given in the previous tables. The tables which follow give the results and include in the first column as before the ratio of the Pianko (3.2) mean to the Livesey (Entropy Flux Mean) mean total pressure. It is evident from (3.2) that the re-heat duct will, with the method of (3.2), give the same results as the Mixed Mean and this is confirmed closely by comparison of the two sets of tables. Note that the confirmation is not absolutely precise because the computation of the Pianko method was by direct substitution into the analytical integral forms whereas the previous tables were achieved by numerical integration. Furthermore the calculations were performed independently with different rounding errors.

TABLE 4.1.IX

Method of Pianko (3.2) Applied to Power Law Profiles

	$\frac{\bar{P}_{tPianko}}{\bar{P}_t}$ Entropy	$\frac{\bar{P}_{tPianko}}{\bar{P}_s}$	$\frac{\bar{A}_{Pianko}}{\bar{A}}$	$\bar{M}$ Pianko	$\frac{\hat{V}}{\bar{V}}$ Pianko	$\frac{\bar{P}_{sPianko}}{\bar{P}_s}$	
Comp'r. or Turb'n.	0.99995	1.0083	1.0	0.0661	3.0120	1.0053	
Comb'n. Chamber	0.99995	1.0083	0.6081	0.1093	1.8245	1.0	$n = 1$
Re-heat Duct	0.99787	1.0062	1.0	0.0663	3.0048	1.0031	
Jet Nozzle	0.99995	1.0083	1.0	0.0661	3.0139	1.0052	
Comp'r. or Turb'n.	0.99991	1.0145	1.0	0.1279	1.5591	1.0029	
Comb'n. Chamber	0.99991	1.0145	0.8924	0.1437	1.3883	1.0	$n = \frac{1}{3}$
Re-heat Duct	0.99990	1.0136	1.0	0.0281	1.5576	1.0020	
Jet Nozzle	0.99991	1.0145	1.0	0.1280	1.5584	1.0029	
Comp'r. or Turb'n.	0.99985	1.0212	1.0	0.1702	1.1736	1.0007	
Comb'n. Chamber	0.99985	1.0212	0.9818	0.1735	1.1505	1.0	$n = \frac{1}{9}$
Re-heat Duct	0.99965	1.0210	1.0	0.1702	1.1733	1.0005	
Jet Nozzle	0.99985	1.0212	1.0	0.1703	1.1730	1.0007	

AXISYMMETRICAL

$M_o = 0.2$ $\qquad\qquad$ $\delta/R_o = 1.0$

TABLE 4.1.X

Method of Pianko (3.2) Applied to Power Law Profiles

	$\frac{\bar{P}_{tPianko}}{\bar{P}_{t\ Entropy}}$	$\frac{\bar{P}_{tPianko}}{\bar{P}_s}$	$\frac{\bar{A}_{Pianko}}{\bar{A}}$	$\bar{M}_{Pianko}$	$\frac{\hat{V}}{\bar{V}}_{Pianko}$	$\frac{\bar{P}_{sPianko}}{\bar{P}_s}$	
Comp'r. or Turb'n.	0.99493	1.0140	1.0	0.0991	2.0105	1.0070	
Comb'n. Chamber	0.99493	1.0140	0.7066	0.1412	1.4134	1.0	$n = 1$
Re-heat Duct	0.99258	1.0116	1.0	0.0994	2.0056	1.0047	
Jet Nozzle	0.99493	1.0140	1.0	0.0992	2.0101	1.0070	
Comp'r. or Turb'n.	0.99498	1.0187	1.0	0.1494	1.3363	1.0029	
Comb'n. Chamber	0.99498	1.0187	0.9182	0.1631	1.2244	1.0	$n = \frac{1}{3}$
Re-heat Duct	0.99422	1.0179	1.0	0.1495	1.3351	1.0021	
Jet Nozzle	0.99498	1.0187	1.0	0.1495	1.3355	1.0029	
Comp'r. or Turb'n.	0.99523	1.0235	1.0	0.1797	1.1117	1.0006	
Comb'n. Chamber	0.99523	1.0235	0.9858	0.1824	1.0954	1.0	$n = \frac{1}{9}$
Re-heat Duct	0.99504	1.0233	1.0	0.1798	1.1115	1.0004	
Jet Nozzle	0.99523	1.0235	1.0	0.1798	1.1111	1.0006	

TWO-DIMENSIONAL

$M_o = 0.2$ $\qquad\qquad$ $\delta/R_o = 1.0$

TABLE 4.1.XI

Method of Pianko (3.2) Applied to Power Law Profiles

	$\frac{\bar{P}_{tPianko}}{\bar{P}_t}$ Entropy	$\frac{\bar{P}_{tPianko}}{\bar{P}_s}$	$\frac{\bar{A}_{Pianko}}{\bar{A}}$	$\bar{M}$ Pianko	$\frac{\hat{V}}{\bar{V}}$ Pianko	$\frac{\bar{P}_{sPianko}}{\bar{P}_s}$	
Comp'r. or Turb'n.	0.99737	1.2037	1.0	0.2791	3.296	1.1402	
Comb'n. Chamber	0.99737	1.2037	0.5991	0.5215	1.796	1.0	$n = 1$
Re-heat Duct	0.94821	1.14438	1.0	0.2953	3.119	1.0772	
Jet Nozzle	0.99124	1.1963	1.0	0.2807	3.278	1.1326	
Comp'r. or Turb'n.	0.99733	1.3800	1.0	0.5593	1.682	1.1159	
Comb'n. Chamber	0.99733	1.3800	0.8851	0.6942	1.377	1.0	$n = \frac{1}{3}$
Re-heat Duct	0.97609	1.3506	1.0	0.5786	1.630	1.0765	
Jet Nozzle	0.99264	1.3735	1.0	0.5636	1.670	1.1071	
Comp'r. or Turb'n.	0.99796	1.6043	1.0	0.7907	1.225	1.0621	
Comb'n. Chamber	0.99796	1.6043	0.9793	0.8502	1.149	1.0	$n = \frac{1}{9}$
Re-heat Duct	0.99242	1.5954	1.0	0.8046	1.206	1.0418	
Jet Nozzle	0.99609	1.6013	1.0	0.7962	1.217	1.0544	

AXISYMMETRIC

$M_o = 1.0$ $\qquad\qquad$ $\delta/R_o = 1.0$

TABLE 4.1.XII

Method of Pianko (3.2) Applied to Power Law Profiles

	$\frac{\overline{P}_{tPianko}}{\overline{P}_t}$ Entropy	$\frac{\overline{P}_{tPianko}}{\overline{P}_s}$	$\frac{\overline{A}_{Pianko}}{\overline{A}}$	$\overline{M}$ Pianko	$\frac{\hat{V}}{\overline{V}}$ Pianko	$\frac{\overline{P}_{sPianko}}{\overline{P}_s}$	
Comp'r. or Turb'n.	0.99897	1.3691	1.0	0.4009	2.313	1.2255	
Comb'n. Chamber	0.99897	1.3691	0.6966	0.6853	1.393	1.0	$n = 1$
Re-heat Duct	0.94278	1.2921	1.0	0.4311	2.157	1.1371	
Jet Nozzle	0.99152	1.3589	1.0	0.4047	2.293	1.2139	
Comp'r. or Turb'n.	0.99804	1.5203	1.0	0.6451	1.473	1.1491	
Comb'n. Chamber	0.99804	1.5203	0.9116	0.7973	1.216	1.0	$n = \frac{1}{3}$
Re-heat Duct	0.97782	1.4895	1.0	0.6710	1.420	1.1014	
Jet Nozzle	0.99319	1.5129	1.0	0.6517	1.459	1.1372	
Comp'r. or Turb'n.	0.99914	1.6919	1.0	0.8341	1.168	1.0723	
Comb'n. Chamber	0.99914	1.6919	0.9837	0.9003	1.093	1.0	$n = \frac{1}{9}$
Re-heat Duct	0.99435	1.6838	1.0	0.8501	1.149	1.0497	
Jet Nozzle	0.99754	1.6892	1.0	0.8409	1.160	1.0632	

TWO-DIMENSIONAL

$M_o = 1.0$ $\qquad\qquad$ $\delta/R_o = 1.0$

TABLE 4.1.XIII

Method of Pianko (3.2) Applied to Power Law Profiles

	$\frac{\bar{P}_{tPianko}}{\bar{P}_{tEntropy}}$	$\frac{\bar{P}_{tPianko}}{P_s}$	$\frac{\bar{A}_{Pianko}}{A}$	$\bar{M}_{Pianko}$	$\frac{\hat{V}}{\bar{V}}_{Pianko}$	$\frac{\bar{P}_{sPianko}}{P_s}$
Comp'r.						
or	0.85933	3.1742	1.0	0.3008	6.5487	2.9810
Turb'n.	0.85933	3.1742	1.0	2.2142	1.2405	0.2903
Comb'n.	-	-	-	-	-	-
Chamber	0.85933	3.1742	0.5487	1.3981	1.6466	1.0
Re-heat	0.56828	2.0991	1.0	0.4986	4.0112	1.7712
Duct	1.29961 *	4.8005	1.0	2.6617	1.1401	0.2186
Jet	0.26809	2.8372	1.0	0.3385	5.8309	2.6208
Nozzle	0.76809	2.8372	1.0	2.0953	1.2766	0.3125

*Contravenes 2nd Law

AXISYMMETRICAL

Comp'r.						
or	0.78596	9.1710	1.0	0.2055	9.5420	8.9048
Turb'n.	0.78596	9.1710	1.0	2.5969	1.1519	0.4617
Comb'n.	-	-	-	-	-	-
Chamber	0.78596	9.1710	0.6372	2.1018	1.2745	1.0
Re-heat	0.3589	4.1878	1.0	0.5114	3.9154	3.5032
Duct	0.7284	8.4988	1.0	2.5157	1.1680	0.4854
Jet	0.6896	8.047	1.0	0.2359	8.3914	7.7415
Nozzle	0.6896	8.0475	1.0	2.4580	1.1801	0.5027

TWO-DIMENSIONAL

$n = 1$ $\quad M_o = 4.0$ $\quad \delta/R_o = 1$

Note: Both subsonic and supersonic results are quoted where appropriate.

4.2 EXHAUST NOZZLE FLOW

Model tests have long been used for the performance predictions of exhaust system hardware concepts and for providing design guidance information early in the engine development cycle. Most model tests are conducted with unheated air with corrections applied to the test results to account for deviations from full-scale engine gas-path flow environment. Table 4.2.I[4.2.1] presents a list of flow-field considerations that the engine nozzle designer must evaluate and quantify before he can utilize the model results. Since nozzle coefficients are the measure of performance for an engine exhaust system, corrections made to the model results are assessed by quantifying the change in the nozzle performance coefficients. There is a problem, however. Nozzle performance coefficients are defined as the ratio of the engine mass flow and force referenced to a corresponding ideal value based on the nozzle stagnation flow properties and nozzle ambient conditions. The problem is in identifying the real changes in nozzle efficiency as a result of variations in flow-field properties and the numerical changes as a result of the method used to define the ideal flow values. The intent of this section is to illustrate numerically how well some of the various flow averaging procedures characterize the rotational, distorted flows of full-scale engine nozzle exhaust systems.

Nozzle Performance Coefficients

Tests were conducted in 1973 at the Arnold Engineering Development Center to evaluate the impact of flow non-uniformities on nozzle performance coefficients[4.2.2] . Undistorted flows and flows representative of a low-bypass mixed-flow turbofan engine (Figure 4.2.1) were duplicated in an experimental model program and the data used to compare nozzle discharge coefficients. Nozzle coefficients for the distorted flows were derived using area-weighting and mass-flow-weighting averaging procedures, and the results were compared with uniform flow coefficients from the same nozzle (Figure 4.2.2). The comparison shows that the non-uniform flow results are a function of the flow distortion profile shape as evidenced by the difference in the results for cases 1 and 2. Also, neither referencing procedure collapses the uniform and non-uniform flow results, although the mass-flow-weighting procedure provides a closer correlation than the area-weighting procedure. Similar results were obtained when comparing the uniform and non-uniform force coefficients; however, the relatively high measurement uncertainty (2 to 3 percent) of the calculated nozzle force coefficients precluded making conclusive comparisons.

Kuchar and Tabakoff[4.2.3] conducted an analytical evaluation of the effects of flow distortion on nozzle thrust coefficients. The study compared thrust coefficients for a given nozzle geometry using both non-uniform and uniform flow profiles. Two types of non-uniform temperature profiles were analyzed: one typical of a non-afterburning subsonic cruise condition and the other representative of a part afterburning condition (Figure 4.2.3). A uniform stagnation pressure was assumed for these calculations. The results of the comparison are presented in Figure 4.2.4. Kuchar and Tabakoff concluded that a mass flow averaging of nozzle total pressure profiles and thrust weighting of total temperature profiles is the correct averaging method for analyzing engine nozzle performance. This mass-thrust averaging method consists of using a known mass flow rate, the nozzle "vacuum" thrust (i.e., exit impulse), and the spatial distributions of stagnation pressure and temperature to calculate nozzle average flow properties. The nozzle exit impulse (I_e) equation in terms of average flow properties is

$$I_e = \frac{(1 + \bar{\gamma}\,\bar{M}_e^2)}{\left(1 + \frac{\bar{\gamma} - 1}{2}\,\bar{M}_e^2\right)^{\bar{\gamma}/(\bar{\gamma}-1)}} (\bar{P}_t A_e) \tag{1}$$

where for two-dimensional flow

$$\bar{\gamma} = \frac{\int \gamma_i \rho_i V_i \, dA}{\dot{m}}$$

and

$$\gamma_i = f(T_{ti})$$

and

$$\bar{P}_t = \frac{\int P_{t_i} \rho_i V_i \, dA}{\dot{m}}$$

The mass flow equation in terms of average flow properties is

$$\dot{m} = \left(\frac{\bar{\gamma}}{R}\right)^{1/2} \frac{\bar{P}_t}{(\bar{T}_t)^{1/2}} \frac{\bar{M}_e}{\left(1 + \frac{\bar{\gamma} - 1}{2}\,\bar{M}_e^2\right)} \bar{\gamma}/(\bar{\gamma} - 1) \tag{2}$$

Equations (1) and (2) are solved for $\bar{M}_e$ and $\bar{T}_t$, and ideal thrust (F_{g_i}) is calculated from

$$F_{g_i} = \dot{m} \left(\bar{T}_t \frac{2\bar{\gamma}R}{(\bar{\gamma} - 1)} \left(1 - \left(\frac{P_0}{\bar{P}_t}\right)^{\bar{\gamma}-1/\bar{\gamma}} \right) \right)^{1/2}$$

where P_0 is altitude pressure.

For the case of limited temperature distortion but significant pressure distortions (i.e., high-bypass turbofan fan nozzles), it may be preferable to mass flow weight the temperature or enthalpy and solve Equations (1) and (2) for $\overline{M}_e$ and $\overline{P}_t$. Mass-thrust averaging methods are commonly used on model programs to correct for flow non-uniformities induced by the model installation and model hardware such as struts, guide vanes, and flow splitters.

Another model flow averaging method is momentum averaging[4.2.4]. Momentum averaging consists of measuring the nozzle entrance stagnation pressure distribution and dividing the entrance area into a number of constant stagnation pressure streamtubes each of which is expanded to ambient pressure. The thrust contribution of each streamtube is summed and an effective total pressure is defined that produces an equivalent thrust. This method, which is similar to the Pianko method presented in section 3.2.2, does not require as much input information as the mass-thrust method and, for the purpose of correlating model and full-scale test results, is generally better than area and mass-flow-weighted averaging methods.

One problem with the nozzle flow averaging methods discussed thus far is that an accurate measurement of the nozzle flow-field properties is required. In actual engine installations, flow-field complexities such as blade wakes, swirl, streamline curvature, mixing, dynamics, induced wave forms from rotating machinery, probe sampling gaps, and afterburner combustion may make it difficult to obtain an accurate assessment of flow profiles. Another problem is that, depending on the flow averaging procedure, the nozzle coefficients can be a function of the aircraft flight conditions. Both of these problems have been dealt with on high-bypass turbofan engine tests and the findings are presented in the next subsection.

High-Bypass-Ratio Turbofan

Figure 4.2.5 shows a schematic of a dual-stream turbofan engine (i.e., fan engine) and the corresponding flow-through model for the same engine. Generally, the fan engine model designers will make an effort to simulate engine hardware features that affect flowthrough performance: features such as nozzle flow splitters, fan case strusts, thrust reverser blocker door links, pylon flow splitter, and turbine rearframe struts. Some of the philosophy used for designing engine models and conducting model tests is contained in Reference 4.2.5. One source of nozzle flow non-uniformities are the wakes generated from the fan guide vanes and struts (Figure 4.2.6). Strut and vane losses are usually a few percent or less of the nozzle total forces but are still important in the engine performance verification process. Oates (Reference 4.2.6) presents a simple example of the influence of wake losses and flow averaging procedures for cascade-type flows by comparing "mixed-out" and mass-flow-weighted averaged pressure-loss coefficients (Table 4.2.II).

The "mixed-out" average pressure loss corresponds to that value of the pressure loss that would exist if the fluids were allowed to mix fully in an ideal, constant-area mixer. Table II shows that at the stagnation pressure ratio of 0.8, there is a factor of two difference in the pressure-loss coefficients. Oates results demonstrate that when comparing fan flow model data, both the flow averaging procedure and axial position of the measurement traverse are important.

Kimzey[4.2.7] reported scale-model and full-scale engine fan nozzle flow and velocity coefficients for a high-bypass turbofan engine (Figure 4.2.7). The nozzle coefficients were derived using an area-weighted stagnation pressure and temperature. Figure 4.2.7 illustrates that not only are there differences in the model and full-scale fan nozzle coefficients, but that the full-scale coefficients are a function of both nozzle pressure ratio and flight conditions. Kimzey hypothesized that because the fan is closely coupled to the nozzle that the fan flow exerts a strong influence on the nozzle coefficients. Therefore, as flight conditions and accordingly ram pressure ratio vary, the fan operating point change is accompanied by a change in fan nozzle inlet profile and thus in nozzle coefficients, which are a function of flight conditions. Rather than adjusting the nozzle coefficients directly for flow distortions, Kimzey generalized the full-scale nozzle coefficients. The coefficients were generalized by expressing the coefficients as a function of both the fan nozzle operating point, which is set by the nozzle pressure ratio, and the fan operating point, which is set by a fan "equivalent" pressure ratio. The specific details of this procedure are contained in Reference 4.2.7.

Another approach to the model full-scale data correlation problem and commonly used by airframers is discussed in Reference 4.2.4. Typically, model nozzle coefficients are adjusted for full-scale Reynolds number effects, geometric differences, and leakage, with remaining discrepancies between model and full-scale results attributed to differences in measured gas-path properties or flow averages. Having made this assumption, a pressure correction factor is determined from the thrust coefficient versus nozzle pressure ratio curve (Figure 4.2.8). As a check, the thrust coefficient pressure correction factor is applied to the nozzle flow coefficient versus pressure ratio curve to determine if the model and full-scale flow coefficients collapse to an acceptable tolerance. If a temperature correction is required in addition to the pressure correction, then the thrust coefficient curve is used to generate the pressure correction, the flow coefficient curve used to generate a temperature correction, and the velocity coefficient curve used for proof of the corrections (Figure 4.2.9). Finally, calculations are made to determine if the corrected nozzle pressure and temperature are consistent with the engine cycle math model. Generally, the pressure or temperature correction is less than two percent of the calculated bulk values. This method does require, however, that the nozzle coefficient data be generalized with nozzle pressure ratio or else a correction factor as a function of both nozzle pressure ratio and flight conditions is required.

Nozzle Flow Averaging Comparison

In this final subsection, the implications of using different flow averaging methods to characterize test data for a full-scale, turbine engine exhaust nozzle are examined. Flow averaging methods discussed in Chapters 3 and 4 are used to calculate engine nozzle mean flow property values and performance coefficients, and the results from each method are compared.

The nozzle calculations are for experimental data from a low-bypass turbofan engine test in which the engine mass-flow rate, thrust, and nozzle flow profiles were measured. Figure 4.2.10 depicts the stagnation pressure and temperature profiles measured at the nozzle inlet plane and includes a sketch of the nozzle geometry. It should be mentioned that the measured nozzle mass flow rate is about one to two percent less than the mass flow rate predicted at the nozzle inlet station using measured total pressure, total temperature, wall static pressure, and an estimate for the wall boundary layer displacement thickness. The reason for this difference can be attributed to both measurement error and streamline curvature of the flow (i.e. flow static pressure is not uniform). For the purposes of the present calculations, the nozzle wall static pressure was adjusted to be consistent with the measured mass flow rate.

The results from the nozzle flow averaging calculations are presented in Table 4.2.III. The values for the flow properties and coefficients using the Dzung and Livesey method were provided by H. Kruse. The values for the Pianko method were provided by M. Pianko. The equations used to calculate the discharge and thrust coefficients are for choked nozzle flow and are given by:

$$C_d = \frac{\dot{m}}{\frac{\bar{P}_t A_{th}}{(\bar{T}_t)^{1/2}}\left[\frac{\bar{\gamma}}{R}\left(\frac{2}{\bar{\gamma}+1}\right)^{(\bar{\gamma}+1)/(\bar{\gamma}-1)}\right]^{1/2}}$$

and

$$C_f = \frac{F_g}{\dot{m}\left(\left(\frac{2\bar{\gamma}}{\bar{\gamma}-1}\right) R\bar{T}_t \left[1-\left(\frac{P_0}{P_t}\right)^{(\bar{\gamma}-1)/\bar{\gamma}}\right]\right)^{1/2}}$$

where A_{th} is the nozzle throat area. The uniform flow performance coefficients presented in Table 4.2.III were obtained from cold-flow model tests of a scaled nozzle geometrically similar to the full scale nozzle shown in Figure 4.2.10. The model nozzle tests were conducted with a uniform inlet flowfield.

A review of the bulk total pressures and temperatures in Table 4.2.III shows the numerical agreement and disagreements in the various calculated values. Kuchar and Tabakoff use a mass flow-weighting pressure averaging procedure, and Pianko and Dzung use a mass flow-weighting temperature averaging procedure, therefore, these respective values are the same as the mass flow-weighted method values. For this particular example, the calculated area and mass flow-weighted flow properties are the same; but in general this will not be true, particularly if there are significant non-uniformities in total pressure. Livesey's method gives a value for the average total pressure which is significantly greater than the other averaging methods and which is also greater than the actual measured pressures. The explanation, as pointed out by Kruse, is that Livesey's method assumes reversible mixing for averaging the flow mean static pressure value, which is calculated from

$$R \ln\left(\frac{\bar{P}_s}{P_0}\right) = C_p \ln\left(\frac{\bar{T}_s}{T_0}\right) - \bar{s}$$

where $\bar{T}_s = 1/m \int T_s \, dm$, and

$$\bar{s} = \frac{1}{m}\left(C_p \int \ln\left(\frac{T_s}{T_0}\right) dm - R\int\left(\frac{P_s}{P_0}\right) dm\right)$$

with $P_s(r) = \text{constant}$, the difference between the mean pressure $\bar{P}_s$ and $P_s(r) = \text{constant}$ only depends on the difference between the two terms,

$$\Delta = \ln \frac{\left(\frac{1}{\dot{m}} \int T_s \, dm\right)}{T_0} - \frac{1}{\dot{m}} \int \ln\left(\frac{T_s}{T_0}\right) dm$$

which is positive for $T(r) \neq \text{constant}$. Another way to think of the problem is that the temperature differences in Livesey's method must increase the calculated mean pressure values, otherwise the mixing would be irreversible. The Livesey method should not be applied to flow with non-uniform temperatures.

Other notable differences in the calculated bulk flow properties are the relatively low values of the total pressure derived from the Pianko method and the total temperature derived from the Kuchar method. This difference, as pointed out by Dunham, is a result of the Pianko and Kuchar methods ignoring the thrust mixing gain potential of a non-uniform nozzle flow. To clarify this point, Dunham used the simple example of a nozzle receiving two inlet streams both with $\gamma = 1.4$, both with stagnation pressure 350 kPa, expanding to 100 kPa and both having a 100 kg/s mass flow. One stream is at stagnation temperature 400°K and the other at 800°K. The following table gives the various averages and the ideal thrust calculated by expanding the "average" flow isentropically:

Method	$\bar{P}_t$, kPa	$\bar{T}_t$, °K	*Thrust*, kN
Mass Flow-Weighting	350	600	120.46
Livesey	430.2	600	128.22
Kuchar and Tabakoff	350	582.8	118.73
Pianko	335.3	600	118.73
Dzung (mixing at Mn 0.36)	349.06	600	120.33
Dzung (mixing at Mn 0.71)	346.51	600	120.04

Dunham explains that both Kuchar and Pianko derive their "ideal thrust" by assuming the two streams expand separately, which ignores the fact that a higher thrust can be obtained by mixing them before expansion. As a result, the Kuchar method gives a total temperature that is lower than other methods and the Pianko method gives a low value for the average total pressure. Dunham's example also shows that mass flow-weighting, in effect, assumes that mixing takes place at such a low Mach number that the fundamental pressure loss attributable to mixing (which is accounted for in the Dzung method) is negligible.

A review of the nozzle performance coefficients in Table 4.2.III is also informative. Depending on the flow averaging method selected, the indicated thrust efficiency lies (ignoring the Livesey method) between 96 and 99 percent. Maximum thrust efficiency should correspond to uniform flow since there are no thrust losses as a result of flow non-uniformities; and, in fact, the Dzung and mass flow-weighting methods which do account for the thrust mixing gain potentials have calculated thrust coefficients less (3 to 4 percent) than the ideal uniform flow case. The Kuchar and Pianko methods give values for the thrust coefficient which are greater than Dzung, because, as previously discussed, the methods do not include the non-uniform flow thrust effects. Kuchar's method will give the highest value for the non-uniform flow thrust coefficients because it calculates the lowest value for the flow bulk temperature. For choked nozzle flows, the influence of flow temperature on the thrust coefficient is greater (about a factor of 1.5 for the present data) than that of pressure. Flow averaging methods that ignore the thrust gain potential of unmixed flows and that predict a low value for the flow bulk temperature, will predict a high value for the non-uniform flow thrust coefficient that can appear to correlate with the uniform flow values.

The only conclusion made with respect to the non-uniform flow discharge coefficients is that the level of the coefficient for the ideal uniform flow is considerably less (4 to 10 percent) than the non-uniform flow values. For the non-uniform flow averaging methods, Pianko's method will give the highest value for the discharge coefficient because it predicts the lowest value for the bulk pressure. For choked flows, the influence of pressure on the discharge coefficient is twice that of the temperature.

The writer also found it informative to apply the present set of data to the cold-flow model to full-scale nozzle coefficient adjustment method described in the section titled, High-Bypass Ratio Turbofan of Chapter 4.2. Recall, in this method a corrected flow temperature and/or pressure is determined by equating the nozzle discharge (or thrust) coefficients from the uniform and non-uniform flow data and verifying the results by applying the corrected value to the nozzle thrust (or discharge) coefficient. For the present data, where the pressure distribution was nearly uniform and the temperature distribution highly non-uniform, the area-weighting discharge coefficient was used to determine the data adjustment. The area-weight coefficient was selected because it is generally used on engine tests because of its convenience. The results for the "Adjusted Coefficient" method are presented in the following table.

	$\bar{P}_t$ psia	$\bar{T}_t$ °R	$\bar{\gamma}$	*Discharge Coefficient* C_d	*Thrust Coefficient* C_f
Uniform Flow			1.4	0.91 – 0.93	0.99 – 1.00
Area-Weighting (Non-uniform Flow)	14.83	1122	1.37	0.99	0.96
Adjusted Coefficient	14.83	945 – 990	1.38	0.91 – 0.93	1.05 – 1.02

As shown in the table, the Adjusted Coefficient method does not collapse the numerical difference between the model and full-scale nozzle thrust coefficients. Similar results have been obtained at the AEDC when using this method on other turbine engine (including high-bypass turbofans) to model data comparisons. The assumption that the principal difference in cold-flow model and full-scale turbine engine nozzle coefficients is attributable to measurement error is not correct.

In summary, for flows with variations in pressure and temperature, the Dzung method is the only method identified that properly accounts for the flow stagnation enthalpy and stream force at the flow measurement station. The Dzung method, however, requires specification of a flow static property distribution at the flow measurement station which will be difficult to define on most turbine engine tests. For a given nozzle configuration, the thrust efficiency of a non-uniform flow will be less (because of the thrust gain potential and mixing losses) than that obtained for uniform inlet flow conditions. No flow averaging method has been identified that gives the same values of nozzle coefficients for a two stream and a one stream nozzle flow, principally because the nozzle efficiencies for these two cases are not the same. The nozzle flow comparisons in this section are based on engine nozzle data with basically only distortions in total temperature. It would be informative to see a flow averaging comparison similar to Table 4.2.III for real data with only pressure distortions and with both pressure and temperature distortions.

TABLE 4.2.I (Ref. 4.2.1)

Model to Full-Scale Nozzle Flow Considerations

(1) Three-dimensional nature of flow in the nozzle.

(2) Corrections for real-gas effects which may arise in applying some model nozzle test data to full-scale nozzles (in particular at high-pressure and low-temperature conditions).

(3) Nonuniformity of pressure and temperature profiles across the exhaust duct at the nozzle entry measurement plane.

(4) The coverage of the pressure and temperature probes, which will not in general give representative mean values.

(5) Local flow direction, including swirl, in the plane of measurement.

(6) Value of γ used for isentropic groups (if Ideal Gas Thermodynamics are not used).

(7) Dissociation of real gases at high temperature, and energy-mode-fixation during rapid nozzle expansion.

(8) Pressure losses between plane of measurement and nozzle entry, particularly with reheat.

(9) Mass-flow leakage from the tailpipe and nozzle.

TABLE 4.2.II (Ref. 4.2.6)

Comparison of Wake Flow-Averaging Methods

a. Flow Conditions:

Primary Stream

Stagnation Pressure = P_{t_1}

Stagnation Temperature = T_{t_1}

Mass Flow = $\dot{m}_1$

Mach Number = 0.6

Ratio of Specific Heats = 1.4

Secondary Stream

Stagnation Pressure = P_{t_2}

Stagnation Temperature = T_{t_1}

Mass Flow = $0.2\,\dot{m}_1$

Ratio of Specific Heats = 1.4

b. Pressure Loss (ΔP_t) Comparison:

$\frac{P_{t_2}}{P_{t_1}}$	$\frac{\Delta P_t \text{ (mixed-out)}}{P_{t_1}}$	$\frac{\Delta P_t \text{ (mass flow weighted)}}{P_{t_1}}$
0.95	0.0090	0.0083
0.90	0.0197	0.0167
0.85	0.0336	0.0250
0.80	0.0625	0.0333

TABLE 4.2.III

Comparison of Flow Averaging Methods
(Results for Figure 4.2.10)

Averaging Method	$\bar{P}_t$, psia	$\bar{T}_t$, ^oR	γ	Discharge Coefficient, C_d	Force Coefficient, C_f
Uniform Flow	---	---	1.4	0.92 ± 0.01	0.995 ± 0.005
Nonuniform Flow	---	---	$f(T_t)$	0.96	0.98
Area-Weighting	14.83	1,122	1.373	0.98	0.97
Mass Flow-Weighting	14.84	1,123	$f(T_t)$	0.98	0.97
Kuchar-Tabakoff	14.84	1,050	1.38	0.94	1.00
Momentum	14.84	1,099	$f(T_t)$	0.97	0.98
Adjusted Coefficient	14.84	982	1.382	0.92	1.04
Pianko (Chapter 3.2)	14.42	1,123	1.37	1.01	0.97
Dzung (Chapter 3.1)	14.81	1,123	$f(T_t)$	0.99	0.96
Livesey (Chapter 4.1)	16.94	1,135	$f(T_t)$	0.88	0.91

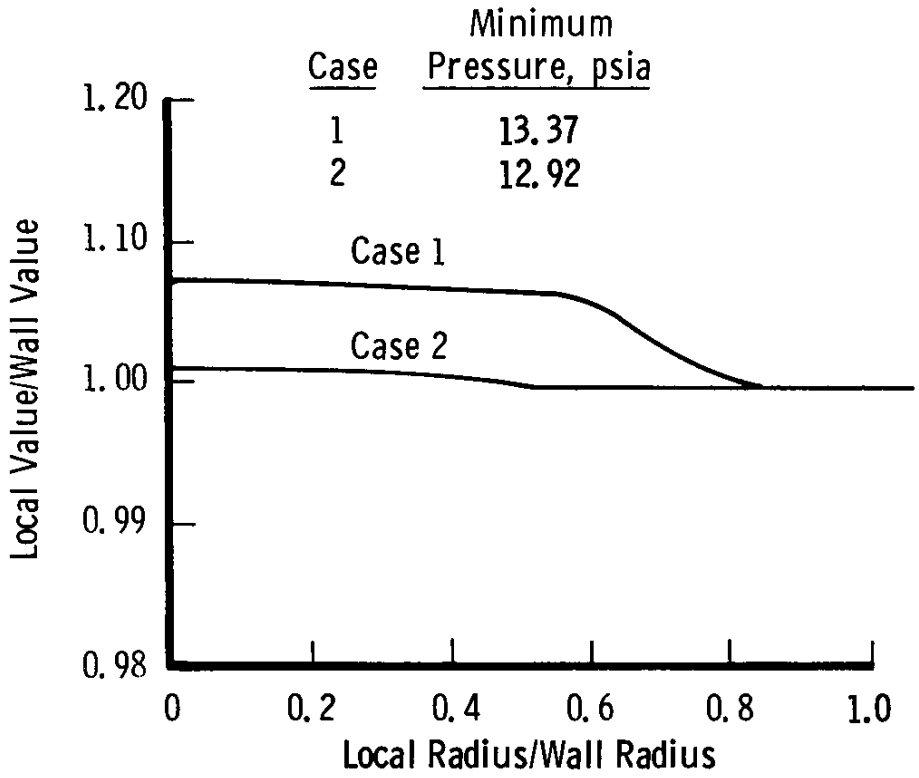

a. Stagnation Pressure

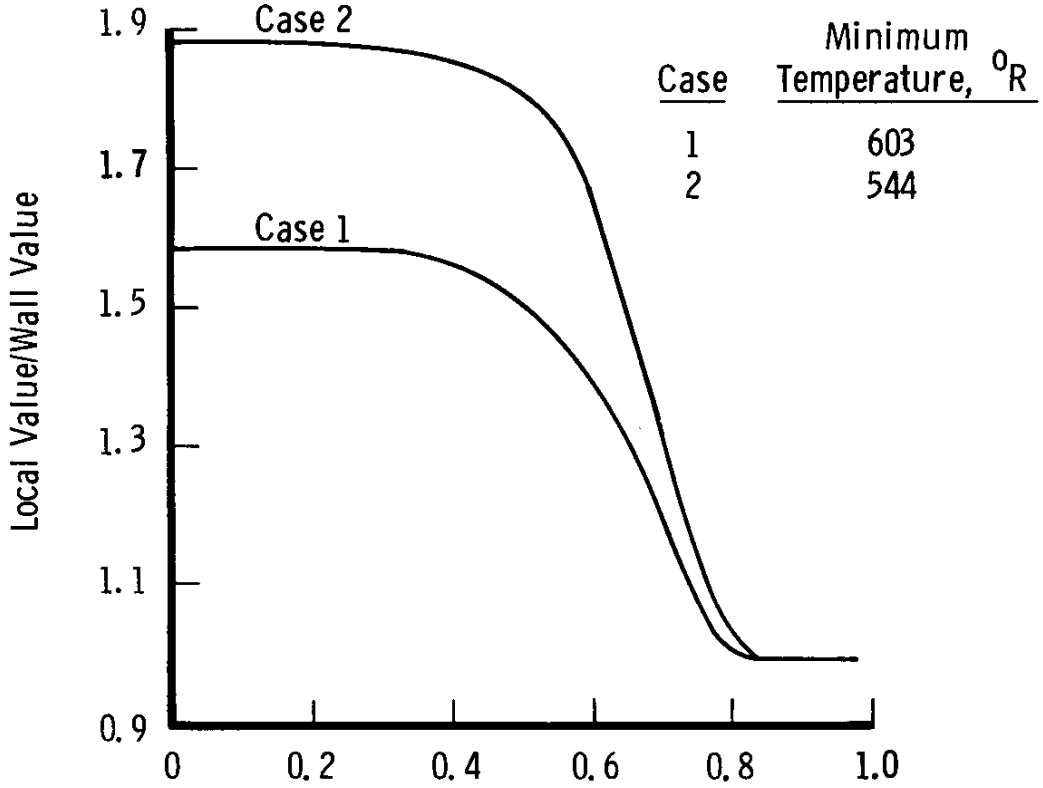

b. Stagnation Temperature

Fig.4.2.1 Nozzle inlet profiles (low-bypass turbofan)

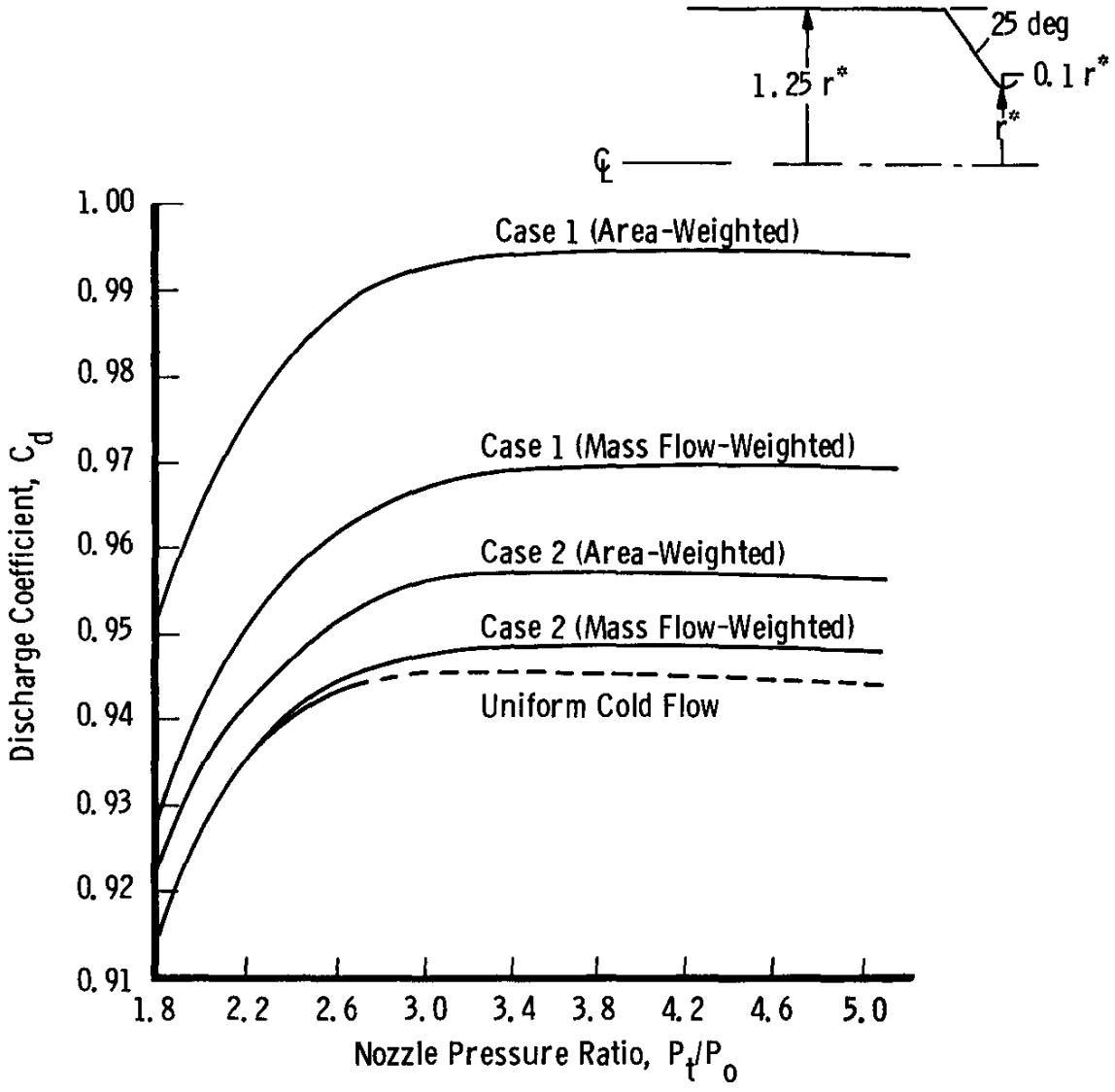

Fig.4.2.2 Influence of flow averaging on nozzle discharge coefficient

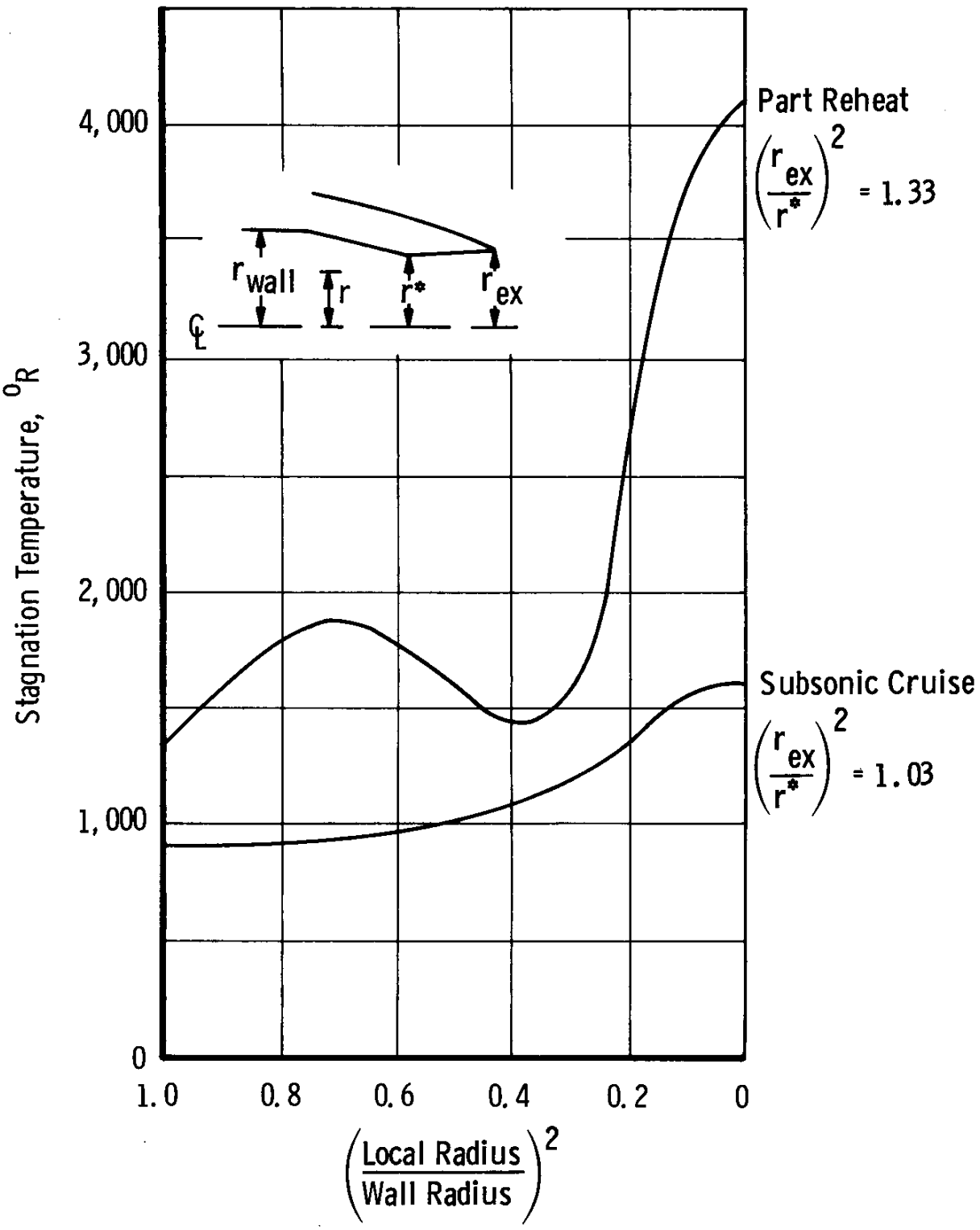

Fig.4.2.3 (Ref.4.2.3) Nozzle inlet temperature profiles

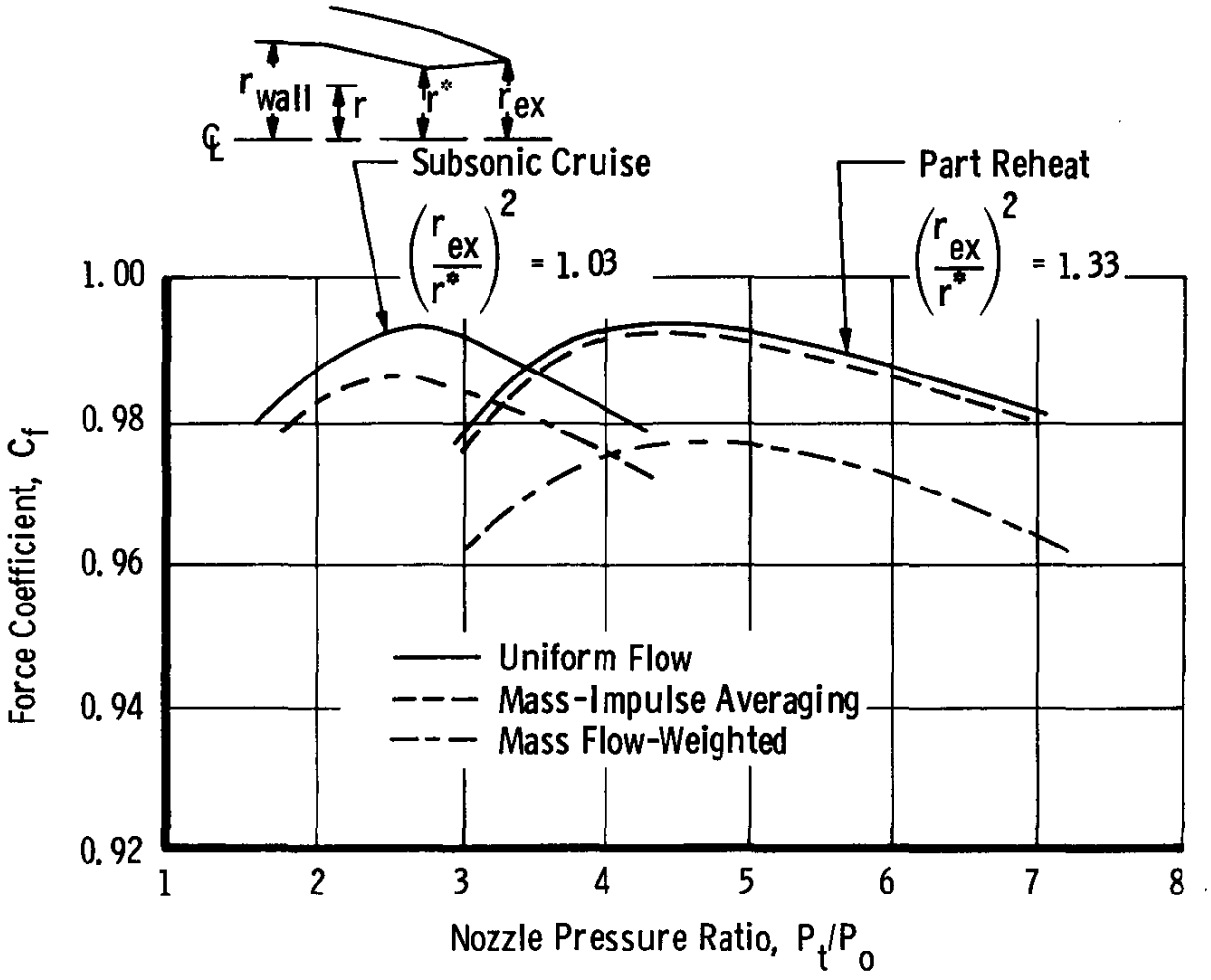

Fig.4.2.4 (Ref.4.2.3) Theoretical influence of flow averaging on nozzle force coefficient

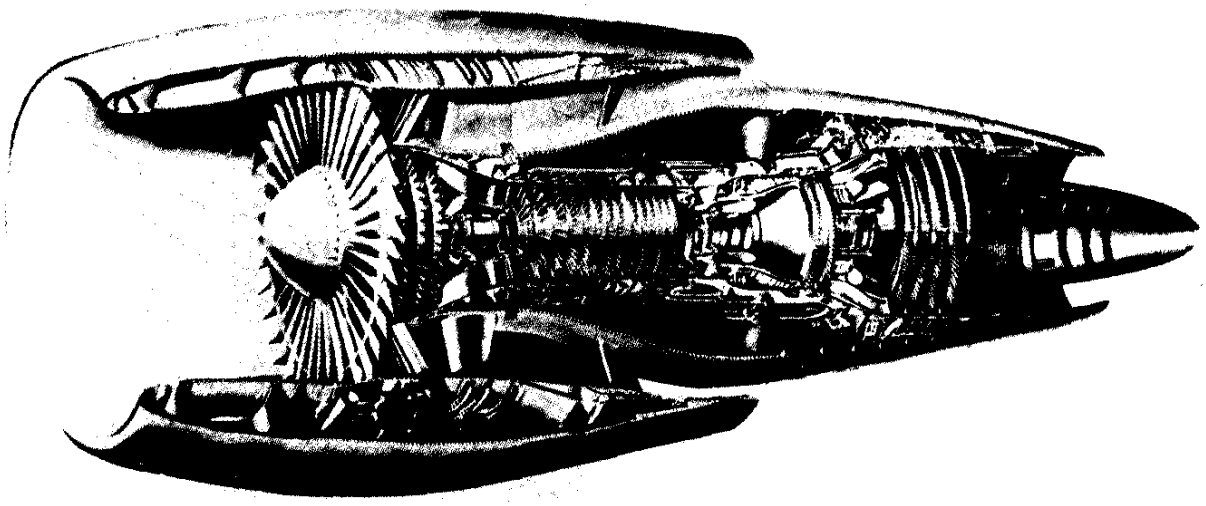

a. Full-Scale Engine

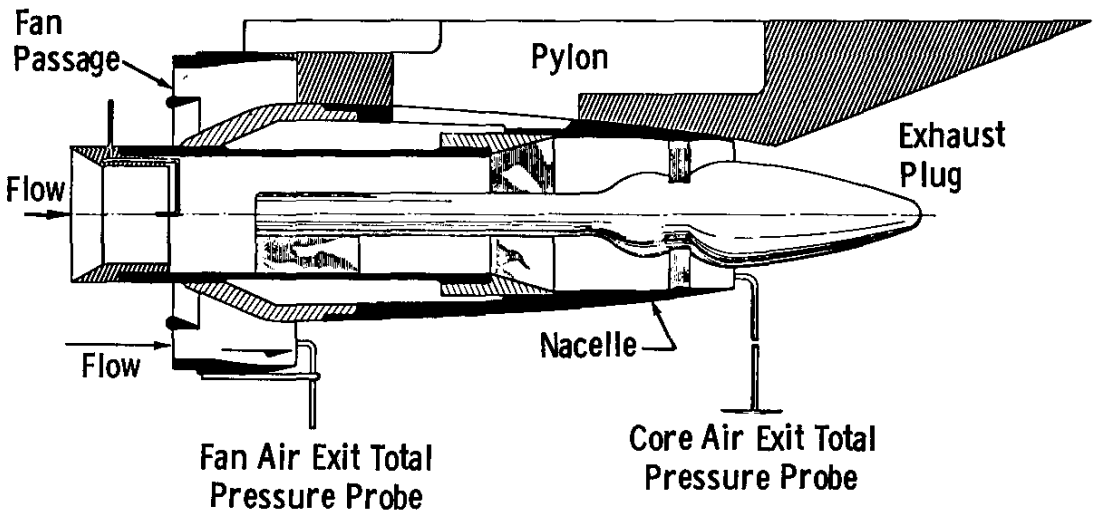

Fig.4.2.5 Schematic of dual stream turbofan engine

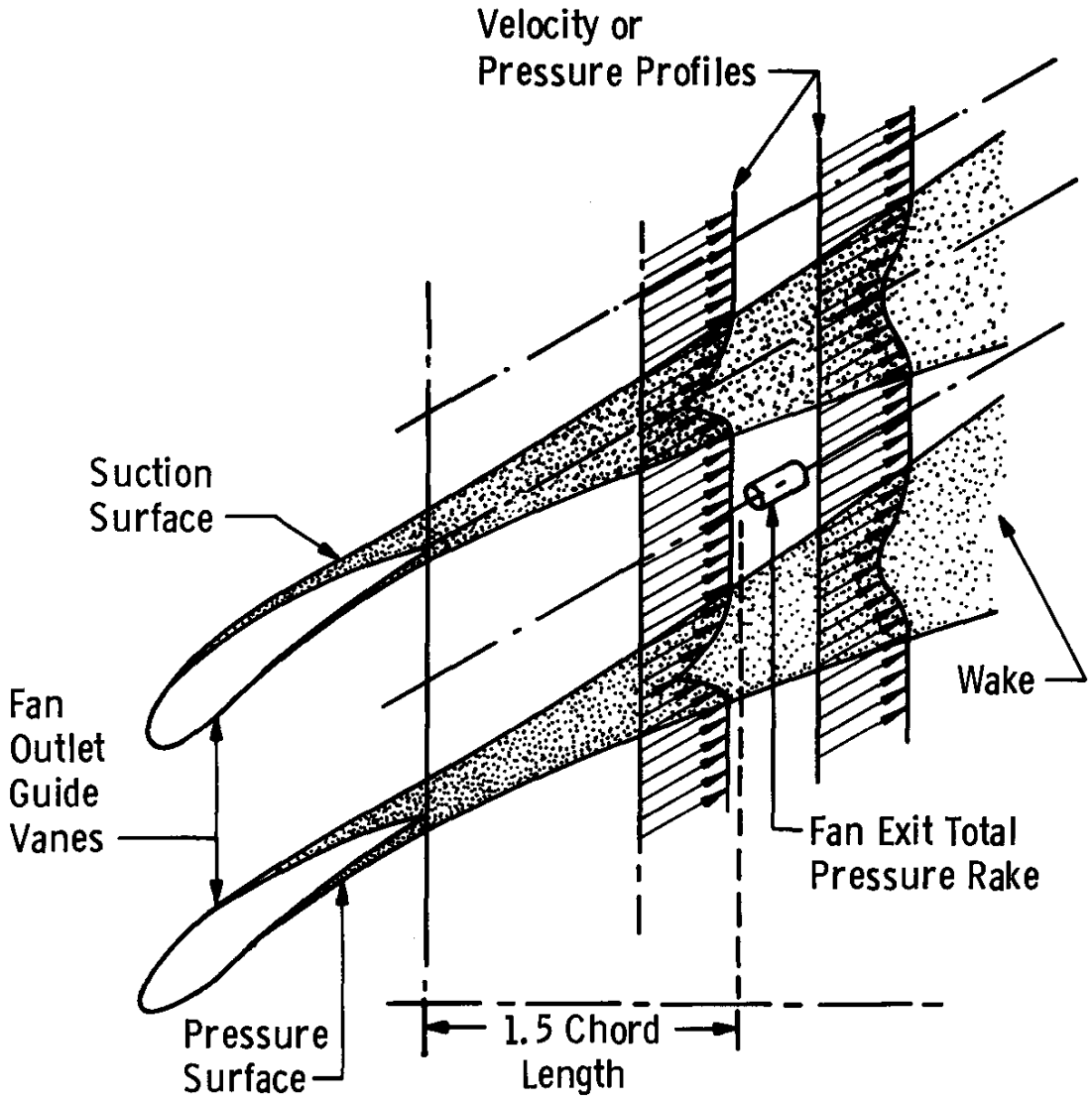

Fig.4.2.6 (Ref.4.2.7) Schematic of fan exit flow profile

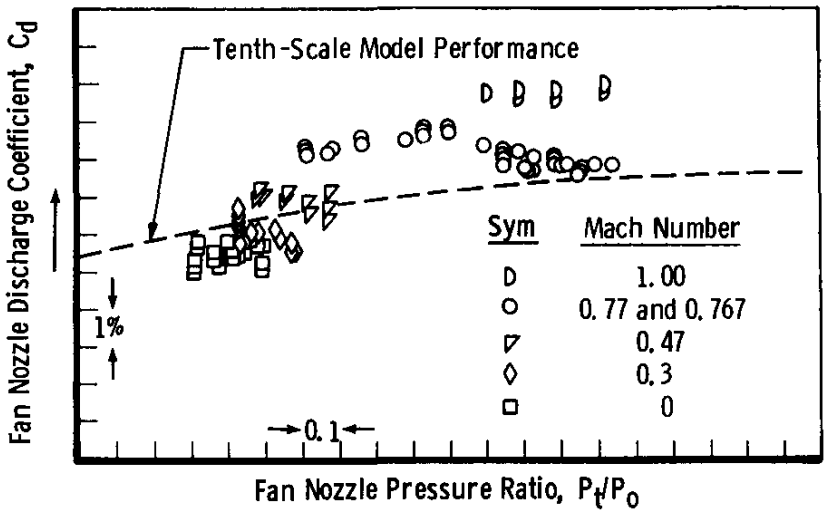

a. Discharge Coefficient

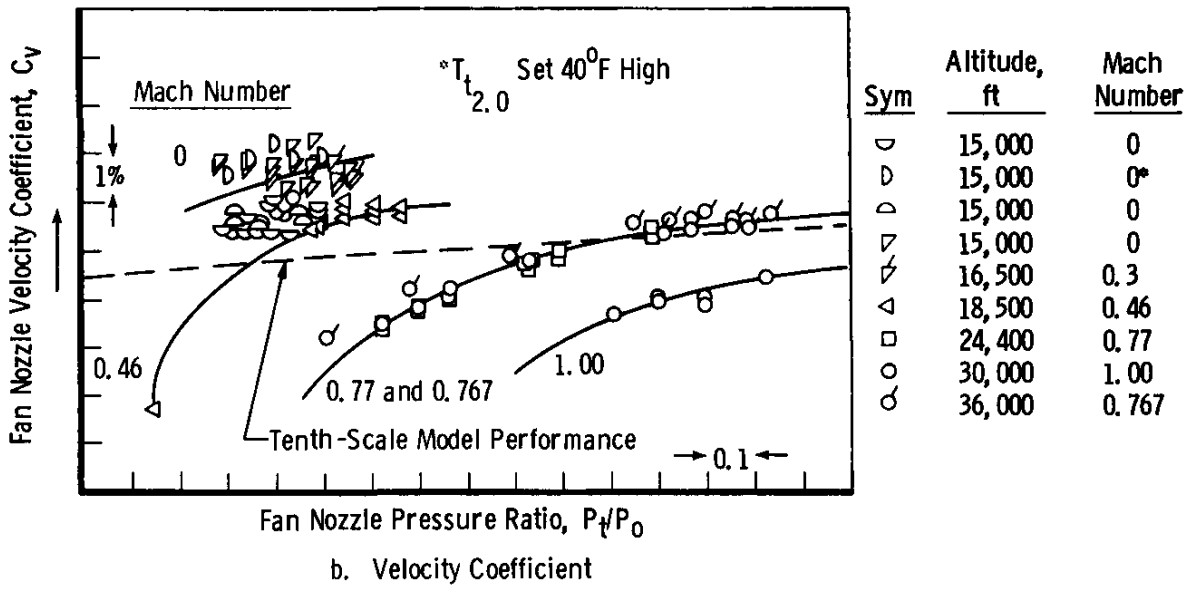

b. Velocity Coefficient

Fig.4.2.7 Comparisons of full-scale fan nozzle data with model results

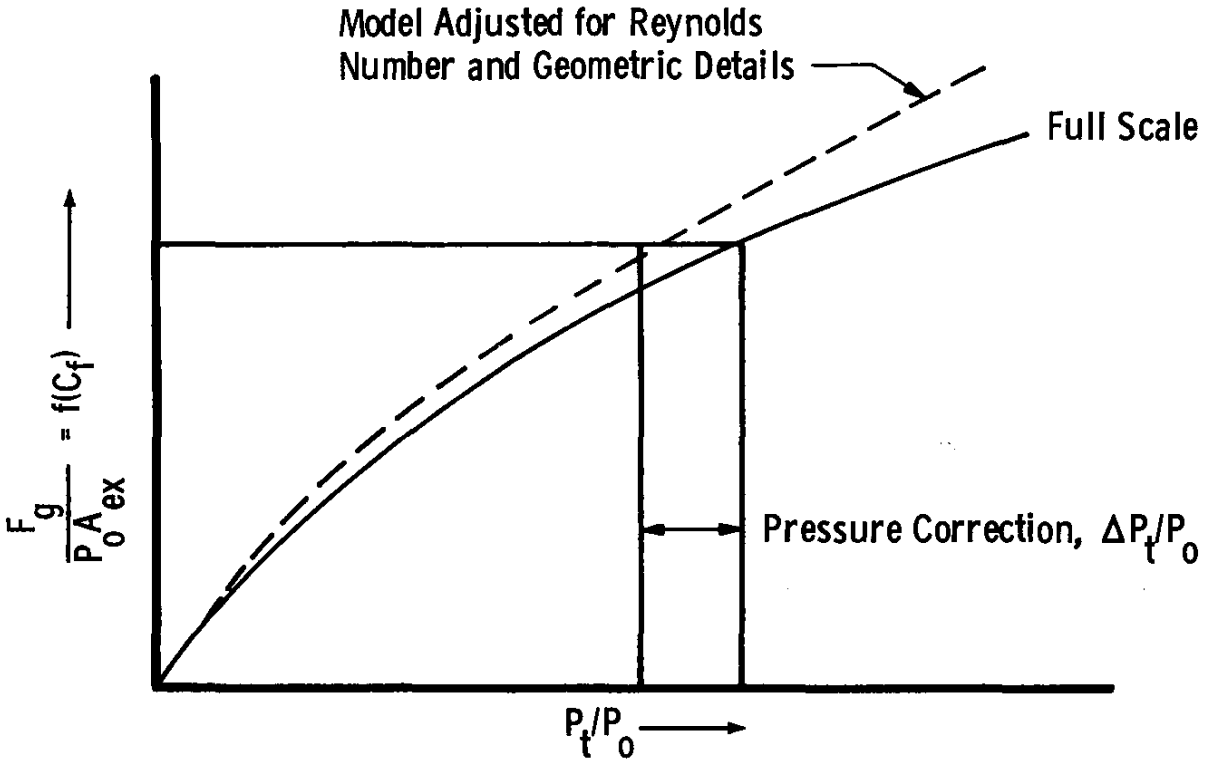

Fig.4.2.8 (Ref.4.2.4) Model to full-scale pressure correction

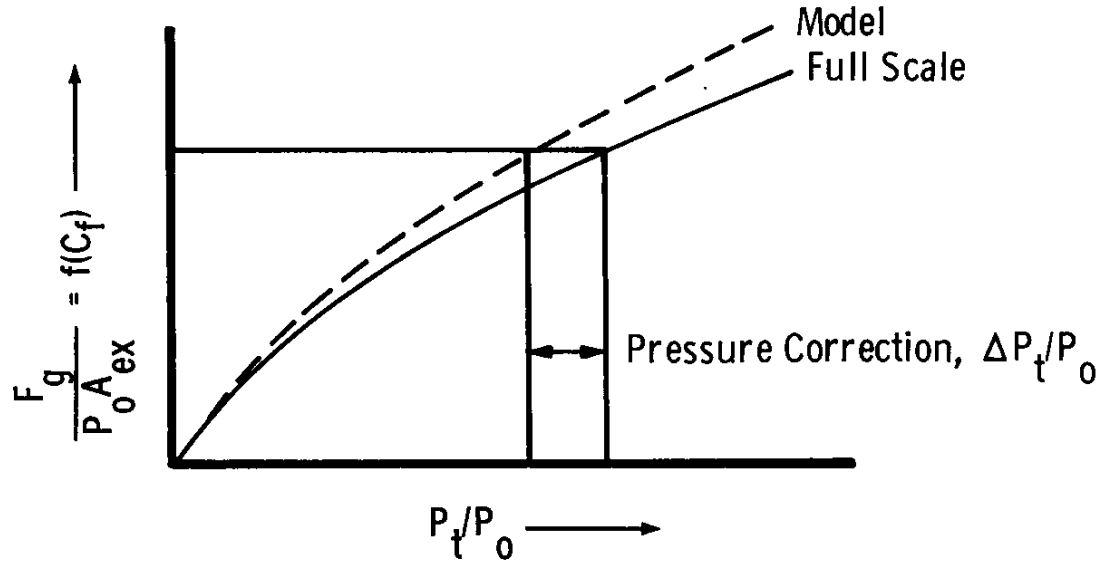

a. Pressure Correction

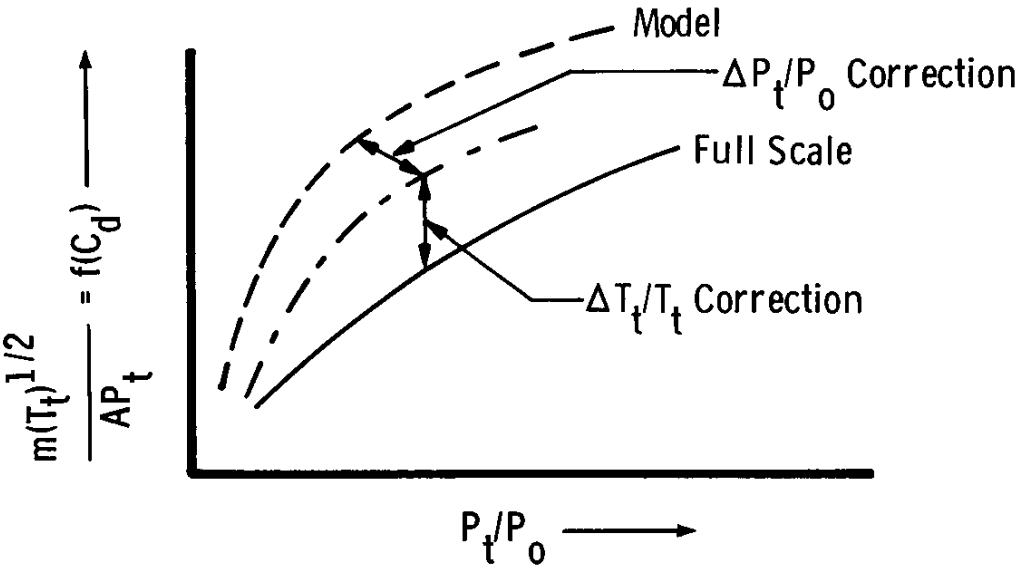

b. Temperature Correction

Fig.4.2.9 Model to full-scale pressure, temperature correction

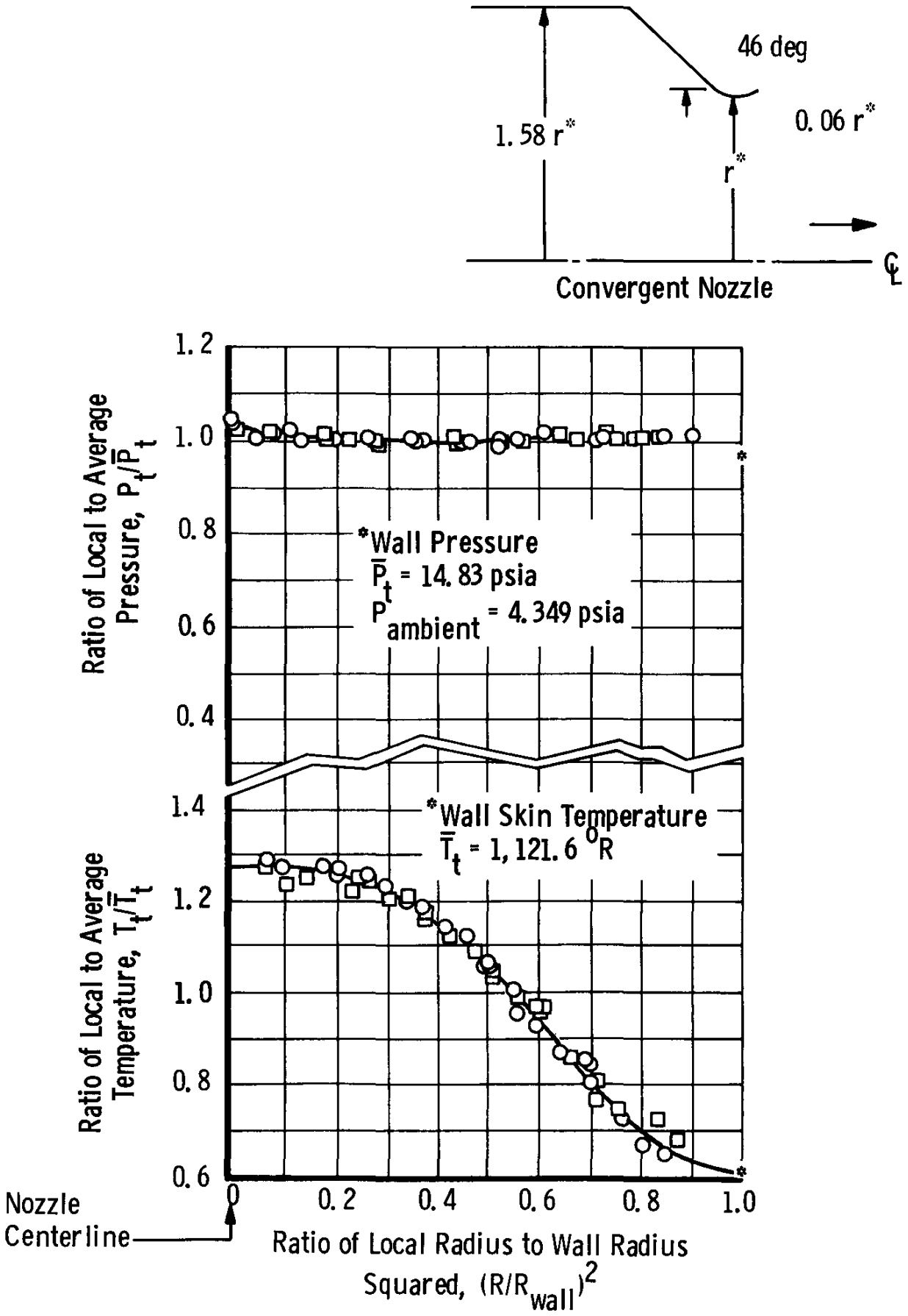

Fig.4.2.10 Measured nozzle total pressure and temperature profiles

4.3 TURBOMACHINERY FLOWS

The purpose of this section is to quantify the flow averaging methods (described in the preceding chapters) by sample calculations using realistic distributions of flow quantities within the engine components compressor and turbine in order to compare and discuss the different results.

The data used for the sample calculations are design data so that there is no influence of any inaccuracy caused by individual measuring techniques. The area- and mass-weighted mean values need no further explanation. Using the Dzung method (see Chapter 2) one gets a consistent set of mean values characterizing the flow. For typical turbomachinery flows these results are compared to a set of mean values called "entropy weighted" mean values because they are essentially based on constant energy/constant entropy mixing, whereas some quantities are mass flow weighted.

Complementary to Chapter 2 these relations are as follows:

$$\bar{\alpha} = \frac{1}{\dot{m}} \int \alpha \, dm$$

$$\bar{h}_s = \frac{1}{\dot{m}} \int h_s dm$$

$$\bar{T}_s = \frac{\bar{h}_s}{C_p}$$

(because of less computational effort c_p is assumed to be constant).

$$\bar{V} = \sqrt{\frac{1}{\dot{m}} \int V^2 \, dm}$$

$$\bar{T}_t = \frac{1}{C_p} \left(\bar{h}_s + \frac{\bar{V}^2}{2} \right)$$

$$\bar{P}_s = P_0 \left(\frac{\bar{T}_s}{T_0} \right)^{C_p/R} \cdot \exp - \frac{\bar{S}}{R}$$

$$\left(\bar{S} = \frac{1}{m} \int S dm \right)$$

$$\bar{P}_t = \bar{P}_s \cdot \left(\frac{\bar{T}_t}{T_s} \right)^{\gamma/(\gamma-1)}$$

In addition the data of some sections of the compressor and the turbine are examined using the "Pianko" method, described in section 3.2. Its application is explained in detail in the following section 4.4.

4.3.1 Compressor

4.3.1.1 Axis symmetric flow

In contrast to turbine or nozzle flow data there are relatively small variations in radial temperature distributions. The data of the single-stage compressor under consideration are as follows:

Geometry:

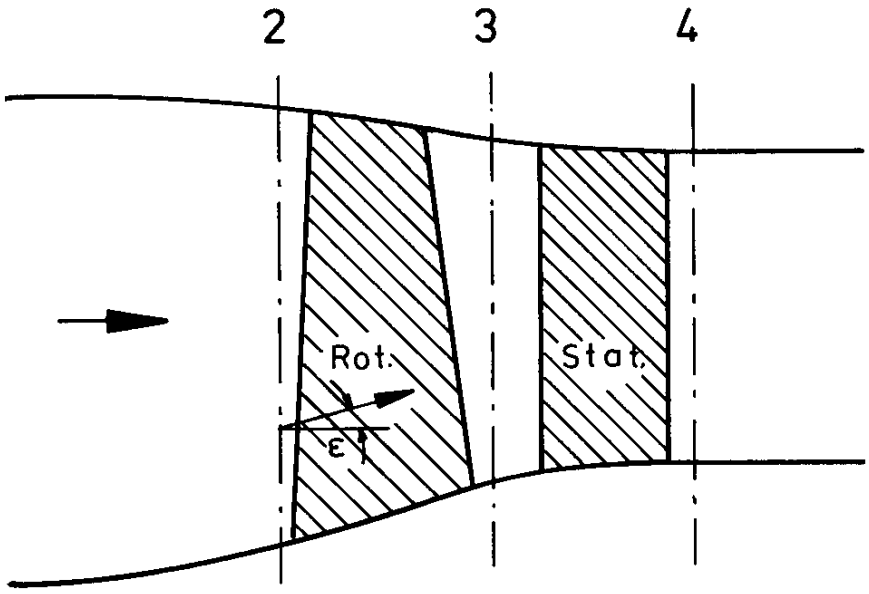

Fig.4.3.1 Geometry

TABLE 4.3.I

Design Data

Section	*Axial Position (mm)*		*Radius (mm)*	
	hub	*tip*	*hub*	*tip*
1	0.	0.	90.00	202.00
2	63.	63.	99.00	199.50
3	113.	113.	113.00	192.00
4	159.	159.	117.48	188.05

Section 2

r (mm)	α_2 (degr.)	T_{t2} (K)	P_{t2} (bar)	ϵ_2 (degr.)	P_{s2} (bar)
100.10	90.00	288.00	1.0133	14.25	0.8634
116.95	90.00	288.00	1.0133	10.33	0.8432
131.66	90.00	288.00	1.0133	6.83	0.8315
144.88	90.00	288.00	1.0133	3.64	0.8251
156.99	90.00	288.00	1.0133	0.69	0.8226
168.24	90.00	288.00	1.0133	−1.59	0.8232
178.78	90.00	288.00	1.0133	−3.73	0.8265
188.73	90.00	288.00	1.0133	−5.74	0.8333
198.18	90.00	288.00	1.0133	−7.63	0.8467

Section 3

r (mm)	α_3 (degr.)	T_{t3} (K)	P_{t3} (bar)	ϵ_3 (degr.)	P_{s3} (bar)
114.52	43.74	333.00	1.5463	13.04	1.0639
126.50	49.44	330.31	1.5504	9.36	1.1125
137.44	52.38	329.33	1.5492	5.93	1.1460
147.58	54.20	329.25	1.5503	2.72	1.1703
157.06	55.32	329.59	1.5537	−0.30	1.1913
166.00	55.58	331.20	1.5536	−2.35	1.1994
174.49	55.02	333.65	1.5594	−4.29	1.2110
182.58	52.91	338.04	1.5578	−6.12	1.2155
190.32	47.87	345.34	1.5298	−7.87	1.2062

Section 4

r (mm)	α_4 (degr.)	T_{t4} (K)	P_{t4} (bar)	ϵ_4 (degr.)	P_{s4} (bar)
119.44	90.00	333.00	1.4349	1.41	1.2245
129.70	90.00	330.31	1.5268	0.95	1.2449
139.20	90.00	329.33	1.5297	0.52	1.2384
148.10	90.00	329.25	1.5331	0.13	1.2433
156.49	90.00	329.59	1.5382	−0.25	1.2471
164.45	90.00	331.20	1.5385	−0.69	1.2467
172.05	90.00	333.65	1.5363	−1.11	1.2449
179.32	90.00	338.04	1.5266	−1.52	1.2437
186.31	90.00	345.35	1.4927	−1.91	1.2403

TABLE 4.3.II

Comparison of Averaging Methods (Compressor, Figure 4.3.1)
(γ = 1.4 = constant)

	Section	$\bar{V}$ (m/s)	$\bar{h}$ (kj/kg)	$\bar{P}_s$ (bar)	$\bar{P}_t$ (bar)	$\bar{T}_s$ (K)	$\bar{T}_t$ (K)	$\bar{\alpha}$ (degr.)	η_{is} (–)
Dzung method	2	175.91	273.69	0.8343	1.0114	272.6	288.0	90.0	
	3	220.22	309.53	1.1811	1.5379	308.3	332.4	52.4	0.8030
	4	189.16	316.06	1.2572	1.5244	314.8	332.6	90.0	
"Entropy-weighted" Mean Values	2	177.93	273.69	0.8322	1.0133	272.2	288.0	90.0	
	3	226.61	308.13	1.1731	1.5521	306.9	332.4	52.6	0.8008
	4	194.72	314.95	1.2435	1.5256	313.7	332.6	90.0	
Pianko method	2			0.8333	1.0133		288.0		
	3 *			1.1770	1.5511		332.7		
	4 **			1.2435	1.5221		332.8		0.7925
	4 ***			1.2424	1.5221		332.8		0.7925
Area weighted	2				1.0133		288.0		0.7795
	4				1.5151		333.0		
Mass weighted	2				1.0133		288.0		0.7915
	4				1.5188		332.6		

* section 3 considered as compressor inlet
** section 4 considered as compressor inlet
*** section 4 considered as combustor inlet

Comparing the isentropic efficiency of the stage (Table 4.3.II), there is a small difference (except for the area weighted value).

But looking at total and static pressure mean values (Table 4.3.II, Figures 4.3.2–5) there may be noticeable differences in the different sections.

At the compressor inlet $P_t(r)$ which is constant in section 2 exceeds the Dzung total mean pressure probably as a consequence of the mixing losses from equalizing the different radial components ($s \cdot \epsilon_2$).

In one case (section 4, Figure 4.3.4) the static mean pressure from the Dzung method is greater than any existent static pressure value within the radial distribution!

In this compressor case with no considerable differences in radial temperature distribution the Dzung mean static pressure always exceeds the "entropy-weighted" pressure.

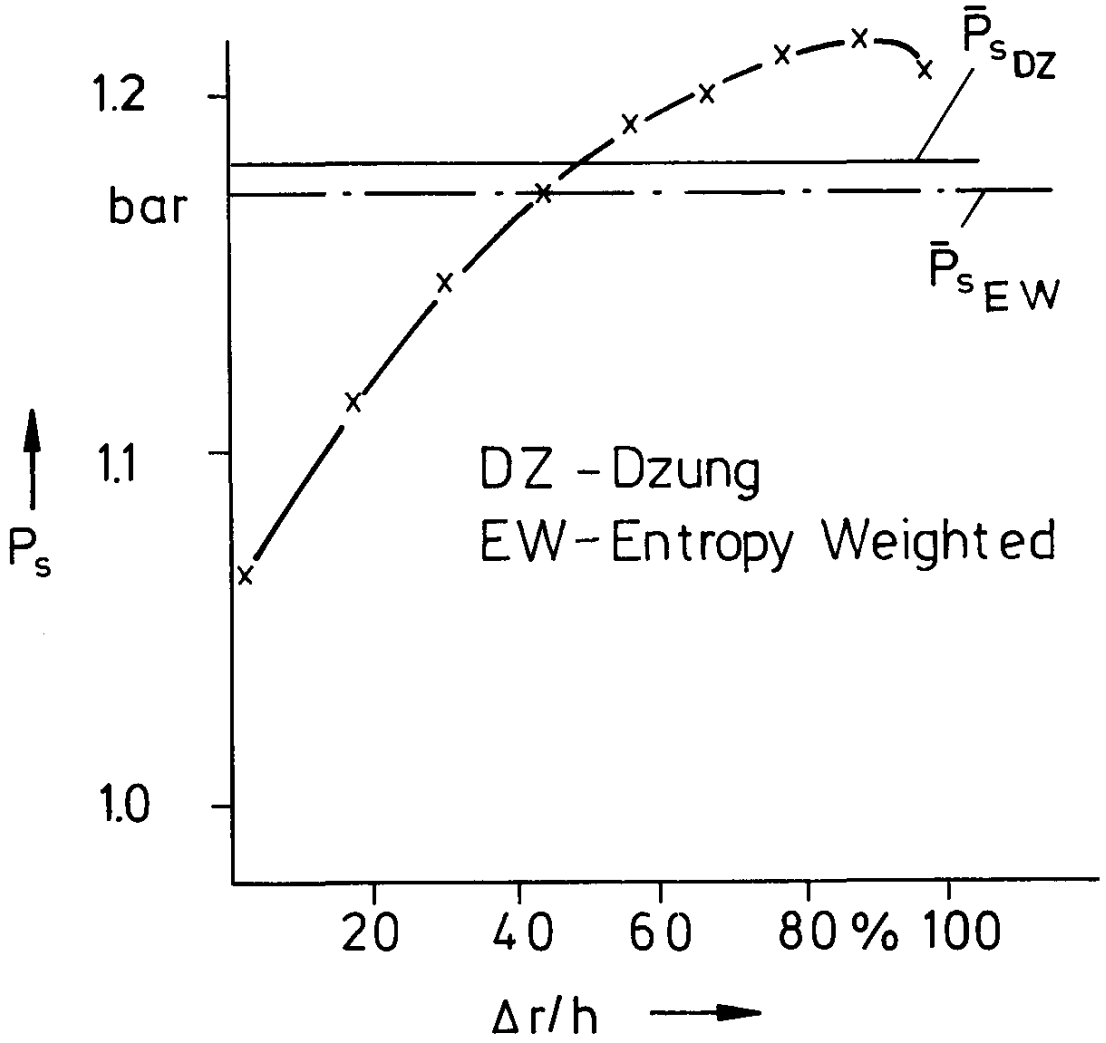

Fig.4.3.2 Section 3: Static pressure distribution

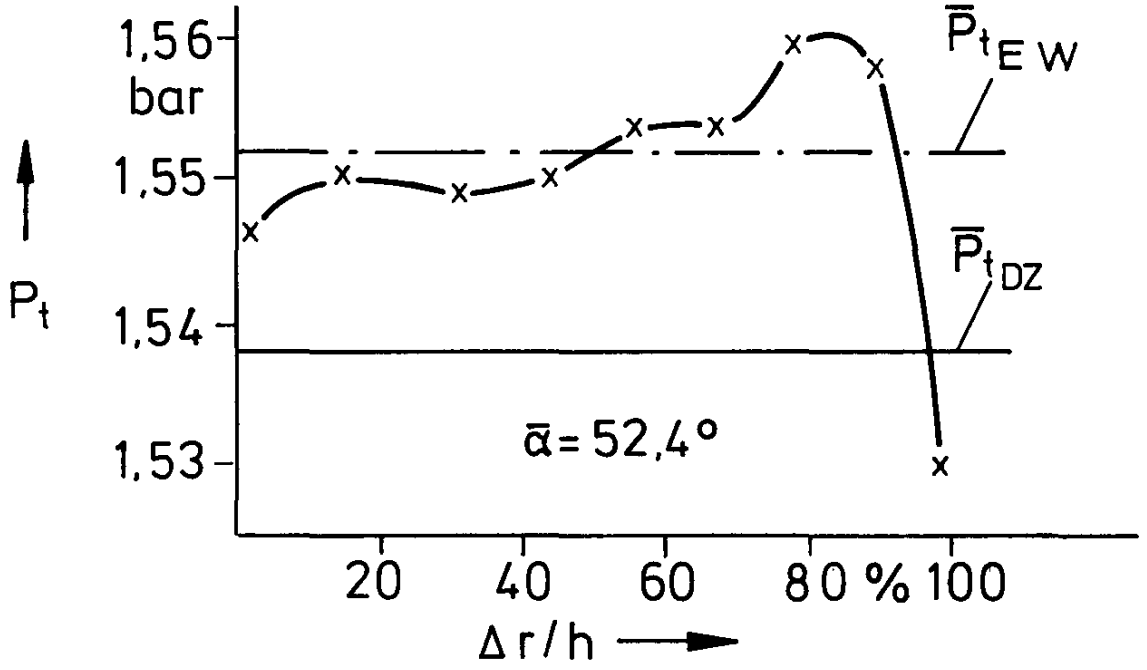

Fig.4.3.3 Section 2: Total pressure distribution

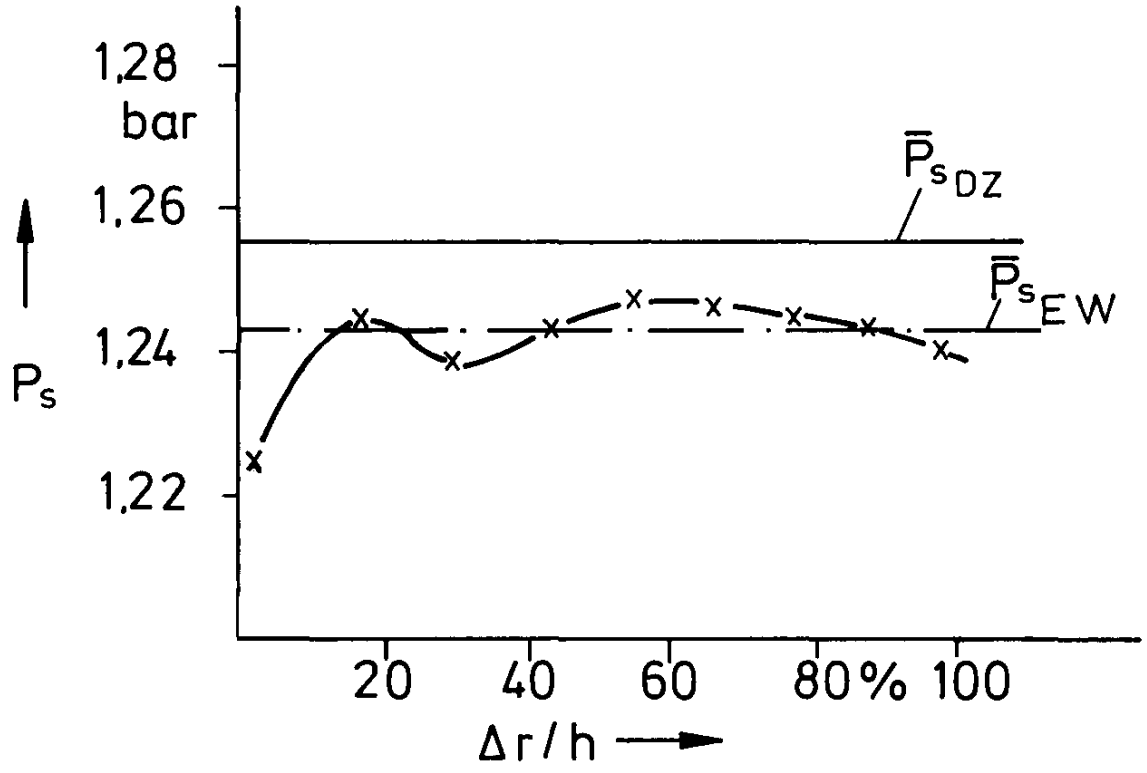

Fig.4.3.4 Section 4: Static pressure distribution

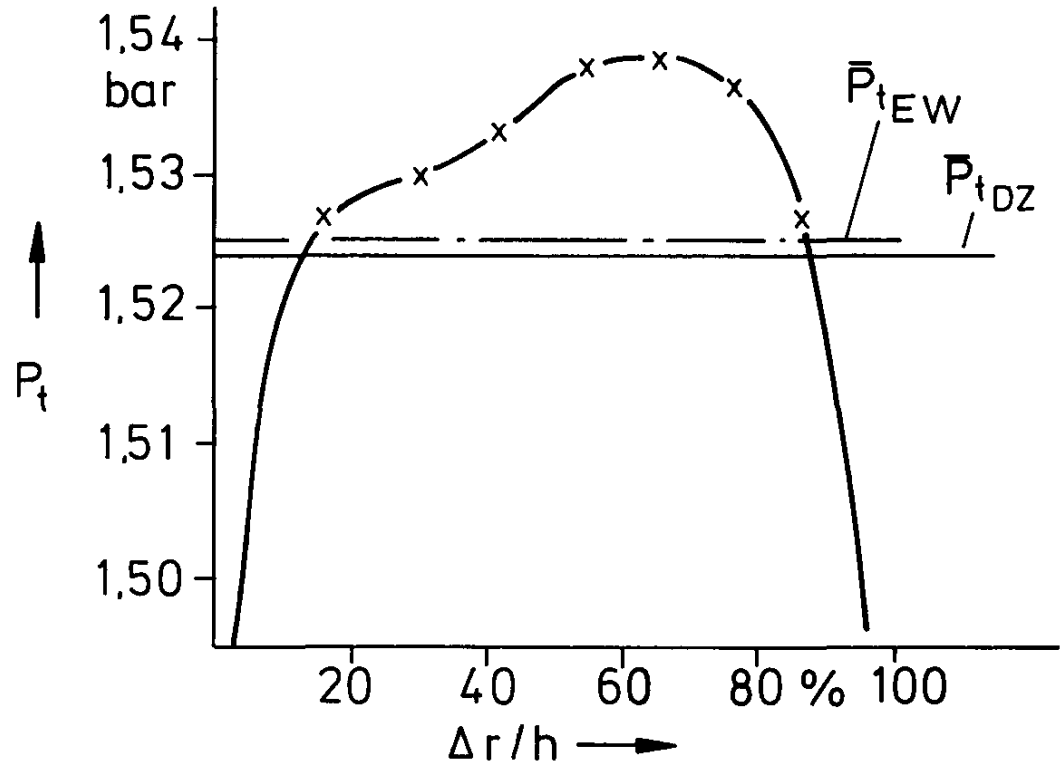

Fig.4.3.5 Section 4: Total pressure distribution

4.3.1.2 Compressor Intake Distortion

When a compressor or engine is tested alone, it is usually supplied with air at effectively uniform stagnation pressure and temperature, so the inlet averaging method is unimportant. When it is tested behind an intake or an intake simulator, on the other hand, the pressure will no longer be uniform, so the averaging procedure may be important. To examine the magnitude of the differences likely to be found in practice, sample calculations have been done on actual test results obtained from full scale intakes at typical low-distortion and high-distortion conditions. Four cases were examined:

(1) intake A, low distortion (equivalent to an engine face time average distortion coefficient $DC_{60} \simeq -0.06$) The distortion coefficient DC_{60} is the difference between the mean pressure in the compressor inlet plane and the mean minimum pressure in a 60° angular sector, divided by the dynamic pressure.

(2) intake A, high distortion ($DC_{60} \simeq -0.31$, a level which might well be high enough, in conjunction with the accompanying time-variant distortion, to cause concern about possible surge)

(3) intake B, low stagnation pressure distortion ($DC_{60} \simeq -0.08$) but a 2.5% static pressure distortion

(4) intake B, high distortion ($DC_{60} \simeq -0.36$) and 3.6% static pressure distortion.

The following table shows the average inlet stagnation pressure recovery as calculated by the various methods:

TABLE 4.3.III

Case	*1*	*2*	*3*	*4*
Area weighted	.9466	.8245	.9716	.9333
Mass weighted	.9487	.8339	.9765	.9518
Entropy weighted	.9485	.8334	.9763	.9507
Pianko mean	.9485	.8332	.9763	.9504
Dzung mean	.9474	.8261	.9744	.9379
Mass-derived	.9453	.8201	.9682	.9263

It will be seen that the entropy-weighted and Pianko mean are virtually the same, and the following percentage differences from them were found for the other methods:

TABLE 4.3.IV

Case	*1*	*2*	*3*	*4*
area weighted	−0.2	−1.1	−0.5	−1.8
mass weighted	0	−0.1	0	+0.1
Dzung mean	−0.1	−0.9	−0.2	−1.3
mass-derived	−0.3	−1.6	−0.8	−2.6

It will be seen that the area weighted and mass-derived pressures cannot be relied upon for accurate work. The mass weighted, entropy and Pianko averages differ only by unimportant amounts, and the Dzung average is slightly lower than them.

4.3.2 Turbine

In this section the mean values of a two stage turbine were calculated using design data with realistic radial temperature distributions. The engine station identification is shown in Figure 4.3.6. The design data of six stations are shown in Table 4.3.V.

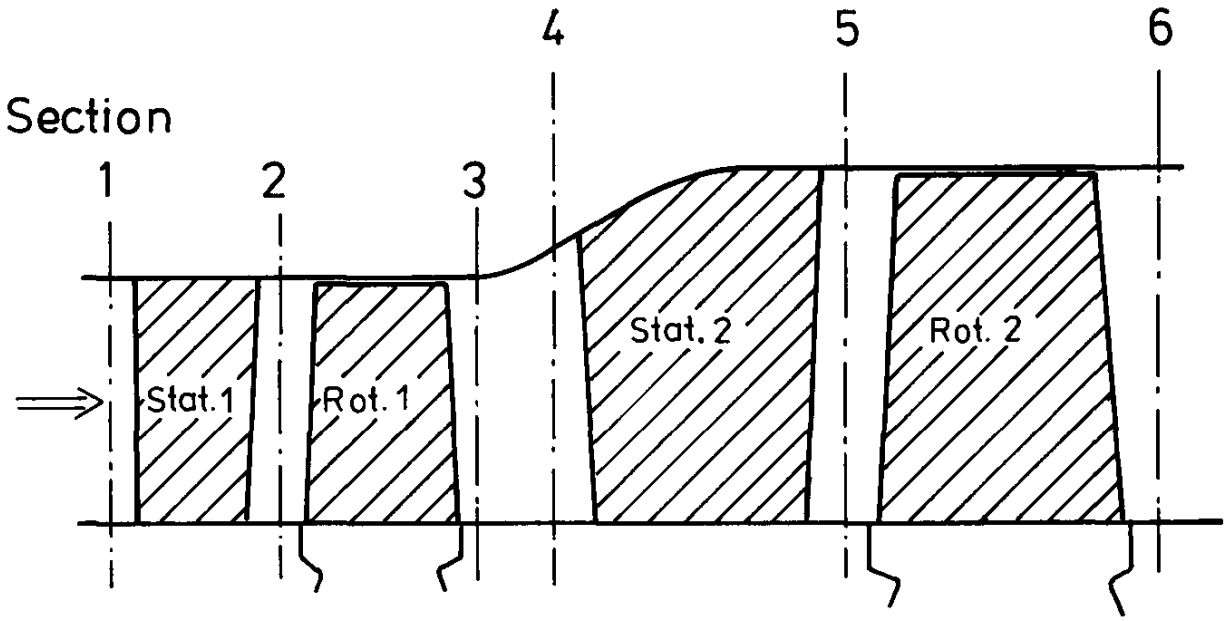

Figure 4.3.6

As well as in the compressor example the entropy weighted mean values always exceed the mean total pressure from the Dzung method, whereas only in some cases is the entropy averaged static pressure (as a consequence of the temperature distribution) somewhat higher than the Dzung mean value.

Although the differences in pressure mean values are small there may occur appreciable differences in pressure loss coefficient or pressure recovery. Considering for instance the pressure loss coefficient of the first stator vane the Dzung method gives:

$$\zeta = 14.2\%$$

and from the entropy weighted mean values one gets

$$\zeta = 12.3\% .$$

Considering the pressure recovery factor

TABLE 4.3.V

Turbine Design Data

Section 1

r (m)	T_s (K)	P_s (bar)	V (m/s)	(degr.)	(degr.)
0.0670	1254.0300	11.7603	120.7400	89.9999	0.0
0.0689	1322.7800	11.7604	123.9700	89.9999	0.0
0.0708	1372.8401	11.7607	126.2400	89.9999	0.0
0.0727	1409.0701	11.7612	127.7300	89.9999	0.0
0.0746	1431.6299	11.7618	128.5900	89.9999	0.0
0.0764	1440.4299	11.7624	128.8000	89.9999	0.0
0.0782	1438.4500	11.7630	128.5800	89.9999	0.0
0.0800	1428.4099	11.7635	127.9900	89.9999	0.0
0.0817	1411.9900	11.7637	127.1900	89.9999	0.0
0.0834	1393.4500	11.7638	126.3200	89.9999	0.0
0.0850	1375.0400	11.7635	125.5800	89.9999	0.0

Section 2

0.0670	1150.5100	7.5852	517.1001	21.0000	0.0
0.0688	1210.6101	7.7306	537.8799	20.7000	-0.2921
0.0706	1257.8899	7.8744	544.6699	20.4045	-0.6935
0.0724	1295.3000	8.0139	542.3601	20.1095	-1.0943
0.0742	1320.8401	8.1480	535.8201	19.8138	-1.5086
0.0760	1334.0601	8.2762	525.7200	19.5183	-1.9845
0.0778	1337.1599	8.3985	513.7200	19.2238	-2.5175
0.0796	1332.5200	8.5152	500.5701	18.9319	-3.1627
0.0814	1321.6499	8.6265	486.6399	18.6453	-3.9717
0.0832	1308.4800	8.7331	472.7100	18.3680	-5.0296
0.0850	1295.1599	8.8356	459.1899	18.1072	-6.4498

Section 3

0.0670	1110.0701	6.1565	209.7200	91.5676	-0.2479
0.0689	1160.8000	6.1558	223.9500	97.5760	0.6881
0.0707	1200.0701	6.1539	231.0500	100.6800	1.2050
0.0725	1229.9399	6.1506	233.9600	102.5418	1.6632
0.0743	1248.7700	6.1457	233.9100	103.6647	2.1216
0.0761	1256.2300	6.1389	231.3100	104.1863	2.5749
0.0779	1254.5200	6.1298	226.9300	104.2809	3.0876
0.0797	1246.0100	6.1183	221.2400	104.0239	3.6982
0.0814	1232.1299	6.1039	214.6200	103.4502	4.5139
0.0832	1216.7000	6.0869	207.5400	102.6264	5.7021
0.0850	1201.7800	6.0671	200.3900	101.5456	7.6165

TABLE 4.3.V (continued)

Turbine Design Data

Section 4

r (m)	T (K)	p (bar)	v (m/s)	(degr.)	(degr.)
0.0670	1113.2200	6.2313	190.4700	91.7260	-0.3065
0.0690	1164.1699	6.2320	204.8100	98.2686	0.5665
0.0710	1203.7100	6.2337	210.9400	101.6579	1.3987
0.0730	1233.9299	6.2360	212.1300	103.7633	2.4090
0.0750	1253.1699	6.2384	209.6900	105.1417	3.5289
0.0770	1261.1101	6.2411	203.9100	105.9559	4.7311
0.0790	1259.9900	6.2442	195.3300	106.4154	6.0337
0.0810	1252.1799	6.2483	184.0300	106.6385	7.4580
0.0832	1239.1799	6.2539	169.8200	106.7218	9.0611
0.0855	1224.8301	6.2620	152.3300	106.8527	10.9483
0.0880	1211.2500	6.2731	130.5100	107.2685	13.3582

Section 5

0.0670	1020.1299	4.0281	513.4600	26.0000	0.0
0.0695	1070.1001	4.1351	521.2200	25.3429	2.1122
0.0720	1110.6001	4.2377	521.4299	24.7043	3.7936
0.0745	1143.0200	4.3362	516.7300	24.0672	5.1231
0.0770	1165.5100	4.4310	507.9900	23.4218	6.1384
0.0796	1177.5500	4.5223	495.6299	22.7621	6.8675
0.0821	1181.1399	4.6103	480.3101	22.0835	7.3187
0.0848	1178.3799	4.6950	462.7100	21.8822	7.4923
0.0874	1170.6101	4.7765	443.0500	20.6545	7.3781
0.0902	1161.4199	4.8545	422.0000	19.8974	6.9714
0.0930	1153.1101	4.9288	398.7700	19.1071	6.3000

Section 6

0.0670	986.7600	3.3116	181.9000	93.6689	-0.2229
0.0704	1026.0000	3.3135	202.5600	96.5749	2.2674
0.0736	1058.2900	3.3181	215.8800	96.3651	3.7590
0.0765	1083.3000	3.3240	226.1700	95.2952	4.6451
0.0792	1099.3301	3.3304	233.9600	93.6229	4.9353
0.0818	1105.8799	3.3365	239.8300	91.5398	4.5179
0.0843	1104.8799	3.3419	244.4100	89.2388	2.9124
0.0866	1098.3601	3.3461	248.5300	86.8217	0.0
0.0889	1087.5901	3.3491	252.7100	84.3815	0.0
0.0910	1076.0701	3.3509	257.0100	82.0740	0.0
0.0930	1065.9900	3.3516	261.6001	79.9974	0.0

TABLE 4.3.VI

Comparison of Averaging Methods (Turbine, Figure 4.3.6)
(γ = 1.3074 = const)

	Section	$\bar{V}$ (m/s)	$\bar{h}$ (kj/kg)	$\bar{P}_s$ (bar)	$\bar{P}_t$ (bar)	$\bar{T}_s$ (K)	$\bar{T}_t$ (K)	$\bar{\alpha}$ (degr.)	η_{is} (–)
Dzung-method	1	126.94	1706.1	11.762	12.000	1397.1	1403.7	90.00	
	2	509.97	1584.1	8.286	11.590	1297.3	1403.8	19.56	
	3	222.36	1490.9	6.130	6.574	1220.9	1241.2	102.14	0.8848
	4	186.08	1498.2	6.259	6.572	1226.9	1241.1	104.26	
	5	471.54	1404.4	4.556	6.300	1150.8	1241.1	22.60	
	6	231.79	1316.0	3.337	3.636	1077.7	1099.7	89.47	
"Entropy Weighted" Mean values	1	126.91	1706.1	11.790	12.029	1397.1	1403.7	90.00	
	2	515.85	1581.1	8.271	11.664	1294.8	1403.8	19.53	
	3	223.39	1490.6	6.142	6.591	1220.7	1241.2	102.04	0.8857
	4	192.12	1497.1	6.257	6.597	1226.0	1241.1	104.15	
	5	484.51	1398.2	4.514	6.361	1145.0	1241.1	22.69	
	6	235.33	1315.2	3.340	3.650	1077.9	1099.7	89.67	
Pianko method	1	127	1706.4	11.7645	12.000	1398.0	1404.6		
	6 *	232.7	1315.6	3.3411	3.643	1077.8	1100		0.8872
	6 **	233	1315.5	3.3370	3.640	1077.7	1100		0.8867
	6 ***	232.9	1315.6	3.3389	3.641	1077.8	1100		0.8868
Area weighted	1				12.000		1402.0		
	6				3.638		1097.4		0.8880
Mass weighted	1				12.000		1403.7		
	6				3.643		1099.7		0.8861

* Section 6 considered as inlet of a turbine
** Section 6 considered as inlet of a reheat channel
*** Section 6 considered as inlet of a nozzle

$$c_p = \frac{\bar{P}_{s4} - \bar{P}_{s3}}{\left(\frac{\bar{\rho}}{2}\bar{V}^2\right)_3}$$

within the diffusor between section 3 and 4 the different results are

$$c_{p(DZUNG)} = 29.7\%$$

and

$$c_{p(EW)} = 26.3\% .$$

The differences in mean enthalpies and in efficiency are negligible.

Some radial distributions and the corresponding mean values for section 2 and 3 are shown in Figures 4.3.7–12.

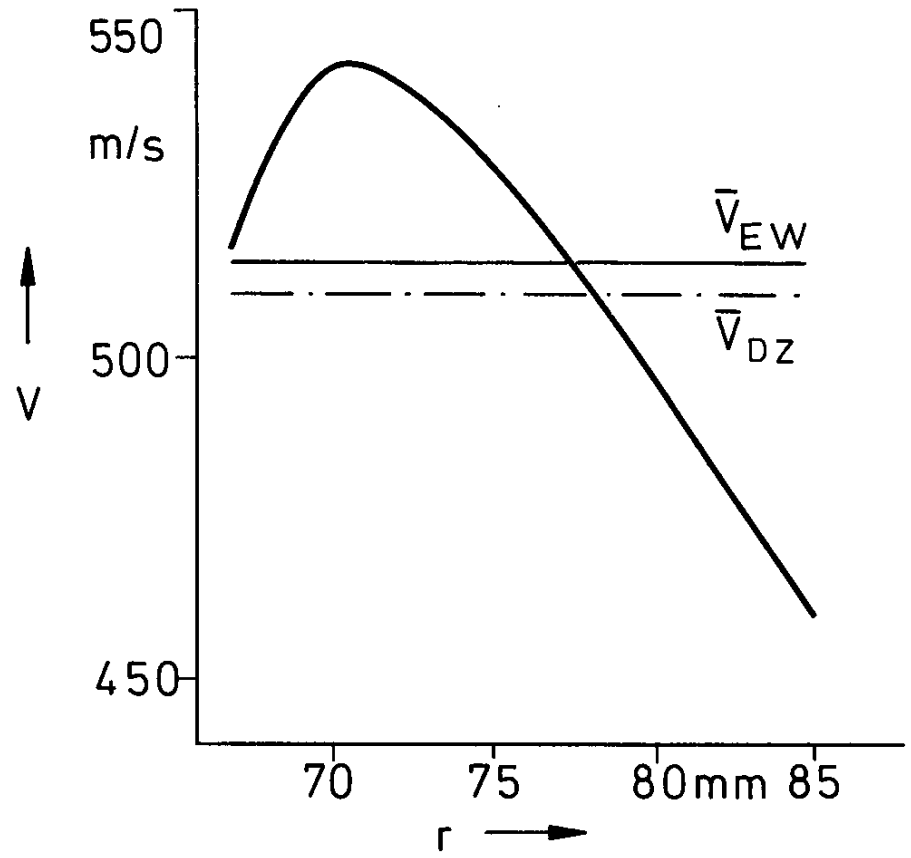

Fig.4.3.7 Section 2, velocity

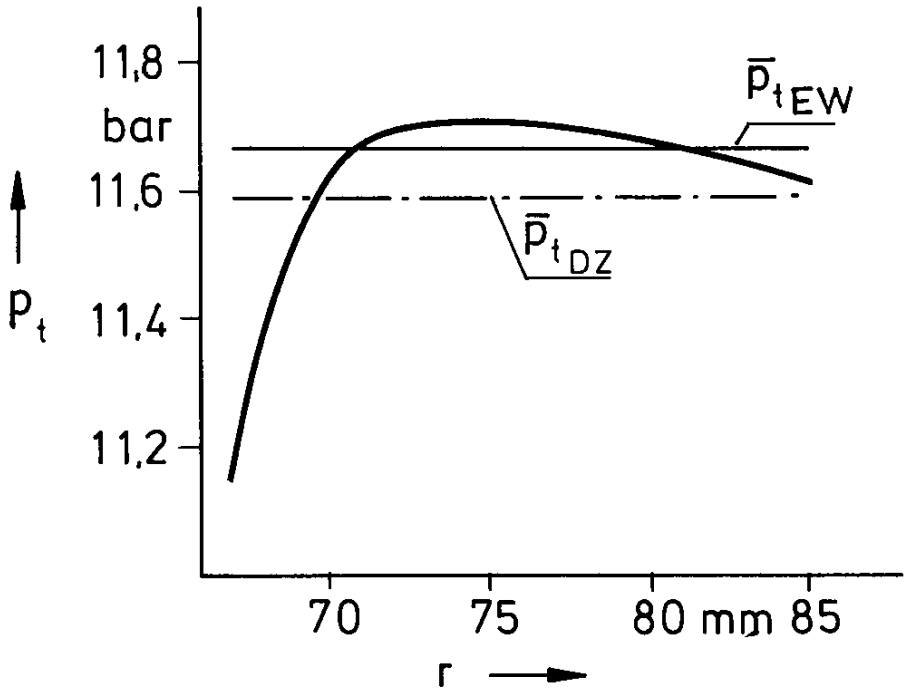

Fig.4.3.8 Section 2, total pressure

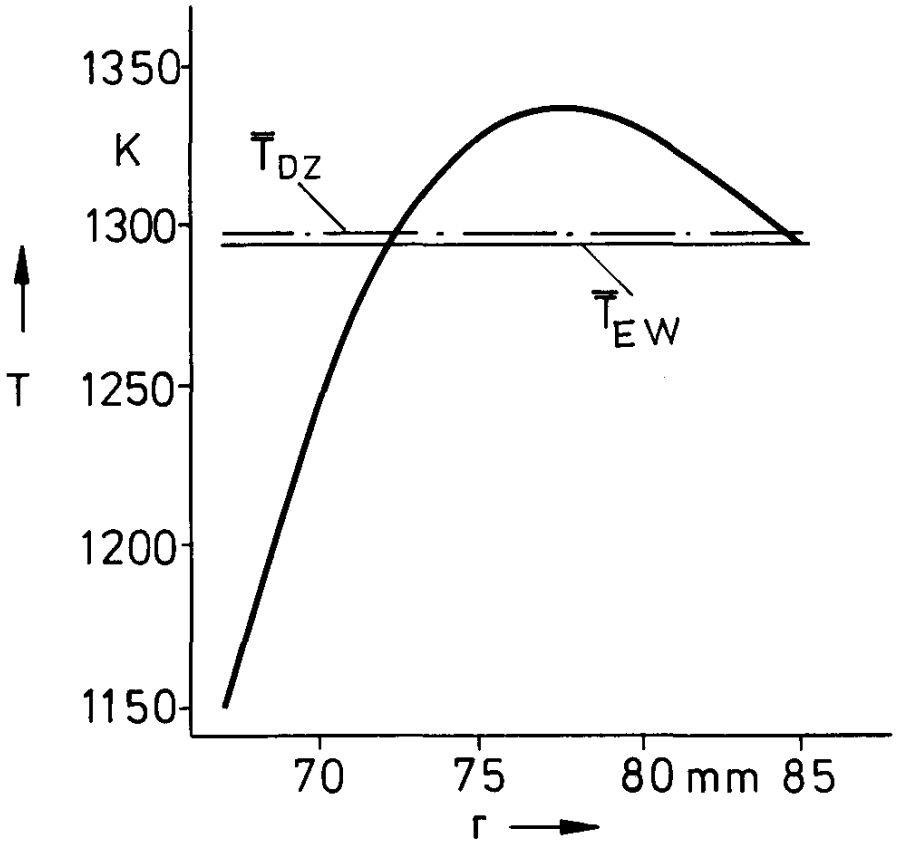

Fig.4.3.9 Section 2, static temperature

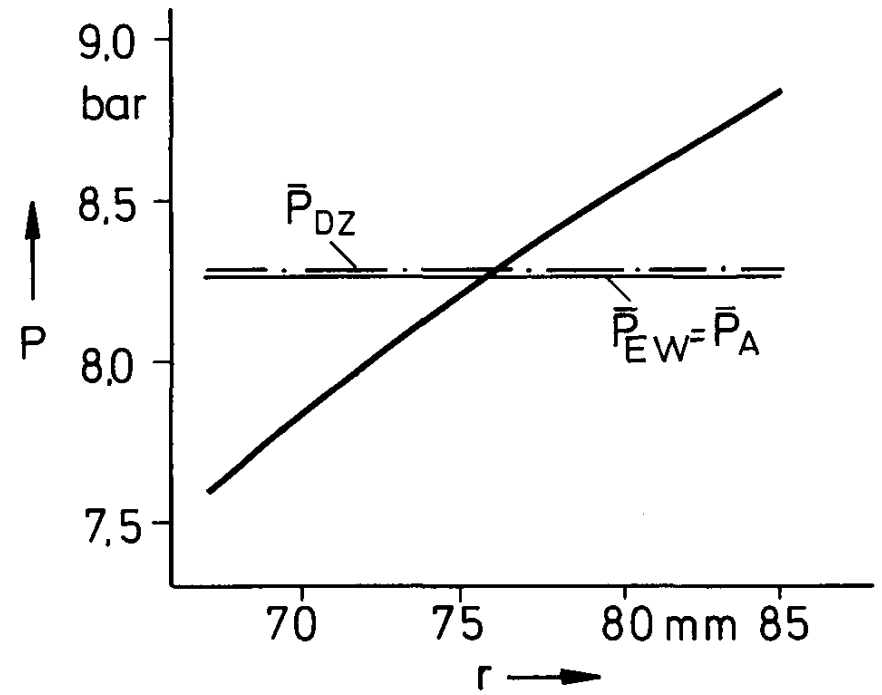

Fig.4.3.10 Section 2, static pressure

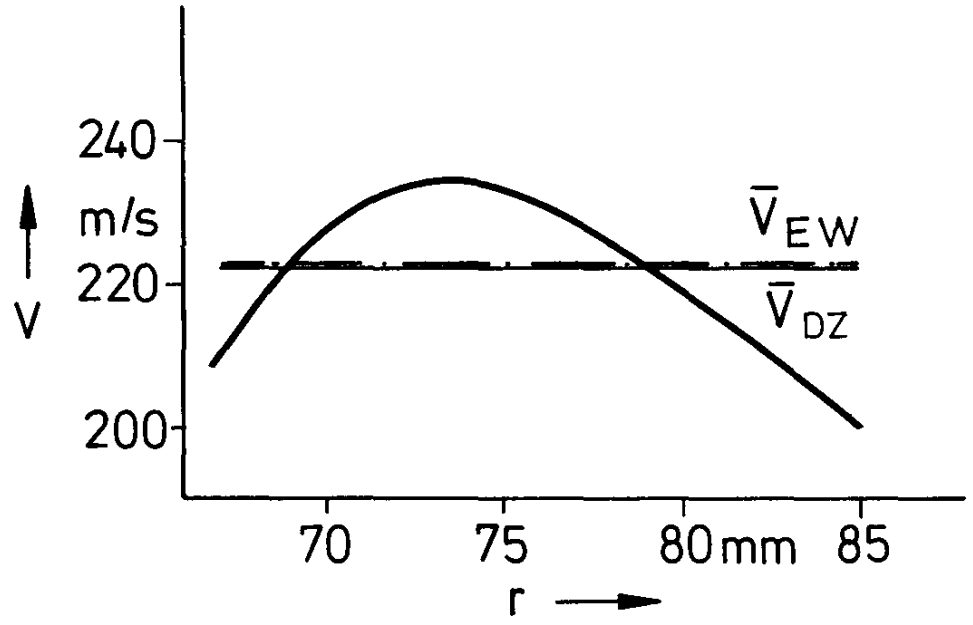

Fig.4.3.11 Section 3, velocity

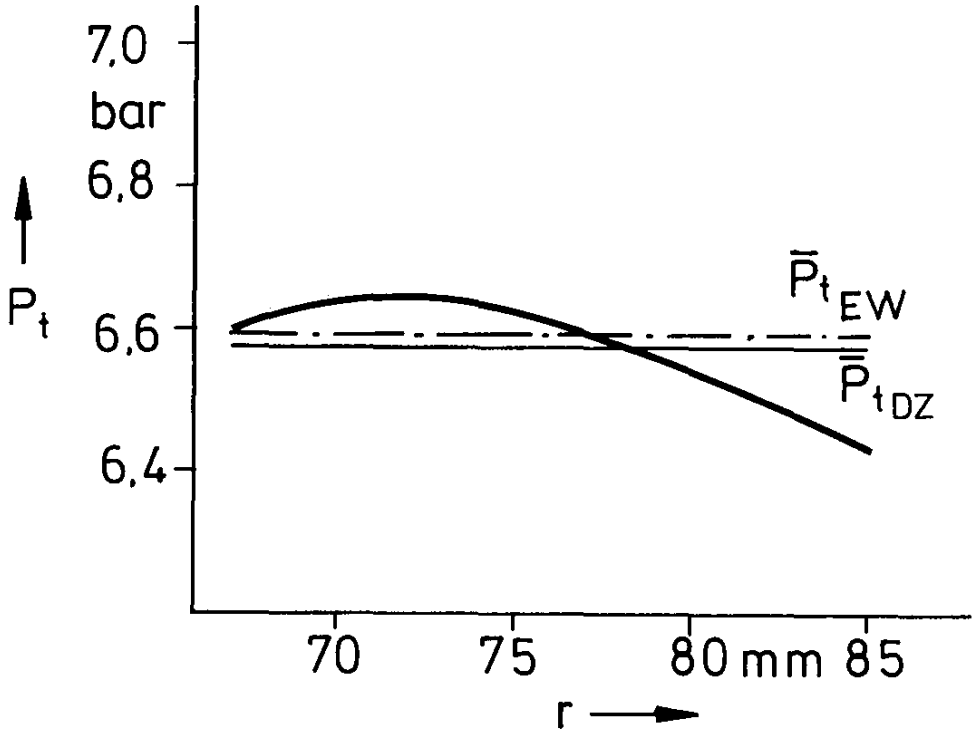

Fig.4.3.12 Section 3, total pressure

4.4 ENGINE SYSTEM ANALYSIS

Notations

The notations used in paragraph 4.4 are identical with those in paragraph 3.2. In addition, the symbol h^* is used.

$$h^* = \frac{h}{R}$$

4.4.1 General

4.4.1.1 Introduction

In the section below, an example is given of an engine to which the Pianko method described in paragraph 3.2 is applied. The engine is a turbojet (see figure below) consisting of the following components: a compressor, a combustor, a turbine, a mixer-diffuser, a reheat duct and an exhaust nozzle.

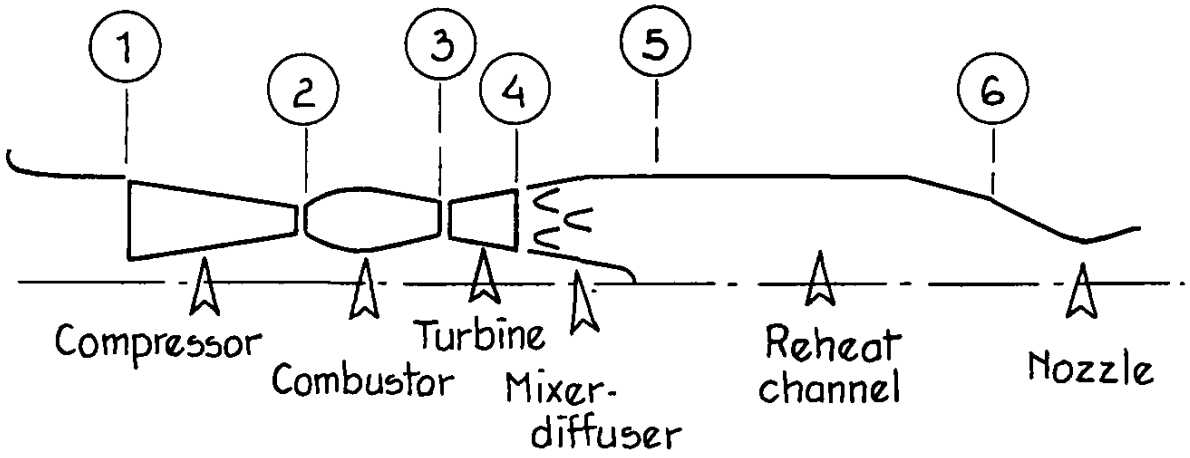

The calculations will be carried out in the planes (1), (2), (3), (4), (5) and (6) where the aerothermodynamic data of the heterogeneous flow are known. The total area is divided into a number of elementary areas ΔA at the centre of which the total pressure P_t, the total temperature T_t, the static pressure P_s, the angle formed by the velocity V with the normal to the section plane, and the fuel/air ratio (FAR) are known.

The various sections (1) to (6) will be designated as:

(1) Compressor inlet
(2) Combustor inlet
(3) Turbine inlet
(4) Mixer-Diffuser inlet
(5) Reheat duct inlet
(6) Exhaust nozzle inlet.

In each of these sections, the average total temperature and the average total pressure will be calculated by the Pianko method explained in paragraph 3.2. For comparison purposes, the results obtained with Dzung's method (applied systematically with $\gamma = \text{const} = 1.4$) will also be given.

4.4.1.2 Data

The data in the various sections are summed up in the following tables.

Important note: The reader will notice that, in all the sections considered, the static pressure is constant and the flow normal to the section. This assumption, which is by no means compulsory, has been chosen only with a view to simplifying calculations.

Section 1

ΔA	m^2	0.1	0.1	0.1	0.1	0.1	0.1	0.1	0.1	0.1	0.1
P_t	bar	0.9	0.92	0.94	0.97	0.98	0.99	1	1	1	1
T_t	K	290	290	290	290	290	290	290	290	290	290
P_s	bar	0.757	0.757	0.757	0.757	0.757	0.757	0.757	0.757	0.757	0.757
angle		0	0	0	0	0	0	0	0	0	0
FAR		0	0	0	0	0	0	0	0	0	0

Section 2

ΔA	mm^2	7918	8824	9841	10840	12470	13330	14330	14330	14330	14330
P_t	bar	18.377	18.079	17.768	17.627	17.113	16.943	16.771	16.771	16.771	16.771
T_t	K	790	780	770	760	750	745	740	740	740	740
P_s	bar	15.3	15.3	15.3	15.3	15.3	15.3	15.3	15.3	15.3	15.3
angle		0	0	0	0	0	0	0	0	0	0
FAR		0	0	0	0	0	0	0	0	0	0

Section 3

ΔA	mm^2	10290	11860	13430	15250	17800	19640	20250	20480	20730	21010
P_t	bar	17.5	17.1	16.8	16.7	16.2	16	15.9	15.8	15.7	15.6
T_t	K	1300	1350	1400	1500	1600	1700	1650	1600	1550	1500
P_s	bar	14	14	14	14	14	14	14	14	14	14
angle		0	0	0	0	0	0	0	0	0	0
FAR		0.0229	0.0229	0.0229	0.0229	0.0229	0.0229	0.0229	0.0229	0.0229	0.0229

Section 4

ΔA	mm^2	104530	113922	79362	65977	59213	51137	56753	59107	58005	68330
P_t	bar	3.408	3.408	3.552	3.765	3.965	4.320	4.128	4.032	4.028	3.801
T_t	K	892	931	1002.5	1116	1229	1336	1289	1238	1185.5	1134
P_s	bar	3.312	3.312	3.312	3.312	3.312	3.312	3.312	3.312	3.312	3.312
angle		σ	0	0	0	0	0	0	0	0	0
FAR		0.0229	0.0229	0.0229	0.0229	0.0229	0.0229	0.0229	0.0229	0.0229	0.0229

Section 5

ΔA	mm^2	95240	95240	95240	95240	95240	95240	95240	95240	95240	95240
P_t	bar	3.6014	3.6235	3.7274	3.8219	3.9374	3.9374	3.9269	3.7694	3.7169	3.7169
T_t	K	1000	1050	1100	1150	1200	1250	1200	1140	1100	1080
P_s	bar	3.5552	3.5552	3.5552	3.5552	3.5552	3.5552	3.5552	3.5552	3.5552	3.5552
angle		0	0	0	0	0	0	0	0	0	0
FAR		0.0229	0.0229	0.0229	0.0229	0.0229	0.0229	0.0229	0.0229	0.0229	0.0229

Section 6

ΔA	mm^2	50000	60000	85000	100000	100000	100000	100000	100000	100000	100000
P_t	bar	3.280	3.285	3.376	3.422	3.642	3.631	3.621	3.421	3.346	3.409
T_t	K	1750	1800	1850	1900	1950	2000	1950	1890	1850	1830
P_s	bar	2.9	2.9	2.9	2.9	2.9	2.9	2.9	2.9	2.9	2.9
angle		0	0	0	0	0	0	0	0	0	0
FAR		0.05	0.05	0.05	0.05	0.05	0.05	0.05	0.05	0.05	0.05

4.4.1.3 Calculation method

In the general case, calculations are made with γ and C_p being variables. For this purpose, the integrals are assumed to be known

$$h^*(T) = \frac{h(T)}{R} = \frac{1}{R}\int C_p(T)\,dT$$

and

$$\Phi(T) = \frac{1}{R}\int \frac{C_p(T)}{T}\,dT$$

as functions of the temperature and fuel/air ratio. It is also admitted that the functions can be inverted, that is to say that knowing the fuel/air ratio and one of the values h^* or Φ enables us to know the temperature.

In an elementary section ΔA, where the fuel/air ratio and the total temperature are known, we calculate

$$\Phi_t = \Phi(T_t) = \frac{1}{R}\int^{T_t} \frac{C_p(T)\,dT}{T}$$

and

$$h^*_t = \frac{h(T_t)}{R} = \frac{1}{R}\int^{T_t} C_p(T)\,dT\,.$$

As the total pressure P_t is known, the specific entropy can be calculated

$$s = R[\Phi_t - \ln P_t]\,.$$

Then, we can calculate the static temperature T_s by means of the function $\Phi_s = \bar{\Phi}(T_s)$ by writing that the entropy calculated with the total values (P_t, T_t) is equal to the entropy calculated with the static values (P_s, T_s), that is:

$$\Phi_s - \ln P_s = \Phi_t - \ln P_t\,.$$

Therefore:

$$\Phi_s = \Phi(T_s) = \Phi(T_t) - \ln \frac{P_t}{P_s}$$

Knowing $\Phi(T_s)$, we can calculate T_s, then the static enthalpy $h_s = h(T_s) = [R \times h^*(T_s)]$. The velocity V is then calculated by

$$V = \sqrt{2[h(T_t) - h(T_s)}$$

If we take into account the state equation $P_s/p = RT_s$, the mass flow running through the section ΔA is

$$d\dot{m} = \frac{P_s \times V \times \Delta A}{RT_s}.$$

Note: When γ may be regarded as constant, the calculations are necessarily simpler.

4.4.2 Compressor Inlet (section (1))

4.4.2.1 Calculations

The section (1) is located upstream of the compressor. The method used to calculate the homogeneous equivalent flow which will yield the total pressure (and the total temperature) is that described in paragraph 3.2.2. However, as the temperature in this section is homogeneous, it seems quite justifiable to carry out the calculation with $\gamma = \text{const}$. In this case, we have (Cf 3.2.7.2)

$$\bar{T}_t = \frac{\int T_t \, d\dot{m}}{\dot{m}} = 290 \text{ K}$$

and

$$\bar{P}_t = \left[\frac{\dot{m}}{\int \frac{d\dot{m}}{P_t^{(\gamma-1)/\gamma}}} \right]^{\frac{\gamma}{\gamma-1}}$$

The table below shows the various calculation steps.

ΔA m^2	0.1	0.1	0.1	0.1	0.1	0.1	0.1	0.1	0.1	0.1
P_t P_a	0.9×10^5	0.92×10^5	0.94×10^5	0.97×10^5	0.98×10^5	0.99×10^5	10^5	10^5	10^5	10^5
T_t K	290									
P_s P_a	0.757×10^5									
$d\dot{m}$ kg/s	16.019	17.087	18.088	19.487	19.930	20.363	20.786	20.786	20.786	20.786
$\frac{d\dot{m}}{P_t^{\gamma-1/\gamma}}$	0.6154	0.6523	0.6863	0.7327	0.7472	0.7612	0.7748	0.7748	0.7748	0.7748

From this table, we derive

$$\dot{m} = \Sigma \, d\dot{m} = 194.1 \text{ kg/s}$$

$$\sum \frac{d\dot{m}}{P_t^{(\gamma-1)/\gamma}} = 7.2944$$

and

$$\bar{P}_t = \left[\frac{194.1}{7.2944} \right]^{1.4/0.4} = 97220 \, P_a$$

Therefore, the average values in the section (1) are:

$$\overline{T}_t = 290 \text{ K}$$

$$\overline{P}_t = 0.9722 \text{ bar}$$

4.4.2.2 Influence of the compressor pressure ratio on the calculated total average pressure

The total pressure $P_t = 0.97220$, as calculated above, is *independent* of the compressor pressure ratio, as it results from a calculation where γ is assumed to be constant.

4.4.2.3 Calculation with the Dzung method

The results are:

$$\overline{T}_t = 290 \text{ K}$$

$$\overline{P}_t = 0.9709 \text{ bar}$$

4.4.3 Combustor Inlet (section (2))

4.4.3.1 Calculations

The section (2) is located upstream of the combustor. The method used to calculate the average values is that described in paragraph 3.2.4. Since the static pressure in the section (2) is uniform (and equal to 15.3 bars), this value will be chosen for the static pressure of the homogeneous flow

$$\overline{P}_s = 15.3 \text{ bar}$$

Note: If the static pressure were not uniform, the value chosen for $\overline{P}_s$ would have been

$$\overline{P}_s = \left[\frac{\int_{A2} P_s^{(\gamma-1)/\gamma} \, d\dot{m}}{\int_{A2} d\dot{m}} \right]^{\gamma(\gamma-1)}$$

according to the formula recommended in paragraph 3.2.4.5.

The calculations are shown in the following table.(page 137 opposite).

We infer from this table that:

$$\dot{m} = \Sigma \, d\dot{m} = 192.9 \text{ kg/s}$$

$$\overline{h}_t^* = \frac{\overline{h}_t}{R} = \frac{\Sigma \, h_t d\dot{m}}{\Sigma \, d\dot{m}} = \frac{518434}{192.9} = 2687.6$$

$$\overline{h}_s^* = \frac{\overline{h}_s}{R} = \frac{\Sigma \, h_s d\dot{m}}{\Sigma \, d\dot{m}} = \frac{501382}{192.9} = 2599.2$$

The following temperatures correspond to the values of $\overline{h}_t^* = 2687.6$ and $\overline{h}_s^* = 2599.2$

$$\overline{T}_t = 754 \text{ K}$$

and

$$\overline{T}_s = 730.7$$

$$\overline{\Phi}_t = \overline{\Phi}(754) = 23.255 \text{ corresponds to } \overline{T}_t = 754$$

and

$$\overline{\Phi}_s = \overline{\Phi}(730.7) = 23.135 \text{ corresponds to } \overline{T}_s = 730.7 \, .$$

SECTION 2

Table of Calculations for Combustor Inlet

ΔA	m^2	0.0079178	0.008824	0.009841	0.01084	0.01246	0.01333	0.014326	0.014326	0.014326	0.014326
P_t	bar	18.377	18.079	17.768	17.627	17.113	16.943	16.771	16.771	16.771	16.771
T_t	K	790	780	770	760	750	745	740	740	740	740
P_s	bar	15.3	15.3	15.3	15.3	15.3	15.3	15.3	15.3	15.3	15.3
V	m/s	283.70	269.3	253.5	245.2	217.09	206.64	195.5	195.5	195.5	195.5
$d\dot{m}$	kg/s	15.900	16.965	17.966	19.353	19.802	20.246	20.671	20.671	20.671	20.671
h_t^*		2824.2	2786	2748.0	2710	2672.1	2653	2634	2634	2634	2634
h_s^*		2683.9	2659.7	2636	2605.7	2590	2597	2567.7	2567.7	2567.7	2567.7
$h_t^* \times d\dot{m}$		44904	47260	49370	52450	52910	53720	54455	54455	54455	54455
$h_s^* \times d\dot{m}$		42674	45120	47360	50420	51290	52210	53077	53077	53077	53077

Applying the method described in paragraph 3.2 (3.2.4.6), we calculate:

$$\overline{P}_t = 15.3 \exp[23.255 - 23.135]$$

$$\overline{P}_t = 17.251 \text{ bar}.$$

The total average values in the section (2) are therefore

$$\boxed{\begin{aligned} \overline{T}_t &= 754 \text{ K} \\ \overline{P}_t &= 17.251 \text{ bar} \end{aligned}}$$

4.4.3.2 Influence of downstream conditions on the calculated total average pressure

The total pressure $\overline{P}_t = 17.251$, as calculated above, is independent of any physical process taking place downstream of the plane 2. It is an *intrinsic value* which depends only on upstream combustor data.

4.4.3.3 Calculation with the Dzung method

The results obtained are:

$$\boxed{\begin{aligned} \overline{T}_t &= 754 \text{ K} \\ \overline{P}_t &= 17.210 \text{ bar} \end{aligned}}$$

4.4.4 Turbine Inlet (section (3))

4.4.4.1 Calculations

The section (3) is located upstream of the turbine. The method used to calculate the average values is that described in paragraph 3.2.3. The calculations will be carried out with γ function of the temperature. The values of the functions $h^*(T)$ and $\Phi(T)$ are taken for the value of FAR = 0.0299. To apply the method described in paragraph 3.2.3, we must know the total pressure P_{te} at the turbine exit, that is to say the total pressure in the plane 4, which is presently unknown.

In carrying out the calculations, we shall assume that there is in the turbine an isentropic expansion down to $P_{te} = 4$ bars. As we shall see in paragraph 4.4.4.2 the influence of P_{te} on the value of the total pressure $\overline{P}_t$ calculated in the plane 3 is very small.

The steps of the calculations are shown on the table opposite.

From the table we derive

$$\dot{m} = \Sigma \, d\dot{m} = 198.8 \text{ kg/s}$$

$$\overline{h}_t^* = \frac{\Sigma \, h_t^* \, d\dot{m}}{\Sigma \, d\dot{m}} = \frac{1189800}{198.8} = 5984.9$$

$$\overline{h}_{te}^* = \frac{\Sigma \, h_{te}^* \, d\dot{m}}{\Sigma \, d\dot{m}} = \frac{826800}{198.8} = 4158.9$$

the following temperatures correspond to the above values of $\overline{h}_t^*$ and $\overline{h}_{te}^*$:

$$\overline{T}_t = 1525 \text{ K}$$

and

$$\overline{T}_{te} = 1102 \text{ K}.$$

With these temperatures, we calculate

$$\overline{\Phi}_t = \Phi(1525) = 26.4706$$

SECTION 3

Table of Calculations for Turbine Inlet

ΔA	m^2	0.01029	0.01186	0.01343	0.01525	0.01780	0.01964	0.02025	0.02048	0.02073	0.02101
P_t	bar	17.5	17.1	16.8	16.7	16.2	16.0	15.9	15.8	15.7	15.6
T_t	K	1300	1350	1400	1500	1600	1700	1650	1600	1550	1500
P_s	bar	14	14	14	14	14	14	14	14	14	14
FAR		0.0229	0.0229	0.0229	0.0229	0.0229	0.0229	0.0229	0.0229	0.0229	0.0229
$d\dot{m}$	kg/s	16.378	17.474	18.502	19.956	20.427	20.884	21.308	21.305	21.296	21.288
$\Phi(T_t)$		25.775	25.938	26.096	26.398	26.681	26.949	26.817	26.681	26.541	26.398
$\Phi(T_{te})$		24.299	24.485	24.661	24.968	25.282	25.562	25.437	25.307	25.173	25.037
T_{te}	K	915.7	958	999.6	1076	1158.6	1237	1201	1165	1129	1094
h_t^*		5002	5218	5436	5874	6316	6760	6538	6316	6094	5874
h_{te}^*		3386.7	3560	3730.6	4048	4397	4732	4579	4426	4273	4122
$h_t^* \times d\dot{m}$		81933	91179	100577	117221	129017	141176	139311	134562	129778	125045
$h_{te}^* \times d\dot{m}$		55474	62207	69023	80782	89817	98823	97569	94296	90998	87749

and

$$\bar{\Phi}_{te} = \Phi(1102) = 25.0708 .$$

From this, we derive $\bar{P}_t$ by

$$\bar{P}_t = P_{te} \exp[26.4706 - 25.0708] .$$

With $P_{te} = 4$ bar , we obtain

$$\bar{P}_t = 16.217 \text{ bar} .$$

Therefore, the total average values in the section 3 are

$\bar{T}_t = 1525$ K
$\bar{P}_t = 16.217$ bar

4.4.4.2 Influence of downstream conditions on the calculated total average pressure

The value $\bar{P}_t = 16.217$ bars calculated above is not an intrinsic value. It depends on the value of the total pressure P_{te} , that is to say the total average pressure at the turbine exit. In the above calculation, we have taken $P_{te} = 4$ bar . In fact, the value of $\bar{P}_t$ which will be calculated below in the plane 4, will be 3.88 bar. The table below enables us to quantify the influence of P_{te} on the value of $\bar{P}_t$ calculated upstream of the turbine.

P_{te} bar	2	3.6	4	10
$\bar{P}_t$ bar	16.213	16.217	16.217	16.220
Divergence/ calculation with $P_{te} = 3.88$	−0.03%	0	0	+0.02%

We note that the fact of having taken 4 bar (instead of 3.88) for P_{te} leads to no error on $\bar{P}_t$ calculated with 3 decimals. Even if we had chosen for P_{te} values as extreme as 2 bar or 10 bar, the errors concerning $\bar{P}_t$ would be below 0.03%, that is to say quite negligible. Therefore, we can conclude that the proposed method leads us to calculate a *virtually intrinsic value* upstream of the turbine.

4.4.4.3 Calculation based on the Dzung method

The results obtained are:

$\bar{T}_t = 1524.2$ K
$\bar{P}_t = 16.210$ bar

4.4.5 Mixer-Diffuser Inlet (section (4))

4.4.5.1 Calculations

The section (4) is located upstream of the mixer-diffuser. In this case, as explained in paragraph 3.2.6, there are several possible options. For instance, we can deal with the section (4) as we would with a turbine inlet or with a reheat duct inlet. However, the velocities in the section 4 are too high to give a realistic representation of a reheat duct inlet. For this reason, to calculate the average values, we shall regard the section 4 as in the upstream turbine plane. The calculation method is therefore identical with that described in the previous paragraph 4.4.4. Here, we have assumed that the total pressure at the hypothetic turbine exit is 2 bar.

The following table provides the steps of the calculation, the results of which are

$\bar{T}_t = 1147.8$ K
$\bar{P}_t = 3.883$ bar

SECTION 4

Table of Calculation for Mixer-Diffuser Inlet

ΔA	m^2	0.104530	0.113922	0.079362	0.065977	0.059213	0.051137	0.056753	0.059107	0.058005	0.068327
P_t	bar	3.408	3.408	3.552	3.765	3.965	4.320	4.128	4.032	4.028	3.801
T_t	K	892	931	1002.5	1116	1229	1336	1289	1238	1185.5	1134
P_s	bar	3.312	3.312	3.312	3.312	3.312	3.312	3.312	3.312	3.312	3.312
FAR		0.0229	0.0229	0.0229	0.0229	0.0229	0.0229	0.0229	0.0229	0.0229	0.0229
$d\dot{m}$	kg/s	16.378	17.474	18.502	19.956	20.427	20.884	21.308	21.305	21.295	21.288
$\Phi(T_t)$		24.1922	24.3673	24.6731	25.1231	25.5339	25.8936	25.7388	25.5652	25.3798	25.1909
$\Phi(T_{te})$		23.6593	23.8343	24.0987	24.4905	24.8495	25.1235	25.0142	24.8641	24.6797	24.5487
T_{te}		781.2	816.4	871.7	959.34	1046	1116.3	1087.7	1049.5	1004.2	973
h_t^*		3290.9	3449.2	3742.8	4216.6	4696.7	5157.6	4954.4	4735.2	4510.9	4292.6
h_{te}^*		2849.21	2987.8	3209.2	3564.9	3922.4	4217.0	4097.1	3937.5	3749.3	3620.7
$h_t^* \times d\dot{m}$		53898	60271	69249	84146	95935	107710	105568	100883	96064	91380
$h_{te}^* \times d\dot{m}$		46664	52209	59377	71141	80119	88068	87301	83888	79845	77077

4.4.5.2 Influence of downstream conditions on the calculated total average pressure

As stated in paragraph 4.4.4.2, the influence of the expansion rate of the turbine on the total average pressure calculated upstream of the turbine is quite negligible. However, the flow given in the section 4 located downstream of the turbine would be identical if there were an exhaust nozzle downstream of this section. In other words, we can calculate the section 4 as a section upstream of an exhaust nozzle. In this case, dealing with the case of an adapted convergent-divergent nozzle, we would have found:

$$\bar{P}_t = 3.835 \text{ bar}$$

that is a value different by −1.2% from the value found previously.

4.4.5.3 Calculation with the Dzung method

The results obtained are:

$$\bar{\bar{T}}_t = 1146.6 \text{ K}$$

$$\bar{P}_t = 3.809 \text{ bar}$$

4.4.6 Reheat Duct Inlet (section (5))

4.4.6.1 Calculations

The outlet of the mixer in the section (5) is upstream of the reheat channel. The calculation method is described in paragraph 3.2.5.

The phases of the calculation are shown in the table opposite.

From this table of calculations, we derive

$$\dot{m} = \Sigma \, d\dot{m} = 198.8 \text{ kg/s}$$

$$h_t^* = \frac{\bar{h}_t}{R} = \frac{\Sigma \, h_t^* \times d\dot{m}}{\Sigma \, d\dot{m}} = \frac{864065}{198.8} = 4344$$

$$J = \Sigma \, P_s \Delta A + \Sigma \, V d\dot{m} = 338600 + 41052 = 379652 .$$

As $A = 0.9524 \text{ m}^2$, $J/A = 398626$.

Therefore, the three equations to be solved are:

$$\begin{cases} \bar{\rho}\bar{V} = 208.73 \\ \bar{h}_t^* = \bar{h}_s^* + \dfrac{\bar{V}^2}{2R} = 4344 \\ \bar{P}_s + \bar{\rho}\bar{V} = 398626 . \end{cases}$$

The solution is

$$\bar{\bar{P}}_s = 359198 \text{ Pa}$$

$$\bar{\rho} = 1.1077$$

$$\bar{V} = 191 \text{ m/s}$$

$$\bar{T}_s = 1131 \text{ K}$$

$$\bar{T}_t = 1146.2 \text{ K}$$

$$\bar{\Phi}_s = 25.1806 \text{ corresponds to } \bar{T}_s = 1131 \text{ K}$$

$$\bar{\Phi}_t = 25.2363 \text{ corresponds to } \bar{T}_t = 1146.2 \text{ K} .$$

SECTION 5

Table of Calculations for Reheat Channel Inlet

ΔA	m^2	0.09524	0.09524	0.09524	0.09524	0.09524	0.09524	0.09524	0.09524	0.09524	0.09524
P_t	Pa	3.6014	3.6235	3.7274	3.8219	3.9374	3.9374	3.9269	3.7694	3.7169	3.7169
T_t	K	1000	1050	1100	1150	1200	1250	1200	1140	1100	1080
P_s	Pa	3.5552×10^5									
$d\dot{m}$	kg/s	10.417	12.036	18.647	22.663	26.515	25.991	26.154	20.419	18.074	18.237
V	m/s	85.749	106.64	171.951	217.21	263.3	268.9	259.88	194.64	166.77	165.21
h_t^*		3732.4	3939.9	4149.3	4360.2	4572.7	4786.7	4572.7	4317.9	4149.3	4065.4
$P_s \frac{V}{RT_s}$		106.541	126.37	195.81	237.92	278.39	272.88	274.61	214.39	189.77	191.48
$P_s \Delta A$		33860									
V x $d\dot{m}$		870.1	1283.5	3206.5	4922.9	6981.8	6989	6797	3974.5	3014.3	3013.1
h_t^* x $d\dot{m}$		37874	47421	77376	98820	121249	124415	119598	88172	74995	74142
h_s^*		3719.6	3920	4097.8	4278	4451.9	4660.7	4455	4252	4100.8	4017.8
T_s	K	996.9	1045.3	1087.8	1130	1171.57	1220.5	1172.3	1124.5	1088.6	1068.7

Then we calculate $\bar{P}_t$ by

$$\bar{P}_t = \bar{P}_s \exp[\bar{\Phi}_t - \bar{\Phi}_s].$$

With $\bar{P}_s = 3.59198$ bar , we find

$$\bar{P}_t = 3.798 \text{ bar}.$$

Therefore, the total average values in the section 5 are:

$\bar{T}_t = 1146.2$ K
$\bar{P}_t = 3.798$ bar

4.4.6.2 Influence of downstream conditions on the calculated total average pressure

We can assume that the reheat channel does not exist and that the plane 6 is upstream of an exhaust nozzle. The calculation of the section 6 as an exhaust nozzle inlet would lead to:

$$\bar{P}_t = 3.803 \text{ bars}$$

that is to say, higher by approximately 0.1%.

4.4.6.3 Calculation with the Dzung method

The results obtained are:

$\bar{T}_t = 1146$ K
$\bar{P}_t = 3.794$ bar

Note: The Pianko method applied above to paragraph 4.4.6.1 is, in principle, identical with the Dzung method. The divergences noted (0.2 K as regards the temperature and 0.1% as regards the total pressure) result from the fact that the calculation in paragraph 4.4.6.1 has been carried out with γ variable, and the calculation by the Dzung method with γ constant and equal to 1.4.

4.4.7 Exhaust Nozzle Inlet (section (6))

4.4.7.1 Calculations

The section 6 is located upstream of the exhaust nozzle. The method used to calculate the average values is that described in paragraph 3.2.2. The calculations will be carried out with γ variable. The functions $h^*(T)$ and $\Phi(T)$ are calculated for FAR = 0.5 . In order to apply the method described in paragraph 3.2.2, we have to know the ambient pressure and the static pressure in the exhaust plane of the nozzle. For the purpose of the calculation, we have chosen here:

$$P_0 = 1 \text{ bar}$$

$$P_{se} = 1.856 \text{ bar}.$$

The phases of the calculation are shown in the table opposite.

From this table we derive:

$$\dot{m} = \Sigma\, d\dot{m} = 204.5 \text{ kg/s}$$

$$h_t^* = \frac{\bar{h}_t}{R} = \frac{\Sigma\, h_t^*\, d\dot{m}}{\Sigma\, d\dot{m}} = \frac{1621260}{204.5} = 7927.9$$

$$F = \Sigma\, \Delta F = 224049 \text{ N}$$

that is $F/\dot{m} = 1095.6$ m/s .

SECTION 6

Table of Calculations for Nozzle Inlet

ΔA	m^2	0.04715	0.05658	0.080155	0.0943	0.0943	0.0943	0.0943	0.08487	0.080155	0.07544
P_t	bar	3.4782	3.4835	3.5800	3.6288	3.8621	3.8504	3.8398	3.6278	3.5482	3.6150
T_t	K	1750	1800	1850	1900	1950	2000	1950	1890	1850	1830
P_s	bar	3.0753	3.0753	3.0753	3.0753	3.0753	3.0753	3.0753	3.0753	3.0753	3.0753
$h^*(T_t)$		7236.7	7472.2	7708.5	7945.3	8182.8	8420.8	8182.8	7898	7708.5	7613.9
$\Phi(T_t)$		27.5336	27.6653	27.7937	27.9189	28.04115	28.1605	28.0411	27.8941	27.7937	27.7427
$\Phi(T_s)$		27.4104	27.5406	27.6417	27.7533	27.8133	27.9357	27.8190	27.7288	27.6506	27.5809
T_s	K	1704.2	1752.4	1790.7	1833.9	1857.5	1906.5	1860	1824.3	1794	1767.6
$h^*(T_s)$		7022.3	7249	7429.4	7633.5	7745	7977.5	7756	7588.3	7445	7320.5
$\Phi(T_{se})$		26.9063	27.0365	27.1366	27.2483	27.3082	27.4306	27.3140	27.238	27.1455	27.0759
T_{se}	K	1528.6	1572.4	1607.2	1645.7	1667	1711.5	1669.2	1637	1610.3	1586
$h^*(T_{se})$		6203.4	6406.3	6566.1	6749	6849	7057	6858.5	6708.4	6580.6	6468.7
$d\dot{m}$	kg/s	10.395	12.38	19.193	23.306	27.264	26.732	26.891	21.011	18.594	18.762
$h^*(T_t) \times d\dot{m}$		75232	92524	147950	185178	223098	225106	220046	165943	143336	142856
V_e		770.6	782.8	809.7	828.7	875.0	884.7	871.8	826.3	804.6	810.7
$\Delta A_e'$	m^2	0.0318	0.03846	0.05890	0.07158	0.08032	0.07996	0.07962	0.06438	0.05755	0.05677
ΔF	N	10732	12983	20582	25440	30731	30494	30259	22872	19887	20069

The three equations to be solved are:

$$\frac{F}{\dot{m}} = \frac{(185600 - 100000)}{\bar{\rho}_e \bar{V}_e} + \bar{V}_e = 1095.6$$

$$h^*(T_{se}) + \frac{V_e^2}{2R} = 7927.9$$

$$\frac{18560}{\bar{\rho}_e} = RT_{se} .$$

Solving these equations, we find

$$\bar{T}_{se} = 1637.3$$

and

$$\bar{V}_e = 836.3 \text{ m/s} .$$

In addition, the value which corresponds to $h_t^* = 7927.9$ is

$$\bar{T}_t = 1895.7 \text{ K}$$

$$\bar{T}_t = 1895.7 \text{ K gives } \bar{\Phi}_t = 27.9098$$

$$\bar{T}_{se} = 1637.3 \text{ K gives } \bar{\Phi}_{se} = 27.2243 .$$

Then, we calculate:

$$\bar{P}_t = \bar{P}_{se} \exp[\bar{\Phi}_t - \bar{\Phi}_{se}]$$

that is

$$\bar{P}_t = 1.856 \exp[27.9098 - 27.2243]$$

$$\bar{P}_t = 3.4730 \text{ bar} .$$

Therefore, the total average values in the section 6 are:

$$\boxed{\begin{aligned} \bar{T}_t &= 1895.7 \text{ K} \\ \bar{P}_t &= 3.6837 \text{ bar} \end{aligned}}$$

4.4.7.2 Influence of downstream conditions on the calculated total average pressure

The pressure $\bar{P}_t$ calculated above depends on the ambient pressure and on the value of the assumed static pressure P_{se} in the exhaust plane. In the three cases calculated:

$$\begin{cases} P_0 = 1 \text{ bar} \\ P_{se} = 1 \text{ bar} \end{cases} \qquad \begin{cases} P_0 = 1 \text{ bar} \\ P_{se} = 1.856 \text{ bar} \end{cases} \qquad \begin{cases} P_0 = 1 \text{ bar} \\ P_{se} = 0.928 \text{ bar} \end{cases}$$

We find the same total pressure $\bar{P}_t$ as calculated (with three decimals) $\bar{P}_t = 3.683$ bar . Therefore, the divergences are lower than 0.01% and can be disregarded.

4.4.7.3 Calculation with the Dzung method

The results obtained are:

$$\boxed{\begin{aligned} \bar{T}_t &= 1896 \text{ K} \\ \bar{P}_t &= 3.678 \text{ bar} \end{aligned}}$$

4.4.8 Synthesis and application of results

The results obtained are summed up in the following table:

Section			*1*	*2*	*3*	*4*	*5*	*6*
Pianko method	$\bar{T}_t$	K	290	754	1525	1147.8	1146.2	1895.7
	$\bar{P}_t$	bar	0.97221	17.251	16.217	3.883	3.798	3.683
Dzung method	$\bar{T}_t$	K	290	754	1524.2	1146.6	1146	1896
	$\bar{P}_t$	bar	0.9709	17.210	16.210	3.809	3.794	3.678
$\Delta\bar{P}_t/P_t$ between Pianko and Dzung methods			−0.1%	−0.2%	−0.04%	−1.9%	−0.1%	−0.1%

We note that the divergences between the temperatures calculated according to the two methods are quite negligible.

In general, the total pressures calculated according to the two methods are also very similar. The total pressure as calculated by the Dzung method is always lower than that calculated by the Pianko method. Generally, the divergences are of the order of 0.1%, except in the section 4, where a divergence of 1.9% appears. This results from the fact that the Dzung method includes *mixing losses*. The latter are especially high because the heterogeneity of the Mach numbers is high in section 4.

Owing to the values of the above table, we can calculate the performance of the engine components. We obtain:

	Polytropic efficiency of compressor	*Pressure loss in combustor*	*Polytropic efficiency of turbine*	*Pressure loss in mixer-diffuser*	*Pressure loss in reheat channel*
Pianko method	0.843	6%	0.859	2.18%	3%
Dzung method	0.843	5.8%	0.848	0.4 %	3%

The divergences between the two methods which appear above regarding the turbine and the mixer-diffuser are relatively high and lead us to believe that a more thorough analysis-comparison would be advisable. This is done in the following paragraph.

4.4.9 Comparison between Dzung and Pianko Methods

4.4.9.1 General

The pressure loss difference between the two methods in the mixer-diffuser is natural. As Dzung method ascribes the mixing losses to the upstream component, it logically ensues that the pressure loss between sections 3 and 4, calculated by this method, is lower than that calculated by the Pianko method which ascribes the mixing loss to the downstream component.

On the other hand, it would be useful to analyse in more detail the difference between the turbine efficiencies. For this purpose, it is necessary to have a reference efficiency independent of any averaging method and giving an overall representation of the turbine qualities. In the following paragraphs, we shall attempt to define a reference isentropic efficiency and a reference polytropic efficiency which can be used as criteria to compare the efficiencies obtained with any method. Such an efficiency will be called "reference efficiency".

Finally, in order that the comparison may not be erroneous due to the numerical process, all the calculations will be made with $\gamma = \text{const} = 1.3$.

4.4.9.2 Results

The table overleaf gives the results of the calculations for both methods:

			Section 3	*Section 4*	*Polytropic efficiency*	*Isentropic efficiency*
Pianko	$\bar{P}_t$	bar	16.2292	3.8839		
	$\bar{T}_t$	K	1524.35	1146.20	0.8640	0.8826
Dzung	$\bar{P}_t$	bar	16.2104	3.8090		
	$\bar{T}_t$	K	1524.35	1146.20	0.8531	0.8732

4.4.9.3 Definition and calculation of the "reference efficiency"

4.4.9.3.1 Isentropic Efficiency

When the flow is homogeneous at the inlet and exit of a turbine engine, the definition of an isentropic efficiency is trivial. In a turbine, the isentropic efficiency is defined as the real enthalpy variation/ideal enthalpy variation ratio:

$$\eta_T = \frac{\Delta H_{t\ real}}{\Delta H_{t\ ideal}}.$$

The ideal enthalpy variation is that which corresponds to an isentropic expansion from the state at the turbine inlet (P_{ti}, T_{ti}) down to the total pressure P_{te} at the turbine exit. If we assume that γ is constant, we obtain:

$$\eta_T = \frac{T_{ti} - T_{te}}{T_{ti}\left[1 - \left(\frac{P_{te}}{P_{ti}}\right)^{(\gamma-1)/\gamma}\right]}.$$

When the flow is heterogeneous at the turbine inlet and exit, the notion of isentropic efficiency can be extended by assuming that the turbine is composed of a large number of turbines operating in parallel.

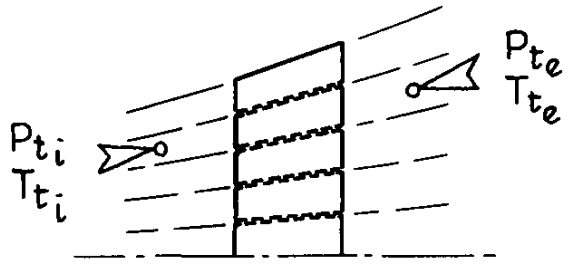

This amounts to figuring out that the various streamlets which flow through the turbine can be individualized. The ideal enthalpy variation of a streamlet which can be individualized in this way is:

$$\Delta H_{ideal} = dh_{ideal} \times d\dot{m}.$$

That is, in the case when γ is constant:

$$\Delta H_{ideal} = c_p\, T_{ti}\left[1 - \left(\frac{P_{te}}{P_{ti}}\right)^{(\gamma-1)/\gamma}\right] d\dot{m}.$$

Then, the "reference isentropic" efficiency becomes equal to:

$$\eta_T = \frac{(\bar{T}_{ti} - \bar{T}_{te})\,\dot{m}}{\int_A T_{ti}\left[1 - \left(\frac{P_{te}}{P_{ti}}\right)^{(\gamma-1)/\gamma}\right] d\dot{m}}$$

where

$$\bar{T}_{ti} = \frac{1}{\dot{m}_i} \int_{A_i} T_{ti}\, d\dot{m}$$

$$\bar{T}_{te} = \frac{1}{\dot{m}_e} \int_{A_e} T_{te}\, d\dot{m}.$$

Remark: The concept of "reference isentropic efficiency" which is explained above for the case of a turbine is also applicable to the case of a compressor.

It is evident that, during tests on a real turbine engine, it is almost impossible to individualize the various streamlets by measurements.

However, the calculation of the "reference efficiency" is possible in certain special cases:

(i) When the flow in the turbine (or compressor) is the result of a calculation.

(ii) When the total temperature and the total pressure are uniform at the inlet.

(iii) When the total pressure is uniform at the exit.

In the present Chapter 4.4 where the turbine is calculated, the various streamlets are given as individualized; it is therefore possible to calculate the reference isentropic efficiency.

The table below shows the details of the calculations:

P_{ti}	bar	17.5	17.1	16.8	16.7	16.2	16.0	15.9	15.8	15.7	15.6
T_{ti}	K	1300	1350	1400	1500	1600	1700	1650	1600	1550	1500
P_{te}	bar	3.408	3.408	3.552	3.765	3.965	4.320	4.128	4.032	4.028	3.801
$d\dot{m}_i$	kg/s	16.377	17.466	18.486	19.924	20.377	20.818	21.247	21.250	21.249	21.250
$T_{ti}\left[1-\left(\frac{P_{te}}{P_{ti}}\right)^{(\gamma-1)/\gamma}\right]$		408.8	419.57	421.9	436.36	443.7	443.31	441.26	432.54	417.62	417.12
$T_{ti}\left[1-\left(\frac{P_{te}}{P_{ti}}\right)^{(\gamma-1)/\gamma}\right]d\dot{m}$		6695.0	7328.6	7799	8694.0	9042.0	9229.0	9375.5	9191.4	8874.1	8864.0

From this table we derive:

$$\dot{m} = \Sigma\, d\dot{m} = 198.4 \text{ kg/s}$$

$$\Sigma\, T_{ti}\left[1-\left(\frac{P_{te}}{P_{ti}}\right)^{(\gamma-1)/\gamma}\right] d\dot{m} = 85092.6$$

As we know, in addition, that:

$$\bar{T}_{ti} = 1524.35$$

and

$$\bar{T}_{te} = 1146.2$$

we obtain:

$$\eta_{ref} = \frac{378.15 \times 198.4}{85092.6}$$

$$\eta_{ref} = 0.8817\,.$$

4.4.9.3.2 Polytropic efficiency

When the flow is homogeneous at a turbine inlet and exit, the polytropic efficiency is defined by the following relation:

$$s_e - s_i = \left(1 - \frac{1}{\gamma_T}\right) [\phi_{te} - \phi_{ti}] \times R$$

where

$$\phi_{te} = \phi(T_{te}) = \frac{1}{R}\int^{T_{te}} \frac{c_p\, dT}{T}$$

$$\phi_{ti} = \phi(T_{ti}) = \frac{1}{R}\int^{T_{ti}} \frac{c_p\, dT}{T} .$$

When the flow which runs through a turbine is heterogeneous, an average polytropic efficiency called "reference polytropic efficiency" can be defined by taking the integral quantities. The reference polytropic efficiency is then defined by:

$$s_e - s_i = \left(1 - \frac{1}{r_{ref}}\right) \times R \times \left[\int_{A_e} \phi_{te}\, d\dot{m}_e - \int_{A_i} \phi_{ti}\, d\dot{m}_i\right].$$

Remark: The same generalization can be applied to a compressor in which the polytropic efficiency is defined by:

$$s_e - s_i = (1 - r_{ref})\, R\, [\phi_{te} - \phi_{ti}] .$$

In the case when γ is constant, we have:

$$s = R \times \ln \frac{T_t^{\gamma/(\gamma-1)}}{P_t}$$

$$\phi(T) = \ln T_t^{\gamma/(\gamma-1)} .$$

The reference polytropic efficiency of the turbine can be easily calculated.

We obtain:

$$r_{ref} = 0.8709 .$$

4.4.9.4 Comparison of efficiencies

	Polytropic	*Isentropic*
Reference efficiency	0.8709	0.8817
Efficiency obtained by the Pianko method	0.8640	0.8826
Efficiency obtained by the Dzung method	0.8531	0.8732

We note that:

(i) The differences between the calculated polytropic efficiencies and the reference efficiency are greater than those between the calculated isentropic efficiencies and the reference efficiency.

(ii) The efficiency calculated by the Pianko method is closer to the reference efficiency.

Chapter 5

CONCLUSIONS AND RECOMMENDATIONS

5.1 CONCLUSIONS

1. No uniform flow exists, in general, which simultaneously matches all the significant stream fluxes, aerothermodynamic and geometric parameters of a non-uniform flow.

Among the following parameters

- mass flow rate
- stagnation enthalpy flow rate
- entropy flow rate
- kinetic energy flow rate
- linear momentum flux
- stream force or dynalpy
- static pressure (when constant)
- area

only four can be correctly matched.

If the flow is swirling it is also possible to match its angular momentum.

2. Since the purpose of defining an equivalent uniform flow is to represent component performance in a thermodynamic cycle calculation, mass and stagnation enthalpy flux must be correctly matched. The choice of the two other conditions may depend on the use which will be made of the average so derived.

3. The study has therefore concentrated on examining a variety of alternative ways of averaging stagnation pressure

- area weighting
- mass weighting
- momentum-averaging (identical to Dzung's method for non-swirling flow)
- "entropy-weighting"

and a new method proposed by Pianko.

Of these methods, the first two have no theoretical justification. The first one (area weighting) is used because of its simplicity. The other methods satisfy theoretically desired requirements. The conditions satisfied by the Pianko method depend on the engine component considered.

The table overleaf shows what quantities are matched by the studied methods.

4. The fundamental difficulty which prevents a single stagnation pressure being correct for all purposes is that a non-uniform flow is not in equilibrium and the process of mixing involves a loss of stagnation pressure. The problem facing the user is whether to debit this probably unavoidable, but not yet incurred, loss to the "average" flow or not. The momentum-averaging (Dzung) and the Pianko method for components other than a reheat ducts inlet debit the full mixing loss to the upstream unit; the mass weighting and Pianko method (for other component than reheat duct) do not. The "entropy-weighting" method effectively assumes that mixing can occur without any such loss.

5. It follows that in representative flow conditions of a gas turbine engine (except the inlet of a nozzle) Dzung average stagnation pressure is, usually lower than the mass weighted and Pianko averages (which are often very close). The "entropy weighted" pressure is almost the same as the mass-weighted average in constant stagnation temperature flow

Method	*METHODS WITH THEORETICAL JUSTIFICATION*						*METHODS WITHOUT THEORETICAL JUSTIFICATION*	
	Momentum Averaging or Dzung	*"Entropy Weighting"*	*Pianko Method*				*Mass Weighting*	*Area Weighting*
			Compressor or Turbine Inlet	*Combustor Inlet*	*Reheat Duct Inlet*	*Exhaust Nozzle Inlet*		
Matched quantities	– Mass flow – Enthalpy – Dynalpy – Area	– Mass flow – Enthalpy – Entropy – Area	– Mass flow – Enthalpy – Stagnation enthalpy variation in an isentropic expansion (or compression)	– Mass flow – Enthalpy – Kinetic energy – Static pressure	– Mass flow – Enthalpy – Dynalpy – Area	– Mass flow – Enthalpy – Ideal thrust in an isentropic expansion	None*	None

* Mass flow may be considered as matched

but unrealistically high when large non-uniformity occurs in stagnation temperature. The area-weighting stagnation pressure is usually the lowest value and has no theoretical basis but is very easily obtained which is one of the principal reasons for its usage.

If the stagnation temperature of the flow is uniform, the "entropy-weighting" method ensures that the second law of thermodynamics is fulfilled. Mass-weighting, in that case, contravenes the second law. This effect is numerically small at Mach numbers commonly found at inter-component planes within a gas turbine, but can be very significant in supersonic flows.

6. Thermodynamic cycle calculations conducted by any of these pressure averaging methods will give the correct final result (engine performance), provided the same method is used throughout the engine. However, the various component efficiencies will not be the same. Specifically, Dzung's method credits the component which first introduces non-uniformity with lower efficiency than other methods (except area weighting).

The efficiency of other components will be little affected. The component which restores uniformity will be credited with a higher efficiency (such as mixer-diffuser).

7. A small number of numerical examples using practical non-uniformities characteristic of gas turbine components were undertaken. They showed that, except for the two-stream nozzle case, the numerical differences between the various "average" total pressures are quite small. Percentage differences referred to the Pianko mean* are summarized in the following table. Differences in numerical integration processes or in specific heat assumptions can amount to ± 0.1%.

		Mass Weighting	*Dzung*	*Area Weighting*
Section 4.2	Compressor Inlet	0.1	−1.3	−1.8
	Outlet	−0.2	0.2	−0.4
	Turbine Inlet	0	0	0
	Outlet	0.1	−0.1	−0.1
Section 4.4	Compressor Inlet	0.1	−0.1	−0.2
	Outlet	−0.2	−0.2	−0.7
	Turbinet Inlet	0.4	0	−0.3
	Outlet	−0.5	−1.9	−3.1
	Reheat Inlet	0.3	−0.1	−0.5
	Outlet	0.1	−0.1	−0.2

The larger figures occurred when there were large Mach number differences across the section (as after the high-distortion intake in the Section 4.3 example and at turbine outlet in the Section 4.4 example).

The Dzung mean total pressure was usually but not always lower; the area mean total pressure was always the lowest.

Although the differences were small, they were sufficient to lead to significant differences in component efficiency figures derived from them. Again using Pianko's efficiency as the datum the following percentage differences were found:

		Mass Weighting	*Dzung*	*Area Weighting*
Section 4.3	Compressor**	−0.2	+1.0	−1.3
	Turbine	−0.1	−0.2	+0.1
Section 4.4	Compressor	−0.1	0	−0.2
	Turbine	−0.5	−1.1	−1.5

* The choice of the Pianko method as a reference for comparison does not mean any preference for application.
** With uniform inlet.

In one example quoted to the Working Group, a difference of $1\frac{1}{2}\%$ in compressor efficiency was found.

If errors of this order are acceptable, the simplest method (area weighting) may be used. Also, if as in many test rigs, steps have been taken to ensure an almost uniform inflow, area weighting is also, obviously, acceptable.

As has been pointed out in paragraph 3, the Pianko and Dzung methods have theoretical justification and give different answers (in some cases significantly different) for the reason explained in paragraph 4. The justification for using mass-weighting or area-weighting must be assessed by examining how far they differ from the theoretically-justified methods. Mass-weighting was acceptably close to the Pianko mean in most of the examples considered, but area weighting showed differences many test centres would consider unacceptable.

The two-stream nozzle, in which the core and fan flows meet before the final nozzle, is a special case. The examples considered showed that it is unrealistic to form an "average" inlet stagnation pressure (by any method) across the two streams taken together and then to expect the nozzle coefficients to agree with those measured under uniform inflow conditions. Indeed the discharge and thrust coefficients cannot in general be simultaneously matched. In the example of Section 4.2 differences in both discharge and thrust coefficient of ± 6.5% were found.

This results from the impossibility to match simultaneously

- the mass flux
- the enthalpy
- the exit nozzle area
- the exit static pressure (or Mach number)
- the ideal thrust.

The possibilities to agree with the measured nozzle coefficient would be

(i) accept not to match one of the above parameters

(ii) accept two different average stagnation pressures: one for the discharge coefficient, one for the force coefficient.

Future work on averaging methods in an exhaust nozzle is needed to explore the various options.

8. When only the stagnation temperature and pressure have been calculated the "average" static pressure may be derived from the geometric area to ensure the correct mass flow, or alternatively when the average static pressure is chosen, an effective area is computed to fit the mass flow.

Some of the averaging methods studied include either a choice of the area or a choice of the static pressure.

9. The study has concentrated almost entirely on how to average flows which are assumed to be accurately measured in practice, although this is rarely so; the rakes or traverses may not provide detailed information on wall boundary layers, and often record stagnation pressure and temperature only, leaving static pressure to be interpolated from wall measurements. It is recognized that even the theoretically best averaging method cannot lead to a correct result if the input data are poor due to incomplete or inaccurate measurements. In some circumstances the error introduced by attempting an averaging method using poor input data may produce a result no more reliable than simple area weighting.

Using independently measured mass flow (when it differs from that derived from traverse plane measurements because of the inaccuracies) to derive average pressure are also considered, and a new correction method is suggested (see Section 4.15).

10. The study has illuminated the differences between the various averaging methods and why they occur. It has led to a single recommendation for temperature averaging but not to a single recommendation for pressure averaging. For pressure averaging the individual user must make the choice best suited to his particular application, in the light of the findings of the study.

5.2 RECOMMENDATIONS

1. Stream stagnation temperature should be averaged by mass-weighting stagnation enthalpy. In many practical cases, mass-weighting stagnation temperature will be adequate. In many test rigs, where stagnation temperature is almost uniform, area averaging of probe readings is acceptable.

2. Except in the case of propelling nozzles, stream stagnation pressure should be averaged by one of two methods, the Pianko or Dzung methods. The choice depends on where the user wishes to debit the mixing loss implied by the non-uniformity. Pianko's method debits it to the components downstream of the traverse plane whereas Dzung's method

debits it to the component upstream of the traverse plane. Mass-weighting may be considered an acceptable approximation to Pianko's method and is easier to specify. Area-weighting should only be used when the static pressure level and distribution cannot be reliably estimated and when the Mach number is small. It is usually closer to the Dzung average than the Pianko average. The "entropy weighting" method should not be used unless the stagnation temperature of the flow is uniform.

If the mixing loss will not necessarily be wholly incurred (as in a system which is designed to accept the non-uniformity) and the stagnation temperature is uniform, then "entropy weighting" gives a true thermodynamic upper bound for average stagnation pressure.

3. In undertaking an engine thermodynamic cycle calculation, the same pressure averaging method should be used for all components used to construct the cycle.

4. More work is needed to resolve some of the anomalies noted during the study, in particular to find a way of characterizing the entropy of a non-uniform stream, to examine by systematic examples the relationship between efficiencies derived by different methods and to find effective ways of using the extra information available when the total mass flow is separately measured. More work is particularly needed to evolve a satisfactory way of dealing with the multiple stream nozzles.

Chapter 6

LIST OF REFERENCES

CHAPTER 2

2.1		*Gas turbine engine inlet flow distortion guidelines.* Aerospace Recommended Practice ARP-1420, SAE, March 1978.
2.2		*Modern prediction methods for turbomachine performance.* AGARD-LS-83, June 1976.
2.3		*Through-flow calculations in axial turbomachinery.* AGARD-CP-195, May 1976.
2.4	Smith, L.H.	*The radial-equilibrium equation of turbomachinery.* Journal of Engineering for Power, Vol.88, Series A, No.1, pp.1–12, January 1966.
2.5	Hesse, W.J. Mumford, N.	*Jet propulsion for aerospace applications.* Second edition, Pitman Publishing Corporation, New York, 1964.
2.6	Smith, R.E., Jr Matz, R.J.	*Verification of a theoretical method of determining discharge coefficients for venturis operating at critical flow.* AEDC-TR-61-8 (AD263714), September 1961.
2.7		*Fluid meters: their theory and application.* Sixth edition, The American Society of Mechanical Engineers, New York, 1971.
2.8	Abbott, W.A. Philpot, P.	*The derivation of airflow from an engine face rake in a distorted flow.* National Gas Turbine Establishment M80010, March 1980.
2.9	Wehofer, S.	*Internal transonic flows with non-uniform inlet conditions.* AIAA Paper 70-635, 6th Propulsion Joint Specialist Conference, June 1970.
2.10	Cline, M.C.	*NAP: A computer program for the computation of two-dimensional, time dependent, inviscid nozzle flow.* LA-5984, Los Alamos Scientific Laboratory, University of California, January 1977.
2.11	Walker, N.D. Thomas, M.W.	*Experimental investigation of a 4-1/2 – stage turbine with very high stage loading factor.* NASA CR-2363, January 1974.
2.12	Urasek, D.C. Lewis, G.W. Moore, R.D.	*Effect of casing treatment on performance of an inlet stage for a transonic multistage compressor.* NASA TM X-3347, February 1976.
2.13	Urasek, D.C. Moore, R.D. Osborn, W.M.	*Performance of a single-stage transonic compressor with a blade-tip solidity of 1.3.* NASA TM X-2645, November 1972.
2.14	Oates, G.C.	*The aerothermodynamics of aircraft gas turbine engines.* AFAPL-TR-78-52, July 1978.
2.15	Dimmock, N.A.	*A compressor routine test code.* Aeronautical Research Council (Great Britain), R&M No.3337, January 1961.
2.16	Milner, E.J. Wenzel, L.M.	*Performance of a J85-13 compressor with clean and distorted inlet flow.* NASA TM X3304, December 1975.
2.17	Osborn, W.M. Moore, R.D. Steinke, R.J.	*Aerodynamic performance of a 1.35-pressure-ratio axial-flow fan stage.* NASA TP-1299, October 1978.

2.18 Smith, D.J.L. Johnston, I.H. Fullbrook, D.J. — *Investigations on an experimental single-stage turbine of conservative design.* R&M No.3541, January 1967.

2.19 Whitney, W.J. Schum, H.J. Behning, F.P. — *Cold-air investigation of a 3-1/2-stage fan-drive turbine with a stage loading factor of 4 designed for an integral lift engine.* NASA TM X-3289, October 1975.

2.20 Johnsen, R.L. Cullom, R.R. — *Altitude test of several afterburner configurations on a turbofan engine with a hydrogen heater to simulate an elevated turbine discharge temperature.* NASA TP-1068, November 1977.

2.21 Goldman, L.J. — *Cooled-turbine aerodynamic performance prediction from reduced primary to coolant total-temperature-ratio results.* NASA TN D-8312, October 1976.

2.22 Dzung, L.S. — *Konsistente mittelwerte in der theorie der turbomaschinen für kompressible medien.* Brown Boveri, M.H., October 1971.

2.23 Traupel, W. — *Theorie stark gestörter strömungen in kanalen und turbomaschinen.* Forschungsvereinigung Verbrennungskraftmaschinen, E.V. Frankfurt/M. Heft R 153, 1971.

2.24 Dudzinski, T.J. Krause, L.N. — *Flow-direction measurement with fixed-position probes.* NASA TM X-1904, October 1969.

2.25 Armentrout, E.C. Hicks, J.C. — *Pressure instrumentation for gas turbine engines, a review of measurement technology.* NASA TM-73864, 1978.

2.26 Scadron, M.D. Warshawsky, I. Gettelman, C.C. — *Thermocouples for jet engine gas temperature measurement.* Paper No.52-12-3 in Proceedings of the ISA, Vol.7, p.142, 1952.

2.27 Gettelman, C.C. Krause, L.N. — *Considerations entering into the selection of probes for pressure measurement in jet engines.* Paper No.51-12-1 in Proceedings of the ISA, Vol.7, p.134, 1952.

2.28 — *Modern methods of testing rotating components of turbomachines (instrumentation).* AGARD-AG-207, April 1975.

2.29 Odgers, J. — *Combustion modelling within gas turbine engines, some applications and limitations.* AIAA Paper No.77-52, 15th Aerospace Sciences Meeting, January 1977.

2.30 Swithenbank, J. et al. — *Combustion design fundamentals.* 14th Symposium (International) on Combustion. The Combustion Institute, Pittsburgh, PA, August 1972.

2.31 Diehl, L.A. Trout, A.M. — *Performance and emission characteristics of swirl-can combustors to a near-stoichiometric fuel-air ratio.* NASA TN D-8342, November 1976.

2.32 Rusnak, J.P. Shadowen, J.H. — *Development of an advanced annular combustor.* NASA CR-72453 and PWA FR-2832, May 1969.

2.33 Fear, J.S. — *Performance of a small annular turbojet combustor designed for low cost.* NASA TM X-2476, February 1972.

2.34 Niedzwiecki, R.W. — *Preliminary tests of a simplified modular turbojet combustor.* NASA TN D-5688, March 1970.

2.35 Wear, J.D. et al. — *Tests of a full-scale annular ram-induction combustor for a Mach 3 cruise turbojet engine.* NASA TN D-6041, October 1970.

2.36 Stenning, A.H. — *Inlet distortion effects in axial compressors.* Journal of Fluids Engineering, Vol.102, No.1, pp.7–13, March 1980.

2.37 Kuchar, A.P. — *An analysis of jet aircraft engine exhaust nozzle entrance profiles, accountability and effects.* AIAA Paper 76-152, 14th Aerospace Sciences Meeting, January 1976.

2.38 Wehofer, S. Rivir, R. — *Measurement of turbine engine transient airflow in ground test facilities.* AEDC-TR-80-21 (AD-A088706), April 1980.

2.39 Barlett, C.R. Turner, E.E. — *Performance evaluation methods for the high-bypass-ratio turbofan.* AIAA Paper No. 75-1206, 11th Propulsion Conference, September/October 1975.

2.40 Wehofer, S. — *Analysis and computer program for evaluation of air-breathing propulsion exhaust nozzle performance.* AEDC-TR-73-29 (AD760541), May 1973.

2.41 Pelton, J.M. — *A computer model for the calculation of thermodynamic properties of working fluids of a gas turbine engine.* AEDC-TR-76-15 (AD-A021859), March 1976.

2.42 Sanders, N.D. — *Performance parameters for jet propulsion engines.* NACA-TN-1106, July 1946.

2.43 — *Gas turbine engine performance station identification and nomenclature.* Aerospace Recommended Practice ARP-755, SAE, November 1973.

2.44 Sola, J.M. Hutcheson, L. Palmer, J.D. — *Performance of a production model TF30-P-3 turbofan engine at simulated flight conditions.* AEDC-TR-69-136 (AD865170L), February 1970.

2.45 German, J.A. Beach, D.W. — *Altitude performance verification of the General Electric TF39-GE-1 turbofan qualification engine (S/N 441-026) in propulsion development test cell (J-1).* AEDC-TR-70-15 (AD865461L), February 1970.

2.46 Davis, M. Palmer, J.D. Skiles, T.W. — *Altitude development of the F100-PW-100 turbofan engine.* AEDC-TR-75-139 (AD-C003933L), November 1975.

2.47 Abernethy, R. Thompson, J. — *Handbook: Uncertainty in gas turbine measurements.* USAF AEDC-TR-73-5 (AD755356), March 1973.

2.48 — *ASTM manual on quality control of materials.* ASTM STP 15-C (available from American Society for Testing Materials, 1916 Race Street, Philadelphia, PA 19103).

2.49 — *Guide for quality control and control chart method for analyzing data.* ASQC Standard B1, B2-1958, ANSI Standard Z1.1, Z1.2, 1958.

2.50 — *Control chart method of controlling quality during production.* ASQC Standard B3-1958, ANSI Standard Z1.3, 1958 (available from American Society for Quality Control, 161 West Wisconsin Avenue, Milwaukee, Wisconsin 53203 or from American National Standards Institute, 1430 Broadway, New York, NY 10018).

2.51 Duncan, A.J. — *Quality control and industrial statistics.* Third edition, Richard D. Irwin, Incorporated, Homewood, Illinois, 1965.

2.52 Cowden, D.J. — *Statistical methods in quality control.* Prentice-Hall, Incorporated, Englewood Cliffs, New Jersey, 1957.

2.53 Juran, J.M., Editor — *Quality control handbook.* Second edition, McGraw-Hill Book Company, New York, 1962.

2.54 Ku, H.H. — *Statistical concepts in metrology.* Chapter 2, Handbook of Industrial Metrology. American Society of Tool and Manufacturing Engineers, Prentice-Hall, Incorporated, New York, NY, 1967. (Reprinted in NBS SP 300-Vol.1, "Precision measurement and calibration – statistical concepts and procedures" (available from the Superintendent of Documents, United States Government Printing Office, Washington, D.C. 20402).

2.55 Pontius, P.E. — *Measurement philosophy of the pilot program for mass calibration.* NBS Technical Note 288 (available from the Superintendent of Documents, United States Government Printing Office, Washington, D.C. 20402).

2.56 Pontius, P.E. Cameron, J.M. — *Realistic uncertainties and the mass measurement process.* NBS Monograph 103 (available from the Superintendent of Documents, United States Government Printing Office, Washington, D.C. 20402).

2.57 Dietrich, C.F. — *Uncertainty, calibration and probability.* The Statistics of Scientific and Industrial Measurement, Adam Hilger, London, 1973.

2.58 Paradine, C.G. Rivett, B.H.P. *Statistical methods for technologists.* 3rd Impression, The English Universities Press Ltd, 1962.

2.59 Weatherburn, C.E. *A first course in mathematical statistics.* Cambridge University Press, New York, 1962.

2.60 Davies, O.L. Goldsmith, P.L. *Statistical methods in research and production.* 4th Edition, Oliver & Boyd, Edinburgh, 1972.

2.61 Urban, L.A. *Parameter selection for multiple fault diagnostics of gas turbine engines.* Journal of Engineering for Power, April 1975.

2.62 Urban, L.A. *Gas turbine parameter interrelationships.* 2nd Edition, HSUAC, Windsor Locks, CT, 1969.

2.63 Skiles, T.W. *Turbine engine flowpath averaging techniques.* Master Thesis, University of Tennessee, Knoxville, August 1981.

CHAPTER 3

Section 3.1

3.1.1 Rosslenbroich, M.E. *Averaging methods in the description of energy conversion in thermodynamic systems.* Z. Flugwiss, Bd. 20, pp.71–76, 1972.

3.1.2 Smith, A.J.W. *Pressure losses in ducted flows.* Butterworths, London, 1971.

3.1.3 Livesey, J.L. Hugh, T. *Suitable mean values in one-dimensional gas dynamics.* J. Mech. Eng. Scie. Vol.8, No.4, pp.374–383, 1966.

3.1.4 Livesey, J.L. *Duct performance parameters considering spatially non-uniform flow.* AIAA Paper No.72-85, 1972.

3.1.5 Tyler, R.D. *One-dimensional treatment of non-uniform flow.* ARC R&M No.2991, 1954.

3.1.6 Traupel, W. *Thermal turbomachines, Volume I.* Springer-Verlag, Berlin. 2nd Edition 1966, 3rd Edition 1978.

3.1.7 Baehr, H.D. *Thermodynamics.* Springer-Verlag, Berlin. 3rd Edition 1973.

3.1.8 *Decrease and performance tests in compressors (VDI-compressor rules).* Deutscher Normenausschuss (German Standards Committee), Edition May 1934.

3.1.9 Hoffmeister, M. *Formation of flow-technical and thermal average values on a turbomachine stage.* Maschinenbautechnik, Bd.12, pp.578–582, 1963.

3.1.10 Wyatt, M.D. *Analysis of errors introduced by several methods of weighting non-uniform duct flows.* NACA TN 3400, 1955.

3.1.11 Scholz, N. *Conduction of systematic measurements on two-dimensional cascades.* Z. Flugwiss, Bd.4, pp. 313–333, 1956.

3.1.12 Amecke, J. *Evaluation of wake measurements in two-dimensional cascades.* AVA-Report 67A49, 1967.

3.1.13 Amecke, J. *Application of the transonic similarity rule on flow through two-dimensional cascades.* VDI-Forsch.-H.540, pp.16–28, 1970.

3.1.14 Dzung, L.S. *Consistent average values in the theory of turbomachines for compressible media.* BBC-Mitt. Bd.58, pp.485–492, 1971.

Section 3.2

3.2.1 Reid, L. Moore, R.D. *Design and overall performance of four highly loaded high speed inlet stages for an advanced high pressure ratio core compressor.* NASA Technical Paper 1337, October 1978.

CHAPTER 4

Section 4.1

4.1.1 Dzung, L.S. *Konsistente mittelwerte in der theorie der turbomaschinen für kompressible medien.* BBC-Mitt. Bd.58, pp.485–492, 1971.

4.1.2 Livesey, J.L. AIAA Paper 72-85, AIAA 10th Aerospace Sciences Meeting, San Diego, 1972.

4.1.3 Livesey, J.L. Hugh, T. Jnl. Mech. Eng. Sci., Vol.8, No.4, pp.374–383, 1966, Vol.9, No.3, 1967, Corrigendum.

Section 4.2

4.2.1 MIDAP Study Group *Guide to in-flight thrust measurement of turbojets and fan engines.* AGARDograph-AG-237, 1979.

4.2.2 Wehofer, S. Matz, R.J. *Turbine engine exhaust nozzle performance with non-uniform inlet flow.* AEDC-TR-75-82 (AD-A014261), August 1975.

4.2.3 Kuchar, A.P. Tabakoff, W. *An analysis of jet aircraft engine exhaust nozzle entrance profiles, accountability and effects.* AIAA Paper No.76-152, AIAA 14th Aerospace Sciences Meeting, January 1976.

4.2.4 Decher, R. et al. *Systems aspects of engine installation.* Chapter 26 of "Aerothermodynamics of Aircraft Gas Turbine Engines". AFAPL-TR-78-52, 1978.

4.2.5 Longhouse, R.E. *TF39 1/10 scale model exhaust system static performance test.* Report No.R67FPD416, General Electric Company, Cincinnati, Ohio, February 1968.

4.2.6 Oates, G.C. *Cascade flows.* Chapter 12 of "Aerothermodynamics of Aircraft Gas Turbine Engines", AFAPL-TR-78-52, 1978.

4.2.7 Kimzey, W.F. *Some insights into high-bypass ratio turbofan engine nozzle performance from full-scale tests in an altitude test cell.* AIAA 6th Propulsion Specialists Conference, June 1970.

WORKING GROUP 14 – MEMBERSHIP

PEP MEMBERS

BELGIUM	Professor Ch. HIRSCH Vrije Universiteit Brussel Dienst Stromingsmechanica Pleinlaan 2 1050 Brussel	
FRANCE	Mr J. FABRI ONERA 29 Avenue de la Division Leclerc 92320 Châtillon sous Bagneux	
	Mr l'Ingénieur en Chef M. PIANKO ONERA 29 Avenue de la Division Leclerc 92320 Châtillon sous Bagneux	*ACTING CHAIRMAN*
GERMANY	Professor Dipl-Ing. F. WAZELT Lehrstuhl für Flugantriebe Technische Hochschule Darmstadt Petersenstrasse 30 6100 Darmstadt	*CHAIRMAN*
ITALY	Professor D. DINI Università degli Studi Istituto di Macchine Via Diotisalvi 3 56100 Pisa	
UNITED KINGDOM	Dr J. DUNHAM National Gas Turbine Establishment Pyestock Farnborough, Hants GU14 0LS	
UNITED STATES	Professor E.E. COVERT Department of Aeronautics and Astronautics Massachusetts Institute of Technology Cambridge, Massachusetts 02139	

NON-PANEL MEMBERS

FRANCE	M. l'Ingénieur Général P. CARRIERE ONERA 29 Avenue de la Division Leclerc 92320 Châtillon sous Bagneux	
	Dr G. MEAUZE ONERA 29 Avenue de la Division Leclerc 92320 Châtillon sous Bagneux	
GERMANY	Mr W. HAPPEL Motoren und Turbinen Union GmbH (MTU) Dachauerstrasse 665 8000 München 50	
	Dr H. KRUSE DFVLR Institut für Antriebstechnik Postfach 90 60 58 5000 Köln 90	

UNITED KINGDOM

Professor J.L. LIVESEY
University of Salford
Royal College of Advanced Technology
Salford, Manchester 5

UNITED STATES

Mr S. WEHOFER
Technology Application Branch – ETF
ARO Inc.
Arnold Air Force Station, Tennessee 37389

LIST OF CONTRIBUTIONS

LIST OF CONTRIBUTORS